

Crystallization of High Silica
Molecular Sieves

Douglas Murray Sinclair

Presented for the Degree of Doctor of Philosophy

University of Edinburgh

1986



Abstract.

Tetraethyl silicate has been hydrolysed under controlled conditions to produce "clear" silicate sols. An investigation of these sols by both trimethylsilylation and reaction with molybdic acid solution did not reveal any major difference between these sols and those produced from fumed silica. However these sols remain clear when heated to temperatures normally used in the synthesis of high silica molecular sieves (353K to 473K) and do not separate into solution plus solid gel as is the case with sols normally used in molecular sieve synthesis. New methods to follow the growth of zeolite crystals have been developed. Since there is no solid gel phase the zeolite crystals can be recovered by filtration and then weighed. Thus crystallization can be followed directly by mass growth measurements. Crystallization from the "clear" sols can also be followed by silicate analysis of the solution phase. These methods are not appropriate for crystallization from gels. Reaction mixtures have been sealed inside glass capillary tubes and the crystals grown at different glass temperatures. The crystal growth of individual crystals can then be followed by optical microscopy. The effects of temperature and chemical composition on the crystallization of ZSM-5 type zeolites has been examined. Apparent activation energies of growth for the different crystal faces have been calculated from Arrhenius plots. Factors which influence the size and shape of the crystals have been determined. Conditions for the growth of relatively large crystals of ZSM-5 have been established. Similar conditions are found to produce larger crystals of some other high silica molecular sieves (e.g. EU-1, ZSM-39 and ZSM-48). The crystallization of silicalite-1 at 368K from reaction mixtures with the composition $1\text{Na}_2\text{O} \cdot 20\text{SiO}_2 \cdot 1960\text{H}_2\text{O} \cdot 80\text{EtOH} \cdot 2\text{TPABr}$ has been studied in detail, using thermal gravimetric analysis, scanning electron microscopy, X-ray powder diffraction, pH measurements and crystal mass measurements. The rate of linear crystal growth has been determined by measurement of the largest crystals at various stages of the crystallization. Nucleation curves have been calculated from the final crystal size distribution and the crystal growth curve. The crystal mass growth curve has also been calculated from the crystal growth curve data and the final crystal size distribution. The calculated mass growth curve is found to be in close agreement with the actual mass growth curve obtained experimentally.

Declaration.

I declare that this thesis, which is of my own composition, is an accurate record of work which I carried out in the Department of Chemistry, University of Edinburgh and at ICI Ltd., New Science Group (formerly Corporate Laboratory), Runcorn, between October 1981 and September 1984. During this period I was supervised by Drs. B.M.Lowe, N.H.Ray and C.Cundy.

During the above period I also attended the following lectures/courses:

Fortran Computing Course	-	E.R.C.C.
Lasers in Chemistry	-	Prof. Donovan/Dr. Fotakis
Fourier Transform Spectroscopy	-	Drs. Craddock, Duncan and Morrison
Interpreting the Results of Crystallography	-	Drs. Gould, Walkinshaw and Welch
Modern Liquid Phase Separation Techniques	-	Prof. Knox
The History of the Chemistry Department	-	Dr. Doyle
The Chemistry of Photographic Processes	-	Dr. Williams
Aspects of Structural Chemistry	-	Dr. Heath
X-ray Discussions	-	Dr. Gould

Acknowledgements.

I must begin by acknowledging the help and encouragement of Barrie Lowe without whom this work may never have reached completion.

I would also like to thank Neil Ray and Colin Cundy for playing their part as supervisors so well, in particular Colin for looking after me on my visits to the New Science Group at Runcorn.

I have also to thank the New Science Group for the work they carried out on my behalf and for the use of their equipment on my visits.

In addition I must thank the S.E.R.C. for their funding throughout the three years of my C.A.S.E. award.

Lastly I would like to acknowledge the help given by my wife, Pamela, as she managed to take on the role of secretary as well as giving both moral and monetary support throughout .

1.6 Objectives 59

1.7 References 62

Chapter 2 Experimental 68

2.1 Introduction 70

2.2 Apparatus 71

2.3 Procedure 72

2.4 Results 73

2.5 Discussion 74

2.6 Conclusions 75

2.7 References 76

<u>Contents.</u>	<u>Page</u>
<u>Chapter 1</u>	1
1.1 Introduction	1
1.2 Natural Zeolites	2
1.3 The Structural Chemistry of Zeolites	4
1.4 Properties and Applications	10
1.4.1 Adsorption	10
1.4.2 Ion Exchange	14
1.4.3 Catalysis	15
1.5 Synthesis	17
1.5.1 General	17
1.5.2 Mechanism of Crystallization	22
1.5.2.1 Reactants	27
1.5.2.2 Nucleation	30
1.5.2.3 Growth	41
1.5.2.4 Crystallization Kinetics	48
1.5.2.5 Role of Cations	56
1.6 Objectives	59
1.7 References	62
<u>Chapter 2</u>	69
2.1 Analysis	70
2.1.1 X-Ray Powder Diffraction	70
2.1.2 Microscopy	72
2.1.2.1 Scanning Electron Microscopy	72
2.1.2.2 Optical Microscopy	74
2.1.3 Thermal Analysis	77
2.1.3.1 Thermal Gravimetric Analysis	78

<u>Contents</u>	<u>Page</u>	
2.1.4	Silicate Analysis	79
2.1.4.1	Procedure	80
2.1.5	pH Measurement	80
2.2	Synthesis	82
2.2.1	High Temperature Reactions	82
2.2.2	Low Temperature Reactions	89
2.3	References	93
<u>Chapter 3</u>	<i>Zedite Synthesis using Tetraethyl Silicate</i>	94
3.1	Introduction	94
3.2	Experimental	102
3.2.1	Materials	102
3.2.2	Preparation of Solutions	102
3.2.3	Trimethylsilylation	103
3.2.4	Reactions with Molybdic Acid	104
3.2.5	Crystallization	106
3.2.6	Analysis	106
3.3	Results and Discussion	108
3.3.1	Hydrolysis of Tetraethyl Silicate	108
3.3.2	Trimethylsilylation	114
3.3.3	Molybdic Acid Analysis	118
3.4	Crystallization	119
3.4.1	Reactions at 353K	119
3.4.2	Reactions at 368K	124
3.4.3	Crystallization of ZSM-5	129
3.5	References	134

<u>Contents.</u>	<u>Page</u>
<u>Chapter 4</u> <i>Zedite Crystal Growth followed by Optical Microscopy</i>	136
4.1 Introduction	136
4.2 Experimental	144
4.2.1 Materials	144
4.2.2 Preparation of Solutions	144
4.2.2.1 Silicate Solutions	144
4.2.2.2 Addition of Aluminium	145
4.2.3 Crystallization	145
4.2.4 Crystal Growth	146
4.3.1 Conditions for the Growth of Large Crystals	147
4.3.1.1 Silica Concentration	147
4.3.1.2 Hydroxide	155
4.3.1.3 Temperature	155
4.3.1.4 Cation	157
4.3.1.5 Summary	160
4.3.2 Temperature Dependence	160
4.3.3 Aluminium Additions	172
4.3.4 Salt Additions	183
4.3.5 Addition of Tetrapropylammonium	189
4.3.6 Ethanol Additions	195
4.3.7 Other Systems	200
4.3.7.1 Zeolite EU-1	201
4.3.7.2 Zeolites ZSM-39 and ZSM-48	207
4.4 Conclusions	216
4.5 References	217

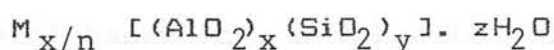
<u>Contents.</u>	<u>Page</u>
<u>Chapter 5</u> <i>Nucleation and Crystal Growth of Silicalite</i>	219
5.1 Introduction	219
5.2 Experimental	228
5.2.1 Materials	228
5.2.2 Preparation of Silicate Solutions	228
5.2.3 Crystallization	228
5.2.4 Analysis	229
5.3 Results and Discussion	233
5.3.1 Crystal Growth	233
5.3.2 Nucleation	247
5.3.3 pH	257
5.3.4 Comparison of Reactions	257
5.4 Conclusions	265
5.5 References	267
<u>Appendix 1</u> Program to Calculate Weights Required for Reaction Mixtures	268
<u>Appendix 2</u> Program to Convert Crystal Size Distribution into a Mass Growth Curve	271
<u>Appendix 3</u>	273

1.1. Introduction.

Crystal growth has been of interest to scientists for a very long time. This is due to the frequent occurrence of crystallization in nature and also because of the various uses of crystallization in industrial processes. The growth of crystals has often been regarded as an "art" rather than an area where the scientific method may be applied. This appears to be especially true in the area of zeolite crystallization. A large proportion of the early work on zeolite crystallization was of an empirical nature and was often very successful in that many different zeolite types were made. The theoretical aspects of zeolite crystallization were sadly left behind. However, there is now more interest in the development of a greater understanding of zeolite crystallization.

Zeolites are porous, crystalline aluminosilicates whose frameworks consist of a three-dimensional network of tetrahedrally co-ordinated silicon or aluminium atoms which are linked together via bridging oxygen atoms. The result is an open, relatively rigid, anionic structure which contains channels which can have free diameters from about 0.25 nm to 0.8 nm. These channels are large enough to allow the passage of small molecules. They also interconnect larger voids which may contain water molecules and also cations to balance the anionic charge of the lattice.

A zeolite may be represented by the formula:



where M is a cation of valence n. M can be any cation providing that it can fit inside the zeolite framework without destroying the structure by its size or electrostatic charge. The ratio of silicon to aluminium determines the net negative charge of the framework. Lowenstein's¹ rule states that no aluminium atom can bridge with another aluminium atom and so constrains the Si/Al ratio to a minimum value of one (providing that the rule holds). Zeolites can be produced with a wide range of Si/Al ratios with values extending from 1 to over 1000, i.e. an essentially aluminium free phase. Olsen et. al.² have reported a Si/Al ratio as high as 4000.

1.2. Natural zeolites.

Natural zeolites have been known for over 200 years. The first zeolite to be discovered was the mineral stilbite,³ in 1756. Since then natural zeolites have been discovered all over the world, although it is only within the last few decades that the number of different varieties and the immense quantities of some deposits have been recognised.⁴ Some of the deposits are in large enough quantities to be exploited commercially (e.g. clinoptilolite and mordenite) while others, which consist of extremely useful zeolites, only occur rarely and in small quantities (e.g. faujasite).

Zeolites appear to occur either as crystals formed

in cavities of basaltic and volcanic rocks or in sedimentary deposits. The mechanism for the formation of natural zeolites is not fully understood. Crystals from igneous rocks appear to be formed by the action of hot aqueous solutions on alkali rich rocks.⁴ The crystals which are formed are often large and well-formed, with the growing faces not in contact with the parent rock. This suggests that the growth mechanism must involve deposition from the solution onto the crystals. The material for growth is supplied by the parent rock which continuously dissolves into the hot alkaline solution. The type of zeolite which is produced will depend not only upon the composition of the parent material but also upon the temperature and pressure of the reaction. Recent studies⁵ have provided evidence that the regions where crystallization took place at higher temperatures contain the least hydrated zeolites.

The sedimentary zeolites are normally agglomerates of crystallites. The crystals are usually small with poorly developed crystal faces. The sedimentary zeolites often form large deposits. They are probably produced by the action of water, alkaline or saline solution on volcanic sediments.⁴ The water or solution penetrates and dissolves some of the sediment to form an aluminosilicate solution from which the zeolite then crystallizes. Further reaction may then occur with the first zeolite dissolving and recrystallizing as a

different species. The sedimentary material provides a much higher surface area than igneous rocks, allowing the nutrient to dissolve much faster. This higher surface area will also provide many more places for crystals to nucleate. This may account for the differences observed between crystals found in igneous rocks and those in sedimentary deposits.

Further information on natural zeolites can be found in comprehensive reviews by Breck⁶ and by Mumpton.⁴

1.3. The structural chemistry of zeolites.

Zeolite structures are particularly fascinating. There are 41 well established zeolite structures, 30 of which are for natural zeolites. The remainder are for synthetic zeolites which have, as yet, no natural counterpart. Several zeolite structures have still to be elucidated, e.g. the natural zeolites cowlesite⁷ and svetlozarite⁸ and quite a few synthetic zeolites, e.g. ZSM-10,⁹ Nu-1¹⁰ and EU-1.¹¹

One of the difficulties in obtaining zeolite structures is that few zeolites can be obtained with a crystal size which will allow single crystal X-ray diffraction work to be carried out. Also, the structures are extremely complex with large unit cells, so that powder X-ray diffraction methods are of only limited help in structure determination. The chemistry of silicates is based upon the tetrahedron and such structures can be extremely complicated (c.f. carbon). Zeolite structures are often displayed as skeletal

diagrams with a T-atom (i.e. a Si or Al atom) at each corner or termination. The oxygens are not normally shown. The T-O-T angle lies between 140° and 150° and consequently the oxygen atoms are displaced from the mid-points of the lines joining each pair of T-atoms. The skeletal diagrams help to portray the complex structures in a slightly simpler way, allowing the channels and voids to be easily seen. An example is shown in figure 1.1¹² where the straight channels of ZSM-5 can be readily observed.

Since zeolites have many diverse structures it is not really possible to describe a structure using only the primary building unit, TO_4 . Secondary structure units comprising of small groups of linked TO_4 units are needed. In 1967 Meier proposed the secondary building units (S.B.U.)¹³ shown in figure 1.2. A S.B.U. is the smallest simple unit that can be used to construct an entire zeolite structure. Thus the structure of ZSM-5 may be constructed entirely of 5-1 units. It must be emphasized that these units have only been proposed in order to aid the description of zeolite frameworks. They are not meant to represent the aluminosilicate species which may be involved in the crystallization of the zeolite structure.

Several other methods of describing the zeolite frameworks have been developed, e.g. stacking of layers, parallel linking of chains etc., but the S.B.U.'s are probably the simplest to understand and

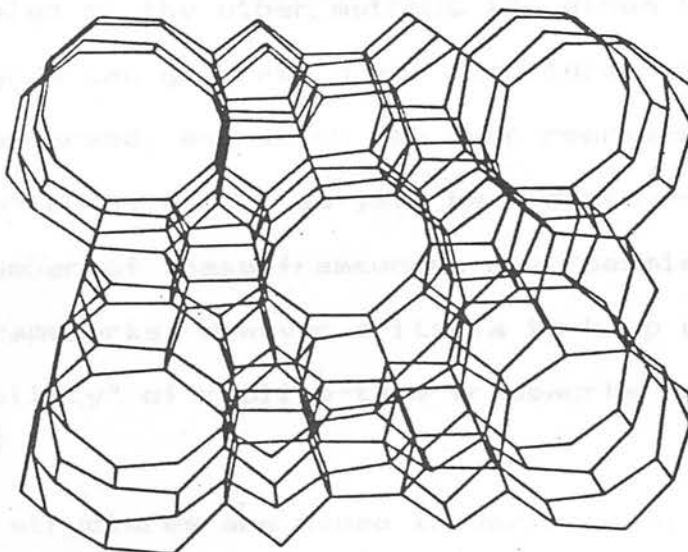


Figure 1.1 The aluminosilicate framework structure of zeolite ZSM-5. Al or Si atoms (T-atoms) are centred at each corner and O atoms are centred near but not at the mid-point of each edge.

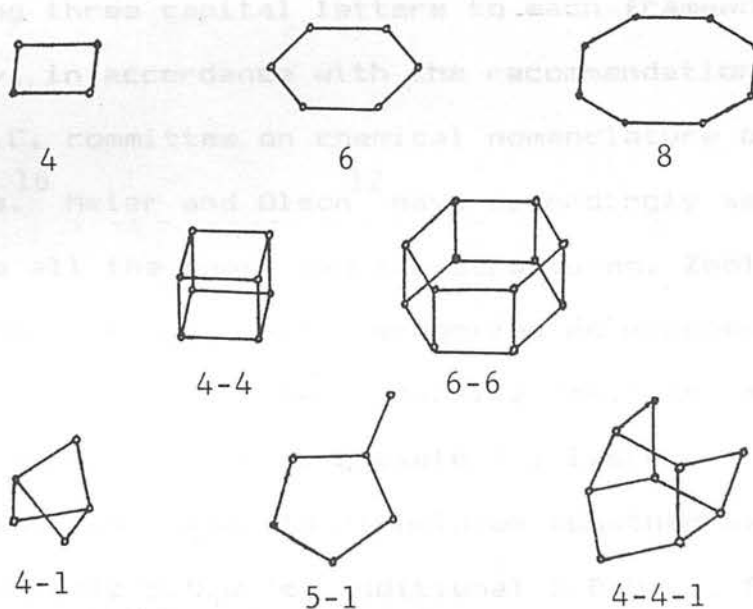


Figure 1.2 The secondary building units (S.B.U.'s) found in zeolite frameworks.

use. Examples of the other methods are given by Barrer.¹⁴ These methods can generate novel structures which have not been observed, and which may even represent zeolites which have not, as yet, been discovered. Only a small number of these frameworks are "permissible" zeolite frameworks. However criteria to help gauge the "permissibility" of zeolite-type frameworks have been proposed.¹⁵

Zeolite structures are named in various ways and often the same type of zeolite has been given several names, each depending upon the laboratory in which it was synthesized. For example, the synthetic zeolites ZSM-4 and omega appear to have the same structure as the natural zeolite mazzite, but this is not obvious from their names. This problem has been resolved by assigning three capital letters to each framework topology, in accordance with the recommendations of the I.U.P.A.C. committee on chemical nomenclature of zeolites.¹⁶ Meier and Olson¹² have accordingly assigned codes to all the known zeolite structures. Zeolite omega (MAZ) is now easily recognized as possessing the same framework structure as mazzite (MAZ) and zeolite ZSM-4 (MAZ). The following table 1.1 lists the well-established zeolite structures together with their characteristic S.B.U.'s, additional S.B.U.'s, typical Si/Al ratios and pore volumes. The structures of related materials are grouped together (after Barrer),¹⁷ but the divisions between these groups are fairly

Table 1.1. Classification of Zeolites

	IUPAC Code	Characteristic SBU's	Additional SBU's	Typical Si/Al	Pore Volume (cm ³ as liquid H ₂ O per cm ³ of crystal)
Analcime Group:					
Analcime	ANA	4	6	2-3	0.18
Chabazite Group:					
Afghanite	AFG	6	4	1	-
Cancrinite	CAN	6	4	1	0.34
Chabazite	CHA	6-6	4,6	1.6-3.0	0.48
Erionite	ERI	6	4	3-3.5	0.36
Gmelinite	GME	6-6	4,6,8	2-2.5	0.43
Levynite	LEV	6		2	0.42
Liottite	LIO	6		1	-
Mazzite	MAZ	4	5-1	2.5	0.37
Offretite	OFF	6	4	2.5-3.5	0.34
Sodalite	SOD	6	4	1	0.34
L	LTL	6	4	2.5-3.5	0.28
Losod	LOS	6		1	0.37
TMA-E (AB)	EAB	6	4	3	-
Clathrate Group:					
Melanophlogite	MEP ^a	5 ^b			-
ZSM-39	MTN ^a	5 ^b			-
Faujasite Group:					
Faujasite	FAU	6-6	4,6	1-3	0.53
Paulingite	PAU	4		3.5	0.48
A	LTA	4-4		1	0.47
RHO	RHO	4	6,8,8-8	3	0.41
ZK-5	KFI	6-6	4,6,8	2-2.5	0.45
ZSM-3	MTH ^a			1.6	0.53
Heulandite Group:					
Brewsterite	BRE	4		2.5-3	0.32
Heulandite	HEU	4-4-1		2.5-3.5	0.35
Stilbite	STI	4-4-1		2.5-3.5	0.38
Laumonite Group:					
Laumonite	LAU	4	6	2	0.35
Yugawaralite	YUG	4	8	2.5-3.5	0.30

Table 1.1. Classification of Zeolites (cont.)

	IUPAC Code	Characteristic SBU's	Additional SBU's	Typical Si/Al	Pore Volume (cm ³ as liquid H ₂ O per cm ³ of crystal)
Mordenite					
Group:					
Bikitaite	BIK	5-1		2	0.20
Dachiarite	DAC	5-1		4	0.26
Epistilbite	EPI	5-1		2.5-3	0.34
Ferrierite	FER	5-1		4-5.5	0.24
Mordenite	MOR	5-1		4.5-5.5	0.26
Natrolite					
Group:					
Edingtonite	EDI	4-1		1.5	0.35
Natrolite	NAT	4-1		1.5	0.21
Thomsonite	THO	4-1		1	0.32
Pentasil					
Group:					
ZSM-5	MFI	5-1		wide	0.32
ZSM-11	MEL	5-1		range	0.32
Phillipsite					
Group:					
Gismondine	GIS	4	8	1-1.5	0.47
Merlinoite	MER	4	8,8-8	2.5	0.36
Phillipsite	PHI	4	8	2-3	0.30
Li-A(BW)		4	6,8	1	0.28

a Codes suggested by Barrer.

b 5-ring SBU proposed by Barrer.

arbitrary and only indicate structural relationships between different frameworks.

1.4. Properties and applications.

The channels and voids of a zeolite give it a very large "internal" surface area which can only be reached by molecules which can pass into the channel system. It is the properties of these cavities which make zeolites very important as catalysts, sorbents and ion-exchangers. It would not be appropriate to give a full account of the uses of zeolites here, but the following sections summarize their main uses. A more complete account can be found in the literature.¹⁸⁻²⁰

1.4.1. Adsorption.

The term "molecular sieve" is often used to describe a zeolite. This is because zeolites can selectively adsorb or reject different molecules according to their size. Several different molecules which can be adsorbed may be separated further due to different rates of diffusion through the zeolite. The main factor which determines whether a molecule can enter a zeolite is the size of the pores which allow access to the zeolite's internal surface. The pore size of a zeolite depends upon the number of atoms which make up the narrowest ring in the channel. Table 1.2 gives the theoretical free dimensions of some rings, assuming an oxygen radius of 0.135 nm and a planar ring. In the actual zeolite the rings are not likely to be planar but will be distorted in some manner, which will result

in a smaller pore size. In the case of zeolites, the pore size is determined by the arrangement of the T-atoms in the ring. The ideal free dimensions of zeolite pore openings are given in Table 1.2. The pore size can also be estimated by the number of T-atoms in the ring. The pore size can also be estimated by the number of T-atoms in the ring. The pore size can also be estimated by the number of T-atoms in the ring.

Table 1.2. Ideal free dimensions of zeolite pore openings.

Number of T-atoms in ring	Ideal dimension/nm
6	0.27
8	0.44
10	0.60
12	0.77

in a smaller pore size. As an example, consider the 10-T atom ring found in ZSM-5. The ideal size, according to table 1.2, is 0.6 nm but the size estimated from the structure is found to be a maximum of 0.54 nm. The pore sizes can also be estimated by the sorption of molecules of known dimensions. These can then be used to probe the zeolite and the pore size can be estimated from the size of the larger molecules which are just denied access. It is often found that molecules which are "larger" than the pore appear to enter the zeolite. This is because neither the zeolite nor the molecules which are adsorbed are composed of rigid bonds or hard spheres. Thermal vibrations can allow molecules to pass into a zeolite at high temperatures even though the molecule cannot enter at low temperatures. A variation in the vibrational amplitude of 0.01 to 0.02 nm can be expected over a temperature interval of 80 to 300K.²¹ This could allow molecules of similar size to be separated and has, in fact, been demonstrated using oxygen and nitrogen. Thus at liquid air temperatures oxygen (critical dimension 0.28 nm) can be separated from nitrogen (critical dimension 0.30 nm) using zeolite Na-A (LTA).²²

It is not just the number of atoms in the smallest ring which can determine the window size. A very important factor can be the type of cation within the zeolite. The classic example of this is found for zeolite A (LTA), where the window size can change from

approximately 0.3 nm when the cation is potassium to approximately 0.5 nm when the cation is calcium. The adsorption characteristics can also be modified by the introduction of small quantities of guest species.²³

The guest species can be of various types, e.g. salts, metal atoms or clusters, polar or non-polar molecules. All these can be used to partially block the zeolite pores.

Another factor which influences the sorption characteristics of zeolites is the electrostatic fields established within the pores. The framework has an anionic charge and local electrostatic fields throughout the structure can interact with the molecules which enter the zeolite. Molecules which possess permanent electric moments can interact strongly with the fields and consequently they are adsorbed much more energetically than molecules which do not possess a permanent dipole. This property allows zeolites to sorb polar molecules from mixtures of molecules which have similar size, e.g. the removal of water from organic solvents.

In high silica zeolites such as ZSM-5 there is very little aluminium in the framework and the sorption characteristics are very different to those described above. These zeolites can only adsorb polar molecules weakly and in fact they exhibit a considerable organophilic behaviour. Small polar molecules such as water are only adsorbed weakly and it is possible to

use high silica zeolites to remove organic molecules from very dilute aqueous solutions.^{24,25}

The commercial applications of zeolites as sorbents are mainly in the areas of purification and separation. Purification includes processes like the drying of gases and the removal of carbon dioxide and sulphur compounds from natural gas. Separation processes include the removal of para-xylene from ortho-, meta- and para-xylene mixtures, and also the separation of normal paraffins from mixtures of normal and iso paraffins.

1.4.2. Ion exchange.

The zeolite cations can move within the framework but are unable to leave it unless they can be replaced by an ion or ions of equivalent charge. This may be brought about by contacting the zeolite with an aqueous salt solution and is known as ion-exchange. The number of cations which can be exchanged depends upon the Si/Al ratio and the structure of the zeolite. The Si/Al ratio determines the maximum exchange capacity of the zeolite; for a given structure the framework with the lowest Si/Al ratio has the highest exchange capacity. In practice the maximum exchange capacity is often not achieved due to an ion-sieving effect. Some ions may be unable to enter the zeolite while others may be only able to enter the main channels. Cation exchange also depends upon the cation charge, the concentration of the species in solution, the anion, the solvent and the

temperature. The effect of these various factors is described by Breck.¹⁸

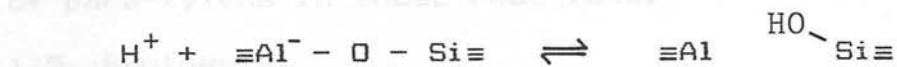
The main use of ion exchange in industry is in the preparation of zeolites as catalysts or sorbents. Indeed, but for their ion exchange abilities, their use in these areas would be much restricted. However they do not have as high an ion exchange capacity as other ion exchangers and consequently the commercial applications which make direct use of their ion exchange properties are somewhat limited. The areas that they are used in tend to make use of their stability to temperature, ionizing radiation and pH. Thus they are used to separate radioisotopes (^{90}Sr and ^{137}Cs), remove NH_4^+ from waste water and, more recently, as a replacement for phosphate builders in detergents (Ca^{2+} removal).

1.4.3. Catalysis.

The effectiveness of a zeolite as a catalyst depends upon the accessibility of the "internal" surface and thus upon the shape and size of the reactant molecules and the window size of the zeolite. The first major catalytic use of zeolites started in 1962 and followed the discovery by Weisz²⁶ that zeolite Y (FAU), could be used as a cracking catalyst. Before that time almost all hydrocarbon cracking catalysts were amorphous aluminosilicates, but these have now been almost totally replaced by ones based on zeolites.

These catalysts have a higher activity and give much higher yields of gasoline. The acid form (H-form) of

the zeolite can be easily obtained by either direct exchange with acid (for high silica zeolites only) or exchange with NH_4^+ ions followed by thermal decomposition (suitable for all zeolites). The acid sites within the H-form arise from silanol groups which are produced from the reaction:²⁷



The presence of the trivalent Al causes the silanol OH to be an extremely powerful proton donor. The acid strength of zeolite catalysts is usually much greater than that of amorphous aluminosilicates. The H-form is not the only one used catalytically. Various cations can be introduced into the zeolites by ion exchange to give forms which are catalytically active and thermally stable e.g. rare earth-Y is used in preference to H-Y.

The channel system can restrict the type of reactant that can reach the catalytic sites, and it can also place constraints on the type of product formed. The internal structure may physically prevent the formation of transition states or stop large product molecules from leaving the zeolite. Thus zeolites are not only shape selective towards the reactant molecule but also towards the product molecules. An example of this is found for ZSM-5. Small molecules such as methanol and ethanol, as well as larger ones like linear esters, can be converted by ZSM-5 to form a narrow range of hydrocarbons which corresponds closely to the range

that makes up petrol.^{28,29} Larger hydrocarbons are not formed. ZSM-5 also exhibits shape-selectivity in xylene isomerization and toluene disproportionation reactions. The ortho and meta forms of xylene are not a good fit for the zeolite channels while para-xylene easily fits into the channels. Consequently, there is a high yield of para-xylene in these reactions.

1.5. Synthesis.

1.5.1. General.

Zeolites are produced by the hydrothermal crystallization of aluminosilicate gels. The temperatures normally used range from about 353K to over 473K. The first attempts to synthesize zeolites were made in the middle of the nineteenth century by geologists who wished to understand the conditions under which they formed in nature. The first successful synthesis of a zeolite is attributed to St. Claire Deville who produced levynite in 1862.

The synthesis of several other zeolites was claimed in the following years by various researchers. Unfortunately there is little evidence to substantiate these early reports. Analytical techniques such as X-ray powder diffraction were not available until very much later.

The conditions used in these early experiments reflected the current ideas on their formation from igneous rocks. Reactions were carried out at very high temperatures, normally greater than 473K, with

compositions which corresponded to the chemical composition of the desired material. Water was not normally considered to be an important variable and an excessive amount was often included. Consequently it is difficult to reproduce these early experiments although some of them may have produced zeolites.

The first really successful work on the synthesis of zeolites began in the late 1940's. Barrer carried out systematic studies³¹ using autoclaves at temperatures above 423K. These studies resulted in the synthesis of many different zeolites including the first with no natural counterpart. Two forms of this material, species P and Q, were prepared.³² Their structure is similar to that of zeolite ZK-5 (KFI), which was synthesized 15 years later using a quite different technique. Barrer used barium salts as mineralizers to convert analcime, a natural zeolite, to the new species. (A mineralizer is a component which is added to the water to form loose complexes with silica and alumina and so shift the dissolution equilibrium so that more silica is in solution). Barrer investigated a series of salts and obtained various degrees of success with this "recrystallization" technique. The technique seems even more remarkable when it is noted that in the example given, the aluminosilicate framework of the product has a more open structure than that of the parent zeolite. Analcime has a framework density of $18.6 \text{ T-atoms nm}^{-3}$ while the KFI structure has a

framework density of $14.7 \text{ T-atoms nm}^{-3}$. However the product zeolite contains occluded salt which probably stabilizes it with respect to the parent zeolite. The recrystallization technique appears to rarely used now.

The use of amorphous aluminosilicate gels as the source of the nutrient was also investigated by Barrer.³³ The first systematic studies in this area resembled the earlier synthetic studies in which aluminosilicate gels were prepared, dried and then reacted with water or alkaline solution at temperatures above 423K .

The major breakthrough in synthesis occurred when Milton and his colleagues at Union Carbide³⁴ successfully crystallized zeolites from reactive gels using temperatures below 373K . The conditions used were similar to those which are now thought to occur in the formation of sedimentary zeolites. These are believed to form under relatively mild conditions. The method involved the use of highly reactive materials, a strong base and low temperatures. The starting materials react together to produce an aluminosilicate gel which can then be crystallized at temperatures up to 373K or sometimes even higher. The gels crystallize quite rapidly, taking from only a few hours to a few days. The success of the method depends upon several important variables. These include the reaction composition, temperature, type of reagent, order of mixing the components, and also the time for which the gel is left at room temperature before it is raised to

reaction temperature.

This method proved to be very successful and led to the production of the novel zeolite, zeolite A (LTA)³⁴, and a synthetic analogue of the mineral faujasite (FAU), zeolite X.³⁵ Both of these zeolites have been found to have important commercial applications. The new method did not require expensive and specialized pressure vessels, hence its investigation was easier and preparation of zeolites by this method was financially more attractive.

Zeolites like A and X are of the "low" silica variety. Their framework is susceptible to attack by acids or steam which can remove the aluminium and cause the structure to collapse. Zeolites with a slightly higher Si/Al ratio were known to have greater stability when subjected to acid or steam (e.g. mordenite with Si/Al of about 5 can resist even severe acid and steam attacks) and this made it desirable to synthesize more siliceous materials. One of the first successes was the synthesis of the zeolite Y (FAU).³⁶ This has a Si/Al ratio of between 1.5 to 3.0 and is sufficiently stable for use as a cracking catalyst. Zeolite Y is now the most important of the commercial zeolite catalysts.

The introduction of tetramethylammonium (TMA) ions into reaction mixtures led to the production of even more siliceous zeolites. Silica rich forms of zeolite A (LTA) were prepared (N-A)³⁷ and ZK-4³⁸ along with several other zeolites including some with previously

unknown structures (e.g. zeolite EAB³⁹). The introduction of the organic cation is thought to produce a higher Si/Al ratio because of a combination of factors. The large cation will take up more space within the zeolite and prevent the use of several cation sites which would normally be used to balance the charge on an aluminium rich framework. It is also possible that the TMA ion influences the type of aluminosilicate ions which are produced in the gel.

Quaternary ammonium ions other than TMA have also proved to be useful and have resulted in a major advance in zeolite synthesis. Their use led to the discovery of a range of high silica zeolites with Si/Al ratios from about 10 to virtually infinity. Novel zeolites with totally different characteristics were produced. The first of these new zeolites to be synthesized was zeolite beta.⁴⁰ This was made with tetraethylammonium (TEA) cations and could be produced with Si/Al ratios up to 200. Other zeolites soon followed, and of these the most important was zeolite ZSM-5 (MFI).⁴¹ This was made with tetrapropylammonium (TPA) cations. The MFI framework structure can be prepared without the addition of aluminium to the reaction mixture and this pure silica molecular sieve was named silicalite.⁴² Other pure silica molecular sieves have been prepared⁴³ and most of these appear to have structures similar to those of high silica zeolites.

Further research has revealed that many organic ions and molecules can assist crystallization. A large number of different amines⁴⁴ have been successfully tried while alcohols,⁴⁵ ketones⁴⁶ and even organic sulphur compounds⁴⁷ appear to be useful. There may still be many more effective organic compounds to be discovered. The exact role of these organic species in the synthesis is still a matter of debate. In some cases, e.g. TPA in ZSM-5 formation, the organic molecule is believed to act as a template which directs the course of the crystallization, whereas in other cases, e.g. hexanediol in ZSM-5 formation, they act merely as void fillers.

1.5.2. Mechanism of crystallization.

The formation of zeolite crystals should obey the same general relationships as those which govern the appearance of any solid crystalline phase from solution. A new phase can only occur if the system is not at equilibrium. The variables in a system must be manipulated so that the chemical potential of the desired phase is lower than any of the other phases in the system. Material will then be transferred to this phase until equilibrium is achieved. A common way to move a system away from equilibrium is to create a supersaturated solution. This is a solution, at some given temperature, where the concentration, C , of the solute is higher than that of a saturated solution, concentration C_0 , where the solid and the liquid phases

are in equilibrium. The deviation from the equilibrium state is one of the main factors which controls crystallization and is often referred to as the degree of supersaturation ($S=C/C_0$).

In zeolite crystallization the most stable phase (i.e. the phase with the lowest chemical potential relative to the nutrient phase) may not be the phase which is produced. This is because there is also a kinetic factor to be considered. The solution may be supersaturated with respect to a number of different phases and it will be the phase which has the lowest barrier to nucleation which will appear first. Over a period of time, this may then transform to the most stable form. This type of behaviour is often found for substances which can exist in the form of several different polymorphs. They tend to produce the least stable phase first and then replace it with a more stable form until the most stable form is obtained (Ostwald's rule of successive transformations). This type of reaction scheme is quite common in zeolite synthesis.

In thermodynamic terms most zeolites are meta-stable species. Many, when left in their synthesis solutions, transform into more thermodynamically stable forms. For example, in high silica systems the original zeolite is often converted into crystalline forms of silica like α -quartz or α -cristobalite. In low silica systems sodalite or zeolite P (GIS) are often the result of

successive transformations, with perhaps faujasite as the original metastable product.⁴⁸ However, although a zeolite like faujasite may be thermodynamically less stable than zeolite P, it will remain stable if removed from the reaction medium. When separated from the synthesis solution there is a very large activation barrier which impedes the spontaneous transformation of the zeolite to another form. In effect there is no mechanistic pathway for the transformation to occur. This may be better understood by considering the non-zeolite case of carbon.

The phase diagram (figure 1.3)⁴⁹ appears to indicate that graphite can be converted to diamond at room temperature and relatively low pressures (about 15 kbar). However this ignores the kinetic factors which are involved. There is a considerable activation barrier which prevents the spontaneous transformation of graphite into diamond or vice-versa. Temperatures of about 3000K and pressures of about 125 kbar would be required to cause the transformation to proceed at a reasonable rate. The importance of kinetic factors is underlined even more by the fact that diamonds have been grown by the deposition from carbonaceous vapours onto diamond seeds at extremely low pressures (as low as 10^{-4} bar) and about 1323K.⁵⁰ This is obviously an area where diamond is thermodynamically unstable with respect to graphite. The atmosphere is supersaturated with respect to diamond but is even more supersaturated

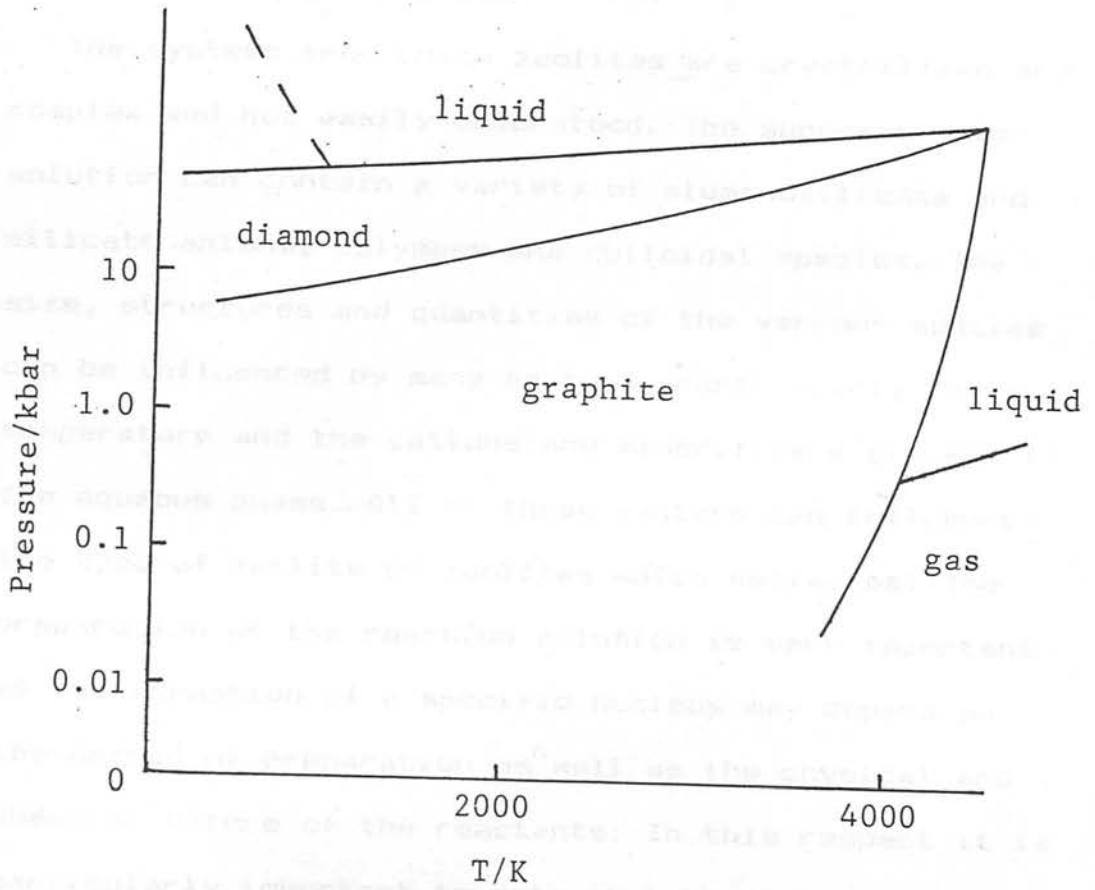


Figure 1.3 The phase diagram for carbon.

with respect to graphite. The presence of diamond seeds allows the diamond to grow, while graphite may also form but it has to nucleate first.

The systems from which zeolites are crystallized are complex and not easily understood. The supersaturated solution can contain a variety of aluminosilicate and silicate anions, polymers and colloidal species. The size, structures and quantities of the various species can be influenced by many factors, particularly the temperature and the cations and mineralizers present in the aqueous phase. All of these factors can influence the type of zeolite or zeolites which nucleates. The preparation of the reaction solution is very important as the formation of a specific nucleus may depend on the method of preparation as well as the physical and chemical nature of the reactants. In this respect it is particularly important to note that these reaction mixtures are heterogeneous and hence the order which the components are mixed may play a crucial role in the crystallization.

The importance of the solution phase of the initial gel has been recognized and various studies⁵¹ have been carried out on the reaction solution and its components at room temperature prior to hydrothermal crystallization. The main hope behind these studies appears to be that a knowledge of the components in solution will lead to a greater understanding of the crystallization process on a molecular scale. It would

appear that many researchers would like to identify the actual "building blocks" of the zeolite. Zeolites have very open and complex structures and are produced from solutions which contain a wide variety of anions of different shapes and sizes. It is a great temptation to examine the solutions in the hope that a specific anion can be identified as the "building block". Indeed some workers^{52,53} appear to be convinced that the "building block" is unlikely to be something as simple as monomer because the structures are so open and complex. Yet the "building blocks" are liable to be relatively simple as large complicated species would need to approach the crystal in the correct orientation and would require to form several bonds in the right sequence.

Thus the synthesis mixture should be prepared, in a manner which is reproducible, from components which are well characterized. The characteristics of the synthesis mixture are not only responsible for the type of nuclei obtained but also for the heat and mass transfer involved during crystal growth. The supersaturated solution must be prepared with care for any crystallization study but this is especially true for zeolite crystallization where there are even more factors involved than usual.

1.5.2.1. Reactants

Studies of aluminate solutions indicate that at high pH the dominant anion is the tetrahedral $\text{Al}(\text{OH})_4^-$ ⁵⁴. The concentration can vary according to pH but $\text{Al}(\text{OH})_4^-$

appears to be dominant in the pH range at which zeolites are formed. The aluminate solution may not be of such great importance in high silica zeolite synthesis since the aluminium is only present as a relatively minor component and in some cases it is not present at all. Silicate solutions appear to be of more interest as they can contain a wide range of anions of various shapes and sizes.

Several methods have been developed for the examination of silicate solutions. The main methods used are ^{29}Si nmr, $^{51}\text{(b)}$,⁵⁵ trimethylsilylation⁵⁶ and, to a lesser extent, reaction with acid molybdate solution.⁵⁷ The molybdate method relies upon the fact that only monomer can react to give yellow molybdosilicic acid. When the monomer is removed the larger polymers depolymerise to form monomer and this can then react with the molybdate ion. This process can continue until all of the silica has reacted. The rate of depolymerisation should be characteristic of the polymer and should be reflected in the rate of increase in intensity of the yellow molybdosilicic acid.⁵⁸ If several different polymer species are present, and depolymerise simultaneously, the results are inevitably difficult to interpret and can only be used to give a qualitative view of the species present.

Trimethylsilylation involves the conversion of silicate anions into volatile, hydrocarbon-soluble derivatives by reaction with trimethylsilyl chloride or

a mixture of the corresponding ether and hydrochloric acid. The trimethylsilyl derivatives can then be extracted into an organic solvent and the lower molecular weight products identified by gas chromatography. If the trimethylsilyl derivative is formed rapidly it will characterize the parent anion unless further reaction or rearrangement took place before the reaction was completed.^{56(b)} This method can give a relatively reliable measure of the distribution of the lower molecular weight anions.

²⁹Si nuclear magnetic resonance spectroscopy has probably been the most successful method of determining the structure of silicate anions in solution. Different chemical shifts are obtained for ²⁹Si atoms in different positions in the silicate anion structures.⁵⁵ Thus chain groups, end groups and so forth can be identified and the anionic structure deduced. High resolution ²⁹Si nmr studies have shown that anions may be positively identified provided they consist of only a few Si atoms. The effect of various parameters on the anion distribution has been investigated.⁵⁹ The extension of the technique to the examination of aluminosilicate solutions could prove to be very useful.

One limitation of the ²⁹Si nmr technique is that with the present equipment it can only be used to examine solutions at moderate temperatures. It would be experimentally difficult to follow an actual

crystallization using ^{29}Si nmr, not only because of the relatively high temperatures required but also because rapid changes in the anion distribution may not be observed as long acquisition times are required to obtain spectra with a reasonable signal to noise ratio. It is known that temperature can change the distribution of anions, and that ions present at room temperature may not be present at higher temperatures. Casci^{59(b)} found that single four rings (see "4" in figure 1.2), which are present at room temperature in TMA silicate solutions, break down and disappear at 333K. It is important to recognize that such changes can take place. The introduction of alkali metal cations into organic silicate solutions often has a similar effect. Casci^{59(b)} found that the addition of sodium ions to aqueous silicate solutions containing hexamethonium cations resulted in the rapid loss of certain silicate anions. It appears that the equilibria involved between the various anions is easily shifted. The only way to be certain which anions are present during a synthesis is to examine the solutions under synthesis conditions.

1.5.2.2. Nucleation

A new phase will not appear just because the solution is supersaturated. There must first occur in the solution a number of small bodies which act as centres of crystallization. These small bodies are called nuclei and are particles which contain the minimum

amount of the new phases to allow them to remain stable and lead an independent existence. There are a number of factors which are found to affect nucleation of crystals other than zeolites and these factors are liable to also operate in zeolite crystallization.

There are two types of nucleation which are generally recognized; homogeneous and heterogeneous. Homogeneous nucleation is where the new phase occurs spontaneously whereas heterogeneous nucleation is where the new phase is artificially induced by, for example, impurities or a "sympathetic" surface. The actual mechanism of nucleation is unknown although it probably involves the initial reaction of a pair of molecules, then the addition of other molecules to the original pair until chains or layers are formed and eventually the lattice structure evolves.⁶⁰ Many of these structures will dissolve as they are extremely unstable, but some may achieve a critical size, become stable, then continue to grow. The reason that the nucleus requires to achieve a critical size becomes clear when the free energy changes associated with the formation of a new phase are considered. The relationship between the free energy due to the formation of a nucleus (ΔG) and the nucleus size (r) is shown in figure 1.4. The free energy, ΔG_s , which is due to the formation of a boundary between phases, is a positive quantity and proportional to r^2 . The free energy, ΔG_v , which is due to the appearance of the new

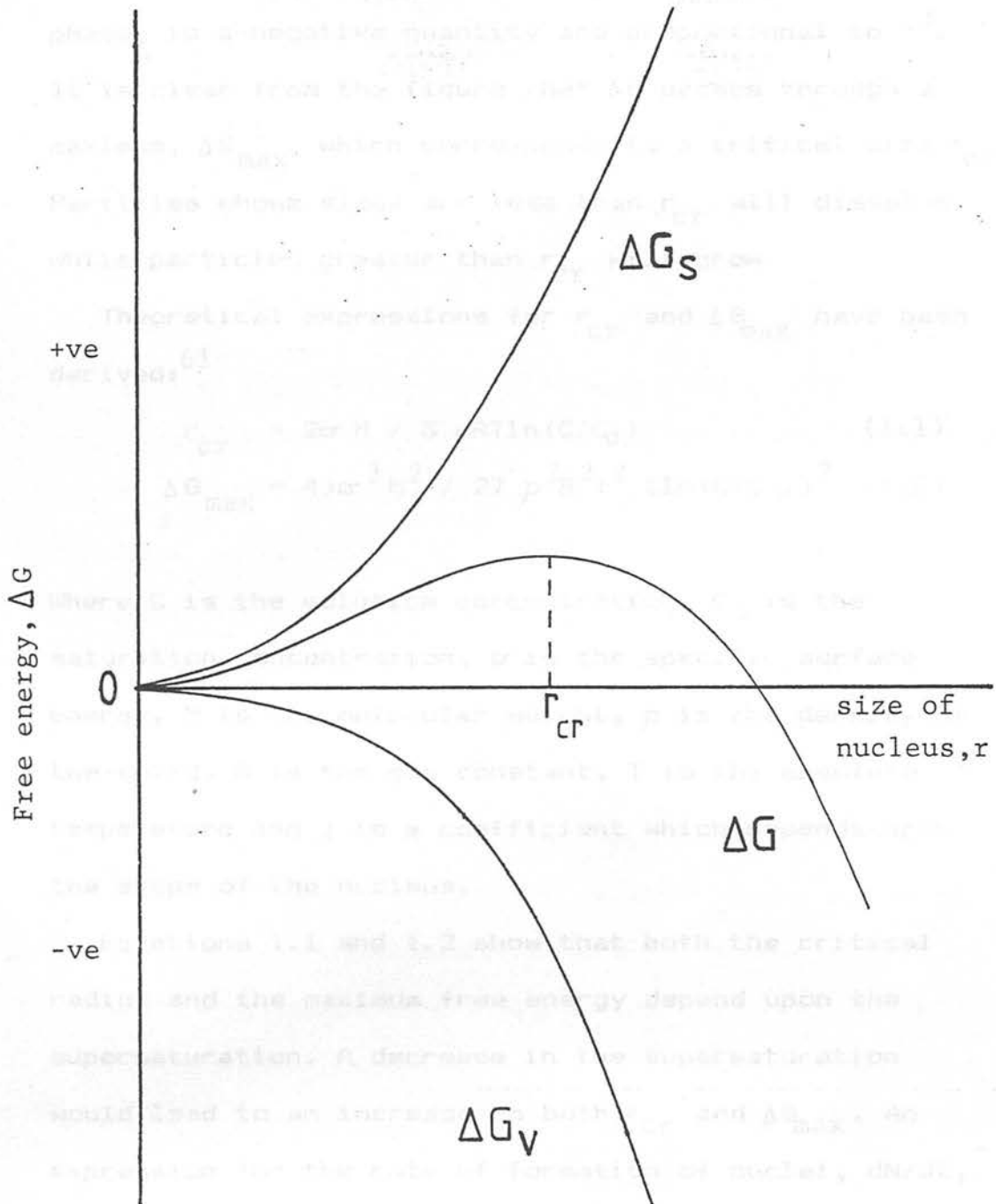


Figure 1.4 Dependence of the change in the free energy due to the formation of a nucleus (ΔG) on the size of a nucleus (r).

phase, is a negative quantity and proportional to r^3 . It is clear from the figure that ΔG passes through a maximum, ΔG_{\max} , which corresponds to a critical size r_{cr} . Particles whose sizes are less than r_{cr} will dissolve, while particles greater than r_{cr} will grow.

Theoretical expressions for r_{cr} and ΔG_{\max} have been derived:⁶¹

$$r_{\text{cr}} = 2\sigma M / 3 \rho R T \ln(C/C_0) \quad (1.1)$$

$$\Delta G_{\max} = 4j\sigma^3 M^2 / 27 \rho^2 R^2 T^2 [\ln(C/C_0)]^2 \quad (1.2)$$

Where C is the solution concentration, C_0 is the saturation concentration, σ is the specific surface energy, M is the molecular weight, ρ is the density of the solid, R is the gas constant, T is the absolute temperature and j is a coefficient which depends upon the shape of the nucleus.

Equations 1.1 and 1.2 show that both the critical radius and the maximum free energy depend upon the supersaturation. A decrease in the supersaturation would lead to an increase in both r_{cr} and ΔG_{\max} . An expression for the rate of formation of nuclei, dN/dt , can also be obtained:

$$dN/dt = A \exp(-j\sigma^3 M^2 / R^3 T^3 \rho^2 [\ln(C/C_0)]^2) \quad (1.3)$$

where A is a constant.

Equation 1.3 indicates that there is a strong dependence of rate of formation of nuclei on the degree of supersaturation. The rate is also dependent upon the temperature and the surface energy. At low degrees of

supersaturation the formation of nuclei will be almost impossible. An increase in the supersaturation and the temperature and a decrease in the surface energy would all lead to an increase in rate. The equation also predicts that the rate should continue to increase as the supersaturation increases, but experiments have found that the rate actually begins to fall again at high supersaturations.⁶² This probably occurs because the increase in supersaturation also results in an increase in viscosity which impedes the formation of the new phase. There will be an optimum saturation level at which the rate is at a maximum. For real systems equation 1.3 should contain a term which allows for viscosity.

Very little systematic work has been carried out on nucleation in zeolite systems. However there are some indications that nucleation depends upon the extent of supersaturation and the temperature. For example, an increase in the amount of base in a zeolite reaction mixture should increase the amount of dissolved silica in the solution. Consequently, the supersaturation can be increased by the addition of alkali metal hydroxides. Curves of crystal yield against time for mordenite (figure 1.5)⁶³ show that the period until crystal growth becomes measurable (the induction time) decreases with increase in alkalinity. The induction time must depend upon the nucleation kinetics and also the growth rate as both these processes must take place

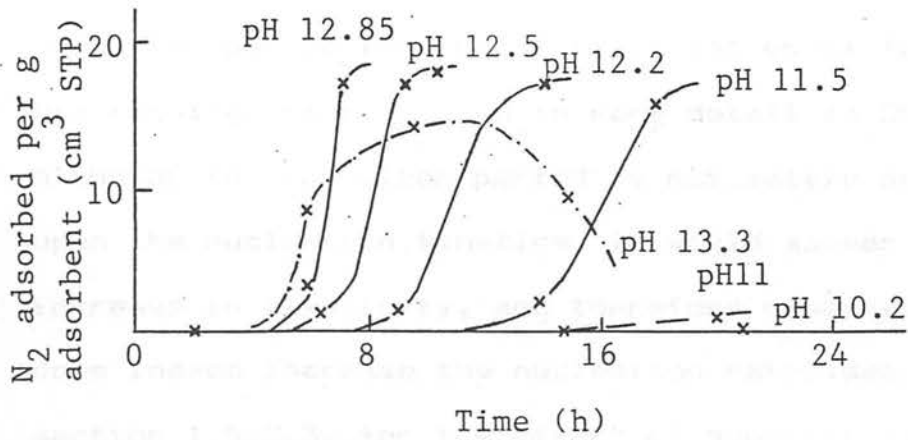


Figure 1.5 Influence of pH on the crystallization rate of mordenite at 573K from amorphous compound.

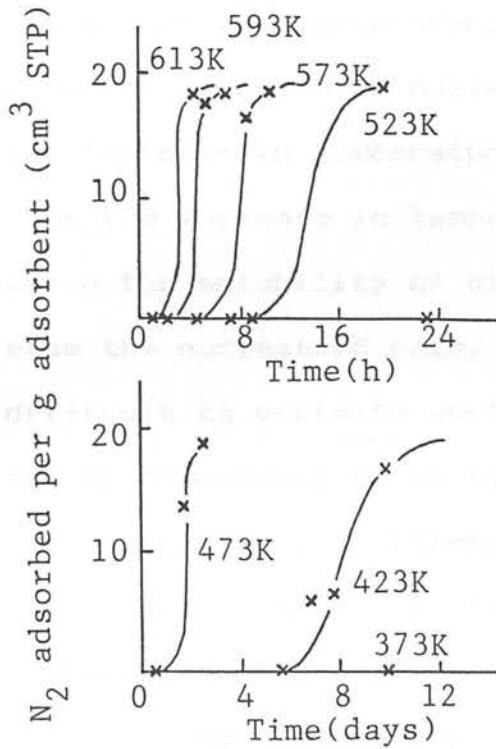


Figure 1.6 Influence of temperature on the crystallization rate of mordenite from amorphous compound.

during the induction period. Zhdanov⁶⁴ has demonstrated that both nucleation and growth take place during the induction period for the crystallization of faujasite. His results are discussed in more detail in Chapter 5. Although the induction period is not solely dependent upon the nucleation kinetics, it would appear that the increase in alkalinity, and therefore supersaturation, does indeed increase the nucleation rate (see also section 1.5.2.3. for the effect of supersaturation on growth).

A similar effect is observed when the temperature is increased. Figure 1.6 indicates that the induction times decrease when the temperature is raised.⁶³ This may be due to the increase in nucleation rate brought about by the increase in temperature. However it should be noted that the increase in temperature will lead to an increase in the solubility of silica and thus would also increase the nucleation rate.

It is difficult to estimate whether a solution crystallizes spontaneously or is aided by the presence of soluble or insoluble impurities. It is certainly difficult to obtain a completely clean solution in zeolite synthesis. Silicate solutions can contain large colloidal and amorphous silica species. The synthesis mixture, from which zeolites are formed, often separates into a solid, amorphous gel phase and a solution phase. The presence of solid particles or solid surfaces can lower the free energy necessary for

the formation of a new phase, especially if there is an affinity between the surface and the phase. There is almost certainly a degree of affinity between the zeolites and the amorphous silicate and aluminosilicate particles which are present in the synthesis mixture. Heterogeneous nucleation is liable to be a very important factor in zeolite synthesis.

The mechanism by which the growth of crystals is initiated by other particles may take different forms, but it is likely that molecules are adsorbed onto the amorphous particles and "held" so that other molecules have a greater chance of reaction with the adsorbed molecules without the potential nucleus dissolving. Complete affinity between the new crystalline phase and the "foreign" particles is found when the two solids are identical or almost identical in composition and structure. This would correspond to "seeding" the solution with crystals of the same material as is to be grown. The addition of seed crystals may not just result in the nucleation of crystals on the surface of the seeds or the growth of the seed. This may not be spontaneous nucleation but the result of the separation of fine particles from the seed when it is introduced into the solution.

Nucleation may also be induced by mechanical means. A stirrer may produce additional foreign particles by abrasion of the stirrer and the reaction vessel surfaces. Stirring will also accelerate the rate of

diffusion of material to the potential nucleus. There does not seem to be a general relationship between stirring speed and nucleation rate, although an increase in the stirring rate also increases the rate of nucleation.⁶⁵ If diffusion had been the only limiting factor then a relatively simple relationship between the nucleation rate and stirring rate should be observed, but this is not normally so. The rate of stirring has been found to influence the induction period in zeolite crystallization. Casci^{59(b)} found that an increase in the rate of stirring resulted in a shorter induction time, although little difference in the induction period was found when the stirring rate exceeded 300 r.p.m.

A third method of nucleation may exist in zeolite crystallization. Zhdanov^{64(a)} has proposed that the amorphous aluminosilicate gels may not be truly amorphous but contain ordered structures which can act as nuclei when released into the solution. This suggestion, termed autocatalytic nucleation, was proposed because studies of zeolite crystallization indicate that the rate of formation of the zeolite increases as the reaction proceeds.^{64(a),66} If the gel contains potential nuclei it will release them when it dissolves. The new nuclei will grow and cause more gel to dissolve and produce more nuclei. Thus the rate of nucleation should increase.

Several expressions have been proposed for

nucleation rates in different situations in zeolite crystallization.⁶⁷⁻⁶⁹

These include:

$$dN/dt = k \quad \text{Constant rate of nucleation (expected for homogeneous nucleation)} \quad (1.4)^{67}$$

$$dN/dt = A \exp(-kt) \quad \text{Exponential decay (expected for nucleation from impurities)} \quad (1.5)^{67}$$

$$dN/dt = A t^n \quad \text{Power law} \quad (1.6)^{68}$$

$$dN/dt = A (\exp(Et)-1) \quad \text{Exponential increase} \quad (1.7)^{68}$$

$$dN/dt = A t^n \exp(-t^p) \quad \text{Rate which exhibits a maxima} \quad (1.8)^{69}$$

A, E, k, n and p are constants. N is the number of nuclei at time t.

These equations, when taken individually, are only likely to describe part of the nucleation process in zeolite crystallization. Homogeneous nucleation (equation 1.4) may take place but it is unlikely that it is the only or the main process which operates. Subotic and Graovac⁶⁷ considered that a general equation for crystallization should include terms for homogeneous, heterogeneous and autocatalytic nucleation. This would involve a combination of equations 1.4, 1.5 and an equation for autocatalytic nucleation. Equations like 1.6 or 1.7 which give an increasing rate of nucleation are of the form expected for an autocatalytic process. The sum of these various

processes produces a complicated equation like equation 1.9.

$$dN/dt = k_1 + A_1 \exp(-k_2 t) + A_2 t^n \quad (1.9)$$

Work by Zhdanov⁶⁴ has indicated that the rate of nucleation, for the crystallization of faujasite and also for zeolite A, increases to a maximum and then decreases. Equation 1.9 does not predict a maximum but will lead to an ever increasing rate as the last term becomes dominant as t increases. The only equation which predicts a maximum is equation 1.8. This combines the power law for nucleation with exponential decay. Barrer postulated⁶⁹ that the rate would have to eventually decrease as the precursor species would have to compete with the growing crystals for the available nutrient. Although equation 1.8 predicts a maximum rate it is unlikely to be a full description of the nucleation rate. It may in fact be a better description of the autocatalytic nucleation process. The dissolution of the gel will release "active sites" into the solution at an increasing rate. If the "active sites" are not true nuclei they may still require time to stabilise and have quite a high solubility. As the reaction proceeds the number of crystals and nuclei produced will increase rapidly so that the demand for nutrient will also increase rapidly. Some of the "active sites" may be unable to stabilise and in fact will dissolve to supply the growing crystals. The removal of these would be described by a decreasing

function. The whole process could perhaps be described by equation 1.8. The complete equation for nucleation would then have the form:

$$\frac{dN}{dt} = k_1 + A_1 \exp(-k_2 t) + A_2 t^n \exp(-t^p) \quad (1.10)$$

This equation can exhibit a maximum and includes terms for homogeneous, heterogeneous and autocatalytic nucleation.

Many workers in zeolite chemistry seem to have limited any investigation of nucleation to a simple description of the induction time even though the work of Zhdanov⁶⁴ has indicated that the induction period is affected by both nucleation and growth. If the nucleation rate bears even a slight resemblance to the situation described by equation 1.10 then a study of nucleation requires much more than a simple examination of induction times. The whole crystallization process must be examined more intimately.

1.5.2.3. Growth.

Once nuclei have formed they begin to grow and become crystals of visible size. The growth of crystals is governed by two main processes:

- (a) the rate of diffusion of material to the growing surfaces and
- (b) the rate of incorporation of material into the surface.

Process (b) may involve several different steps, e.g. adsorption onto the surface, migration on the surface, followed by final surface reaction. In the case of

zeolites the surface reaction must involve the formation of covalent bonds with the elimination of water or hydroxide. The ions involved must also lose their solvation shells in the process. These processes are liable to require more energy than, for example, the growth of an ionic salt, so the growth is liable to be slower than that of say sodium chloride. This is normally the situation when crystals are obtained by chemical reaction.⁷⁰

The rate of crystal growth depends upon which of the above processes, if any, is dominant. Most of the factors which affect nucleation also affect crystal growth through their influence on the above processes. The growth rate is strongly influenced by the extent of supersaturation. As the supersaturation is increased the concentration of nutrient is increased and the rate of growth is increased.⁷¹ The increased concentration of nutrient leads to a faster growth rate because there are more zeolite "building blocks" available in the solution and hence there will be faster transport of these "blocks" to the surfaces of the growing crystals, a higher concentration of "blocks" at the crystal surface and a faster surface reaction to build up the crystal. The extent of supersaturation can influence which step in the growth process is the most important. At low supersaturations the rate of diffusion is important while at high supersaturations the rate of the surface reaction has increased influence. Diffusion

becomes less important when the solution is stirred. The growth rate will increase with increase in stirring speed, until a constant rate is achieved.⁷² The increase in relative velocity between the crystal and the solution should decrease the concentration gradient between the the crystal and the solution so that the reaction is only influenced by the rate of the surface reaction.

Supersaturation is normally the factor which influences the growth rate most strongly. Supersaturation is the driving force for a reaction. In the discussion of nucleation (section 1.5.2.2) it was shown that an increase in alkalinity, and therefore supersaturation, led to shorter induction times (figure 1.5).⁶³ The slope of the growth curves for mordenite also become steeper as the alkalinity is increased. The crystallization curve is influenced by both the nucleation rate and the crystal growth rate. It seems likely that the changes to the crystallization curve brought about by the addition of alkali are caused by changes in both the nucleation and the growth rates. An increase in supersaturation leads to an increase in the rates of both nucleation and growth.

There are several other factors which influence the growth rate. The diffusion process is affected not only by agitation but also by the viscosity of the solution and the temperature. An increase in the viscosity will restrict the mobility of the solute molecules and

decrease the diffusion rate. In a similar manner, a decrease in the temperature will lead to a decrease in the rate of diffusion.

The surface reaction is influenced by impurities and by temperature. Impurities may be adsorbed onto certain faces of the crystal and change the rate of growth of these faces. Dyestuffs are known to produce effects of this nature.⁷³ The temperature should also affect the surface reaction⁷⁴ as there will be an activation barrier to be surmounted when the bonds are being formed. An increase in the temperature should help increase the rate of the surface reaction.

The effect of temperature can be seen in figure 1.6.⁶³ Just as an increase in alkalinity shortens the induction time and makes the crystallization curve steeper, an increase in temperature has a similar effect. It would appear that temperature also affects both the growth and nucleation rates.

The growth rate of a crystal can be obtained by the measurement of the rate of displacement of a crystal face from the crystal centre. Crystal faces do not all grow at the same rate and in fact the slowest growing faces can disappear. There appear to have been only a few studies on the linear growth rates of zeolite crystals.^{64,75} One of these⁷⁵ involved the introduction of seed crystals of faujasite into a solution whose composition was known to normally only nucleate zeolite F but which could supply nutrient to the seed crystals

of faujasite. It was reasoned that only the seed crystals would grow and therefore reflect the kinetics of faujasite growth. The linear growth rates could be obtained from percentage crystallinity versus time plots if several assumptions were made. These included:

(i) The increase in volume, V , of the crystals is proportional to the free surface area, S , of the seeds such that:

$$dV/dt = k S(x) \quad (1.11)$$

where x is the fraction of formula units of faujasite present at time t . k is the rate constant.

(ii) The number of crystals of faujasite remain equal to the number of seeds added, with the linear growth rate independent of crystal size. Thus the expression

$$dx/dt = 3 k x^{2/3} x_0^{1/3} \bar{r}_0^{-1} \quad (1.12)$$

can be obtained, where x_0 is the number of formula units of seeds added and \bar{r}_0 is the average radius of the seeds. Integration of equation 1.12 yields the expressions:

$$k = [(x/x_0)^{1/3} - 1] \bar{r}_0 / t \quad (1.13)$$

and

$$x = x_0 (1 + k t / \bar{r}_0)^3 \quad (1.14)$$

Equation 1.13 can be used to obtain values of k which will have the dimensions of length/time. The validity of the equations can be checked by using equation 1.14 to generate the crystallization curve. It was found that it gave a good fit to the experimental

results and thus it appeared that the model gives a good description of the crystallization. However at high values of x the theoretical values deviate from the experimental observations. This is because it was assumed that k would remain constant through the whole reaction. Zhdanov⁶⁴ has shown that this is not the case and that the growth rate falls off near the end of the reaction when the amount of nutrient is almost completely finished. Zhdanov measured linear growth rates directly by making measurements on the largest crystals in a reaction mixture at various times throughout the crystallization. He found that the sizes increased linearly with time until near the end of the reaction, when there was a gradual decline in growth rate. Zhdanov's work is discussed in more detail in Chapter 5.

Growth rates obtained using equation 1.13 were found to be dependent upon the Si/Al ratio of the product crystals and also appeared to be proportional to the concentration of silicate (expressed as $(\text{SiO}_2)_{\text{sol}}$) in the mother liquor. Table 1.3^{75(a)} shows that samples with less excess alkalinity (Na-Al) have smaller amounts of dissolved silica and smaller linear growth rates. This would be expected if the growth rate depends upon the supersaturation. The concentration of aluminium in solution should also be important in this system. Since the Si/Al ratio of the product increases when the excess alkalinity is decreased, the reduction

Table 1.3 Linear growth rates, k , for faujasite grown from batches with different excess alkalinity $(\text{Na-Al})^a$.

$\text{SiO}_2 / \text{Al}_2\text{O}_3$	$(\text{Na-Al}) / \text{SiO}_2$	$\text{H}_2\text{O} / \text{Al}_2\text{O}_3$	$(\text{SiO}_2)_{\text{sol}} (\text{M})$	$10^3 k$ ($\mu\text{m h}^{-1}$)	Si/Al of product
2.5	2.5	200	0.515	200	1.39
2.5	2.0	200	0.500	145	1.50
2.5	1.5	200	0.477	90	1.65
2.5	1.0	200	0.435	49	1.95
2.5	0.78	200	0.400	28	2.20
2.5	0.78	200	0.400	22	2.20
2.5	0.78	200	0.396	25	2.22

a Compositions are mole ratios

in aluminium content may also be responsible for the smaller growth rate.

1.5.2.4. Crystallization kinetics

The various stages in the crystallization (formation of a supersaturated solution, nucleation and growth) all affect the kinetics of the process as a whole. Each of these stages is governed by various factors so that the kinetics of the whole process must be a function of many variables. The degree of supersaturation is the main factor which governs the kinetics but temperature, stirring speed, composition, concentration and types of impurities etc. also influence the kinetics of the process. The process is so complex that it is unlikely that it could be adequately described by a single equation which would be of practical use. Normally, the process is broken down into various stages which are studied separately.⁷⁶

Although there have been many studies of zeolite crystallization kinetics, they have almost always been limited to the determination of crystal yield as a function of time. Such measurements produce a growth curve which is normally S-shaped. The induction period is the period during which the crystals grow to a size and in such quantities that they can be detected by X-ray powder diffraction of the predominantly amorphous solid phase. The induction period is followed by the crystallization stage where the crystals continue to grow and nucleation may also continue. It should be

noted that the induction period is not the period of time until nucleation takes place. It has been frequently implied that no nucleation occurs until crystals can be detected in the solid phase, and consequently the induction period can be used to give some information about nucleation, e.g. activation energies for nucleation.⁷⁷ Work in the crystallization of non-zeolite materials has shown that this period is simply the time required for a sufficient number of crystals to grow to a size which can be detected.⁷⁶ Zhdanov^{64(a)} recognized that this was also true for zeolites but some workers still like to associate the induction period solely with the time taken for nucleation.

Although the crystallization process for zeolites is obviously very complex there have been several attempts to describe the crystallization curve mathematically.^{64,67,68,78}

Equations which have been proposed include:

$$Z_t/Z_f = k_1 t^a \quad (1.15)^{64(a)}$$

$$Z_t/Z_f = 1 - \exp(-k_1 t^a) \quad (1.16)^{64(b),78}$$

$$Z_t/Z_f = k_1 t^3 + k_2 t^4 + k_3 t^{(a+3)} \quad (1.17)^{67}$$

$$Z_t/Z_f = 4Ak_1^3 \left[6(\exp(Et)-1)/E^3 - 6t/E^2 - 3t^2/E - t^3 - t^4 / 4! / 3E \right] \quad (1.18)^{68}$$

where Z_t is the mass of crystals at time t and Z_f is the final mass of crystals. k_1 , k_2 , k_3 , a , A and E are constants. The constant a in equations 1.15 and 1.16 is meant to indicate the type of nucleation which is taking place. Values less than 4 indicate a decreasing

rate of nucleation while values greater than 4 should represent an increasing rate.

All of these equations assume a linear growth rate, i.e. the growth is proportional to time, and combine an expression for this with an expression for the nucleation rate. Consequently any problems found with the nucleation rate equation will probably be magnified in the crystal mass growth equation. For example, equation 1.15 is not really an adequate representation of the crystallization curve. The value of Z_t/Z_f deviates from the experimental observations near the end of crystallization because there is no allowance made for the exhaustion of nutrient. The equation cannot reveal any detailed information about the nucleation stage and is really far too simplistic. Equation 1.17 also suffers from the failure to include an allowance for exhaustion of nutrient. Nucleation and growth appear to continue for ever and are not affected by the change in nutrient conditions at the end of a reaction. Both equation 1.15 and equation 1.17 allow Z_t/Z_f to become greater than 1 and continue to increase unless the points generated by the equations are actually halted at $Z_t/Z_f = 1$. An allowance has at least been made in equation 1.17 for different types of nucleation where $k_1 t^3$ represents the contribution from heterogeneous nucleation, $k_2 t^4$ represents the contribution from homogeneous nucleation, and $k_3 t^{(a+3)}$ represents the contribution from autocatalytic

nucleation.

Equation 1.16 overcomes the problem of the continuous increase in Z_t/Z_f . The equation is based upon a linear growth rate and random nucleation. It makes an allowance for the exhaustion of nutrient and is found in many cases to be a good representation of the experimental S-shaped crystallization curves.^{64(b)} Barrer⁷⁹ has shown that it cannot be used in certain cases. Also it does not give any quantitative information about the nucleation or the growth rates except to predict whether the nucleation rate increases, decreases or remains constant.

Equation 1.18 is based upon a constant linear growth rate and an exponential increase in nucleation rate (see equation 1.7). The parameter k_1 represents the linear growth rate which is assumed to be constant until the end of the reaction. This is unlikely and it will probably gradually decrease near the end of the reaction as shown by Zhdanov.⁶⁴ The nucleation rate expression is also unlikely to be a true representation of the actual nucleation rate. Equation 1.18 is possibly more applicable to the initial stages of the crystallization than the final ones. The same model can be used to predict the crystallite size distribution by means of equation 1.19

$$d(Z_t/Z_f) = 4 A r^3 (\exp[E(t_e - r/k)] - 1/3k) dr \quad (1.19)$$

in which r is the radius of the crystals and t_e is the time when $Z_t/Z_f = 1$, i.e. the completion of



crystallization.

Size distributions calculated by this equation deviate slightly from the experimental results because of the inadequacies of equation 1.18.

The determination of particle size distribution can play a very important part in the study of crystallization kinetics. The distribution depends upon the crystallization conditions and can reveal information about the way crystals are formed. The final distribution is a result of the crystal growth rate and the nucleation rate. If a value can be obtained for the linear growth rate then it should be possible to obtain information on the nucleation rate using the particle size distribution. This is information which cannot be obtained from the crystallization curve directly. The nucleation part of crystallization can then be examined. Zhdanov⁶⁴ has shown that it is possible to obtain information about the nucleation rate by using the final particle size distribution combined with linear growth rate information. Zhdanov argued that if all the crystals in a system grow with the same rate then the final particle size distribution reflects the nucleation rate, e.g. the largest crystal to be produced must have nucleated first while the smallest crystal must have been the last to nucleate. If the crystal growth rate is known and it is the same for all the crystals then it is possible to give an approximate time of

nucleation for each crystal size. Thus in principle it should be possible to determine the nucleation kinetics. Zhdanov's method is discussed more fully in Chapter 5.

Some workers have felt that the induction period is governed mainly by the rate of nucleation while the growth rate governs the rest of the crystallization curve. Consequently attempts have been made to obtain "activation energies" for nucleation and crystallization by measuring induction periods and crystallization times at different temperatures. Table 1.4 lists some of the values obtained for zeolite ZSM-5 with various Si/Al ratios. It is obvious that the activation energy values obtained vary widely and in some cases the activation energy obtained by one group is completely different to that of another group, even though the Si/Al ratios are similar. It would also appear that in some cases the activation energy for nucleation is larger than that for crystallization yet in other cases it is very much smaller. This method of obtaining activation energies is not really valid.

Zhdanov⁶⁴ has shown that during the induction period the rate of nucleation increases rapidly and is also accompanied by crystal growth. Thus both nucleation and growth are taking place in the induction period and the crystal mass growth period, and it does not seem that either nucleation or growth dominates either period.

A more satisfactory method of obtaining activation

Table 1.4. Apparent activation energies for nucleation (E_n) and crystallization (E_c) of zeolite ZSM-5 (MFI)

$\text{SiO}_2/\text{Al}_2\text{O}_3$	Main Cations	E_n /kJmol ⁻¹	E_c /kJmol ⁻¹	Reference
28	TPA,Na	107.0	81.2	77(a)
	TPA	38	46	77(b)
70	TPA,Na	25	29	77(b)
	TPA,Na	20	42	80
90	TPA,Li	31.4	94.1	81
90	TPA,K	62.8	98.3	81
90	TPA,Na	35.6	83.7	81
70	TPA,Na	134	-	81
86	TEPA,Na	270.4	206.8	82
800	TEPA,Na	249.5	276.3	82
86	TPA,Na	199.5	238.6	82
59	TPA,NH	40.7	66.5	83

Note: TPA = tetrapropylammonium

TEPA = triethyl-n-propylammonium

energies is the method of Kacirek and Lechert.⁷⁵ They introduced seed crystals of faujasite into each batch with a composition from which only zeolite P had been found to nucleate. The growth of the seeds reflected the kinetics of the faujasite growth since no other faujasite was expected to nucleate. It is possible to obtain crystal growth rates (see section 1.5.2.3) at different temperatures using this method. An activation energy for growth can be calculated. Determination of activation energy for nucleation would not be possible with this method as no faujasite crystals can nucleate in the chosen composition. Zhdanov⁶⁴ was also able to calculate activation energies for growth by measuring the linear growth rates of crystals at different temperatures (see Chapter 5).

Care should be taken even when interpreting the activation energies obtained by the above methods. Both nucleation and growth rates depend upon the degree of supersaturation. An increase or decrease in temperature may affect the solubility of the zeolite "building units" and cause a different growth rate partly because of the different supersaturation.

The activation energies which have been obtained for zeolite growth all tend to be quite high. If the reaction was controlled by diffusion of chemical nutrient to the crystal surface then values of ca. 20 kJmol^{-1} would be expected. Also, stirred reactions should show a marked difference to static reactions. It

would therefore seem likely that the activation energies obtained are for the surface reaction where the aluminosilicate units add to the growing surface with covalent bonds breaking and forming and molecules of water or hydroxide ions being removed.

1.5.2.5. Role of cations

Amongst the different factors that can affect a zeolite crystallization, one of particular interest is the role played by the cation in determining the zeolite structure formed. It is well known that faujasite zeolites form more easily from mixtures which contain sodium ions while zeolite L requires potassium ions. It has been suggested^{13,85} that the alkali metal ions help to stabilize particular structures e.g. it has been proposed that the hydrated sodium ion is responsible for the formation of the double four ring (4-4 in figure 1.2), the double six ring (6-6 in figure 1.2) and other even larger, structural subunits (such as the sodalite cage).¹³ Indeed, it has been suggested that the sodium ion or the hydrated sodium ion forms the "nucleus" of these structural subunits. The reported absence⁸⁶ of sodium ions from the centre of the sodalite cage, suggests that the simple "nucleus" idea may be too simple. However there are certainly many zeolites which exhibit a close relationship with certain cations such that it appears that the cation has a structure-directing function. This structure-directing effect has been termed templating.

The mechanism of the templating is not really clear. Whilst it is possible that a "nucleus" type of mechanism could account for the ability of a given cation to produce a particular zeolite in preference to others, it should be noted that other factors may be at work. For example different cations can produce synthesis gels with totally different physical characteristics. The cations may affect the nucleation process and consequently influence the type of zeolite formed in that way rather than by acting as "nuclei" for certain structural subunits. Perhaps both conjectures are partly correct. There are certainly many zeolites, such as mordenite, analcime and others, which only contain single rings and consequently their formation cannot be explained by a cation structure-directing model as above.^{84(a)}

Zeolite synthesis with organic cations has produced further support for the "nucleus" idea. The tetramethylammonium (TMA) ion is trapped within the cages of sodalite⁸⁷ and zeolite omega³⁹ and it appears that these structures are formed around the TMA ions. Templating here can perhaps be explained by the way in which the cation fits neatly into the sodalite and gmelinite cages respectively. The tetrapropylammonium (TPA) ion is found to occupy most of the channel intersections in zeolite ZSM-5.^{42,88} Again it fits neatly into the zeolite structure and occupies almost all the void space. It has been proposed⁸⁸ that the TPA

ions order the SiO_2 and AlO_2^- units into a framework in the same way that organic molecules stabilize water clathrates.

While this "clathration" mechanism of templating is attractive, it cannot satisfactorily explain how many other organic molecules, e.g. unsymmetrical organics^{82,89} or even neutral molecules,^{45,46} aid the crystallization of certain zeolites. While there is no doubt that the TPA ion is a good fit inside ZSM-5, there are many other organic molecules which have been used to produce ZSM-5, e.g. ethanolamine,⁹⁰ pentaerythritol,^{45(b)} hexanediol,⁹¹ propylamine,⁹² etc. Some of the molecules used do not even become trapped within the zeolite but are free to move about and can in fact even be washed out of the zeolite channels. It may be that the organic component simply helps to stabilize a particular zeolite by filling the channels. In such cases it seems unlikely that the organic species has any structure-directing ability, and in such cases the formation of specific zeolites must depend on other factors, for example interaction between alkali metal cations and aluminosilicate material.

Organic molecules can also affect the aluminosilicate starting solution.⁹³ Some organics, e.g. catechol, can form a complex with silica and thereby increase its solubility, while others, e.g. amines, can raise the pH of the solution and produce a similar effect. Some polymers can retard dissolution of

silica because they are adsorbed onto the surface of colloidal silica particles. The formation of organosilicate and organoaluminosilicate species has also been observed and there has been some speculation as to whether any of the species found could contribute to the growth of a zeolite (perhaps as "building units").

There is no doubt that cations certainly play an important part in determining which zeolite structure will form from a particular reaction mixture. It is not known whether they do this through their influence on the distribution of silicate and aluminosilicate anions in the gel through acting as "nuclei" for particular structural subunits, or via some other mechanism. However the cation is only one of several factors which influence the formation of a particular zeolite structure. The gel composition, pH, temperature, starting materials etc. also play a major role.

1.6. Objectives

The aim of the work described in the chapters which follow was to develop new procedures, more suitable for the scientific investigation of zeolite crystallization than those previously used. It was hoped that these new procedures would also reveal how large zeolite crystals could be produced. Large crystals are needed for single crystal X-ray diffraction, and basic studies in zeolite catalysis. In the latter case the use of large crystals reduces the contribution from crystal surface

reactions.

Synthetic zeolites are usually crystallized from aluminosilicate gels which are prepared by the vigorous mixing of aqueous solutions of soluble silicates and aluminates, or their precursors. This method is quite good for the preparation of a large batch of zeolite but does not lend itself to the investigation of the mechanism of zeolite crystallization. The reaction mixture normally consists of an amorphous gel phase and an aqueous phase. The composition and properties of these phases can depend on many factors including the extent of the initial mixing. It is difficult to prepare the solutions reproducibly. In order to avoid some of these problems it was decided to investigate an alternative to the materials normally used as the silica source in the synthesis of high silica zeolites. The benefits and drawbacks of this material (tetraethyl silicate) over other traditional sources are described in Chapter 3.

In zeolite synthesis the progress of zeolite crystallization is normally followed by bulk methods of analysis, e.g. X-ray powder diffraction, thermal analysis, gas adsorption etc. These methods reveal how much crystalline zeolite is present in a mixture of amorphous and crystalline material. They cannot tell very much about the crystals themselves, e.g. the size and shape of the crystals, or the way in which they grow. A common technique used in studies of crystal

systems other than zeolites is to follow the growth of crystals with an optical microscope. A problem with zeolite crystals is that they are often too small (c.a. 0.1 to 1 μm) for their growth to be followed optically. Consequently ways of growing larger crystals were investigated. Once the conditions for the growth of larger crystals had been ascertained the effects of various parameters on growth could then be investigated and studied by optical microscopy. This work is described in Chapter 4 .

These studies gave information on the growth of zeolite crystals but not on their nucleation, especially in bulk crystallizations. The work described in Chapter 5 tells how several different techniques were combined to give a better understanding of both nucleation and the growth stages of the crystallization process.

1.7. References.

1. W. Lowenstein, Amer. Mineral., 1954, 39, 92.
2. D.H. Olson, W.O. Haag and R.M. Lago, J. Catal., 1980. 61, 390.
3. A. Cronstedt, Akad. Hanal. Stockholm, 1756, 120, 18.
4. F.A. Mumpton, "Natural Zeolites: Occurrence, Properties, Use", Ed. L.B. Sand and F.A. Mumpton. Pergamon Press, Oxford, 1978, 3.
5. H. Kristmannsdottir and J. Tomasson, "Natural Zeolites: Occurrence, Properties, Use", Ed. L.B. Sand and F.A. Mumpton. Pergamon Press, Oxford, 1978, 277
6. D.W. Breck, "Zeolite Molecular Sieves", Wiley-Interscience, 1974, 47.
7. W.S. Wise and R.W. Tschinich, Amer. Mineral., 1975, 60, 951.
8. M.N. Maleyev, Int. Geol. Rev., 1977, 19, 993.
9. J. Ciric, U.S. Pat. 3 692 470, 1972.
10. T.V. Whittam, German Pat. Appl. 2 748 276, 1978.
11. J.L. Casci, B.M. Lowe and T.V. Whittam, Eur. Pat. Appl. 42 226, 1981.
12. W.M. Meier and D.H. Olson, "Atlas of Zeolite Structure Types", Structure Commission of the International Zeolite Association, Polycrystals, Pittsburgh, 1978.
13. W.M. Meier, "Molecular Sieves", Society for Chemical Industry, London, 1968, 10.
14. R.M. Barrer, "Hydrothermal Chemistry of Zeolites", Academic Press, London, 1982, 9.

15. R. Gramlich-Meier and W.M.Meier, J. Solid State Chem., 1982, 44, 41.
16. "Chemical Nomenclature, and Formulation of Compositions, of Synthetic and Natural Zeolites", prepared by a special I.U.P.A.C. commission under the chairmanship of R.M. Barrer. I.U.P.A.C. yellow booklet, 1978.
17. Ref. 14, p18.
18. Ref. 6, chapters 7 and 8.
19. L.B. Sand and F.A.Mumpton (editors), "Natural Zeolites: Occurrence, Properties, Use", Pergamon Press, Oxford, 1978, 546pp.
20. P.B. Weisz, Pur Appl. Chem., 1980, 52, 2091.
21. Ref. 6, p640.
22. Ref. 6, p639.
23. R.M. Barrer, J. Inclusion Phenomena, 1983, 1, 105.
24. R.W. Grose and E.M. Flanigen, U.S.Pat.4 061 724, 1977.
25. N.B. Milestone and D.M. Bibby, J. Chem Tech. Biotechnol., 1981, 31, 732.
26. P.B. Weisz and V.J. Frilette, J. Phys. Chem., 1960, 64, 382.
27. Ref. 14, p27
28. S.L.Meisel, J.P. McCullogh, C.H. Lechtaler and P.B.Weisz, Chemtech., 1976, 6, 86
29. C.D. Chang and A.J. Silvestri, J. Catal., 1977, 47, 249
30. J. Thomas, S. Ramden and G.R. Millward, New

Scientist, 18th. Nov. 1982, 435.

31. For example, R.M. Barrer, Trans. Faraday Soc., 1944, 40, 555

32. R.M. Barrer, J. Chem. Soc., 1948, 127.

33. For example, J. Chem. Soc., 1948, 2158.

34. (a) R.M. Milton, U.S. Pat. 2 882 243, 1955.

(b) D.W. Breck, W.G. Eversole, R.M. Milton, T.B. Reed and T.L. Thomas, J. Am. Chem. Soc., 1956, 78, 5963

35. (a) R.M. Milton, U.S. Pat. 2 882 244, 1959.

(b) D.W. Breck, W.G. Eversole and R.M. Milton, J. Am. Chem. Soc., 1956, 78, 2338.

36. D.W. Breck, U.S. Pat. 3 130 007, 1964.

37. R.M. Barrer and P.J. Denny, J. Chem. Soc. , 1961, 971

38. G.T. Kerr, J. Inorg. Chem., 1966, 5, 1537.

39. R. Aiello and R.M. Barrer, J. Chem. Soc. (A), 1970, 1470

40. R.L. Wadlinger, G.T. Kerr and E.J. Rosinski, U.S. Pat 3 308 069, 1967.

41. R.J. Argauer and G.R. Landolt, U.S. Pat. 3 702 886, 1972.

42. E.M. Flanigen, J.M. Bennett, R.W. Grose, J.P. Cohen, R.L. Patton, R.M. Kirchner and J.V. Smith, Nature, 1978, 271, 512.

43. For example, (a) D.M. Bibby, N.B. Milestone and L.P. Aldridge, Nature, 1979, 280, 664.

(b) R.W. Grose and E.M. Flanigen, U.S. Pat. 4 104 294, 1978.

44. For example, M.K. Rubin, E.J. Rosinski and C.J. Plank, U.S. Pat. 4 151 189, 1979.
45. For example, (a) C.J. Plank, E.J. Rosinski and M.K. Rubin, U.S. Pat. 4 175 114, 1978.
- (b) T.V. Whittam, Eur. Pat. Appl. 0 054 386, 1982.
46. J.A. Kaduk, U.S. Pat. 4 323 481, 1982.
47. T. Onodera, T. Sakai, Y. Yamasaki and K. Sumitani, U.S. Pat. 4 320 242, 1982.
48. F.G. Dwyer and P. Chu, J. Catal., 1979, 50, 263.
49. P.W. Atkins, "Physical Chemistry", Oxford University Press, 1978, 184.
50. B.V. Deryagin and D.V. Fedoseev, Scientific American, Nov. 1975, 102.
51. For example, (a) W.C. Beard, "Molecular Sieves", Ed. W.M. Meier and J.B. Uytterhoeven, American Chemical Society Advances in Chemistry series No. 121, 1973, 162
- (b) R.O. Gould, B.M. Lowe and N.A. MacGilp, J. Chem. Soc. Chem. Comm., 1974, 720.
- (c) E.G. Derouane, J.B. Nagy, Z. Gabelica and N. Blom, Zeolites, 1982, 2, 299.
52. H. Kacirek and H. Lechert, ACS Symp. Series, 1977, 40, 244.
53. R.M. Barrer, Zeolites, 1982, 1, 130.
54. For example, R.J. Moolenaar, J.C. Evans and L.D. McKeever, J. Phys. Chem., 1970, 74, 3629.
55. R.K. Harris and R.H. Newman, J.C.S. Faraday II, 1977, 1204.
56. For example, (a) C.W. Lentz, Inorg. Chem., 1964, 3,

374.

(b) L.S. Dent Glasser and S.K. Sharma, Br. Polym. J., 1974, 6, 283.

57. R.K. Iler, "The Chemistry of Silica", Wiley, New York, 1979, 138.

58. R.K. Iler, J. Colloid Interface Sci., 1980, 75, 138.

59. For example, (a) E. Lippmaa, M. Magi, A. Samoson, G. Engelhardt and A.R. Grimmer, J. Am. Chem. Soc., 1980, 102, 4889.

(b) J.L. Casci, Ph.D. Thesis, University of Edinburgh, 1982.

60. J.W. Mullin, "Crystallization", Butterworths, London, 1961, 102.

61. For example, (a) Ref. 60, p104

(b) E.V. Khamskii, "Crystallization from Solutions", Consultants Bureau, New York, 1969, 22

62. Ref. 60, p106.

63. D. Domine and J. Quobex, "Molecular Sieves", Society for Chemical Industry, 1968, 78.

64. (a) S.P. Zhdanov, Advan. Chem. Ser., 1971, 101, 20

(b) S.P. Zhdanov and N.N. Samulevich, "Proceeding of the 5th. International Conference on Zeolites", Ed. L.V.C. Rees, Heyden, London, 1980, 75.

65. J.W. Mullin and K.D. Raven, Nature, 1961, 190, 251.

66. G.T. Kerr, J. Phys. Chem., 1966, 70, 1047.

67. B. Subotic and A. Graovac, "Proceeding of the 5th. International Conference on Zeolites", Ed. L.V.C. Rees, Heyden, London, 1980, 54.

68. W. Meise and F.E. Schwochow, "Molecular Sieves",
Ed. W.M. Meier and J.B. Uytterhoeven, American Chemical
Society Advances in Chemistry Series No. 121, 1973, 169
69. Ref. 14, p136.
70. T.G. Feyrov, E.B. Trevis and A.P. Kasatkin,
"Growing Crystals from Solution", Consultants Bureau,
New York, 1969, 47.
71. For example, (a) P.H. Egli and S. Zerfoss, Faraday
Soc. Discussion No.5, 1949, 61.
(b) Ref. 60, p116
(c) Ref. 61 (b), p32.
72. J.M. Coulson and J.F. Richardson, "Chemical
Engineering", Pergamon Press, London, 1955, 2, 817.
73. H.E. Buckley, Faraday Soc. Discussion No.5, 1949,
243.
74. Ref. 60, p127.
75. (a) H. Kacirek and H. Lechert, J. Phys. Chem., 1975,
79, 1589.
(b) H. Kacirek and H. Lechert, J. Phys. Chem., 1976,
80, 1291.
76. Ref. 61 (b), p43.
77. For example, (a) A. Erdem and L.B. Sand, J. Catal.,
1979, 60, 241.
(b) K-J. Chao, T.C. Tasi, M-S. Chen and I. Wang, J.
Chem. Soc. Faraday Trans. 1, 1981, 77, 547.
78. D. Turnbull, "Solid State Physics", Ed. F. Seitz
and D. Turnbull, Academic Press, London and New York,
1956, 3, 252.

79. Ref. 14, p148.
80. V. Lecluze and L.B. Sand, "Proceeding of the 5th. Internatonal Conference on Zeolites", Ed. L.V.C. Rees, Heyden, London, 1980, 41.
81. R. Mostowicz and L.B. Sand, Zeolites, 1982, 2, 143.
82. S.B. Kulkarni, V.P. Shiralkar, A.N. Kotasthane, R.B. Borade, and P.Ratnasamy, Zeolites, 1982, 2, 313.
83. M.Ghamami and L.B. Sand, Zeolites, 1983, 3, 155.
84. (a) E.M. Flanigen, Adv. Chem. Ser. 1973, 121, 119.
(b) R.M. Barrer, Zeolites, 1981, 1, 130.
85. R.M. Barrer, Chem. Ind. London, 1968, 1203.
86. V. Gramlich and W.M. Meier, Z. Kristallogr., 1971, 133, 134.
87. C. Baerlocher and W.M. Meier, Helv. Chim. Acta., 1969, 52, 1853.
88. E.G. Derouane, S. Detremmerie, Z. Gabelica and N. Blom, Appl. Catal., 1981, 1, 201.
89. P. Chu, U.S.Pat. 3 709 979, 1973.
90. W.J. Ball and K.W. Palmer, Republic of S. Africa Pat. Appl. 787 037, 1978.
91. J.L. Casci, B.M. Lowe and T.V. Whittam, Eur. Pat. Appl. 42 225, 1981.
92. H. Bremer and W. Reschetilowski, Z. Chem., 1982, 22, 275.
93. Ref. 57, p58 and 150.

Chapter 2

Experimental

The experimental techniques which were required for this work fall into two different categories; those used for the synthesis of the zeolites and those used for their analysis. This Chapter gives a full description of the apparatus used for the synthesis of the zeolites while later chapters describe any additional technique used. The analytical techniques generally used are also described in this Chapter although additional, special techniques are discussed in the relevant section.

The techniques described in the first section of this Chapter are connected with the identification and characterization of the products obtained. The major tool used in the identification of zeolites is X-ray powder diffraction, where the X-ray powder pattern is used as a "fingerprint" of the compound, even if the actual structure cannot be determined. Only X-ray powder diffraction work was carried out in this project as the crystals were too small for single crystal X-ray structure determination. The other analytical techniques used gave information on the size and the shape of the crystals (by microscopy), the amount of material in the zeolite channels (by thermal analysis) and information about the synthesis solution (by silicate analysis and pH measurements).

The second section of this Chapter describes the

apparatus used for the synthesis of the zeolites. Reactions at temperatures above 373K were carried out in stirred stainless steel autoclaves or Teflon-lined steel bombs. Work at lower temperatures was carried out in stirred polypropylene bottles.

2.1 Analysis

Carbon, hydrogen and nitrogen analysis was carried out by either the departmental analytical service at Edinburgh University Chemistry Department or the analytical service provided at the ICI research laboratories at the Heath, Runcorn.

2.1.1 X-Ray Powder Diffraction

Synthetic zeolite crystals are normally examined by X-ray powder diffraction as they are usually too small for single crystal work. The minimum practical size for a crystal for single crystal work is about 0.1mm. Most synthetic zeolite crystals are smaller than 10 μ m.

The interplanar spacings, d , of a crystal can be obtained from the Bragg Law:

$$n \lambda = 2 d \sin \theta$$

where λ is the wavelength of the X-rays, θ is the angle of incidence of the rays to the crystal and n is a whole number. From this equation it can be seen that a family of planes of a particular spacing diffract at only one angle of incidence. Thus when X-rays strike the planes of atoms which make up the crystal structure, a series of diffraction lines are obtained which are characteristic of that material. A zeolite

powder contains many crystallites, each of which are able to diffract radiation in accordance with Bragg's Law. The crystallites are at various orientations so that the reflections obtained come from the various planes present in the crystals. There are often reflections from different planes which coincide so that there is a loss of information when compared with single crystal data. However the pattern generally contains enough lines to be characteristic of the material and it can serve as an excellent fingerprint for the zeolite and hence its ready identification.

X-ray powder diffraction patterns were obtained using a Philips powder diffractometer. This comprised of a PW1965/60 goniometer mounted on a PW1730 highly stabilised X-ray generator. The samples were loaded by a PW1170 automatic sample changer. A PW1394 motor control unit controlled the scanning, and the output was analysed by a PW1390 channel control unit which fed to a PM8203 pen recorder. A fine focus copper X-ray tube was used to give Cu K α radiation (wavelength = 0.154 nm) and diffracted X-rays were monochromated before detection. The machine was regularly calibrated using a piece of microcrystalline quartz stone. Reflections from $2\theta = 4^\circ$ to $2\theta = 40^\circ$ were those normally observed. The 2θ values and intensities which were obtained from the diffraction pattern were converted to d-spacings and relative intensities using the program TTOD, written by Dr. B.M.Lowe. The zeolite

could then be identified by comparing the d-spacings and intensities with those for known zeolites. In practice a computer program, IDENT, written by Dr. B.M.Lowe, was used to compare the d-spacings and intensities of the synthesis materials with those of known zeolites.

2.1.2 Microscopy

2.1.2.1 Scanning Electron Microscopy

The scanning electron micrographs which are shown in this work were obtained with a Cambridge Stereoscan 604 instrument. All samples were washed thoroughly and then dried overnight at 369K. Each sample was then mounted on an aluminium stub before it was placed in the microscope. The procedure used initially was to fix the sample to the aluminium stub by means of double-sided adhesive tape. Very little sample was used (much less than 1 mg) and it was spread as thinly as possible in order to prevent the formation of large agglomerates. The sample was then coated with a thin film of gold. This was done by evaporating the gold over the sample using a Polaron E5100 Series II cool sputter coater. The thickness of the gold film was approximately 50 nm. The gold film helps to conduct electrons away from the surface and prevents the non-conductive zeolite from "charging". Charging occurs when charge builds up on the surface and prevents maximum resolution of detail. It was found that this method of fixing the sample to the stub was not entirely satisfactory. The adhesive

tape insulates the zeolite from the metal stub so that the samples had to rely entirely upon the gold film to conduct the electrons away. Samples with large surface areas, (quite common for zeolites) were not covered as completely with gold as was small area samples and consequently charging occurred. A new procedure was developed to try to prevent this. A small amount of sample was placed on a polished stub and a drop of ethanol or acetone added to the sample. The solid and solvent were then lightly mixed and the solvent was allowed to evaporate. The solid adheres very slightly to the stub. The gold film was then evaporated over the sample. This method proved to be much more successful. Samples tended to spread out more thinly and evenly and charging was much rarer. Only samples with a very high surface area could still cause problems.

To ensure that a representative sample was obtained, samples were always mixed well before they were fixed to the stubs. Likewise, several different areas of stub were examined. The electron micrographs provide information about the crystal size and shape as well as the distribution of sizes throughout the sample. They can also reveal any amorphous material and impurities present in the sample. The electron microscope provides better resolution and depth of focus than an optical microscope. The main drawbacks in its use are the time required to prepare the samples, charging, and the fact that samples which contain a lot of amorphous material

can have the crystal features hidden by this solid.

2.1.2.2. Optical microscopy

An optical microscope is essentially an elaborate magnifying glass. It has an advantage over the scanning electron microscope in that it is easier and quicker to use. Samples do not have to be carefully washed, dried and then coated with a metal film. There is no time wasted while the air is pumped out of the sample chamber as in the electron microscope. In recent years the majority of zeolite studies have concentrated on the use of the electron microscope. This is not really surprising as it is indeed a very useful tool. The electron microscope used in this work could magnify objects by up to 50 000 times and could be used to resolve fine details which were less than $0.05 \mu\text{m}$ apart. It also had the tremendous advantage of a much greater depth of field than is possible with an optical microscope. The three-dimensional image produced by the electron microscope is much superior to the flat optical microscope image. The problem with an electron microscope is that samples have to be dry and carefully prepared and there is always the chance that the sample will "charge". Indeed the fact that the sample has to be dried can be of extreme importance when there is a lot of gel or amorphous material present. Zeolite crystals which are present within the gel can be lost completely. The gel or amorphous material also contracts on drying and may mislead the observer on the

extent of zeolite/gel contact as well as the nature of the amorphous material.

An excellent way around this problem is to use an optical microscope. Samples can be viewed "wet" and consequently zeolite crystals dispersed in an aluminosilicate gel can be seen since few gels are completely opaque. Crystals can be observed in the medium from which they are growing and do not need to be separated from their mother liquor. The magnification which can be achieved by an optical microscope is limited by the wavelength of light. Consequently, for 600 nm light, objects closer than about 0.6 μm cannot be resolved. Also, only a "flat" image can be obtained, especially when high magnifications are employed.

The optical micrographs which are shown in this work were obtained with a Vickers M41 Photoplan microscope fitted with a Pentax ME Super camera. Samples were normally diluted with a little distilled water, then a drop of sample was placed on a microscope slide and covered with a cover slip. An alternative to this procedure was to put the samples into flat, rectangular, open-ended glass micro-capillary tubes (microslides).¹ These microslides were made from heat-resistant glass (Pyrex) and had precise optical path lengths. Samples could be sealed within the microslide by melting its ends in a hot flame. The microslides proved to be extremely useful as it was

possible carry out small-scale synthesis experiments with reaction mixtures sealed in the slides. (see Chapter 4). Samples were normally viewed with bright field illumination. They were also examined using a polarized light source and a polaroid analyser. Isotropic crystals remain visible when the sample is rotated between crossed polars, whereas crystals which exhibit double refraction will fade out in a few definite positions when rotated between crossed polars.

If increased contrast of a specimen was desired, Rheinberg illumination² was employed. This is basically a method of "optically staining" a sample without having to contaminate it with dye. Suitable Rheinberg filters were constructed for the microscope from coloured optical filter plastic films. The filters consisted of an outer ring of one colour separated from a coloured central stop by a narrow opaque ring. The filters were placed just under the condenser. The outer ring colour effectively becomes the colour of the specimen and the inner stop becomes the colour of the background. The most effective colour combination was found to be a yellow ring with a red central stop which gave a yellow sample on a red background.

The size of any crystal viewed through the optical microscope could be obtained accurately by using a slide marked with an accurate scale. The scale was photographed at various magnifications so that the size of any sample could be found by comparison of a

photograph of the sample with the photograph of the scale at the same magnification.

2.1.3. Thermal analysis

Thermal analysis consists of the measurement of some physical property of a sample whilst it is heated at a fixed rate. The observation may be recorded as a function of temperature or time. Thus thermal gravimetric analysis (t.g.a.) is the measurement of the weight loss or gain as a function of temperature. Differential thermal analysis (d.t.a.) is the measurement of temperature changes in a sample (compared to a thermally inert material) as a function of temperature. These are probably the most useful thermal analysis techniques in zeolite chemistry. Only thermal gravimetric analysis was used in this work.

One of the most important aspects of thermal analysis is the rate of heating. It must be constant and reproducible as the sensitivity and resolution depend upon the rate. In t.g.a. low heating rates give improved resolution but unchanged sensitivity,

Thermal gravimetric analysis measures the weight loss of a sample as a function of temperature and can therefore be used to determine the water and/or the organic content of a zeolite. A fairly low heating rate is required when both water and organic are within the lattice of the zeolite if separation of both types of loss is to be observed. Complete separation may not always be achieved but a low heating rate will give a

better indication of the weight loss of each.

2.1.3.1. Thermal gravimetric analysis.

T.g.a. was carried out with a Stanton-Redcroft TG770 thermal balance. Before examination, samples were normally equilibrated with water vapour by placing them in a desiccator over saturated sodium chloride solution. The desiccator was then placed in a water bath at 298K for 16 hours. Samples were ground finely, then placed in the platinum sample holder (ca. 5-10 mg of sample) and the furnace raised to surround the sample. The heating rate was normally set at 10K min^{-1} and the final temperature could be set up to 1773K, although it was usually set at 1273K. The temperature and weight were recorded by a Kipp and Zonen BD9 two channel chart recorder. The sample weight was either recorded directly or as a percentage of the full-scale deflection (F.S.D.) of the recorder. This could be set at 100%, 50% or 20% of the sample weight, so that the percentage weight loss could be determined directly. The balance was calibrated before each run using weights supplied by the manufacturers for this purpose. The balance was always allowed to warm-up for 10 minutes after being switched on before the calibration was carried out. Air was passed over the sample during the heating in order to remove the combustion products.

The normal operating conditions are shown below:

Atmosphere/Flow Rate	Air/ 4.5ml min^{-1}
Chart Speed	120mm hour^{-1}

Sample Weight	5-10 mg
Heating Rate	10K min ⁻¹
Temperature(F.S.D.)	20mV
Weight(F.S.D.)	50%

2.1.4. Silicate analysis

The concentration of silica in solution was determined by the molybdic acid method. The reaction of molybdic acid with monomeric silica to form the yellow silicomolybdate ion has long been used to determine soluble silica and also to characterize polysilicic acids and colloidal silica particles (see Chapter 3). In this work the concentration of silica in solution was required not only at the start and finish of a molecular sieve synthesis but also during the reaction to provide information about the mechanism and kinetics of the crystallization process.

The method used was based on that of Truesdale and Smith.³ In this the yellow alpha molybdosilic acid is produced rather than the more intense but less stable beta form.

The reagent used was a buffered molybdate solution, 0.2M in acetic acid and sodium acetate, and 0.1M in molybdenum, prepared from 12.01 gdm⁻³ acetic acid (A.R.), 27.22 gdm⁻³ sodium acetate trihydrate (A.R.), and 17.656 gdm⁻³ (NH₄)₆Mo₇O₂₄·4H₂O. The pH of the solution was adjusted to pH 4.0±0.1 using 2.5M H₂SO₄ (A.R.). The buffered molybdate solution tends to precipitate a white solid after approximately two days.

Because of this a fresh solution was always prepared before each series of analyses.

2.1.4.1. Procedure

The solutions tested were normally c.a. 0.5 molar in silica. Since only monomeric silica reacts with the molybdic acid, 0.1 ml of the test solution was added to 1 ml of 10 molar sodium hydroxide to convert any polymer or colloidal silica to sodium silicate. This solution was then diluted to 250 ml to give a solution which contained about 12 mg silica per litre. The maximum amount of silicon per litre should not exceed 12mg (i.e. 25 mg SiO_2).

To 25 ml of this solution was added 25 ml of the buffered molybdate solution. The optical density could be measured at 390 nm using 1cm cells after allowing the colour to develop fully over 15 to 30 minutes. The reaction time for molybdosilicic acid formation at pH 4.2 and 290K is 10 minutes. The reaction rate increases with decreasing pH and increasing temperature. The reference cell contained a solution made from 25 ml buffer plus 25 ml distilled water.

High levels of TPA can interfere with the test by forming a precipitate. However the amount generally used (c.a. 0.05 molar) did not appreciably affect the results.

2.1.5. pH measurement

An extremely useful method for determining when a zeolite crystallization has been completed is the

measurement of the pH of the reaction mixture.^{4,5} It is a method which does not require the solid phases to be separated from the reaction mixture and then washed, dried and equilibrated with vapour. The determination of the pH samples throughout a reaction is a rapid and simple qualitative method for monitoring the progress of the reaction. Since high silica zeolites are less soluble in water than the amorphous alumino-silicate gel solids from which they are crystallized, their formation is normally associated with a rise in pH.

The pH measurements in this work were made with an EIL plastic bodied combination pH electrode type 1180/200/UKP fitted to a Philips PW9409 digital pH meter. The apparatus was regularly standardised in a reference buffer solution (pH = 9.2) and the uncertainty in the absolute accuracy of measurements on solutions with $\text{pH} < 13$ is believed to be less than 0.1 units. Differences > 0.03 between pH readings obtained at different times are considered to be significant.

The electrode was carefully washed in distilled water between readings. The samples of reaction mixture (c.a. 8 cm^3) were placed in stoppered glass vials and allowed to cool to room temperature. The pH reading generally drifted when the electrode was first introduced into the sample but after approximately ten minutes the value remained relatively stable. Consequently pH readings were only noted after the electrode had been equilibrated with the sample for 10

minutes.

2.2. Synthesis

2.2.1. High temperature reactions

High temperature reactions were carried out in stirred autoclaves or static steel bombs or glass capillary tubes. The autoclaves which were used were designed and constructed by Baskerville and Lindsey Ltd. They had a capacity of 500 ml, and were agitated with stirrers. The stirring speed could be regulated and monitored from the autoclave's control panel. The autoclaves were constructed from stainless steel or stainless steel and inconel (a nickel based alloy containing c.a. 13% chromium, 6% iron and some manganese). Temperature control was by Gullton-West MC36 four-term temperature controllers. The temperature inside the autoclave was measured by a thermocouple which was placed in a thermocouple "pocket" which protruded into the reaction vessel. An important feature of the autoclaves was a facility for sampling the reaction mixture at any time during the reaction. Figure 2.1 is a schematic diagram of the autoclave and shows the thermocouple pocket along with the sampling pipe and stirrer inside the reaction vessel.

The autoclaves also had three safety devices. The pressure gauge incorporated a reed switch which operated a trip. If the pressure exceeded a pre-set value the heater would be switched off automatically. The control panel also incorporated a thermal cut-out

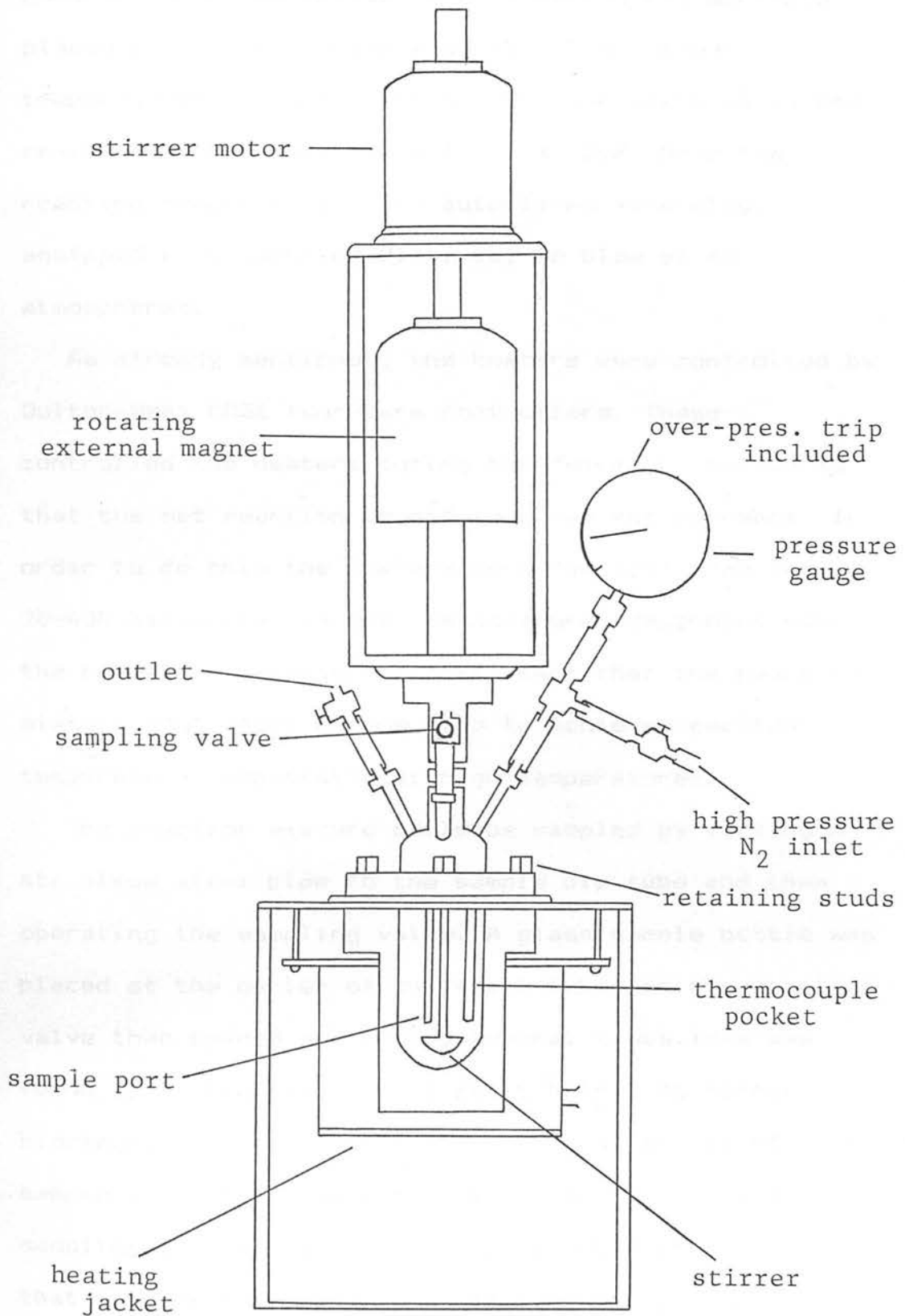


Figure 2.1. Schematic diagram of stirred autoclave

control which was activated by a second thermocouple placed in the thermocouple pocket. The cut-out temperatures could then be set at some value above the reaction temperature (normally c.a. 20K above the reaction temperature). The autoclaves were also equipped with bursting discs set to blow at 45 atmospheres.

As already mentioned, the heaters were controlled by Gulston-West MC36 four-term controllers. These controlled the heaters during the "warm-up" period so that the set reaction temperature was not overshoot. In order to do this the heaters were "pulsed" from about 20-40K below the reaction temperature (depending upon the reaction temperature). This meant that the reaction mixture could take a long time to achieve reaction temperature, especially at high temperatures.

The reaction mixture could be sampled by fitting a stainless steel pipe to the sample dip tube and then operating the sampling valve. A glass sample bottle was placed at the outlet of the steel tube and the sample valve then opened and closed several times. This was found to be the best method as it helped to release blockages in the sample pipe. The first few ml of sample (c.a. 5 ml) were normally discarded as the sampling tube within the autoclave could trap material that was not typical of the reaction mixture. After sampling the material left in the tube could be "back flushed" into the main body of the solution with high

pressure nitrogen. This could lead to a slight increase in pressure inside the autoclave, so it was normally only carried out to help release blockages or if the reaction mixture was so thick that a blockage was liable to occur if some was left in the tube. The amount of sample taken was normally in the region of 10 ml.

The size of the autoclave limited the number of samples which could be taken. The autoclave had a total volume of 500ml but it was important to leave room for the expansion of the reaction mixture at high temperatures. The volume used never exceeded 400ml. The autoclave could not be over-sampled as the dip tube does not descend below the stirrer head (see figure 2.1). Consequently, the last 100 to 150 ml of solution cannot really be removed via the sample tube. This limits the number of 10 ml samples to between 15 and 20 for a 400 ml starting solution and 5 ml run off for each sample.

The autoclaves were always cleaned between reactions using an aqueous solution of sodium hydroxide (1M), stirred at 300 r.p.m. and at a temperature of 393K. After 1 hour approximately 50ml of the solution was removed through the dip pipe. The autoclave was then allowed to remain running for a further 30 to 60 minutes and the heater then switched off. When cool, the autoclave was dismantled and washed. The sampling tube was rinsed thoroughly with water. It was noted

that although the reaction vessel, stirrer and thermocouple port appeared to have all traces of zeolite crystals removed from them by this procedure, washings from the sample tube were found to contain traces of zeolite crystals (visible by optical microscope). A second washing with hydroxide at 393K did not remove all traces of zeolite. Only washing the sample port with large quantities of water appeared to have any effect. The crystals probably stick to the inside of the sample tube. The hydroxide will only be capable of attacking the outer layer, which is loosened and can be washed off. Care had to be taken that no crystals remained in the sample tube. The steel bombs which were used were designed by Dr. B.M. Lowe. The bombs consisted of a stainless steel body and cap with a Teflon insert and cap, as shown on the schematic diagram in figure 2.2. The small hole in the steel cap was a safety feature. Any excessive pressure built up inside the bomb should seep through the Teflon seal and release through the hole. It was calculated that the bombs should be able to withstand very high pressures. The bursting pressure (BP) for metal tubes can be calculated from equation 2.2.

$$BP = 2t S/D \quad (2.2)$$

where t is the thickness of the tube wall, S is the tensile strength of the metal and D is the internal tube diameter. For the steel bombs;

$$S = 5.9 \times 10^8 \text{ Pa}$$

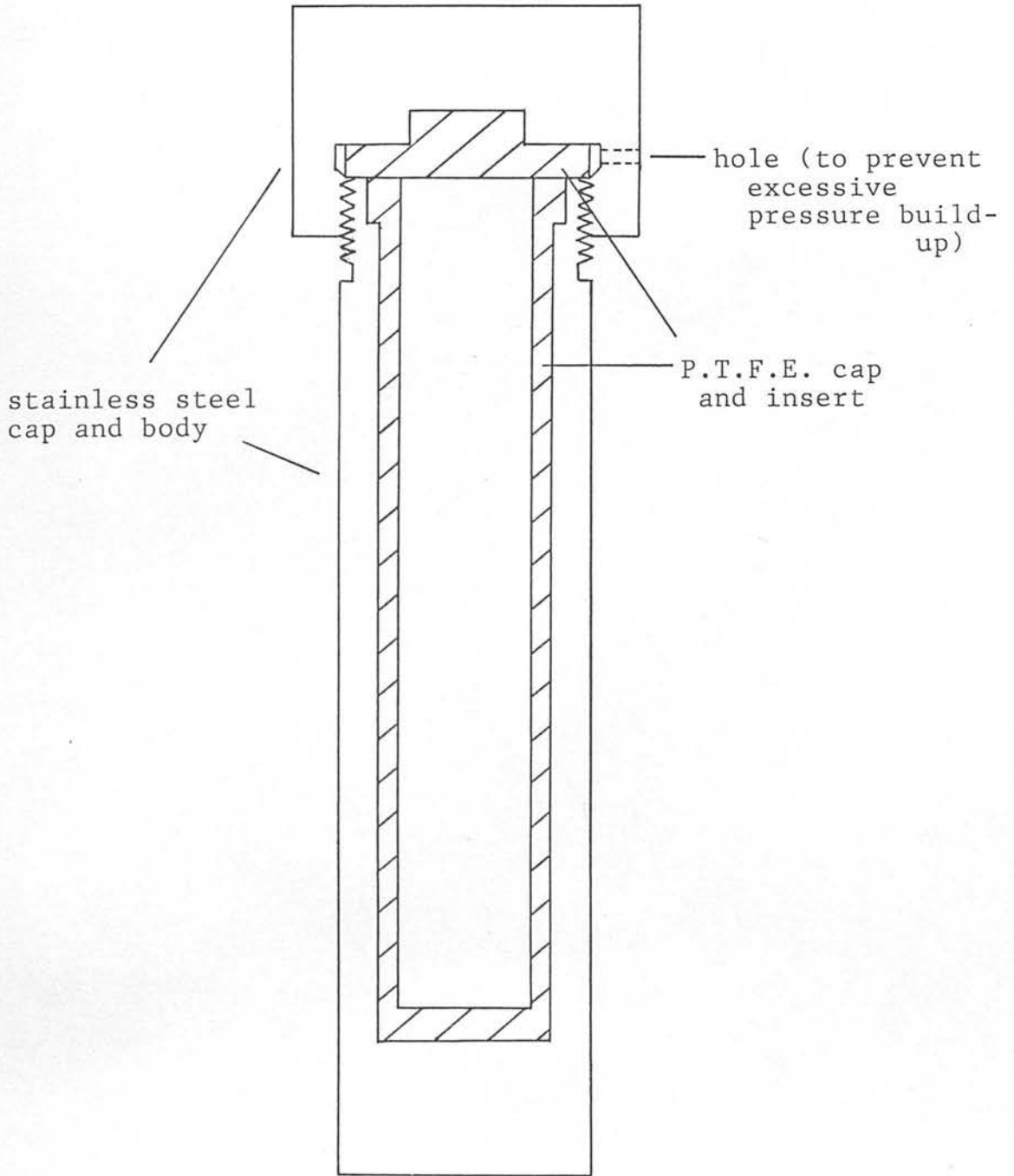


Figure 2.2. Diagram of a steel bomb (actual size)

$$t = 6.25 \times 10^{-3} \text{ m}$$

$$D = 2.5 \times 10^{-2} \text{ m}$$

therefore $BP = 2.95 \times 10^8 \text{ Pa}$

This is an extremely high pressure. The Teflon insert would probably distort long before this pressure is reached.

The bombs originally had a capacity of only 14 ml but the walls of the teflon insert were made narrower and the capacity increased to approximately 35 ml. However, just as for the autoclaves, the bombs were never filled completely full but only to 4/5 the possible capacity so that there was always room for the expansion of the reaction mixture at high temperatures. Bombs were heated by placing them in an oven set at the required temperature. Sampling was not as simple as for the autoclave reactions. The small quantity kept in the bomb meant that there was little point in removing a sample. Also, since reactions were static, most crystals grew on the sides or at the bottom of the teflon insert. This meant that to take a sample of crystals would disturb the whole reaction. The bombs also took a long time to cool down to a temperature at which they could be opened safely, even when they were cooled by running cold water over them. Consequently the bombs were rarely used except to provide sufficient sample for X-ray while the progress of the reaction was followed in a glass capillary tube. The bombs were always cleaned between reactions by filling them with

an aqueous solution of sodium hydroxide (1M) and placing them at 393K for an hour. If any zeolite deposit still remained, this operation was repeated. The insert was then washed thoroughly with distilled water.

Small scale crystallizations were carried out in either glass melting point tubes or "microslides". Material was drawn up into a tube by capillary action, then each end of the tube sealed in a hot flame. The tube was then placed into a pre-heated metal block. The metal blocks had several holes drilled in them in which to place the tubes. The progress of a reaction could be followed by removing the tube from the block, examining it by optical microscopy and then returning it to the heated block.

2.2.2. Low temperature reactions

The reaction vessels used were wide-necked, "screwtop" polypropylene bottles which had been adapted to take stirrers. The stirrer consisted of a stainless steel shaft and paddle which was fitted through a plastic guide set in the lid. The original design had oil-lite bushes set at the top and bottom of the guide to ensure smooth running (see figure 2.3) but it was found that this allowed liquid to escape by evaporation. Also, on occasion, the product was contaminated with oil. The evaporation problem was overcome by using spring loaded rubber washers which close upon the shaft and reduce evaporation (figure 2.3)

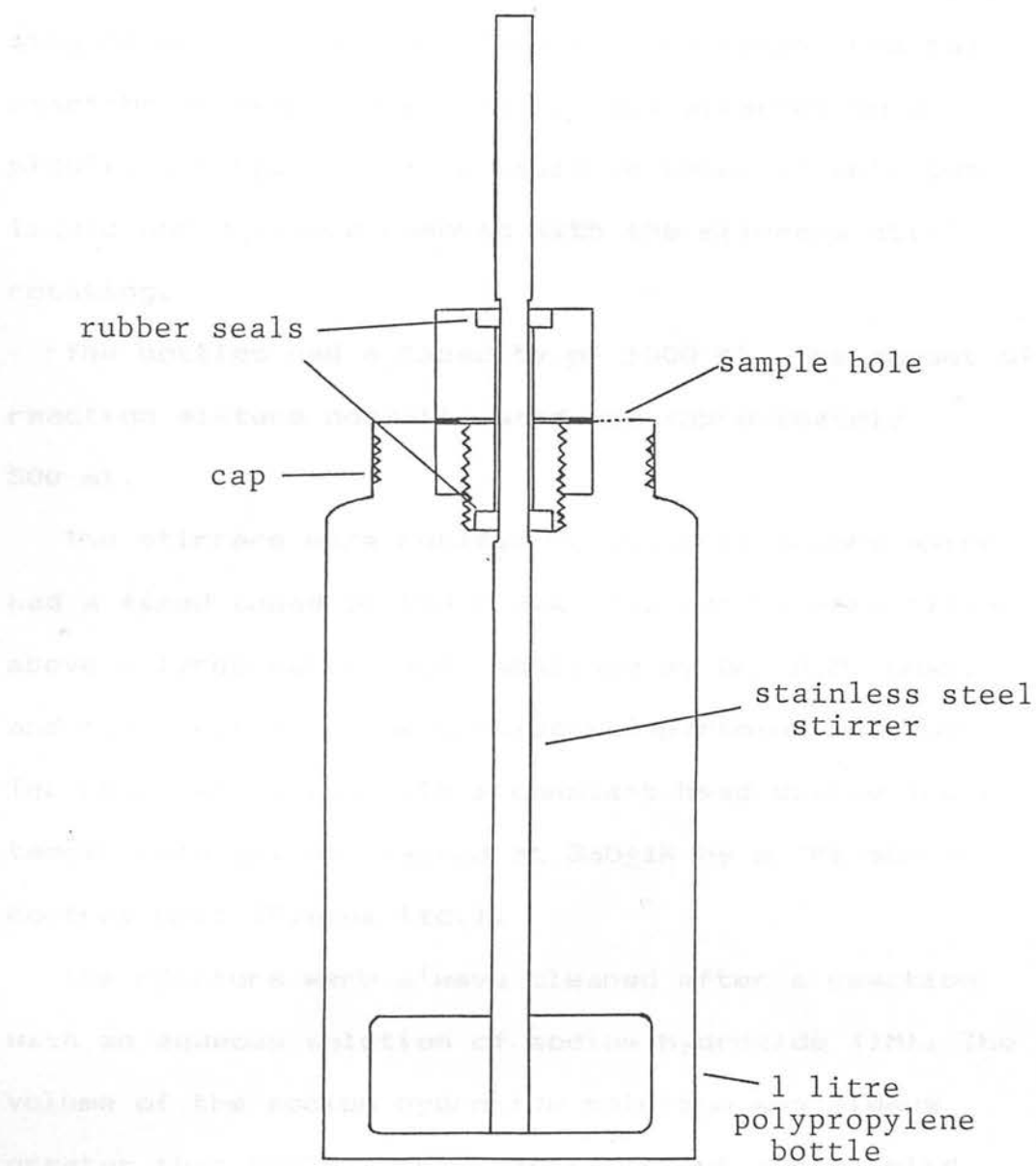


Figure 2.3. Schematic diagram of stirred plastic reaction vessel.

A hole was drilled in the lid to allow samples to be removed. This was always firmly sealed with a plastic stopper when not in use. Samples were taken from the reaction by means of a plastic tube attached to a plastic syringe. The tube could be inserted into the liquid and a sample removed with the stirrers still rotating.

The bottles had a capacity of 1000 ml. The amount of reaction mixture normally used was approximately 500 ml.

The stirrers were rotated by electric motors which had a fixed speed of 150 r.p.m. The motors were fitted above a large water bath, designed by Dr. B.M. Lowe, and constructed in the Chemistry Department workshop. The bath was fitted with a constant head device and its temperature was maintained at $368 \pm 1\text{K}$ by a "Fi-monitor" control unit (Fisons Ltd.).

The reactors were always cleaned after a reaction with an aqueous solution of sodium hydroxide (1M). The volume of the sodium hydroxide solution was always greater than 500 ml. This was important since solid material was often deposited at the solution / vapour / container boundary during crystallization (due to evaporation). The sodium hydroxide solution was stirred at 368K for a minimum of four hours. The vessel was then removed and rinsed thoroughly with water. It was then checked for any remaining white deposits of zeolite. If large, hard deposits were found on the

stirrer these were usually removed with scouring wire-wool pads (e.g. Brillo pads) before cleaning with hydroxide. It was found, by experience, that the hydroxide alone could not completely remove a thick aluminosilicate deposit.

Static reactions were carried out using "screw-top" polypropylene bottles of about 60 ml capacity. These were placed in the same thermostat bath as above.

2.3. References.

1. "Microslides" produced by CAMLAB Ltd.
2. G. Needham, "Practical Use of the Microscope", C.C. Thomas, Springfield, IL., 1958, 281
3. V.W. Truesdale and C.J. Smith, *Analyst*, 1975, 100, 203 and 797
4. J.L. Casci and B.M. Lowe, *Zeolites*, 1983, 3, 186
5. B.M. Lowe, *Zeolites*, 1983, 3, 300

Chapter 3. Zeolite Synthesis using Tetraethyl Silicate.

3.1. Introduction.

The importance of the composition and the method of preparation of the reaction mixture has already been discussed in chapter 1. Most reaction mixtures are gels in which an amorphous solid phase is dispersed in an aqueous solution phase. This type of mixture is extremely difficult to prepare reproducibly and consequently it is hard to investigate the mechanism of zeolite crystallization from gels. Some of the problems associated with the preparation of reaction mixtures are related to the nature of the solid materials and the method used to mix them into a heterogeneous reaction mixture. Very often the type of silica used to prepare the reaction mixture has a marked effect on the progress of the reaction. In an attempt to avoid these problems it was decided to investigate an alternative to the solid silicas normally used in the synthesis of high silica zeolites. The material chosen for investigation was tetraethyl silicate ($\text{Si}(\text{OEt})_4$). This has rarely been used in zeolite synthesis, as other cheaper silica sources are generally preferred. On the few occasions that it has been used^{1,2} the tetraethyl silicate has been hydrolysed quite rapidly in order to form a silicate solution. The hydrolysis reaction is shown in equation 3.1.



The monomer, $\text{Si}(\text{OH})_4$, which is produced by hydrolysis

of tetraethyl silicate, is very reactive and quickly polymerises. The hydrolysis reaction has been studied extensively.³ Tetraethyl silicate is not miscible with water but can be slowly hydrolysed when the two are stirred together. The hydrolysis reaction takes place at the interface between the two liquids. Hydrolysis is much more rapid when a catalyst, e.g. an acid or base is present. In general, acid is a more powerful catalyst, but was not thought to be suitable for this work since zeolite synthesis requires basic conditions. The hydrolysis reaction is normally first order in base.³ Most studies of the hydrolysis of tetraethyl silicate use a mutual solvent to aid the reaction, and only enough water is added to complete the hydrolysis. This method has recently proved to be a useful route to the low temperature formation of glass, formed from the gel produced after hydrolysis.⁴

The use of a mutual solvent is undesirable in the preparation of zeolite reaction mixtures, as it constitutes yet another component to be controlled. However, preliminary experiments showed that the slow release of silicate species into aqueous solution could be carried out without a mutual solvent, and with only a small amount of catalyst. It was originally hoped that silicate species could be fed slowly into solution to start and continue zeolite growth. Unfortunately this proved to be an unsatisfactory method, mainly due to the very fast polymerisation of the hydrolysed

tetraethyl silicate, at normal crystallization temperatures. However it was found that the basic silicate solutions which were produced by the hydrolysis reaction could be used directly in zeolite synthesis. Under certain conditions tetraethyl silicate could be hydrolysed to give water clear silicate solutions for compositions which when prepared by other means would be opaque gels. It is known that hydrolysis of tetramethyl silicate with an organic base as a catalyst, can also produce clear solutions,⁵ but these formed a gel when inorganic ions were added. The solutions made in this project were hydrolysed by inorganic bases.

These solutions were then investigated in order to determine if they were very different to the cloudy silicate dispersions of a similar composition, prepared from fumed silica. Trimethylsilylation (TMS) did not reveal any major differences between clear and cloudy solutions. However the TMS technique can only reveal the distribution of the small silicate anions, and it was therefore apparent that the chief differences lay in the nature of the colloidal species present. It should be noted that whilst the hydrolysis products appeared to be solutions, and are referred to as such throughout this thesis, they do in fact contain very small colloidal silica particles.

A more general problem with zeolite synthesis is that of reproducibility. If the clear silicate

solutions could be prepared reproducibly then this would be an advantage. Iler^{6,7} has shown that it is possible to obtain an estimate of the particle size of the colloidal species present in a silicate solution by reaction with molybdic acid. It can also be used as a way to characterize soluble silicates. The reaction of molybdic acid with silicate solutions and its use in characterizing silica polymers and particles has been reviewed by Iler.⁷ Only the monomer $\text{Si}(\text{OH})_4$ can react with molybdic acid to form the yellow silicomolybdic acid. Larger silicate species must depolymerise to form monomer in order to react with molybdic acid. Once the silicate polymers or colloidal particles have begun to depolymerise they continue to do so until they have reacted completely with the molybdic acid. This reaction occurs slowly enough at pH about 1.2 to allow the rate of development of the yellow colour to be followed by spectrophotometry.

Iler found that it was possible to obtain an approximate size of the colloidal species present from the rate constants obtained for the reaction of molybdic acid with silicate solutions. Since the TMS technique had already shown that the solutions used in this work contain only a small quantity of monomer and a large concentration of larger sized particles which would only react slowly, the method described by Iler proved to be unsatisfactory since there were only very small changes observed with this method. The rate of

development of the yellow colour depends upon the rate at which the silicate polymers and colloidal particles depolymerise. The rate of depolymerisation is slower for larger particles. Consequently, when the concentration of silica specified in the Iler method is used there is an extremely slow development of the yellow colour. This was partly because a molybdate concentration of at least seven times that required for the complete reaction of silica is specified in the Iler method. However, since the molybdic acid only reacts with monomer then, even the addition of a solution which has an excess of silica, compared with the molybdate ion concentration, is quite satisfactory in the initial stages of the reaction as most of the silica is "locked up" and will not react immediately. Thus an approximate idea of the nature of the silicate solution could be obtained by analysis of the rate of reaction of the silicate when added directly to the molybdate reagent. As monomer is removed, the larger particles begin to dissolve. The smallest particles have the highest solubility and dissolve first; as each particle becomes smaller its solubility increases and its rate of dissolution also increases until it has completely dissolved. Thus once a particle begins to dissolve it continues to dissolve until it completely disappears. The rate of development of colour depends upon the number of particles remaining at any one instant i.e., the rate of reaction with the molybdate

reagent depends on the concentration of unreacted silica in the solution. This method allowed different batches of solution, with the same composition, to be examined and their reaction rates compared.

Reproducibility of reaction with molybdic acid was taken as an indication of reproducibility of mixture preparation.

Finally, the "clear" silicate solutions were examined for any potential advantage in zeolite crystallization. Since only tetrapropylammonium bromide (TPABr) had to be added to the silicate solution, the synthesis of silicalite-1 was investigated. This very simple composition made it an ideal zeolite for study. It was found that the reaction mixture remained clear even at the reaction temperature and the silicalite could be observed to form from the clear solution. Other workers have produced zeolite from clear solutions. For example, Ueda and Koizumi⁸ achieved the synthesis of analcime and mordenite from "clear" solutions. They did this by the formation of a gel as normal and then dissolving it in basic solution. Consequently their solutions were extremely basic and certainly much more basic than those used here. Figure 3.1 shows two possible routes to zeolite crystals. Route 1 is the one normally found in zeolite crystallization. Route 2 bypasses the gel formation and goes straight to zeolite crystals (as found by Ueda and Koizumi). This alternative route was investigated to

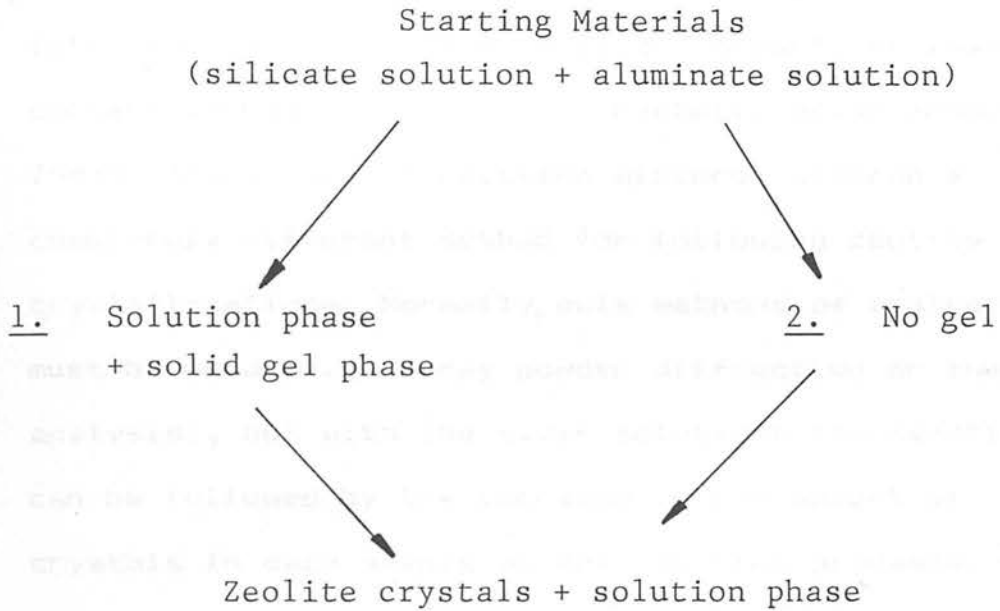


Figure 3.1. Two possible routes to the formation of crystals. Route 1 is the route normally found in zeolite crystallization.

see if it had any advantages over the normal route.

It was found that when aluminium was introduced into the reaction mixtures produced by the hydrolysis of tetraethyl silicate they remained "clear", at least for certain compositions, and on crystallization produced ZSM-5. These "clear" reaction mixtures offered a completely different method for following zeolite crystallizations. Normally, bulk methods of analysis must be used (e.g. X-ray powder diffraction or thermal analysis), but with the clear solutions the reaction can be followed by the increase in the weight of crystals in each sample as the reaction proceeds. This is infinitely superior to the x-ray powder diffraction method which depends on the nature of the amorphous solid phase remaining unchanged throughout the crystallization. Of course with these "clear" reaction mixtures the only solid phase present was pure crystalline zeolite and hence x-ray diffraction could not be used to follow the crystallization.

3.2. Experimental.

3.2.1. Materials.

The following materials were used:

Fumed silica (B.D.H., cab-o-sil M5)

Tetraethyl silicate (B.D.H., G.P.R. grade)

Aluminium hydroxide (B.D.H., G.P.R. grade)

Sodium hydroxide (Fisons, analar grade)

Sodium bromide (Fisons, analar grade)

Tetrapropylammonium bromide (Fluka, purum)

Ethanol (B.D.H., analar grade)

Distilled water was always used.

3.2.2. Preparation of solutions.

Hydrolysis reactions were initially carried out in both glass and polypropylene containers. Glass was useful for initial, "scouting" experiments as the progress of the reaction could be easily observed, but it could dissolve in the alkaline solutions and contaminate them. Therefore polypropylene containers were normally used. Large quantities of solution were prepared in one litre polypropylene bottles, while small quantities were prepared in 60ml. polypropylene bottles. A computer program (see appendix 1) was used to calculate the weights required for reaction mixtures. Solutions were prepared for hydrolysis in the following manner: the required quantity of sodium hydroxide was dissolved in the required amount of water, then one of two different methods were employed.

Method 1. Any salt, e.g. TPABr , required by the composition was added to the hydroxide solution and allowed to dissolve. If aluminium was required then aluminium hydroxide was dissolved in a strong sodium hydroxide solution (at least 10M). The required quantity of aluminium was then added as this sodium aluminate solution. The tetraethyl silicate was then added to the solution. A teflon-coated magnetic follower was placed in the polypropylene bottle which was then sealed with a screw cap. The solutions were then normally stirred quite rapidly so that the tetraethyl silicate liquid was broken into droplets and mixed with the aqueous layer.

Method 2. This was very similar to method 1 except that any salts or sodium aluminate required were added after the hydrolysis and normally just before the solution was used for crystallizations.

Static hydrolysis reactions were carried out in a similar manner to method 1 except that the solutions were never stirred and the tetraethyl silicate was allowed to float on top of the aqueous layer.

3.2.3. Trimethylsilylation.

The procedure used was based on that described by Sharma et.al.⁹ The trimethylsilylating reagent was prepared from hexamethyldisiloxane (20 ml), propan-2-ol (30 ml), water (12.5 ml) and 12M hydrochloric acid (15 ml). These were mixed together and stirred at room temperature for one hour. This reagent was then cooled

to 273K and a sample of the solution to be analysed added, with vigorous stirring for 5 minutes. Samples contained about 5 millimole SiO_2 . The solution was then removed from the ice bath and stirred more gently for about 4 hours while the temperature rose to room temperature. A solution of n-tetradecane in hexamethyldisiloxane (1 ml of a 0.065M solution) was added as an internal chromatographic standard. The organic layer was then separated, washed with water (3 portions of 30 ml) and stirred for 16 hours with Amberlyst 15 ion-exchange resin (2 g). The clear liquid was then decanted and analysed by gas-liquid chromatography. This analysis was carried out in the laboratories of I.C.I. p.l.c. using a model 2151 AC(G) Carlo-Erba gas chromatograph with a glass capillary column (10 m x 0.3 mm bore) coated with silicone rubber (OV1; Phase Separation Ltd.) and a flame ionisation detector. The column temperature was raised at 7.5K min^{-1} from an initial value of 393K to a final value of 598K which was maintained until the chromatogram was complete. Retention times and peak areas were computed and stored by a Commodore PET computer. By reference to standard retention times each peak could be identified and the amount present determined from the peak area. The computer could then print out these results.

3.2.4. Reactions with molybdic acid.

The composition of the molybdic acid reagent was based on that described by Alexander¹⁰ as later modified by

Iler.⁷ A stable 1 litre stock solution of ammonium molybdate was prepared from 100 g of $(\text{NH}_4)_6\text{Mo}_7\text{O}_{24}\cdot 4\text{H}_2\text{O}$, and 47 g of concentrated ammonium hydroxide (28% NH_3). The molybdic acid reagent contained 5 ml of the stock solution, 25 ml distilled water and 10.5 ml of 1.5N H_2SO_4 , and had a pH of about 1.2. About 0.5 ml of the silicate solution (0.5-1M SiO_2) was injected with rapid stirring into 20 ml of the reagent plus 4.5 ml distilled water, to give a total volume of 25 ml. At pH 1.2 the silicomolybdate ion is first generated as the yellow beta form which fades to a less intense yellow alpha form. At the pH selected the absorbance of a standard sample decreased by less than 5% in 1 hour. The optical density was measured at a wavelength of 410 nm at a constant temperature of 288K. The amount of silica in the sample is in excess of the molybdate ion so all the silica cannot convert to silicomolybdic acid. However, since only $\text{Si}(\text{OH})_4$ can react with molybdic acid, when the monomer is removed the polymeric silica must start to depolymerise. The rate of development of colour depends on the concentration of silica particles which remain. The concentration of silica in the samples was chosen so as to give measurable readings. When samples with a silica concentration closer to that normally recommended (to give at least sevenfold excess of molybdate ion over that required for complete conversion of all the silica), colour development was extremely slow and impossible to measure accurately.

3.2.5. Crystallization.

The reactions were carried out in the 1 litre polypropylene reactors described in Chapter 2. The reaction mixtures were agitated by means of stainless steel stirrer bars connected to electric motors. The stirring speed was 150 r.p.m. The reaction mixtures could be sampled through a hole drilled into the reactor lid. This was always firmly stoppered during the reaction. Each bottle was normally filled with 500g of solution. This large quantity of solution helped to minimise the effect due to loss of water through small leaks in the seals. The level of solution in the bottles could be monitored (with the stirrer switched off) by use of a dip-stick. In this way large losses could be compensated for by the addition of distilled water (kept at the reaction temperature). The reactors were placed in a 368K water bath or in a 353K thermostat bath. The reactions were either stirred immediately or allowed to remain static for 24 hours before stirring was commenced.

3.2.6. Analysis.

Samples (8 ml) were collected in glass sample bottles. They were allowed to stand for at least 24 hours before their pH was measured (as described in Chapter 2). Any solid material present in the sample sank to the bottom of the sample bottle during this period unless an amorphous gel phase had formed during the crystallization. Most samples were then filtered,

washed several times with warm water, then dried for 16 hours at 368K. Samples were then identified by X-ray powder diffraction using a Philips powder diffractometer (Cu K α radiation) as described in Chapter 2. For the stirred reactions at 368K (see section 3.4.2), a sample of the clear aqueous phase was removed and the silicon content determined using the molybdic acid method described in Chapter 2. Samples were then filtered (0.2 μ m filter) and washed several times with warm water. With those samples which contained amorphous gel some of the fine solid was lost in this process. The solid was dried for 16 hours at 368K, then equilibrated over saturated sodium chloride solution at 293K for 16 hours. Samples were then weighed and a portion calcined (for silicate reactions only) in order to obtain the weight of silica in the solid phase in the sample. The weight of silicon in the solid phase per litre of the reaction solution was found by dividing the weight of silicon in the sample by the sample volume. It was assumed that the calcined sample only contained silica.

When enough sample was available it was examined by X-ray powder diffraction using a Philips powder diffractometer (Cu K α radiation) as described in Chapter 2.

3.3. Results and discussion.

3.3.1. Hydrolysis of tetraethyl silicate.

Since it was hoped that the tetraethyl silicate could be used to "feed" growing crystals, initial experiments examined the type of solution obtained from different methods of hydrolysis. Table 3.1 summarizes the results for stirred hydrolysis (with no mutual solvent).

Hydrolysis, at a temperature which is really a minimum for zeolite crystallization (353K), proved to be very fast (Runs H1 and H2) and resulted in a white opaque solution, very similar in appearance to a solution of similar composition prepared from, for example, fumed silica. Highly alkaline solutions at room temperature could also result in very rapid hydrolysis and even the precipitation of silica (Run H3). The composition for H3 appeared to lie somewhere on a borderline between solutions which give precipitated silica and "clear" solid gels. Reaction H4 had the same composition but was stirred slightly more slowly. The initial progress of the reaction could be followed approximately by the change in the width of the tetraethyl silicate layer which sits on top of the aqueous layer when the solution is not being mixed. Figure 3.2 (curve 1) shows the width of the layer as time progressed. The initial part of the reaction appears to be first order as shown by the straight line graph in figure 3.3. Curve 2 in figure 3.2 shows how the pH of the aqueous solution falls as the hydrolysis proceeds. This shows that the

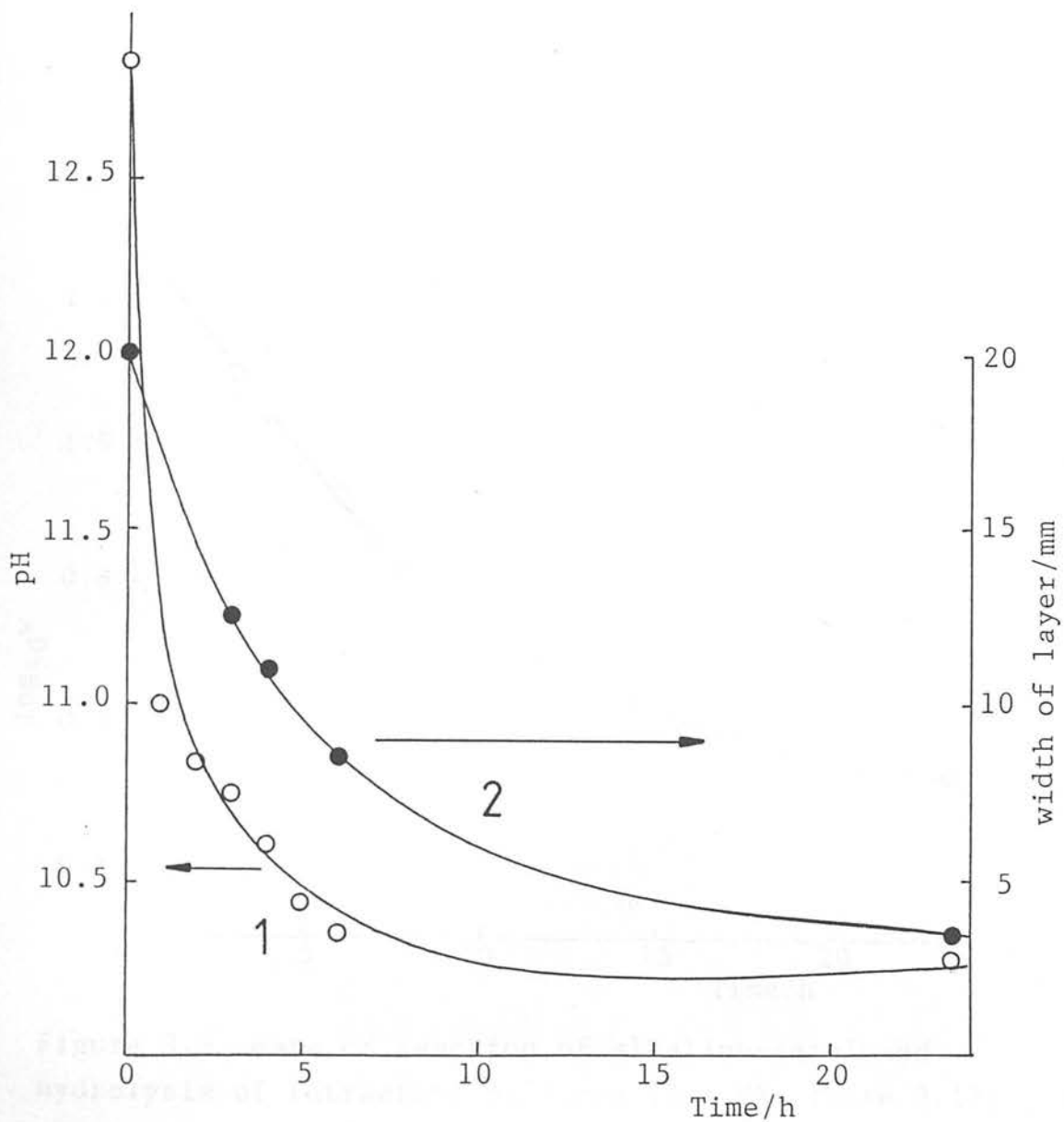


Figure 3.2. Change in the pH of the aqueous phase (curve 1) and in the width of the tetraethyl silicate layer (curve 2) as a function of time for Run H4 (see table 3.1).

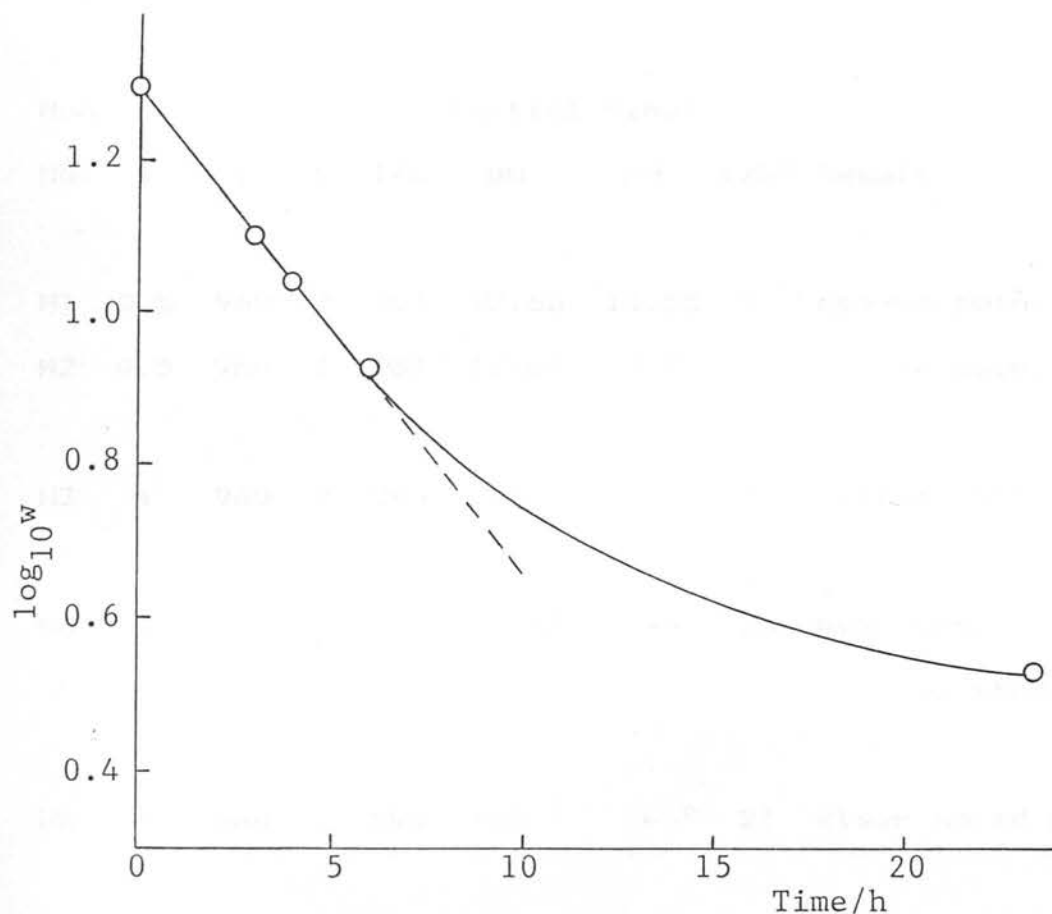


Figure 3.3. Rate of reaction of alkaline-catalyzed hydrolysis of tetraethyl silicate (Run H4, table 3.1), where w is the width of the tetraethyl silicate layer at time t . The reaction initially follows a first order rate but no longer follows a simple order after the pH of the aqueous solution levels off (see figure 3.2, curve 2).

Table 3.1. Hydrolysis of tetraethyl silicate.

All reaction mixtures have the composition $x\text{Na}_2\text{O} \cdot 20\text{SiO}_2 \cdot y\text{H}_2\text{O} \cdot z\text{TFABr} \cdot \text{BOEtOH}$.

Run No.	x	y	z	T/K	Initial Final		t/h*	Result
					pH	pH		
H1	0.5	960	2	353	12.65	10.55	3	opaque soln.
H2	0.5	960	2	353	12.65	9.90	4	opaque soln.
H3	1	960	2	293	>13	--	4	silica pptd.
H4	1	960	2	293	12.83	--	28	hydrolysis not completed
H5	1	960	2	293	>13	--	21	clear solid gel
H6	1	1960	2	293	12.67	10.41	65	clear soln.
H7	0.5	1000	0	293	12.70	10.92	19	clear soln.
H8	0.5	500	0	293	>13	11.10	19	clear soln.

* t = time for hydrolysis

catalyst is in fact removed as the reaction progresses due to the formation of silicate anions. The removal of catalyst appeared to be a problem at this composition since the hydrolysis reaction for H4 appeared to almost stop while reaction H5 gave a clear solid gel.

When the water content was approximately doubled (Run H6), the resulting solution was clear and apparently, much more stable. When the salt (TPABr) is omitted during the hydrolysis then solutions which are more concentrated (in silica) can be prepared, e.g. Runs H7 and H8.

The compositions (H7, H8) which do not contain salt remain as clear solutions indefinitely. The effect of the addition of salts to the hydrolysed tetraethyl silicate solutions is tabulated in table 3.2. The addition of the salt leads to further polymerisation of the silicate polymers which eventually results in a clear solid gel.

Analysis by ^1H and ^{13}C nuclear magnetic resonance only detected the presence of ethanol. Hence the clear solutions produced by the hydrolysis of the tetraethyl silicate do not contain any detectable unreacted tetraethyl silicate. (This analysis was carried out by the Analytical service at I.C.I. Laboratories, Runcorn.). If any tetraethyl silicate had remained intact then it would certainly be very quickly hydrolysed when the solution was raised to the high temperatures normally required for zeolite

Table 3.2. The effect of the addition of salts to a hydrolysed tetraethyl silicate solution of composition $0.5\text{Na}_2\text{O} \quad 20\text{SiO}_2 \quad 80\text{EtOH} \quad 1000\text{H}_2\text{O} \quad x\text{MBr}$.

Salt	x	Time taken to form a solid gel/h
M = Na	4	0.01
	2	0.1
	1	0.3
	0.5	70
M = TPA	4	20
	2	65
	1	340
	0.5	--

crystallization (over 353K).

Static hydrolysis reactions were also carried out (table 3.3) but were not very satisfactory. The tetraethyl silicate layer floats on top of the aqueous layer. If aluminium is present in the aqueous layer then a white solid membrane is quickly formed between the layers. (e.g. SH4-6 in table 3.3). The addition of excess salt also results in the rapid formation of a membrane (see SH7 and 8). Hydrolysis reactions at 353K were quite fast and often resulted in the crystallization of a zeolite (see table 3.3). The composition (SH2) with no aluminium or excess salt present did not form a membrane, although it did produce silicalite-1. After these experiments static hydrolysis was abandoned because of the length of time required and the other problems associated with it. The clear solutions produced by stirred hydrolysis seemed to promise a more fruitful route to zeolite synthesis.

3.3.2. Trimethylsilylation.

It has already been noted that some of the reaction mixtures produced by stirred hydrolysis were completely clear, whereas the same compositions prepared with amorphous silica were opaque. The origin of this difference must lie in the nature and relative proportions of the silicate, polysilicate and colloidal silica present. The distribution of small silicate anions (up to anions which contain 8 silicon atoms as well as anions with charges of -10 and -12) could be

Table 3.3. Static hydrolysis of tetraethyl silicate.

All reaction mixtures have the composition $a\text{Na}_2\text{O} \cdot 20\text{SiO}_2 \cdot b\text{Al}_2\text{O}_3 \cdot c\text{H}_2\text{O} \cdot d\text{NaBr} \cdot e\text{TPABr} \cdot \text{BOEtOH}$.

Run No.	a	b	c	d	e	T/K	Time /day	Product
SH1	1	0	960	-	2	293	50 [*]	clear solid gel.
SH2	1	0	960	-	2	353	25	silicalite.
SH3	1	0	960	-	2	323	29	clear solid gel.
SH4	40	20	4960	-	-	293	50 [*]	amorphous solid.
SH5	40	20	4960	-	-	353	4	zeolite A.
SH6	25	5	1210	-	-	353	4	zeolite X.
SH7	1	0	960	200	2	323	50 [*]	cloudy soln. with
SH8	1	0	960	20	2	323	50 [*]	amorphous solid at interface.

* solutions removed after this time.

measured using the trimethylsilylation technique. Several different samples were examined at both room temperature and at 363K. Table 3.4 lists some typical results. The percentage by weight of the small anions is compared for several different samples. The results show that solutions hydrolysed with TPABr present have a slightly lower monomer content (e.g. compare T1 and T2 with T3 and T4). Aging of the gel does not seem to lead to a large reduction in monomer content. When the gels were heated the amount of monomer increased (e.g. compare T4 with T4Ha and b). However, there is very little difference in the anion distribution between a reaction at 363K which contains TPABr (T4Hb) and one which does not (T4Ha) even though T4Hb produced silicalite while T4Ha never crystallized. The silicate anion distribution found for these tetraethyl silicate solutions did not seem to offer any reason for the different properties of these solutions. In particular they had a very high polymeric content similar to that of opaque reaction mixtures. Indeed the anion distributions are not very different from what might be expected of a 0.5M sodium polysilicate solution (e.g. see T5).

Identification of these small anions was also considered important since the "building bricks" for the zeolite are likely to be small units (perhaps even monomer) rather than large complex units which would have to form several bonds to join together. The

Table 3.4. Distribution of anions in silicate solutions*
 - effect of temperature and addition of TPABr on
 solutions of composition $1\text{Na}_2\text{O} \cdot 20\text{SiO}_2 \cdot 196\text{OH}_2\text{O} \cdot 80\text{EtOH}$
 $\times\text{TPABr}$.

Run NO.	T/K (a)	t/ day (b)	x	Weight % Si present as anions with											
				no. of Si atoms										charge	
				1	2	3	4	5	6	7	8	12	>12		
T1	293	75	2	1.2								0.1		98.2	
T2	293	14	2	1.4									0.3	98.3	
T3	293	35	0	2.5										97.5	
T4	293	8	0	1.7	0.1							0.1		98.2	
T5	293	8	0	2.6	0.2									97.1	
T2H	363	3	2	4.8	0.4								0.1	94.7	
T4Ha	363	3	0	5.4	0.5	0.1								94.0	
T4Hb	363	3	2	5.0	0.4	0.1								94.5	

* All silicate solutions were prepared from tetraethyl silicate except T5, which was prepared from fumed silica (cab-o-sil).

(a) Temperature at which trimethylsilylation was carried out.

(b) Time at temperature, T, before trimethylsilylation was carried out.

trimethylsilylation results do show a rise in monomer content when the solutions are heated to the reaction temperature. Yet more than a high monomer content is needed as comparison of reaction mixtures T4Ha, which did not crystallize, and T4Hb, which gave silicalite, shows.

3.3.3. Molybdic acid analysis.

One problem with zeolite synthesis is that of reproducibility. The hydrolysed tetraethyl silicate solutions could be prepared in a systematic manner but it was necessary to have a method to check if different batches of the same composition were sufficiently identical. As mentioned earlier, it was decided to use the well known reaction with molybdic acid for this purpose.

Only the monomer $\text{Si}(\text{OH})_4$ reacts with molybdic acid. When the solution becomes unsaturated due to the removal of monomer, larger particles begin to dissolve and become smaller. As the particles dissolve their solubility rapidly increases with their diminishing size. Smaller particles therefore tend to dissolve first and continue to do so until they disappear. The rate of reaction of the polymeric silica with molybdic acid is therefore the rate at which the polymer dissolves to form monomer. The rate of this reaction is the rate of development of the yellow colour due to the formation of silicomolybdic acid.

The result of the reaction of a hydrolysed solution

(composition $1\text{Na}_2\text{O}$; 20SiO_2 ; $1960\text{H}_2\text{O}$; 80EtOH) with molybdic acid is shown in figure 3.4. The curve represents the reaction of molybdic acid with the solution 1 day after hydrolysis had finished. Similar results were also obtained 7 days after hydrolysis. The crosses represent a reaction with the same composition, again seven days after hydrolysis. These results show that similar compositions have similar compositions after at least seven days aging. With a more concentrated silicate solution the rate of colour development is much slower. This is shown in figure 3.5 where a solution (composition $0.5\text{Na}_2\text{O}$; 20SiO_2 ; 80EtOH ; $500\text{H}_2\text{O}$) is compared with the solutions portrayed in figure 3.4.

Unfortunately it was found that the addition of TPABr led to a slightly cloudy solution which interfered with the analysis. This meant that solutions hydrolysed in the presence of TPABr could not be tested.

3.4. Crystallization

In section 3.3.1. it was noted that some of the static hydrolysis reactions produced zeolite at 353K. The "clear" solutions produced by the stirred hydrolysis were also investigated to see how well they could replace traditional silica sources.

3.4.1. Reactions at 353K.

Initial reactions at 353K were disappointing with thick opaque gels formed very soon after stirring commenced

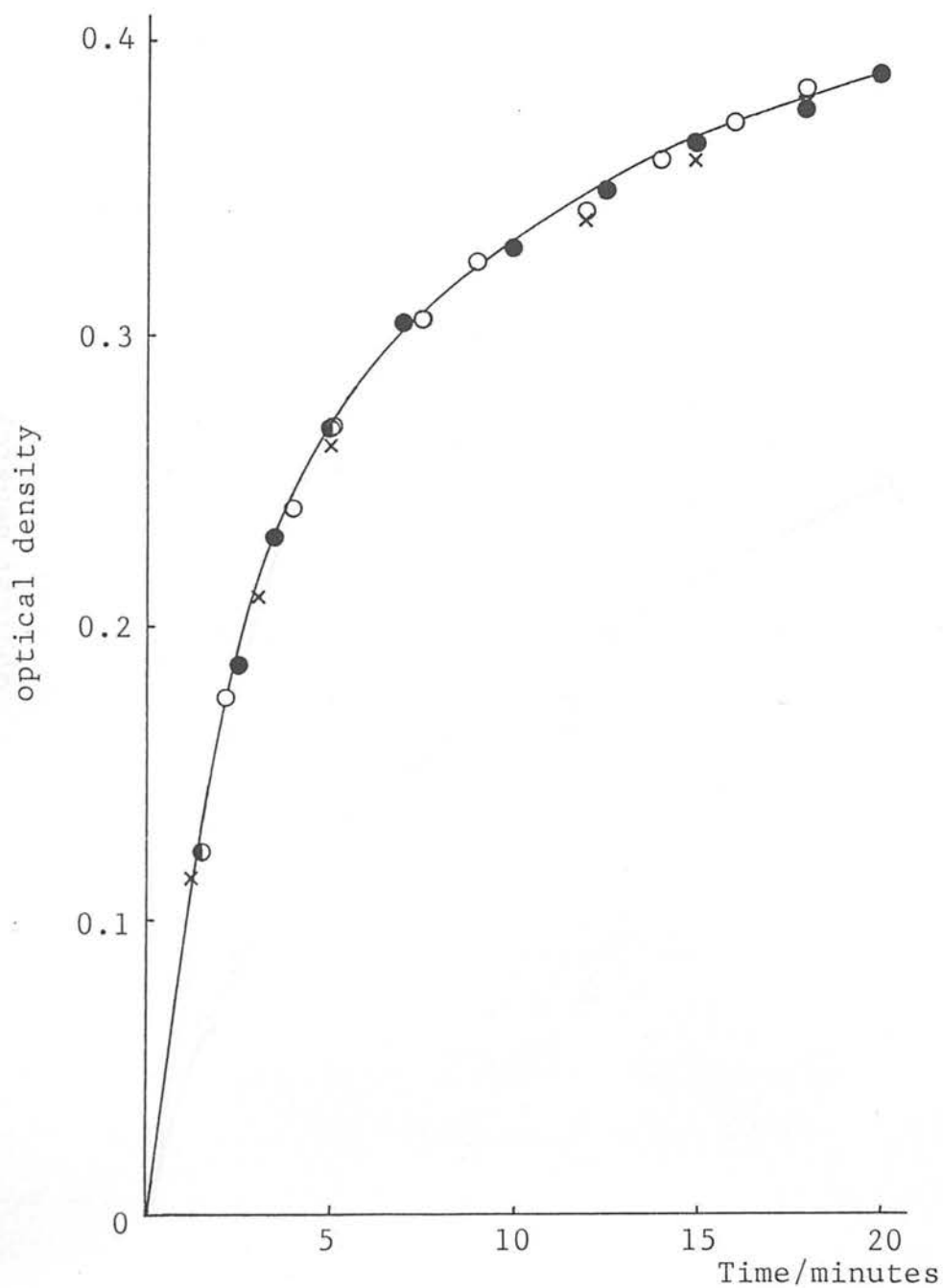


Figure 3.4. Reaction of molybdic acid with a hydrolysed tetraethyl silicate solution (composition $1\text{Na}_2\text{O} \cdot 20\text{SiO}_2 \cdot 1960\text{H}_2\text{O} \cdot 80\text{EtOH}$) 1 day (-o-) and 7 days (-●-) after hydrolysis. The crosses represent a reaction of the same composition 7 days after hydrolysis.

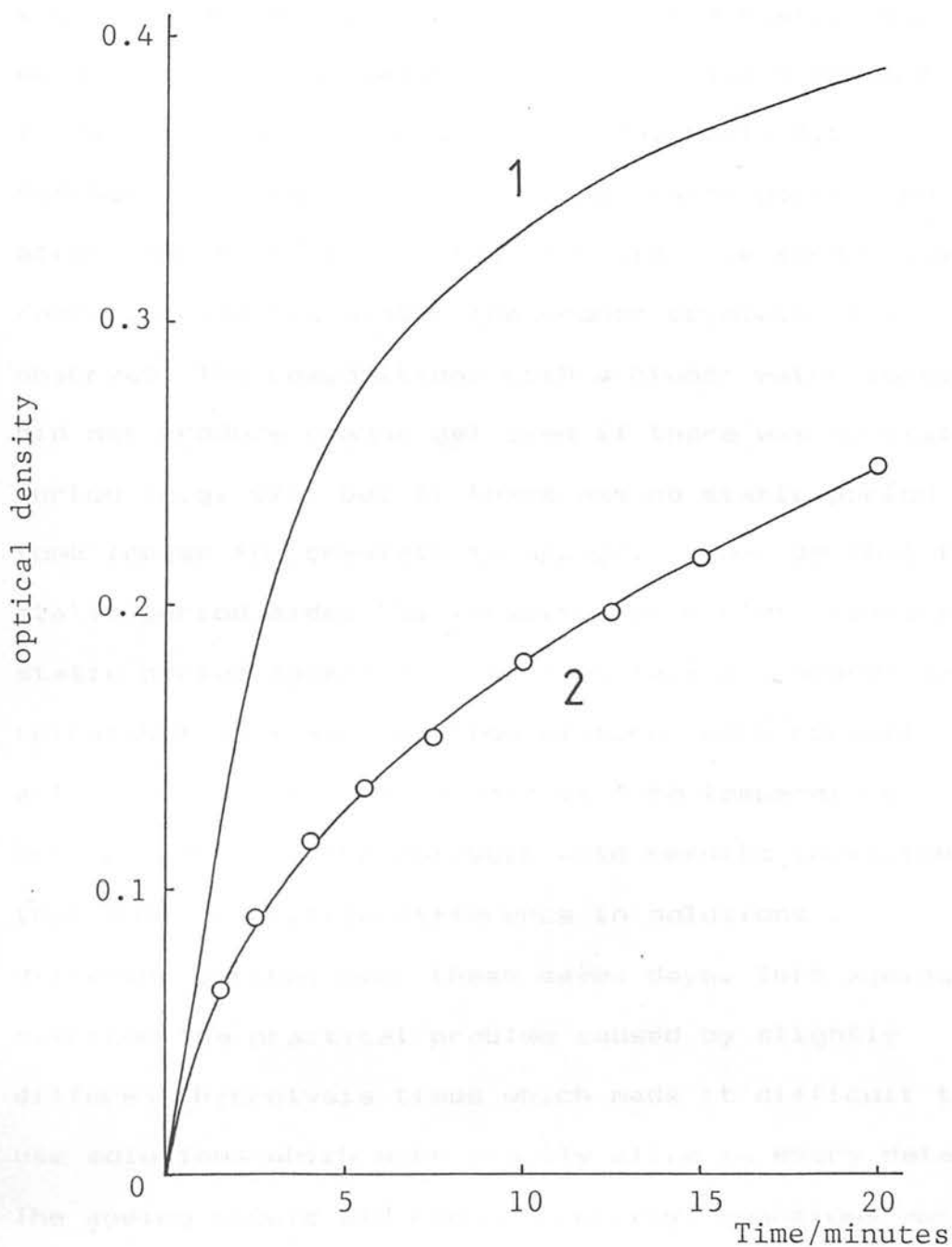


Figure 3.5. Reaction of molybdic acid with a hydrolysed tetraethyl silicate solution (composition $1\text{Na}_2\text{O} \cdot 20\text{SiO}_2 \cdot 80\text{EtOH} \cdot 1960\text{H}_2\text{O}$), (curve 1) compared with the reaction of a more concentrated solution (composition $0.5\text{Na}_2\text{O} \cdot 20\text{SiO}_2 \cdot 80\text{EtOH} \cdot 500\text{H}_2\text{O}$), (curve 2). Both reactions carried out 7 days after hydrolysis.

e.g. runs S1 and S2 in table 3.5. Yet a static reaction made from the same batch as S2 crystallized without the formation of an opaque gel (run S2a, table 3.5).

Further reactions showed that the static period could affect the formation of the crystals. The longer the reaction remained static the sooner crystals were observed. The compositions with a higher water content did not produce opaque gel even if there was no static period (e.g. S7), but if there was no static period it took longer for crystals to appear. It may be that the static period aided the formation of nuclei. Since the static period appeared to be important all hydrolysed tetraethyl silicate reaction mixtures were normally allowed to age for seven days at room temperature before reaction. The molybdic acid results indicated that there is little difference in solutions from different batches over these seven days. This ageing overcame the practical problem caused by slightly different hydrolysis times which made it difficult to use solutions which were exactly alike in every detail. The ageing should aid reproducibility. Reactions were also allowed to remain static for at least 24 hours at the reaction temperature. This static period should help aid the crystallization of the zeolite but later results suggested that it may not be necessary (see 3.4.2.). These reactions were of particular interest because the silicalite crystallized without the formation of an intermediate amorphous gel. The

Table 3.5. Synthesis of silicalite from stirred solutions at 353K.

All reaction mixtures have the composition $a\text{Na}_2\text{O} \cdot 20\text{SiO}_2 \cdot b\text{H}_2\text{O} \cdot 2\text{TPABr} \cdot 80\text{EtOH}$ and produced silicalite.

Run No.	a	b	T/K	t / 1 day	t / 2 day	t / 3 day	t / 4 day	Comments
S1	1	960	353	-	0	11	4	via opaque gel
S2	1.6	1420	353	0.67	0	13	13	via opaque gel
S2a [#]	1.6	1420	353	0.67	13	13	4	no gel
S3	1.5	1460	353	3	1	13	3	no gel
S4	1	1960	353	25	3	16	1	no gel
S5	1	1960	353	1	1	25	5	no gel
S6 [*]	1	1960	353	1	1	27	5	no gel
S7	1	1960	353	0	0	25	12	no gel

t_1 = static ageing at room temperature

t_2 = static ageing at 353K

t_3 = time taken to crystallize at 353K; t_3 includes t_2

t_4 = time at 353K before crystals observed

[#]This reaction was never stirred

^{*}TPABr added after time t_1

crystallization and growth of the silicalite can only be from the solution phase and is independent of the solid gel phase normally found in zeolite crystallization. Most zeolites are synthesized from alkaline aluminosilicate gels where the heterogeneous phases (amorphous solid and aqueous solution) both contribute to the zeolite formation. This led to the proposal of two different hypotheses for zeolite crystallization, namely in the gel phase¹¹ or from solution phase.¹² The absence of an amorphous gel phase in the silicalite crystallizations obviously precludes the gel phase hypothesis in this case.

3.4.2. Reactions at 368K.

The importance of a gel phase could now be examined by a comparison of silicalite crystallizations from solution with those via an amorphous gel. Because the zeolite is produced from a clear solution the normal method of following the progress of the crystallization is unsuitable. X-ray powder diffraction is normally used to follow zeolite crystallization. When crystallization occurs from gels the growing crystals are mixed with the amorphous material. Consequently X-ray powder diffraction can also show how the percentage crystallinity increases until no amorphous material is present. When there is no gel phase there is no amorphous material and consequently each sample is the same when X-rayed at different times during the crystallization. What does change is the amount of

crystalline material per unit volume of sample, and the concentration of silica in solution. This opened up two entirely new ways of following a zeolite crystallization. The amount of solid material per ml could be obtained at different times during crystallization and also the amount of dissolved silica per ml could be determined as well. A comparison was therefore made between a reaction which produced zeolite via a gel and one which bypasses this stage.

The procedure outlined above was carried out for two reactions with the same composition but prepared from different silica sources. The composition used was the same as that used for reactions S4 to S7, all of which produced silicalite from clear solutions. Both reactions were prepared in the same manner using method 1 described in section 3.2.2., except that in one case cab-o-sil and ethanol were added instead of tetraethyl silicate. Both solutions were aged at room temperature for seven days and then allowed to remain static at 368K for a further 24 hours. The tetraethyl silicate solution remained clear while the cab-o-sil solution produced a cloudy gel. The change in pH (curve 1) and silica content in the solution phase (curve 2) and solid phase (curve 3) are shown for each reaction in figure 3.6 and 3.7. It can be seen that the clear solution system shows a marked decrease in silica concentration (solution phase) matched by an increase in the silica concentration (solid phase). This occurs

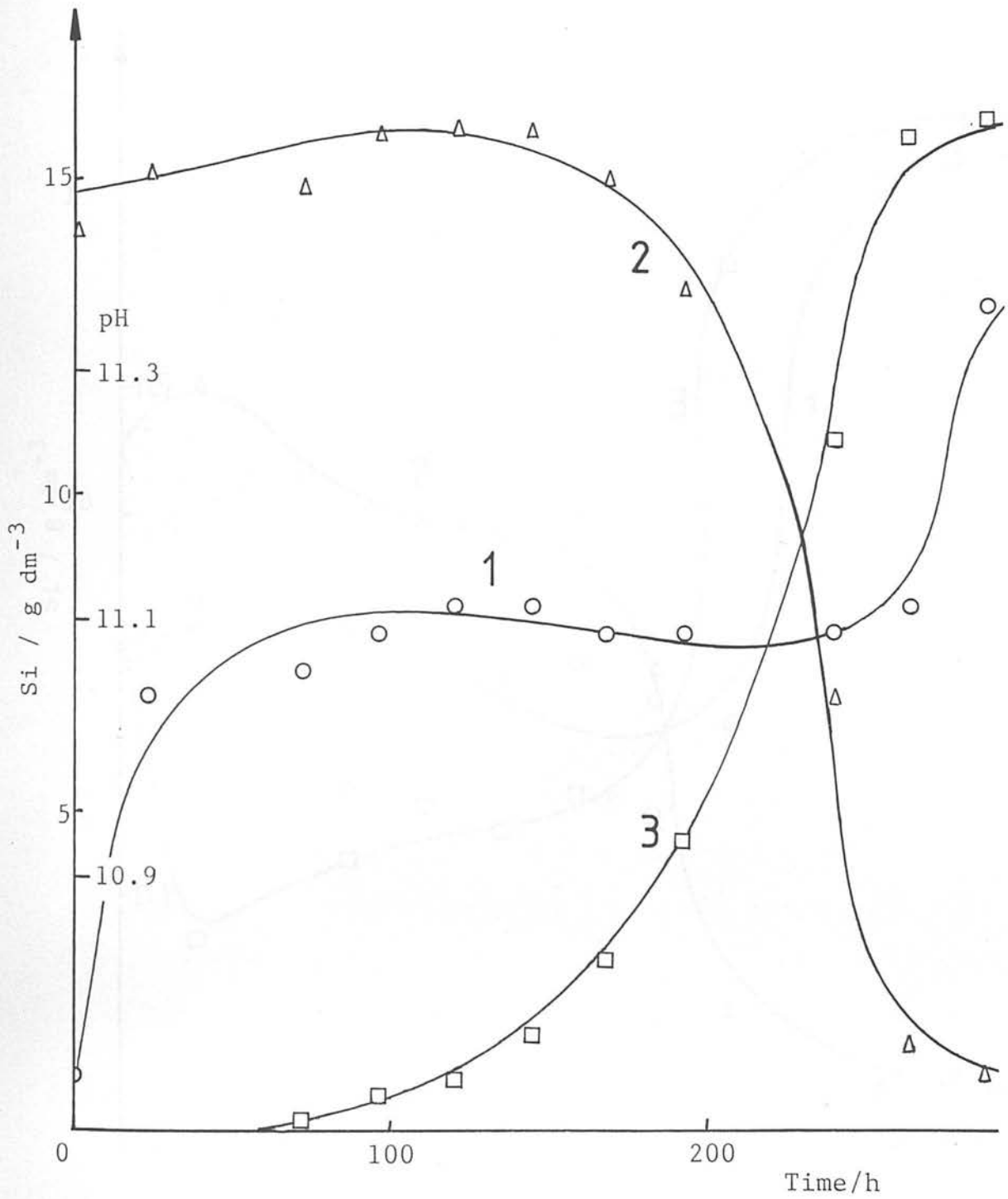


Figure 3.6. pH (curve 1); silicon content in the solution phase (curve 2) and solid phase (curve 3) as a function of time for a reaction mixture of composition $1Na_2O\ 20SiO_2\ 1960H_2O\ 2TPABr\ 80EtOH$. Silica source = tetraethyl silicate.

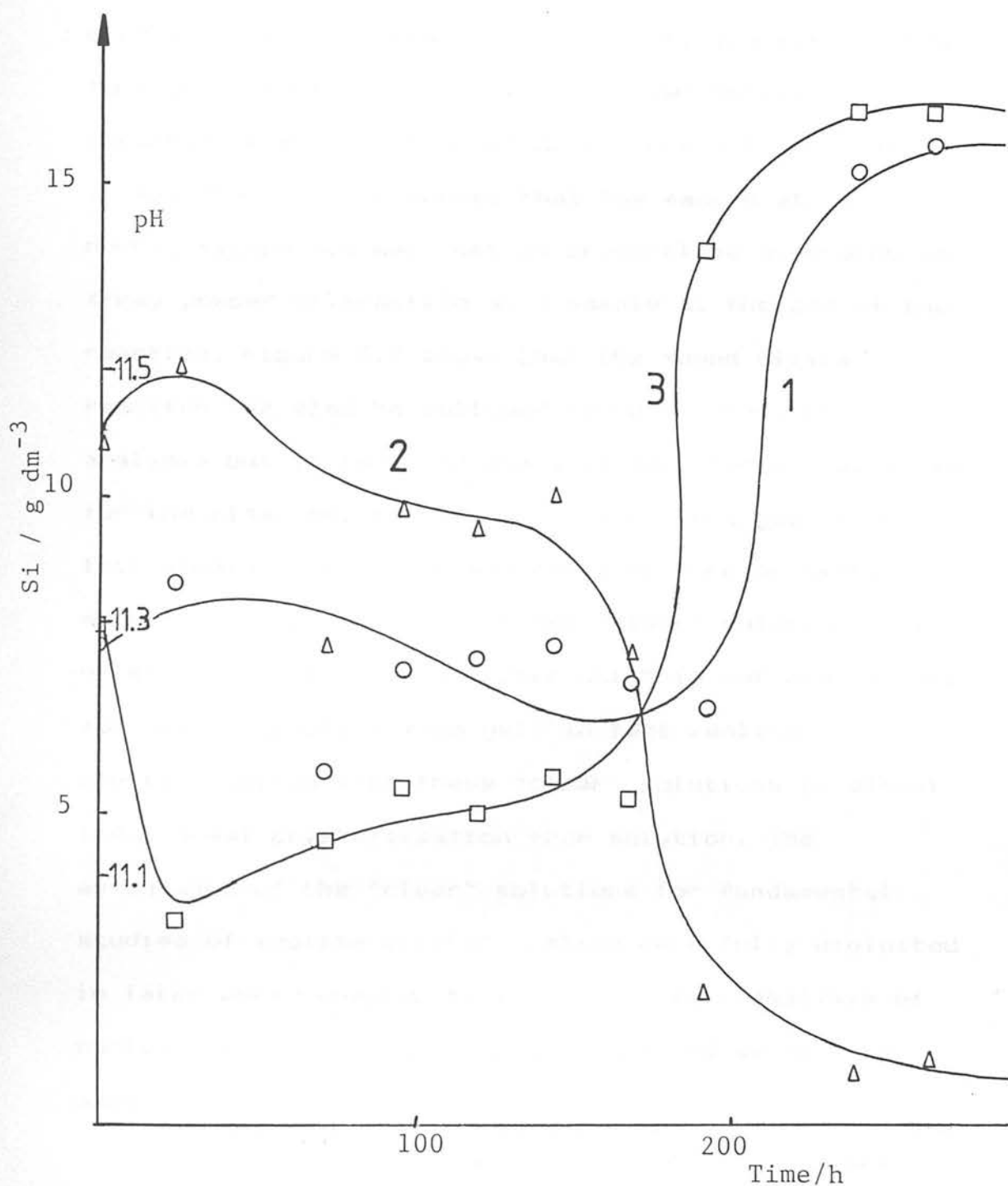


Figure 3.7. pH (curve 1); silicon content in the solution phase (curve 2) and solid phase (curve 3) as a function of time for a reaction mixture of composition $1\text{Na}_2\text{O} \cdot 20\text{SiO}_2 \cdot 1960\text{H}_2\text{O} \cdot 2\text{TPABr} \cdot 80\text{EtOH}$. Silica source = fumed silica (cab-o-sil)

just before the rapid increase in pH which normally occurs at the end of a zeolite crystallization. As expected the solid phase curve is very similar in shape to the S-shaped crystallization curves normally obtained. When enough material was present in a sample it was found, for example, that the sample at 240 hours, figure 3.6 was just as crystalline according to X-ray powder diffraction as a sample at the end of the reaction. Figure 3.7 shows that the fumed silica reaction can also be followed by this method of analysis but it is by no means as satisfactory as it is for the clear solutions where the solid phase is in fact always crystalline and not a mixture of amorphous material and crystals. Thus the "clear" solution does offer a new method of analysis which is not appropriate for crystallization from gel. In fact zeolite crystallization from these "clear" solutions is almost like normal crystallization from solution. The advantages of the "clear" solutions for fundamental studies of zeolite crystallization were fully exploited in later work (Chapter 5) in which a full analysis of nucleation and crystal growth in stirred systems is made.

The "clear" solutions do not appear to offer any advantages as far as the speed of crystallization is concerned. If anything the cab-o-sil reaction is somewhat faster than the tetraethyl silicate reaction. The difference could be due to the number of nuclei

produced in each reaction. The fumed silica may produce more nuclei or offer more nucleation sites than the clear solution. This could lead to a shorter crystallization time as the larger number of crystals would use up the available nutrient at a faster rate (see Chapter 5).

3.4.3. Crystallization of ZSM-5.

When aluminium was introduced into the reaction mixtures produced by the tetraethyl silicate, the reaction mixtures remain clear, even at reaction temperature, provided the reaction mixture composition has a higher water content. Since the aluminium is added as a sodium aluminate solution the final reaction mixture composition also has a higher base content. If aluminium is present in the reaction mixture the zeolite ZSM-5 is produced rather than silicalite. Both silicalite and ZSM-5 have similar X-ray powder diffraction patterns. They only differ from one another in chemical composition. Silicalite is an all silica form of ZSM-5. (*see appendix 3*)

Typical compositions and crystallization times are shown in table 3.6 for reactions which produce ZSM-5. It can be seen from the table that the time that the aluminium is added is important. If the aluminium is present before the tetraethyl silicate is hydrolysed (method 1, section 3.2.2) then the crystallization takes much longer than if the aluminium is added after the hydrolysis (method 2, section 3.2.2). It appears

Table 3.6. Synthesis of ZSM-5 from stirred solutions at 368K.

All reaction mixtures have the composition $3\text{Na}_2\text{O}$ 20SiO_2
 $x\text{Al}_2\text{O}_3$ $y\text{H}_2\text{O}$ 2TPABr 80EtOH .

Run No.	Method	x	y	t ₁ /day	t ₂ /day	t ₃ /day
Z1	1	0.2	2960	7	1	42
Z2	2	0.2	2960	7	1	5.4
Z3	1	0.33	2960	7	1	81
Z4	2	0.33	2960	7	1	13.3
Z5	2	0.2	2420	7	1	12

Method 1: hydrolysis in aluminate solution.

Method 2: aluminate added just before heating.

t₁ = static ageing at room temperature

t₂ = static ageing at 368K

t₃ = time taken to crystallize at 368K; t₃ includes t₂

that the presence of aluminium during the hydrolysis leads to a delay in nucleation. Figure 3.8 shows the pH profiles for reactions Z1 and Z2 which have the same composition (see table 3.6) but Z1 was prepared by method 1 and Z2 by method 2. No crystals were observed in reaction Z1 until after Z2 had crystallized completely.

Since the ZSM-5 reactions crystallize from "clear" solutions just like the silicalite reactions, it is possible to follow these reactions by finding the weight of product per unit volume at different stages of the reaction. This can be seen in figure 3.9 for reaction Z5. Thus even reaction mixtures which contain aluminium can be treated almost as normal crystallizations from solution.

The effect of aluminium on the crystal growth is discussed further in Chapter 4.

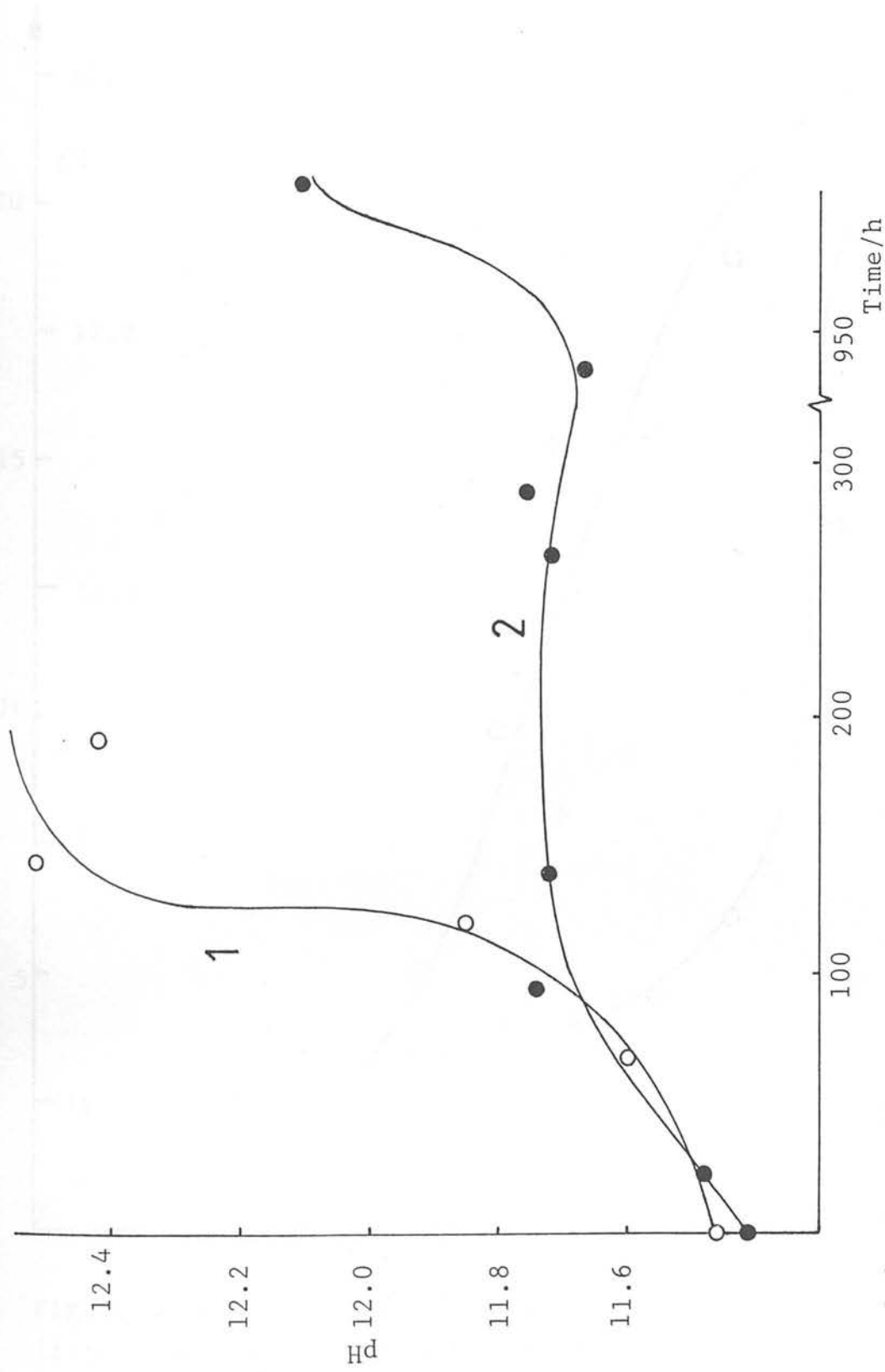


Figure 3.8. Crystallization of ZSM-5 (Run 22 (curve 1), Run 21 (curve 2)) followed by pH measurements.

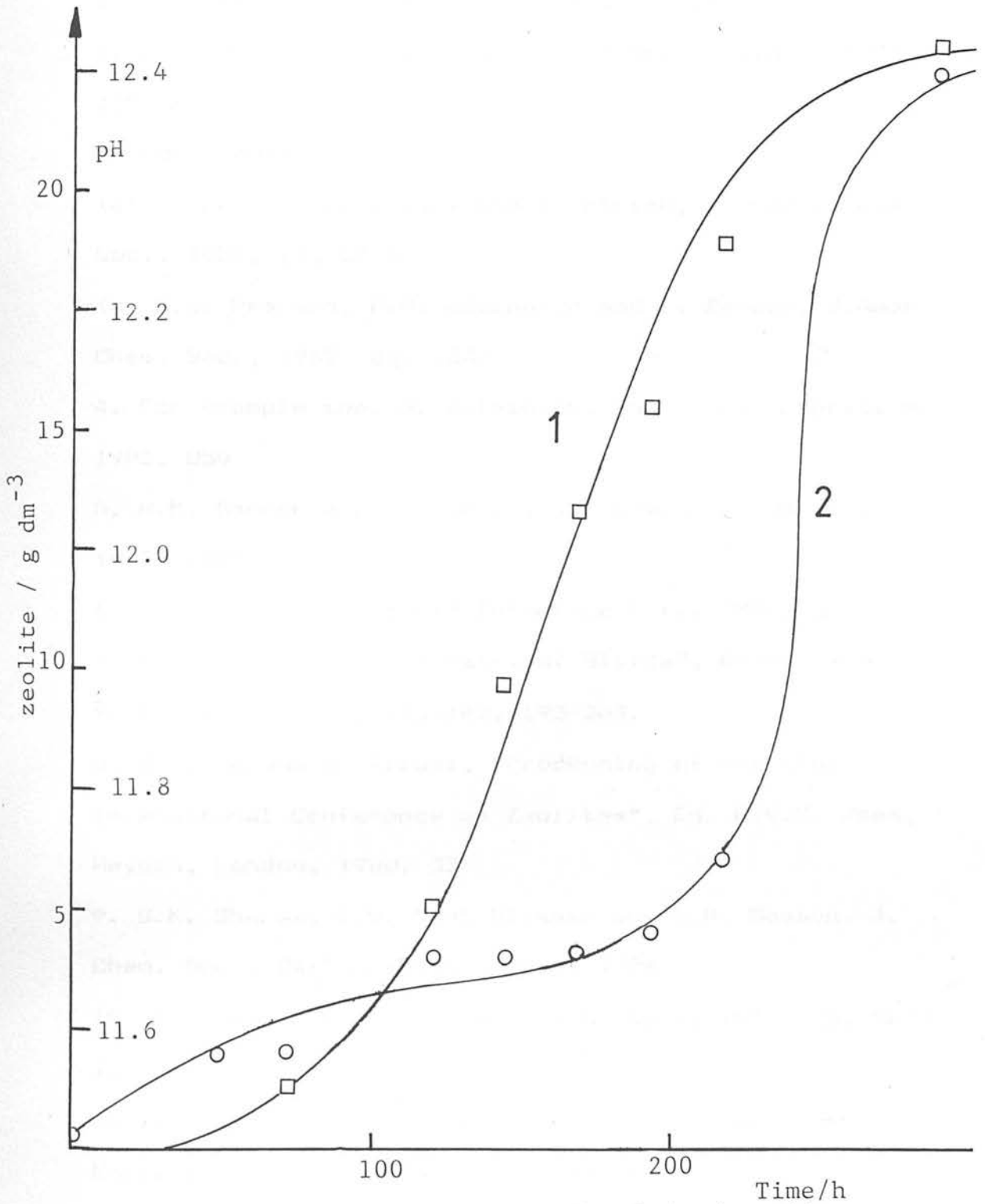


Figure 3.9. Reaction Z5: Weight of calcined zeolite per litre (curve 1) and pH (curve 2) as a function of time.

3.5. References.

1. G.T. Kerr, J. Phys. Chem. 1966, 70, 1047
2. E.W. Valyocsk, European Patent Application 0012572, (1979).
3. For example
 - (a) R. Aelion, A. Loebel and F. Eirich, J. Amer. Chem. Soc., 1950, 72, 5705
 - (b) R.G. Pearson, D.N. Eddington and F. Basolo, J. Amer. Chem. Soc., 1962, 84, 3233
4. For example see, G. Wilkinson, Chemistry in Britain, 1982, 850
5. R.M. Barrer and W. Sieber, J. Chem. Soc. Dalton, 1977, 1020
6. R.K. Iler, J. Colloid Interface Sci., 1980, 75, 138
7. R.K. Iler, "The Chemistry of Silica", Wiley, New York, 1979, 95-97, 138-142, 195-203.
8. S. Ueda and M. Kozumi, "Proceeding of the 5th. International Conference on Zeolites", Ed. L.V.C. Rees, Heyden, London, 1980, 33
9. S.K. Sharma, L.S. Dent-Glasser and C.R. Masson, J. Chem. Soc., Dalton Trans., 1973, 1324
10. G.B. Alexander, J. Amer. Chem. Soc., 1953, 75, 5655
11. For example
 - (a) D.C. Breck and E.M. Flanigen, "Molecular Sieves", Society of Chem. Industry, London, 1968, 47
 - (b) B.D. McNicol, G.T. Pott and K.R. Loos, J. Phys. Chem., 1972, 76, 3388
 - (c) R. Aiello, C. Colella and R. Sersale, Adv. Chem.

Ser., 1971, 101, 51

12. For example

(a) G.T. Kerr, J. Phys. Chem., 1966, 70, 1047

(b) J.Ciric, J. Colloidal Interface Sci., 1968, 28, 315

(c) A. Culfaz and L.B. Sand, Adv. Chem. Ser., 1973,
121, 141

Chapter 4 Zeolite Crystal Growth Followed by Optical Microscopy.

4.1 Introduction

The size, shape and structure of zeolite crystals are very important factors in zeolite catalysis. Large zeolite crystals are desirable for basic studies of catalysis and sorption by zeolites. The use of large crystals reduces the contribution from crystal surface reactions and allows the effect of internal surface reaction and diffusion to be examined. Large crystals ($>100 \mu\text{m}$) are also needed for structure determination by single crystal X-ray diffraction measurements. The main efforts of industrial workers have been directed at the production of small crystals in order to minimise intracrystalline diffusion.¹ This step is a rate-limiting step in catalysis and affects the whole process. However some sorption work² has suggested that large crystals of certain zeolites may offer advantages over small crystals.

The majority of synthetic zeolites tend to be formed with a small crystal size (c.a. $0.1-10 \mu\text{m}$).³ Large crystals of the more stable, compact zeolites have been obtained at high temperatures (e.g. 0.5 mm diameter analcime has been grown at 573K ⁴) but zeolites with more open frameworks cannot be obtained at these high temperatures. Table 4.1 lists some successful attempts at the growth of larger than normal zeolite crystals. From the table it can be seen that the zeolite ZSM-5 and its all silica analogue, silicalite-1, can be grown

Table 4.1 Larger than normal zeolite crystals

Zeolite	Crystal size claimed/ μm	Conditions used	Reference
Low Si/Al: Analcime	500	High temperature	4
Sodalite	12000	Temp. gradient	5
A	up to 75	Counter diffusion conditions (Al and Si solutions allowed to diffuse through a gel then meet)	6
P	" " 150		
X	" " 40		
A	100	Low temperature and a buffering agent	7
X	140		
Y	40	Dilute system, low pH	8
P	>100	Crystallized from glass. (No other information)	9
S	300		
Mordenite	>400		
High Si/Al: ZSM-5	200	Dilute system, low Na	10
"	100	Includes TMA. Control OH/SiO ₂ and TMA/SiO ₂ ratios.	11
"	140	(NH ₄ ⁺) ₂ O-Li ₂ O system	12
Silicalite	>200	NaF added	13

to give a larger than normal crystal size (crystals in the region of 0.1 mm or more). This makes silicalite-1 an ideal candidate for the study of the effect of various factors on the growth of large crystals. Silicalite-1 also has the advantage of a very simple composition. As it is a silica molecular sieve no aluminium is added to the reaction mixture, thus simplifying its preparation and structure.

Some of the important factors which influence nucleation and growth of crystals were discussed in Chapter 1 and are listed in table 4.2. To produce large crystals it is necessary to limit the nucleation rate and increase the growth rate. It is clear from table 4.2 that to limit nucleation zeolite reaction mixtures should be free from impurities, static, low in hydroxide, and sodium ion content and have a high viscosity, and that reactions should be carried out at low temperatures. However, low temperatures and hydroxide ion concentrations will also limit growth, so obviously some sort of compromise must be made. The studies described in the previous chapter showed how zeolite could be crystallized from a "clear" colloidal dispersion. The tetraethyl silicate hydrolyzed mixtures appeared to offer a totally new approach to the study of zeolite crystal growth. The absence of an opaque gel makes it easier to see the crystals by optical microscopy. In conventional zeolite synthesis the progress of zeolite crystallization is normally

Table 4.2 Factors which influence nucleation and growth

Factor	Effect
Reagent impurities	Can act as nucleation centres
Agitation	Favours the formation of nuclei by increasing the rate of diffusion of nutrient to the nuclei, ¹⁴ so that the nuclei grow rather than dissolve. Additional solid particles may also be produced by abrasion.
Temperature	Growth and nucleation rates both increase with temperature.
Hydroxide	In general, an increase in the hydroxide content leads to faster growth and nucleation rates. ¹⁵
Cation	Certain ions (e.g. sodium) appear to aid nuclei formation. Other ions may inhibit nucleation. ¹²
Viscosity	In general an increase in viscosity gives fewer nuclei. ¹⁶

followed by bulk methods of analysis e.g. X-ray powder diffraction and thermal analysis. These methods are unable to tell very much about the crystal morphology (i.e. size and shape) or the way in which the crystals grow. Since initial studies indicated that it was possible to grow silicalite from sols produced by the hydrolysis of tetraethyl silicate to sizes larger than $1 \mu\text{m}$, it seemed that the silicalite system was an ideal one for further study. The growth of crystals could be followed by optical microscopy, provided large enough crystals could be formed. The purpose of the studies described in this chapter was to find a suitable method for the study of zeolite crystal growth which would allow the shape and size of crystals to be observed as they grew. The effect of various changes in conditions on the growth of the crystals could then be observed directly.

In order to achieve this aim, conditions had to be found which were suitable for the growth of larger than normal crystals. If all the zeolite crystals only reached a maximum size of $1 \mu\text{m}$ it would not be possible to study their growth by optical microscopy. The optical microscope is to be preferred over the scanning electron microscope (s.e.m.) as this requires the growing crystal to be removed from its mother liquor for examination. This chapter describes how a suitable method was developed to observe the growth of crystals with the use of an optical microscope. For these

studies it was necessary to seal the reaction mixture in a glass capillary tube before placing at the reaction temperature. Subsequently the capillary tube could be removed from the oven and then returned after examination with the optical microscope. It was found that ordinary glass melting point tubes were adequate for this work but much better results were obtained when "microslides"¹⁷ were used. These are flat, rectangular, open-ended glass micro-capillary tubes with precision optical path lengths. They are made from heat-resistant glass and can easily be filled by capillary action.

This method of observing the course of the reaction allowed growth rates of the different crystal faces to be observed for different temperatures and different compositions. Conditions were found which could produce silicalite crystals of 50 μm to over 200 μm in size. The temperature dependence of the rate of silicalite crystal growth was then investigated.

The effect of various changes to the silicalite composition was then investigated. Aluminium was introduced into the composition and the effect on growth and crystal shape observed. Salts were also added (sodium halides and tetramethylammonium (TMA) halides) to see if the growth and crystal shape could be altered. The importance of the presence of tetrapropylammonium (TPA) bromide was also investigated by altering the amount of TPA present in the otherwise

similar compositions. The changes observed to shape and growth could then be attributed to the presence or lack of TPA. Since ethanol was formed when the tetraethyl silicate hydrolysed, an attempt was also made to see if this ethanol affected the crystallization of silicalite. Different amounts of ethanol were added to the otherwise similar compositions and the growth and shape of the crystals studied.

Finally the conditions used to grow larger silicalite crystals were applied to other zeolite systems. The zeolites chosen were all high silica zeolites; EU-1,¹⁸ ZSM-48¹⁹ and ZSM-39.²⁰ These zeolites were chosen because they could crystallize from compositions which were similar to those for silicalite. They were also relatively easy to crystallize. Zeolite EU-1 is a high silica zeolite with an unknown structure. A typical EU-1 reaction produces ellipsoidal crystals 0.5 to 4.0 μm long and 0.2 to 3.0 μm wide.¹⁸

Zeolites ZSM-39 and ZSM-48 are both high silica zeolites. The structure of ZSM-39 has been determined²¹ but the structure of ZSM-48 still remains unknown. ZSM-39 and -48 can crystallize together from compositions which contain no aluminium. Both zeolites can be obtained from compositions which contain silica, sodium and TMA. ZSM-39 crystals tend to have octahedral habit and it has been reported that single crystals $>10 \mu\text{m}$ could not be grown.²¹ However a structure

determination²² has been carried out on a single crystal of dodecasil-3C (an isotype of ZSM-39) and although the crystal size was not given it was probably greater than 50 μm . No size is given for ZSM-48 crystals reported in the literature.¹⁹

4.2 Experimental.

4.2.1. Materials.

The following materials were used:

- Fumed silica (B.D.H., cab-o-sil M5)
- Tetraethyl silicate (B.D.H., G.P.R. grade)
- Aluminium hydroxide (B.D.H., G.P.R. grade)
- Sodium hydroxide (Fisons, analar grade)
- Lithium hydroxide (Fisons, analar grade)
- Cesium hydroxide (Fluka, pract.)
- Tetramethylammonium hydroxide (Fluka, pract.)
- Tetrapropylammonium hydroxide (Fluka, pract.)
- Cesium bromide (Fluka, pract.)
- Sodium bromide (Fisons, analar grade)
- Tetramethylammonium bromide (Fluka, purum)
- Tetrapropylammonium bromide (Fluka, purum)
- Hexamethonium bromide (Fluka, purum)
- Sodium chloride (Fisons, analar grade)
- Tetramethylammonium chloride (B.D.H., G.P.R. grade)
- Sodium iodide (Fisons, analar grade)
- Tetramethylammonium iodide (B.D.H., G.P.R. grade)
- Ethanol (B.D.H., analar grade)
- Distilled water was always used.

4.2.2 Preparation of solutions

4.2.2.1. Silicate solutions

Mixtures were prepared in 60ml polythene bottles. The hydroxide was dissolved in the required amount of water. The tetraethyl silicate was then added to the solution. Teflon-coated magnetic followers were then

added and the bottles sealed. The solutions were stirred quite rapidly until all of the tetraethyl silicate had hydrolysed and a "clear" silicate solution produced. If the composition required the addition of a salt (organic or inorganic), this was normally added after the hydrolysis had been completed. In Chapter 3 it was noted that if the salt was present at the start of hydrolysis a solid gel was normally formed.

4.2.2.2. Addition of aluminium.

The tetraethyl silicate was hydrolysed, as described above, using approximately half the required amount of hydroxide and two-thirds of the water. The remainder of the hydroxide and water were used to dissolve the aluminium hydroxide. When the aluminium hydroxide was dissolved the salt (if any) was added to this solution. The aluminate solution was then added, with very rapid stirring, to the silicate solution.

4.2.3. Crystallization.

Samples from the prepared solutions were then immediately drawn up into either glass melting point tubes or Camlab "microslides". The tubes were carefully sealed by melting each end. They were then placed in a metal block which had been drilled to accommodate several tubes. The pre-heated block helped to eliminate any effects due to a slow warm-up to the reaction temperature.

Larger quantities of the reaction mixture were placed in 30 ml capacity Teflon-lined stainless steel

bombs in order to obtain enough product for X-ray analysis.

4.2.4. Crystal growth.

The growth of the crystals was followed using a Vickers M41 Photoplan optical microscope fitted with a Pentax ME Super camera. The glass tubes were removed from the block, photographed and returned to the block at regular time intervals.

Samples from the steel bombs were examined by X-ray powder diffraction (as described in Chapter 2). The bombs contained the same reaction mixtures as the capillary tubes so that any crystals produced could be identified by X-ray diffraction. The work described in section 4.3.1 was carried out with glass melting point tubes. The more detailed work described in later sections was done using the Camlab microslides.

4.3.1. Conditions for the growth of large crystals.

The initial experiments were carried out in melting point tubes. Although it was possible that the glass in these tubes could be leached into the solution, there was no physical sign of attack on the glass until near the end of the reaction. This took the form of etch marks along the capillary tube (figure 4.1). Even when microslides were used the glass could become pitted (figure 4.2) in very alkaline conditions. This could eventually obscure the view of any crystals within the tube. The attack on the glass is more likely at the end of the reaction since the nutrient in the solution phase is then almost exhausted. During crystallization the hydroxide released on crystallization of the zeolite or silica molecular sieve attacks the polymeric silica material present in the reaction mixture, but at the end of the reaction when the silica has been consumed the hydroxide ion concentration rises sufficiently for the glass to be attacked. This only occurs at the end of the reaction and does not invalidate the results obtained in the earlier stages of the reaction. Thus despite this attack on the glass, the results provided by these experiments give a very useful and reliable indication of the effect of various parameters on final crystal size.

4.3.1.1. Silica concentration.

A reaction mixture of composition:

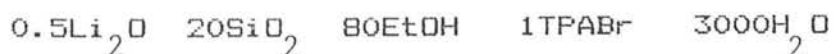


Figure 4.1. (overleaf).

Etch marks along a melting point tube for a reaction mixture of composition $0.5\text{Li}_2\text{O}$ 20SiO_2 80EtOH 0.5TPABr $1500\text{H}_2\text{O}$ at 423K for 12 days.

Figure 4.2. (overleaf).

(a) and (b). Pit marks on a microslide capillary tube for a reaction mixture of composition $1\text{Na}_2\text{O}$ 20SiO_2 $0.3\text{Al}_2\text{O}_3$ 80EtOH 0.5TPABr $1500\text{H}_2\text{O}$ at 448K for 4 days.



Fig.1.

100 μ m

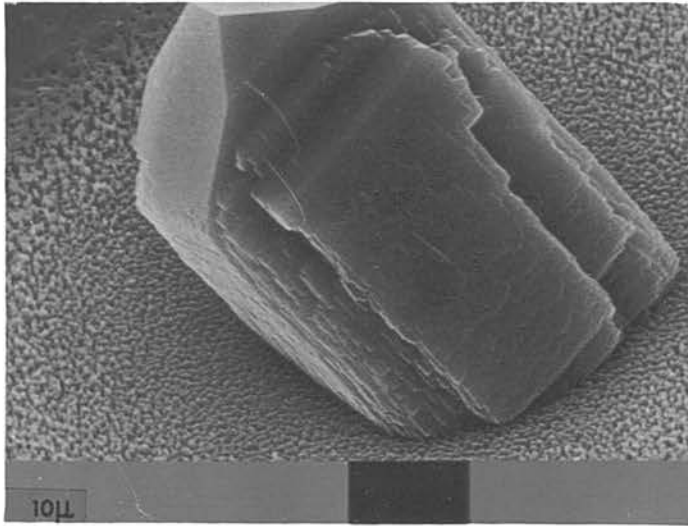
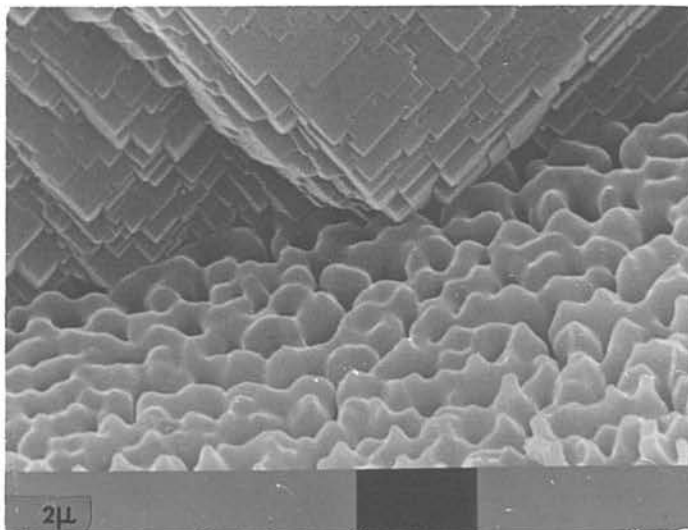


Fig.2.

a



b

was prepared and then known amounts of water were added to samples from this mixture (see table 4.3). This effectively changed the concentration of silica for each of the samples. All the samples were placed at 423K. The largest crystals produced in each sample is shown in table 4.3. (The dimension measured was the crystal length as shown in figure 4.3). The results in table 4.3. show that as the reaction mixture is diluted, the size of the final crystals is reduced. For most of the growth period, the crystal growth appears to be constant. These linear growth rates were almost constant for each reaction mixture irrespective of its water content. This is shown in figure 4.4 for reactions C1a to c. These similar growth rates were quite suprising. It was thought that the change in the water content should change the supersaturation which would then affect the growth rate. The similar growth rates imply that the concentration of the silicate species, which build the crystals, remains almost constant irrespective of the water content. The addition of water must lead to the dissolution of larger quantities of silicate species; otherwise the concentration of the "building" units would fall and the linear growth rate would be reduced. The main difference created by the addition of water is in the termination time; the reaction mixture with most water is the one where crystal growth is the first to stop, probably due to lack of nutrient. This implies that the

Table 4.3. The effect of silica concentration on the final crystal size.

Temperature = 423K

Run No.	Composition					Length of largest crystal in final product / μm
	Li ₂ O	SiO ₂	EtOH	TPABr	H ₂ O	
C1a	0.5	20	80	1	3000	65
C1b	0.5	20	80	1	4000	65
C1c	0.5	20	80	1	5000	50
C2a*	0.5	20	40	1	3000	30
C2b*	0.5	20	40	1	4000	25
C2c*	0.5	20	40	1	5000	20
C3a	1.0	20	80	1	3000	95
C3b	1.0	20	80	1	6000	40

* The silica source for the C2 reactions was a 50:50 mixture of Cab-o-sil (fumed silica) and tetraethyl silicate.

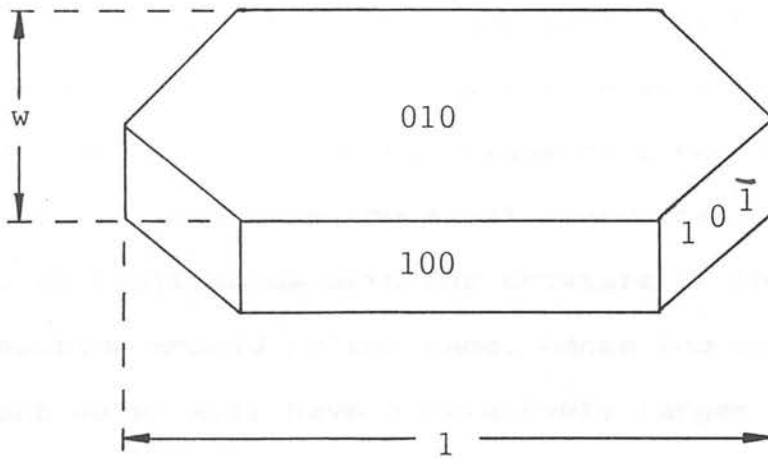


Figure 4.3. Typical silicalite crystal. The crystal contains straight channels, perpendicular to the (010) face and parallel to (100), which connect with zig-zag channels along (101) and (10 $\bar{1}$). The crystal length, l , and width, w , were normally measured.

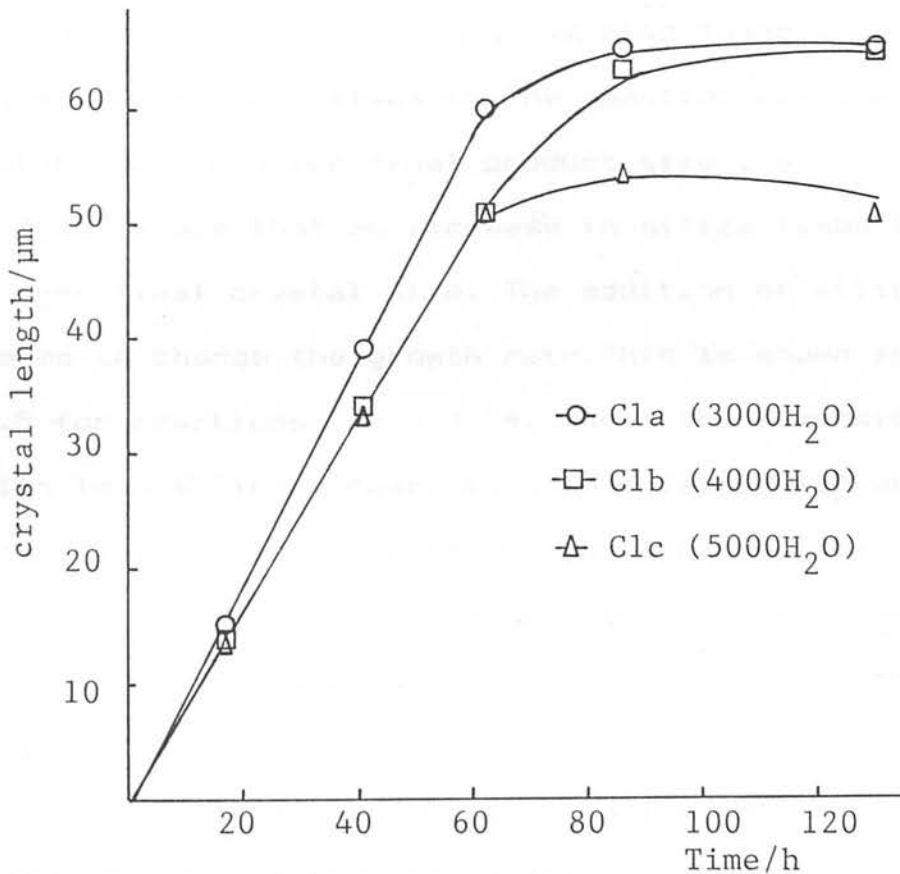


Figure 4.4. Crystal length growth, at 423K, for reactions C1a to c (see table 4.3)

number of nuclei produced in each case is not very different. If the same number of nuclei are produced in each reaction then only the composition with the highest nutrient content can continue to feed the crystals after the other reactions have run out of nutrient. In each case the final concentration of silica in equilibrium with the crystals at the end of the reaction should be the same. Hence the mixture with the most water will have a relatively larger percentage of the total silica left in solution at the end of the reaction. This provides another cause of the early termination of the crystallization from the most dilute reaction mixture.

The silica concentration was also changed by the addition of more silica to the reaction mixture. The values obtained for final product size, shown in table 4.4, indicate that an increase in silica leads to a larger final crystal size. The addition of silica also seems to change the growth rate. This is shown in figure 4.5 for reactions C3a and C4, where the composition with less silica appears to give a faster linear growth rate. This is to be expected since the additional silica is likely to remove some more of the hydroxide from solution and affect the concentration of the crystal building blocks.

These results indicate that an increase in the concentration of the silica will provide more nutrient and can lead to larger crystals. However it would seem

Table 4.4. The effect of silica concentration on final crystal size.

Temperature = 423K

Run No.	Composition					Length of largest crystal in final product / μm
	Li_2O	SiO_2	EtOH	TPABr	H_2O	
C3a	1.0	20	80	1	3000	95
C4	1.0	40	160	1	3000	105
C5	1.0	20	80	0.5	1500	60
C6	1.0	30	120	0.5	1500	90

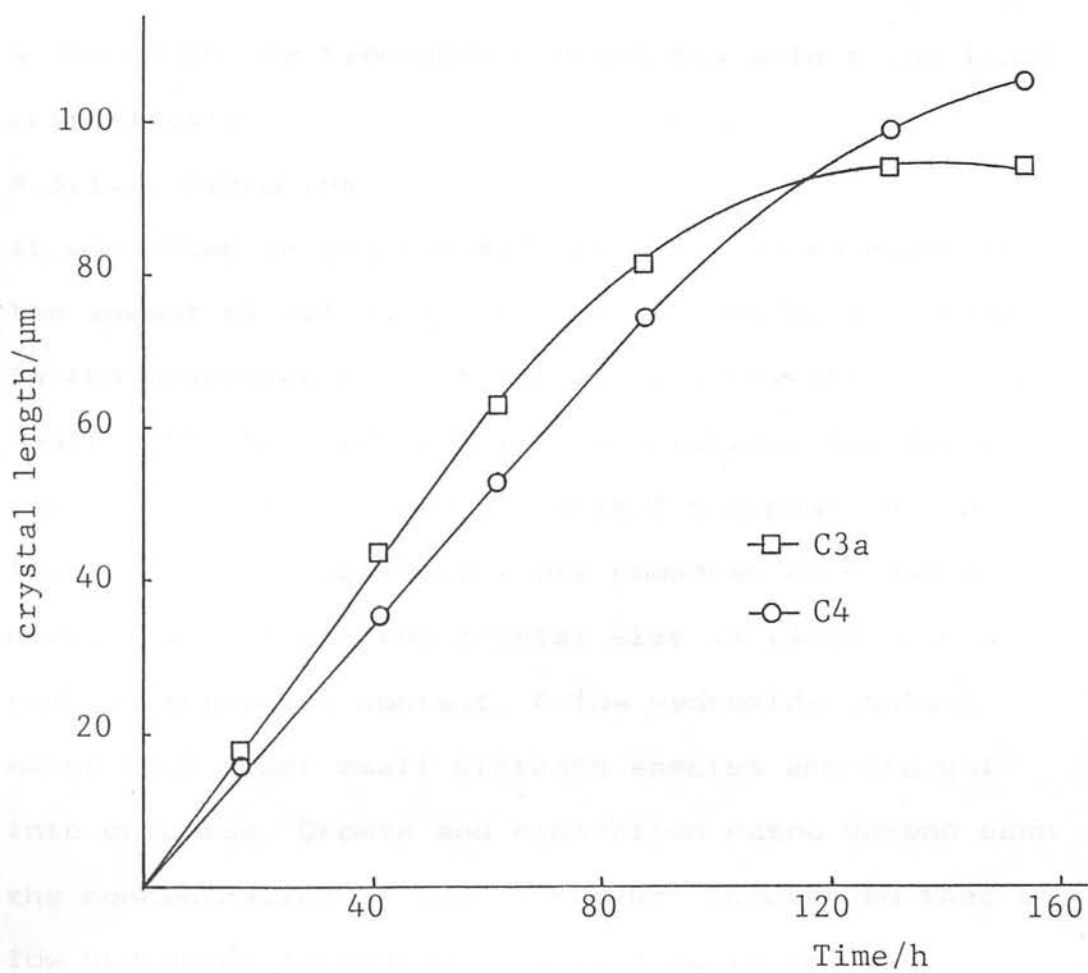


Figure 4.5. Crystal length growth at 423K for reactions C3a and C4 (see table 4.4).

that the concentration of hydroxide ion was also important. An increase in the silica content of the reaction mixture is known to reduce the pH of the solution phase (see, for example, table 3.1, Chapter 3) and it may possibly affect the supersaturation. A low supersaturation is needed to produce large crystals, so a change in the hydroxide content may affect the final crystal size.

4.3.1.2. Hydroxide

It was shown in section 4.3.1.1. that an increase in the amount of silica could also be seen as a decrease in the hydroxide content since the extra silica could react with the hydroxide in the solution. The values for crystal sizes shown in table 4.5 appear to support this. Several compositions are compared here and in every case but one the crystal size is larger for a reduced hydroxide content. A low hydroxide content means that fewer small silicate species are brought into solution. Growth and nucleation rates depend upon the concentration of the "building" species so that a low hydroxide content will give rise to reduced nucleation and growth rates. A low supersaturation is needed for the production of large crystals in other systems. These reactions indicate that this is also the case with the synthesis of silicalite.

4.3.1.3. Temperature.

The effect of temperature on crystal growth is discussed in more detail in section 4.3.2. Initial

Table 4.5. The effect of hydroxide.

Temperature = 423K

Run No.	Composition					Length of largest crystal in final product / μm
	M_2O	SiO_2	EtOH	TPABr	H_2O	
C4	0.5	20	80	0.5	1500	105
C5	1.0	20	80	0.5	1500	60
C1a	0.5	20	80	1.0	3000	65
C3a	1.0	20	80	1.0	3000	95
C7	0.5	20	80	0.5	1000	120
C8	0.75	20	80	0.85	1000	60
C9	1.0	20	80	0.85	1000	50
C10	0.5	20	80	0.5	1500	110
C11	1.0	20	80	0.5	1500	50

M = Li for Runs C4 to C3a

M = Na for Runs C7 to C11

results with the capillary tubes are shown in table 4.6. These results indicate that there is no definite optimum temperature for the growth of large crystals. In some cases low temperatures gave the largest crystals while in other cases the higher temperatures gave the largest crystals. The only way to make proper sense of these results would be to examine both growth rates and crystal size distributions. Size distributions would give some indication of the nucleation rate i.e. if it was constant, increasing or decreasing. Unfortunately the melting point tubes did not lend themselves to either the study of growth rate or size distributions due to the curvature of the tubes. These experiments served to emphasize the necessity for a better technique which would provide growth rates for individual crystals.

4.3.1.4. Cation.

Sodium hydroxide, lithium hydroxide and TPA hydroxide were all used as the source of hydroxide ions. Lithium was used because work by Nastro and Sand¹² had suggested that the lithium system can produce much larger crystals than the sodium one. However the results in table 4.7 show that this is not the case under the conditions used in this work. Sodium systems gave crystals as large, if not larger than lithium ones. The largest difference in size was obtained when the hydroxide was added as TPA hydroxide. The reaction mixtures had the compositions:

Table 4.6. The effect of temperature.

Run No.	Composition					T/K	Length of largest crystal / μm
	M ₂ O	SiO ₂	EtOH	TPABr	H ₂ O		
C3a	1.0	20	80	1.0	3000	423	95
C3c	1.0	20	80	1.0	3000	453	85
C4	0.5	20	80	0.5	1500	423	100
C4a	0.5	20	80	0.5	1500	453	85
C12	0.25	20	80	0.5	750	423	100
C12a	0.25	20	80	0.5	750	448	100
C13	0.5	20	80	-	1000	423	150
C13a	0.5	20	80	-	1000	448	250
C14	0.5	20	80	-	750	423	200
C14a	0.5	20	80	-	750	448	260

M = Li for Runs C3 and C4

M = Na for Runs C12

M = TPA for Runs C13 and 14

Table 4.7. The effect of the cation.

Temperature = 423K

Run No.	Composition						Length of largest crystal / μm
	Li_2O	Na_2O	SiO_2	EtOH	TFABr	H_2O	
C4	0.5	-	20	80	0.5	1500	105
C10	-	0.5	20	80	0.5	1500	110
C5	1.0	-	20	80	0.5	1500	60
C11	-	1.0	20	80	0.5	1500	50
C15	0.5	-	20	80	0.5	1000	70
C7	-	0.5	20	80	0.5	1000	120
C16	1.0	-	20	80	1.0	1500	50
C17	-	1.0	20	80	1.0	1500	85

0.5 TPA₂O 20 SiO₂ 80 EtOH 1000 H₂O (C13a)

and 0.5 TPA₂O 20 SiO₂ 80 EtOH 750 H₂O (C14a)

Those reactions produced very large crystals. Crystals from reactions C13a and 14a are shown in figure 4.6.

These crystals were over 200 μm long. It appears that inorganic cations aid nucleation and that if they are not present, much larger crystals can be obtained

4.3.1.5. Summary

The results given in Sections 4.3.1.1 to 4.3.1.4 show that it is possible to grow crystals of silicalite of 50 to over 200 μm in size. Crystals can easily be observed with an optical microscope. It is obvious from the results that it is not enough to just observe the final crystal size. The crystal size depends upon the growth rate and the nucleation rate. The circular capillary tubes were not suitable for the determination of crystal growth rates or the study of the final product size range. The curved face of the capillaries distorted the crystals. Also loose crystals fell, under gravity, to the bottom of the capillary tube where it was impossible to see them clearly with the microscope. Only the flat, hollow microslides were suitable for more informative studies. These slides could be marked with a permanent marker and the growth of crystals at that point followed.

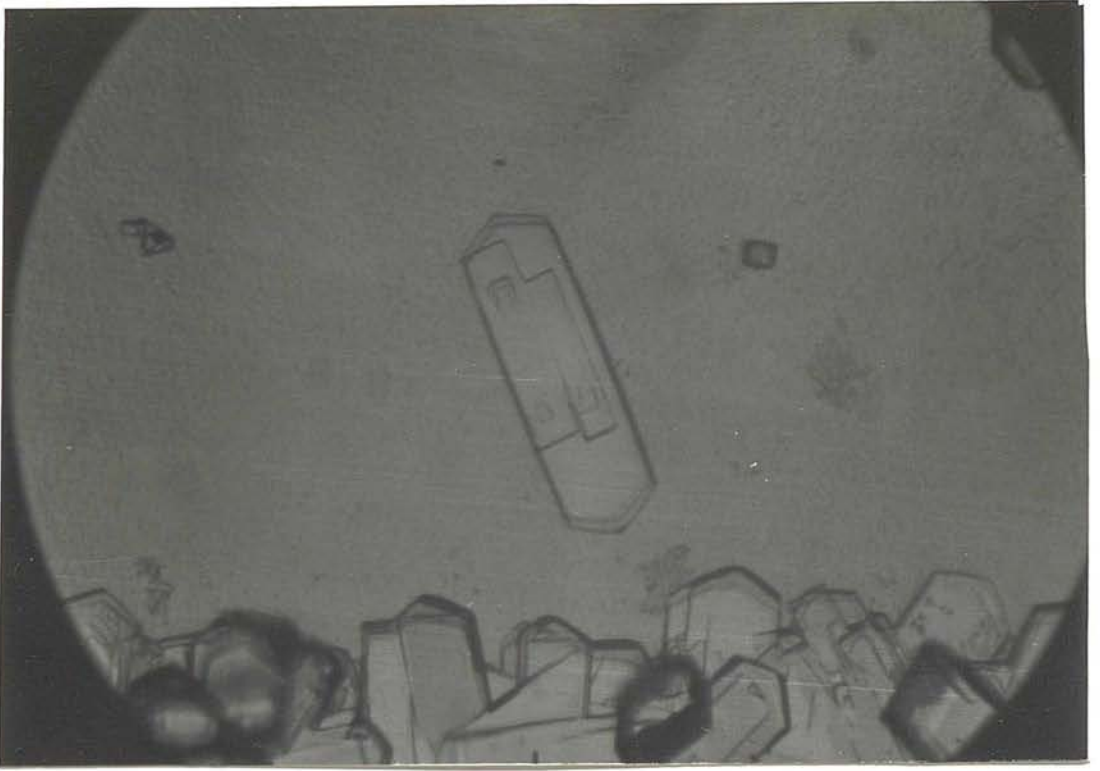
4.3.2. Temperature dependence.

The temperature dependence of the rate of crystal growth for the silicalite-1 system was determined by

Figure 4.6. (overleaf).

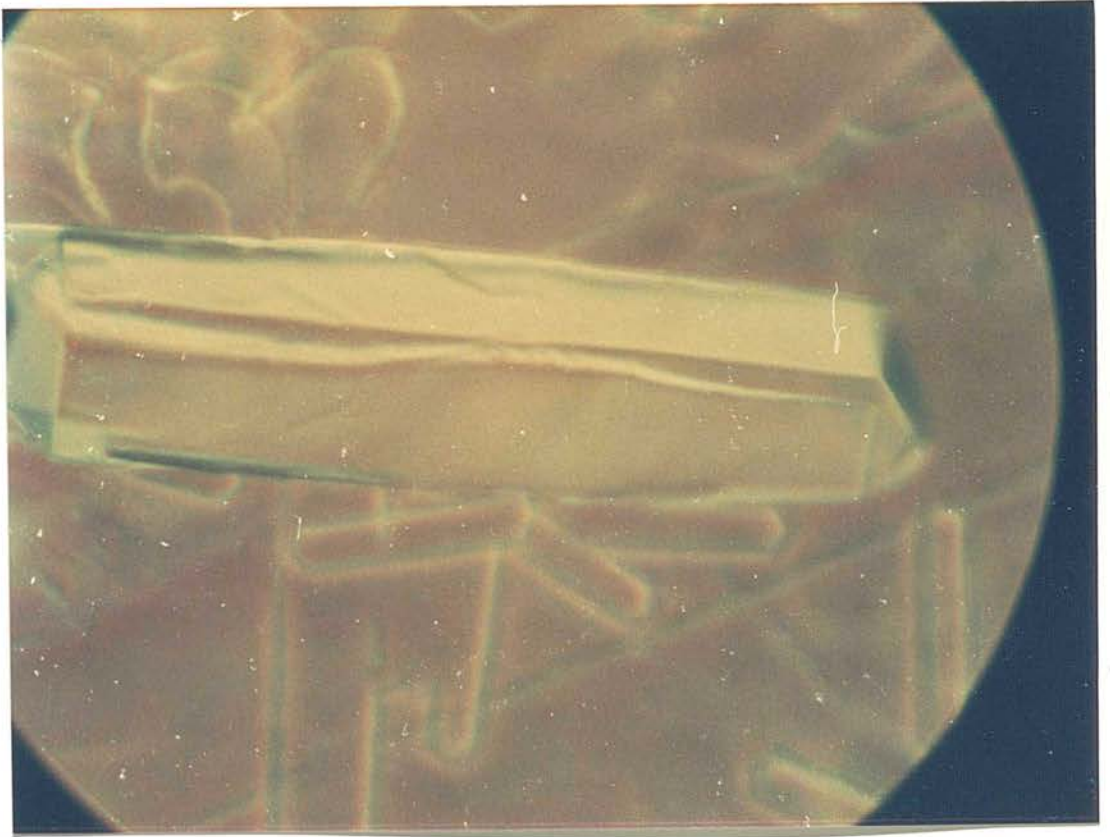
(a) Optical photomicrograph of a silicalite crystal from a reaction mixture of composition $0.5\text{TPA}_2\text{O}$ 20SiO_2 80EtOH $750\text{H}_2\text{O}$ at 448K for 2 days.

(b) Optical photomicrograph of a silicalite crystal from a reaction mixture of composition $0.5\text{TPA}_2\text{O}$ 20SiO_2 80EtOH $1000\text{H}_2\text{O}$ at 448K for 2 days.



a

100 μ m



b

50 μ m

the microslide method. The composition chosen for investigation was :

1 Na₂O 60 SiO₂ 240 EtOH 1500 H₂O 3TPABr

This composition has a low hydroxide content and a high silica content so it was expected to produce crystals which were large enough to be seen with an optical microscope. Reactions were carried out at 368K, 393K, 413K, 433K and 448K. Linear growth rates for both the crystal length and width were measured at each temperature. The growth rates are given as $0.5 \Delta l / \Delta t$, where Δl is the change in the crystal length in time Δt . The length growth rates are given in table 4.8. These growth rates were obtained by the measurement of the same crystal (if possible) at different stages in its growth. Figure 4.7 shows some different stages in the growth of crystals at 413K. The length growth curve is shown in figure 4.8 (curve 1). The growth rate is obtained from the linear portion at the start of this curve. The linear portions of the growth curves at each temperature are shown in figure 4.9. The growth rate at 368K is quite low. A growth rate of $0.011 \mu\text{m h}^{-1}$ would take over 27 weeks to produce a crystal which was over $100 \mu\text{m}$ long. Although low temperatures are usually advised for the growth of large single crystals it can be seen that this may not be practicable with zeolites and silica molecular sieves.

The crystal width was generally more difficult to measure since it was usually much smaller than the

Table 4.8. Crystal length growth rates for silicalite-1.

Temperature T / K	$1/T / 10^3 \text{K}^{-1}$	length growth $R_l / \mu\text{m h}^{-1}$	$\ln R_l$
368	2.72	0.011	-4.48
393	2.54	0.061	-2.80
413	2.42	0.228	-1.48
433	2.31	0.55	-0.59
448	2.23	1.17	0.16

Table 4.9. Crystal width growth rates for silicalite-1.

Temperature T / K	$1/T / 10^3 \text{K}^{-1}$	length/width ratio	width growth $R_w / \mu\text{m h}^{-1}$	$\ln R_w$
368	2.72	2.1	0.005	-5.25
393	2.54	2.3	0.027	-3.61
413	2.42	3.1	0.074	-2.60
433	2.31	4.4	0.126	-2.07
448	2.23	6.0	0.195	-1.63

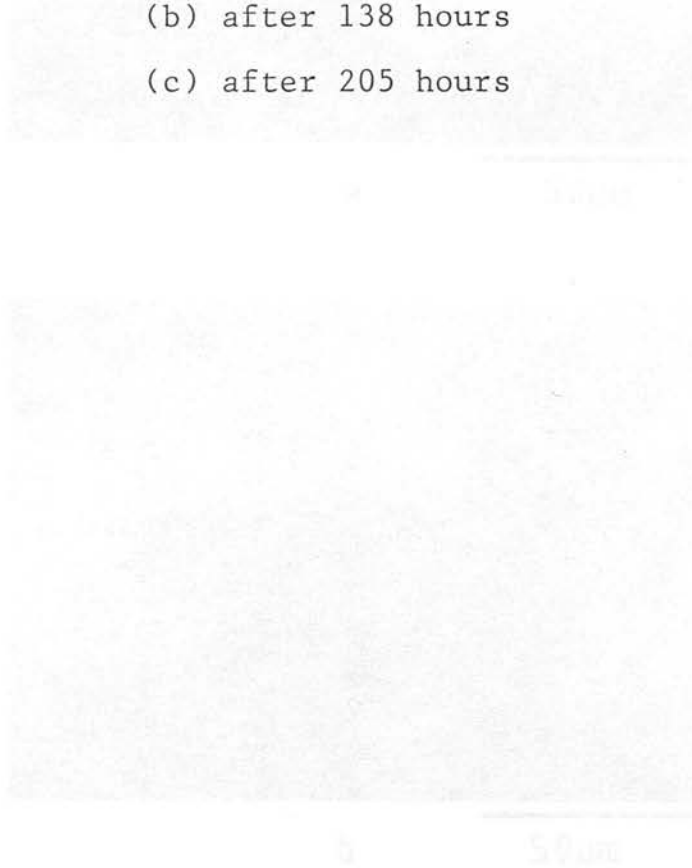
Figure 4.7. (overleaf).

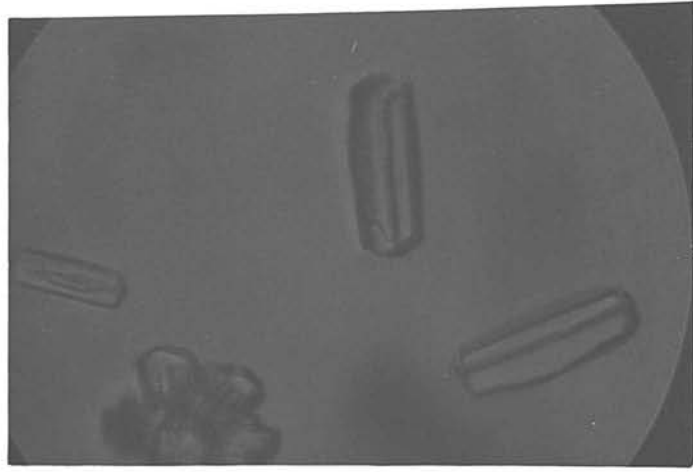
Optical photomicrographs of silicalite crystals from a reaction mixture of composition $1\text{Na}_2\text{O} \cdot 60\text{SiO}_2 \cdot 240 \text{EtOH} \cdot 1500\text{H}_2\text{O} \cdot 3\text{TPABr}$ at 413K.

(a) after 111 hours

(b) after 138 hours

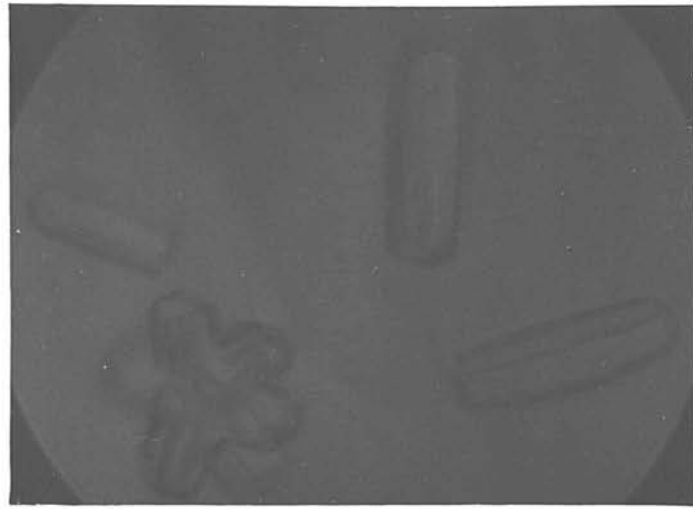
(c) after 205 hours





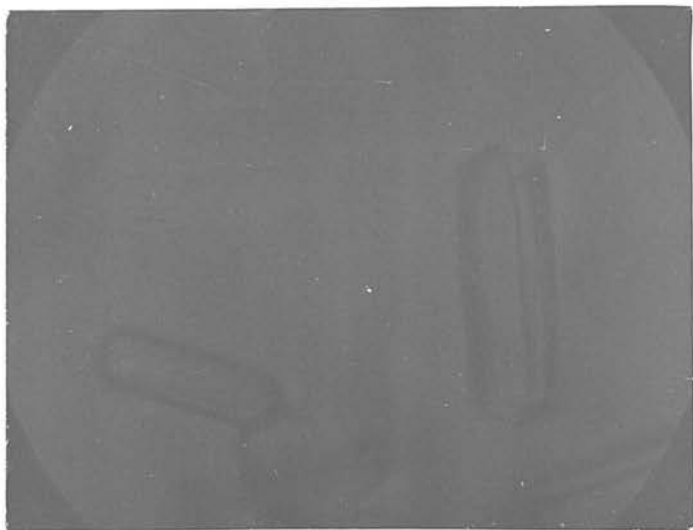
a

50 μ m



b

50 μ m



c

50 μ m

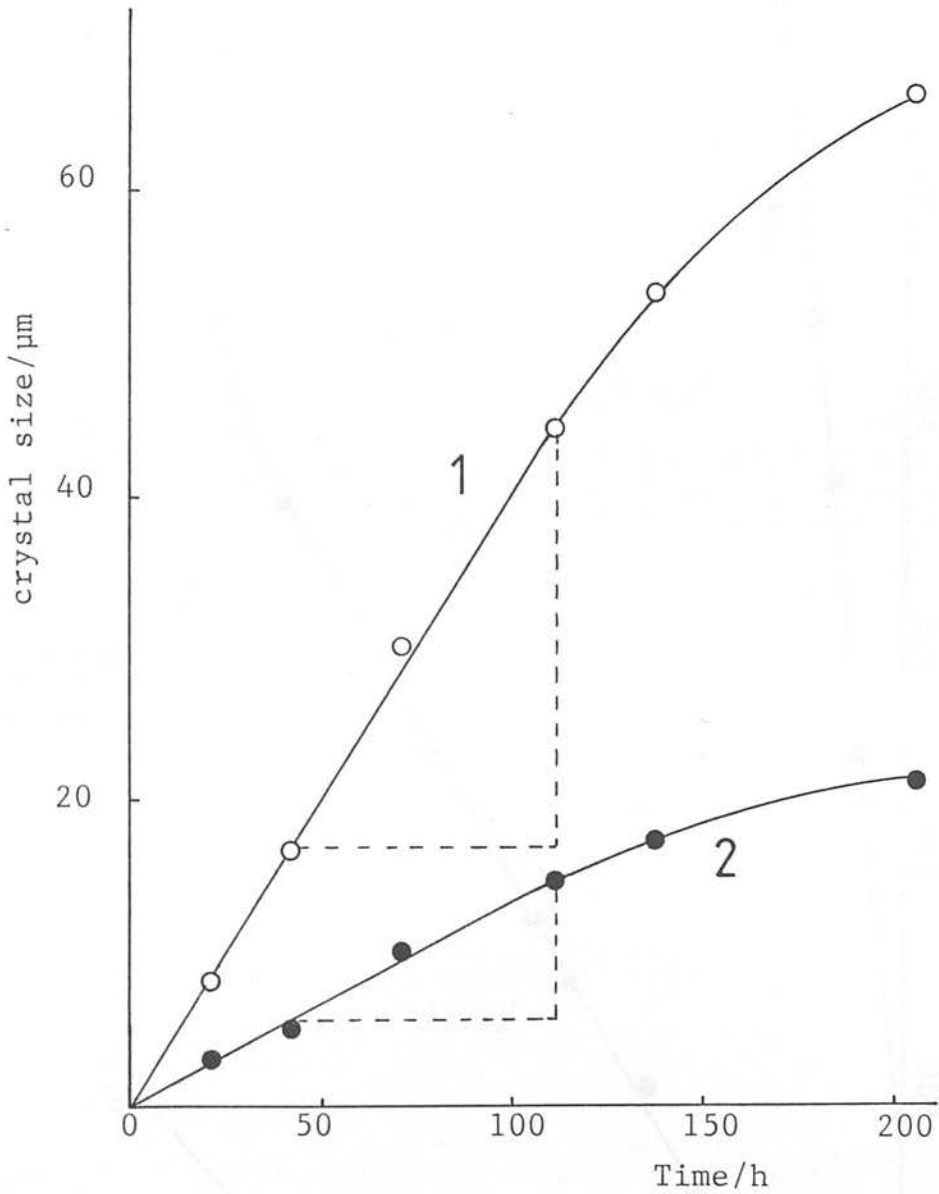


Figure 4.8. Crystal length growth (curve 1) and width growth (curve 2) for a reaction mixture of composition $1\text{Na}_2\text{O} \ 60\text{SiO}_2 \ 240\text{EtOH} \ 1500\text{H}_2\text{O} \ 3\text{TPABr}$ at 413K . The dashed line indicates a smaller crystal which appears to have nucleated at approximately 42 hours according to both the length growth and width growth curves. This crystal has the same length and width growth rate as larger crystals.

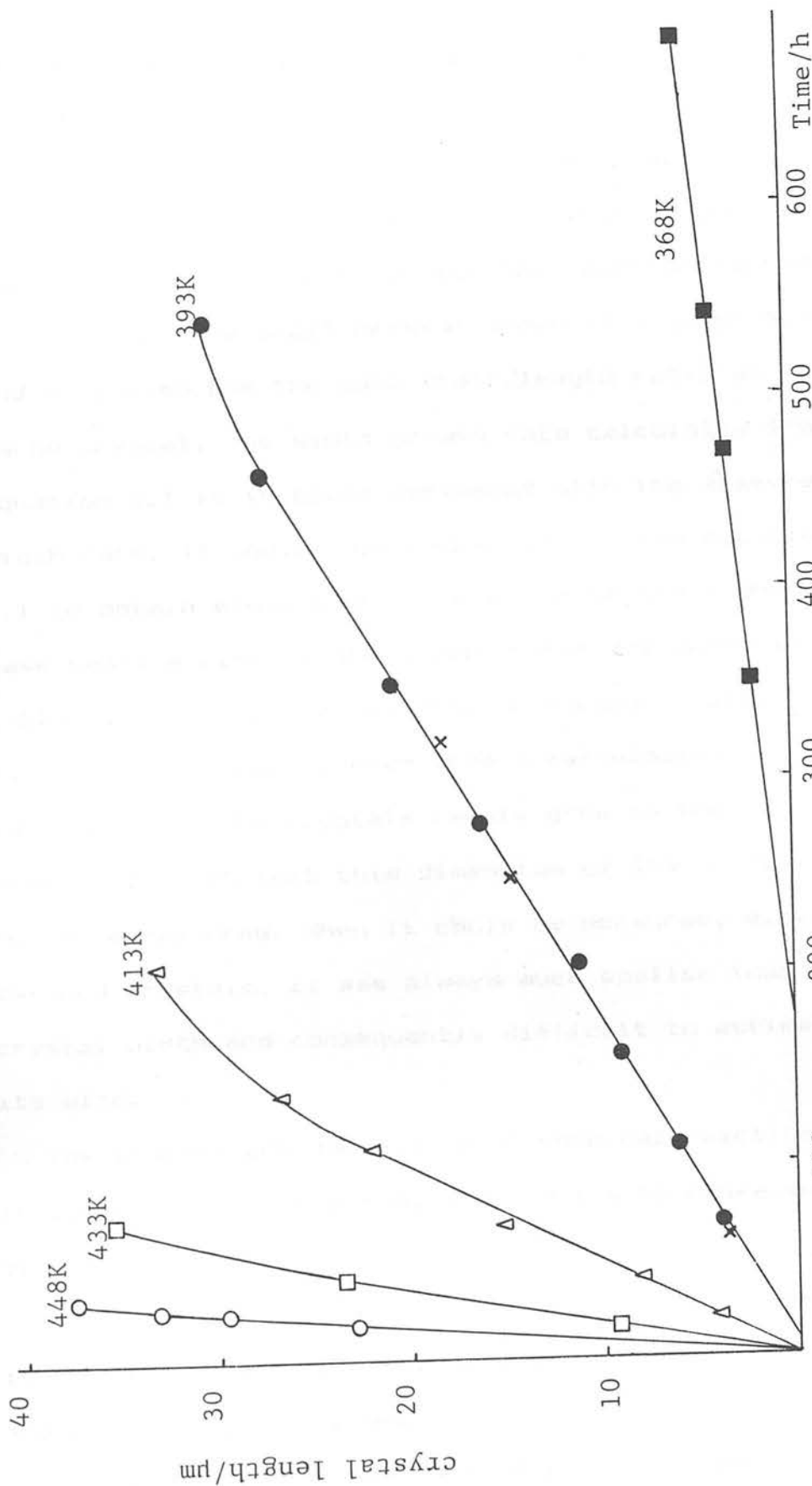


Figure 4.9. Crystal length growth for silicalite crystals from a reaction mixture of composition $1\text{Na}_2\text{O} \cdot 60\text{SiO}_2 \cdot 240\text{EtOH} \cdot 1500\text{H}_2\text{O} \cdot 3\text{TPABr}$. The crosses indicate a second reaction at 393K in order to check the reproducibility of the reaction.

length. However, when it could be measured it was found that :

$$\frac{\text{width linear growth rate}}{\text{length linear growth rate}} = \frac{\text{final width}}{\text{final length}} \quad (4.1)$$

This is shown in figure 4.8 for the reaction carried out at 413K. The small crystal shown in figures 4.7b and 4.7c also has the same width/length ratio as the large crystal. The width growth rate calculated from equation 4.1 is in close agreement with the measured width rate. It would seem reasonable to use equation 4.1 to obtain width growth rates for crystals which have small widths. Width growth rates are shown in table 4.9. It was not possible to obtain crystal "depth" growth rates, even from a calculation such as equation 4.1. The crystals rarely grew in the microslide such that this dimension of the crystal could be measured. When it could be measured, e.g. on twinned crystals, it was always much smaller than the crystal width and consequently difficult to estimate its size.

The temperature dependence of chemical reactions including crystallization, can usually be represented by the Arrhenius Equation,

$$k = A \exp (-E_a/RT) \quad (4.2)$$

in which k = rate constant, A = pre-exponential factor and E_a = activation energy.

When the log of the rate of crystal length growth is plotted against the reciprocal of absolute

temperature, a linear dependence is obtained as shown in figure 4.10. This gives an activation energy, E_a , for crystal length growth of 79 kJ mol^{-1} and a pre-exponential factor, A , of $2.0 \times 10^9 \mu\text{m h}^{-1}$. A similar plot is shown for width growth in figure 4.11. This corresponds to a smaller activation energy (61.5 kJ mol^{-1}) and a smaller pre-exponential factor ($3.4 \times 10^6 \mu\text{m h}^{-1}$). It may be better to call these activation energies "apparent" activation energies. The rate of a reaction depends upon the concentrations of the reactant species in solution, and whilst at each temperature these remain constant (as evidenced by the linear growth rates), they will inevitably have different values at different temperatures, even though the overall stoichiometry of the reaction mixture remains constant.

The apparent activation energies obtained here are merely for one of the stages in the crystallization process. The activation energy for the whole process may be different if some process, other than crystal growth, limits the the rate of crystallization. The activation energy for the whole growth process has been estimated for silicalite-1 and ZSM-5 by several workers.²³⁻²⁸ The values obtained are shown in Chapter 1 in table 1.4. These apparent activation energies were obtained by taking the slope, at 50% crystallization, from crystallization curves (or crystal mass growth curves). It is obvious from table 1.4 that there has

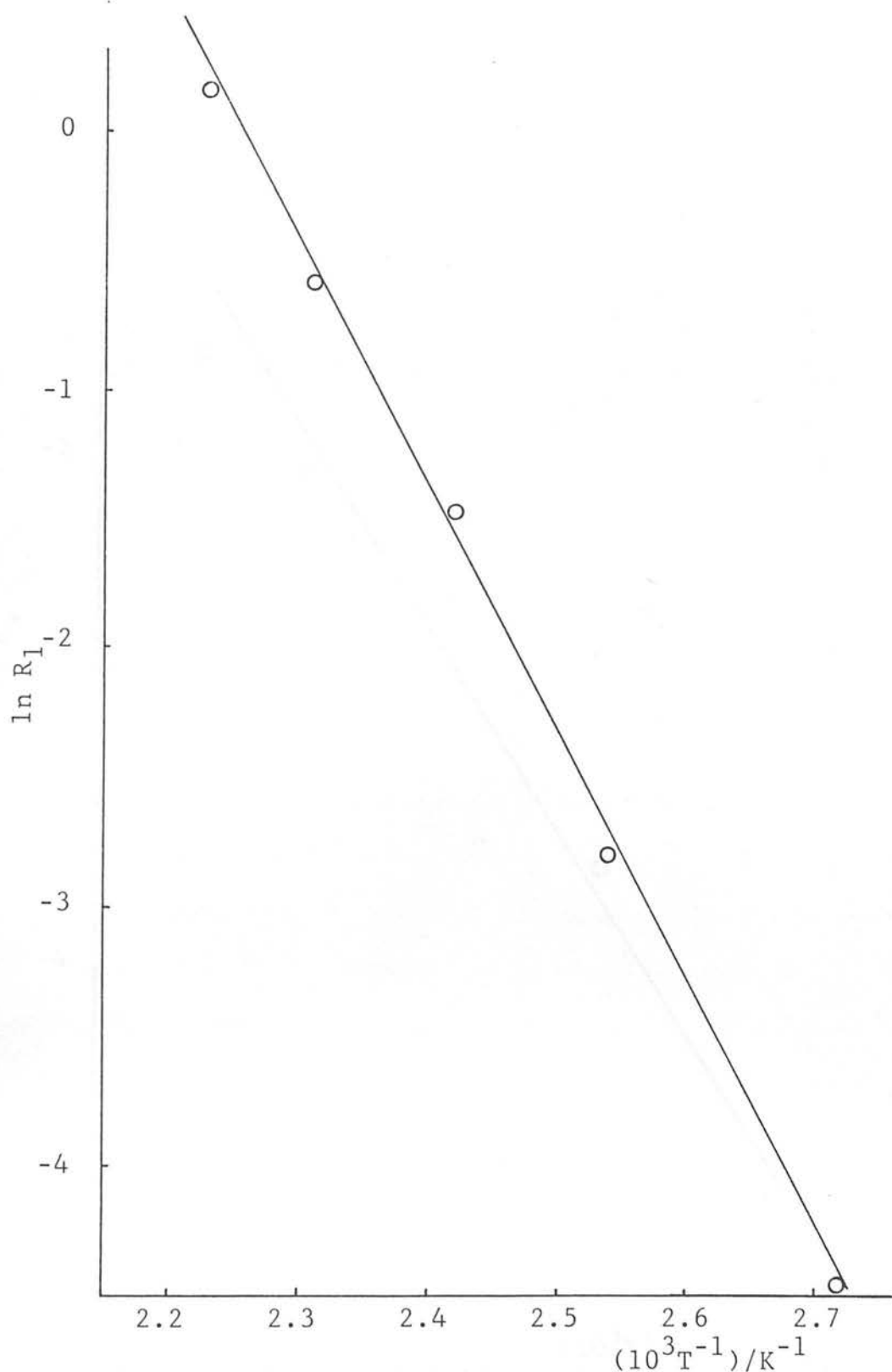


Figure 4.10. Arrhenius plot for silicalite crystallization (length growth) from a reaction mixture of composition $1\text{Na}_2\text{O}$, 60SiO_2 , 240EtOH , $1500\text{H}_2\text{O}$, 3TPABr . Line is given by $R_1 = 2.0 \times 10^9 \exp(-7.9 \times 10^4/RT)$.

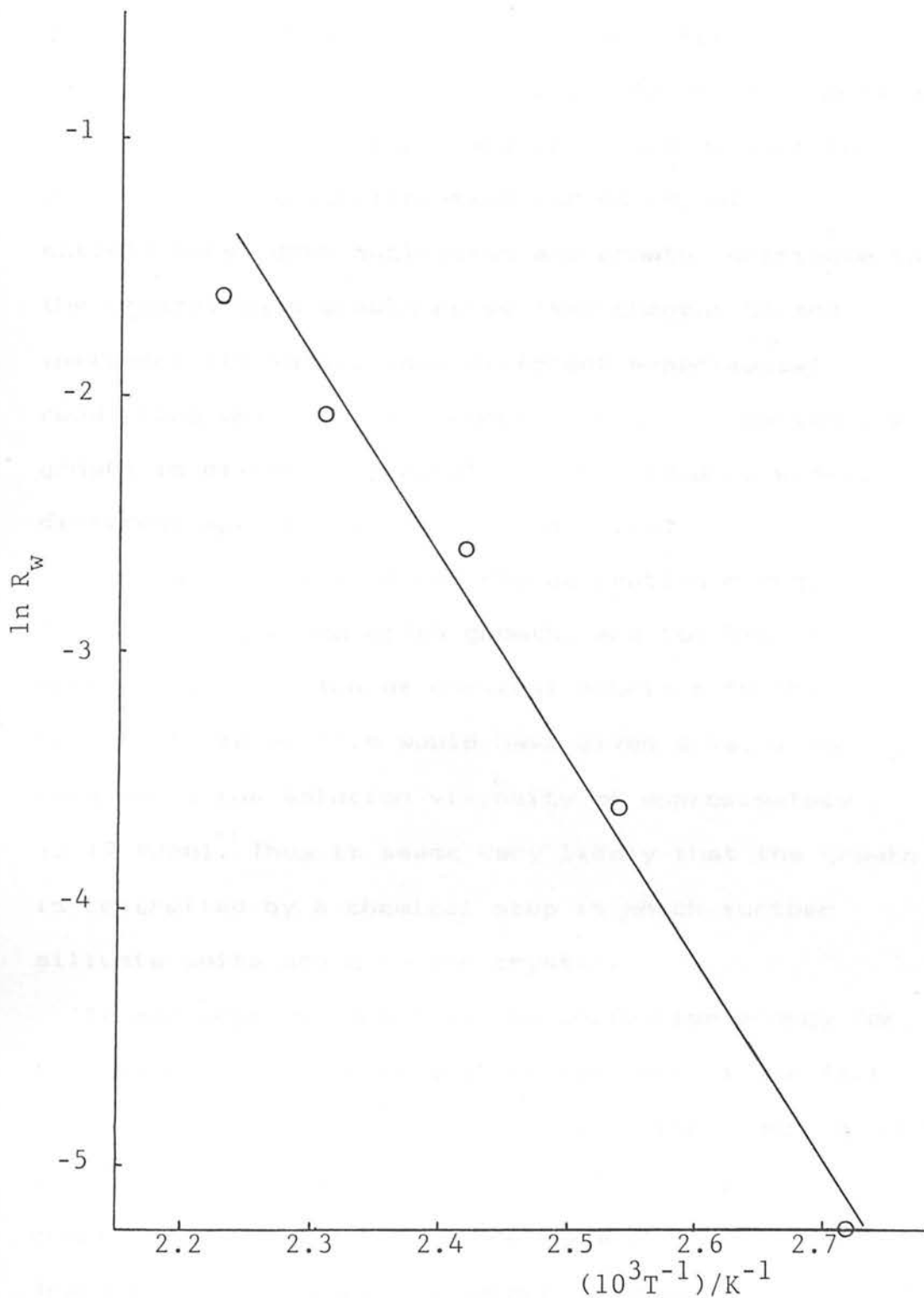


Figure 4.11. Arrhenius plot for silicalite crystallization (width growth) from a reaction mixture of composition $1\text{Na}_2\text{O}$, 60SiO_2 , 240EtOH , $1500\text{H}_2\text{O}$, 3TPABr . Line is given by $R_w = 3.4 \times 10^6 \exp(-6.15 \times 10^4/RT)$.

been a wide range of apparent activation energies found for ZSM-5 and silicalite-1, several of which are of the same order as those found in this work for crystal length growth. It has already been stated (see section 1.5.2.4) that the method used to obtain activation energies from crystallization curves is not satisfactory. Both nucleation and growth contribute to the crystal mass growth curve (see chapter 5) and influence its shape. Thus different experimental conditions which may influence crystal nucleation and growth in different laboratories may lead to widely different apparent activation energies.

The values obtained for the activation energy, E_a , for both length and width growth, are too high for control by diffusion of chemical nutrient to the crystal surface. This would have given a value for E_a related to the solution viscosity of approximately $16-17 \text{ kJmol}^{-1}$. Thus it seems very likely that the growth is controlled by a chemical step in which further silicate units add onto the crystal.

It may seem curious that the activation energy for the *direction* with the fastest growth rate, is in fact larger than that for the *direction* with the lower growth rate. This large apparent activation energy is compensated for by a large pre-exponential factor A . Transition state theory interprets the pre-exponential factor of the Arrhenius equation as :

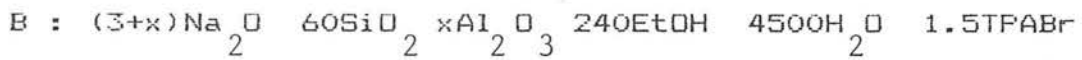
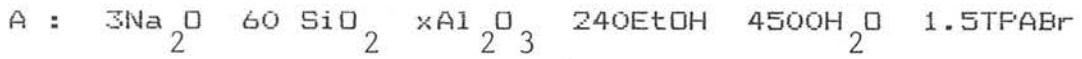
$$A \propto \exp \left[\left(\Delta S^\ddagger \right) / R \right] \quad (4.2)$$

where $(\Delta S^\ddagger)^\circ$ is the entropy change in going from the reagents to the activated complex. If A for the width growth is smaller than that for length growth then this implies that the formation of the activated complex in width growth involves a greater decrease in entropy i.e. the complex is more rigidly bound. Of course the entropy term does not just include the silicate ions which are involved in the bond formation at the crystal surface, but also the solvent molecules which are orientated about these molecules, and which are released along with hydroxide ions as the silica framework forms. Of course the entropy term would differ for each face if different silicate building units were involved. However, it would seem unlikely that there are different species involved in building the different crystal faces. Nevertheless there may be different steric restrictions involved in the orientation of the reactant molecules to form the activated complex and this could well account for the different pre-exponential factors. The 101 face (figure 4.3) grows faster than the other faces. The channel openings on this face offer easier access to a TPA molecule since a molecule which approaches normal to the 101 face would "see" the full channel opening. An approach normal to the 100 face would only "see" part of the opening.

4.3.3 Aluminium additions.

Two similar basic compositions were investigated. These

were :



These compositions have a higher base content than that used for silicalite-1 in section 4.3.2. This was because the addition of aluminium required a higher base and water content to ensure that the reaction mixtures remained clear and did not separate into two distinct phases. Composition B had more base than composition A in order to compensate for the addition of the aluminium. This is because the aluminium was added as $\text{Al}(\text{OH})_3$ which must consume hydroxide ions to form $\text{Al}(\text{OH})_4^-$ ions. This reduces the "free" base in the system and may affect the supersaturation of the solution. The amount of aluminium, x , was varied from 0 to 1 i.e. $60 < \text{SiO}_2/\text{Al}_2\text{O}_3 < \infty$. The reactions were carried out at temperatures between 363 and 433K and growth rates obtained. Compositions and length growth rates for compositions A and B are shown in table 4.10 for the different temperatures. In general the growth rates tend to be very similar for compositions A and B. The growth rates were used to obtain Arrhenius plots to compare with those for silicalite-1.

The values of E_a and A obtained from the length growth results are shown in table 4.11. The activation energy for length growth was approximately independent of x and had an average value of 80 kJ mol^{-1} . It can be seen from table 4.11 that although the addition of

Table 4.10. Length growth rates for different amounts of aluminium in the initial reaction mixture.

Run No.	Moles Al_2O_3 (x)	Length growth rates ($0.5 \Delta l / \Delta t$) / $\mu\text{m h}^{-1}$ at					
		363K	368K	391K	393K	413K	433K
1A	1.00	0.011		0.063		0.25	
1B	1.00	0.012		0.073		0.26	
2A	0.75		0.018		0.079	0.29	
2B	0.75		0.017		0.081	0.29	0.84
3A	0.50	0.014		0.087		0.32	
3B	0.50	0.014		0.093		0.34	
4A	0.25		0.019		0.100	0.35	
4B	0.25		0.020		0.093	0.33	0.99
5	0.00	0.015		0.096		0.37	

Table 4.11. Apparent activation energies (E_a) and pre-exponential factors (A) for length growth for different amounts of aluminium.

Run No.	Moles Al_2O_3 (x)	$E_a / kJ mol^{-1}$	$A / 10^9 \mu m h^{-1}$
1A	1.00	79	2.6
1B	1.00	83	10.0
2A	0.75	77	1.4
2B	0.75	79	3.0
3A	0.50	79	3.3
3B	0.50	81	5.5
4A	0.25	80	5.1
4B	0.25	79	3.6
5	0.00	81	6.6

mean:80 mean:4.0

std. dev.:1.7 std. dev.:3.0

aluminium reduces the length growth rate the activation energy remains unchanged. It may be that the addition of aluminium reduces the supersaturation of the solution slightly, which would lead to a slower growth rate. The data given in table 4.12 shows that width growth values do not decrease when aluminium is added but in fact increase slightly at higher temperatures. The result of this reduction in length growth but slight increase in width growth is to give crystals which are no longer elongated but are much squarer than those obtained in the aluminium free system. This is shown in figure 4.12 for crystals grown at 433K. This higher temperature was not very suitable for the measurement of crystal growth rates but it does emphasize the differences caused by a change in the amount of aluminium present. The crystals obtained in aluminium free reaction mixtures are much more elongated than those where aluminium has been added. It is almost as if the addition of aluminium aids width growth but poisons length growth.

The values in table 4.13 show that as x is increased from 0 to 1, the activation energy and the pre-exponential factor increase to values similar to those obtained for length growth. This implies that the addition of aluminium affects the way the "building units" attach themselves to the growing crystal. The increased value for the pre-exponential factor implies that when the aluminium is present there is a more favourable entropy change on the formation of the

Table 4.12. Width growth rates for different amounts of aluminium in the initial reaction mixture.

Run No.	Moles Al_2O_3 (x)	width growth rates $(0.5 \Delta w / \Delta t) / \mu\text{m h}^{-1}$ at					
		363K	368K	391K	393K	413K	433K
1A	1.00	0.008		0.047		0.21	
1B	1.00	0.010		0.059		0.22	
2A	0.75		0.014		0.061	0.18	
2B	0.75		0.012		0.053	0.16	0.48
3A	0.50	0.011		0.056		0.17	
3B	0.50	0.010		0.061		0.19	
4A	0.25		0.015		0.063	0.18	
4B	0.25		0.014		0.059	0.15	0.43
5	0.00	0.010		0.058		0.15	

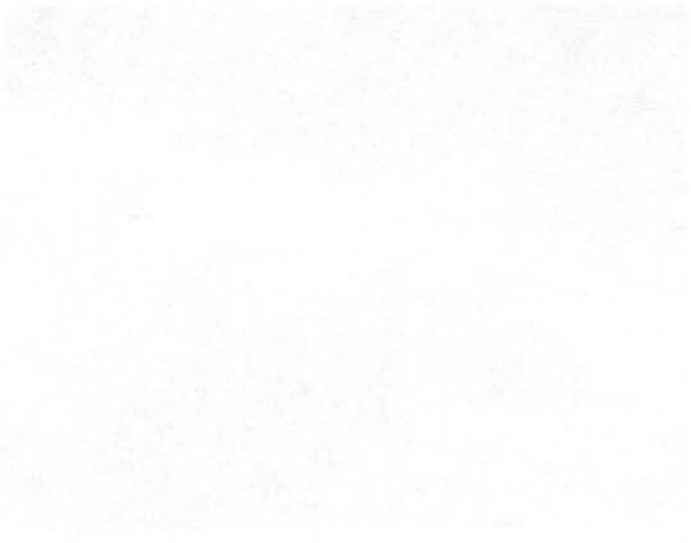
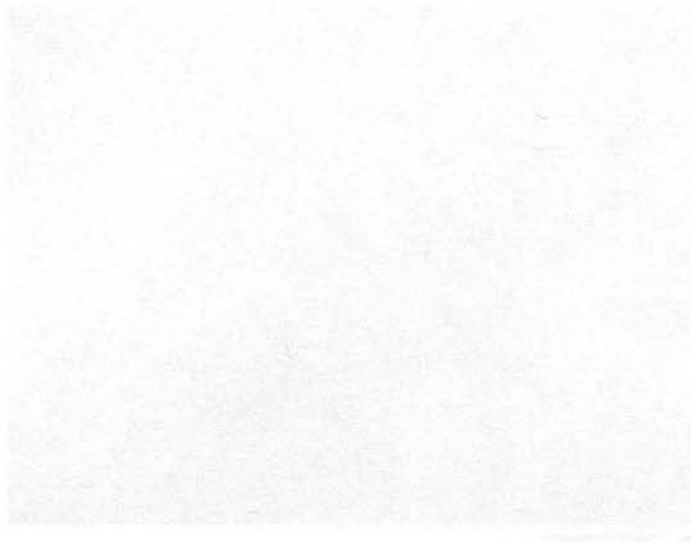
Figure 4.12. (overleaf).

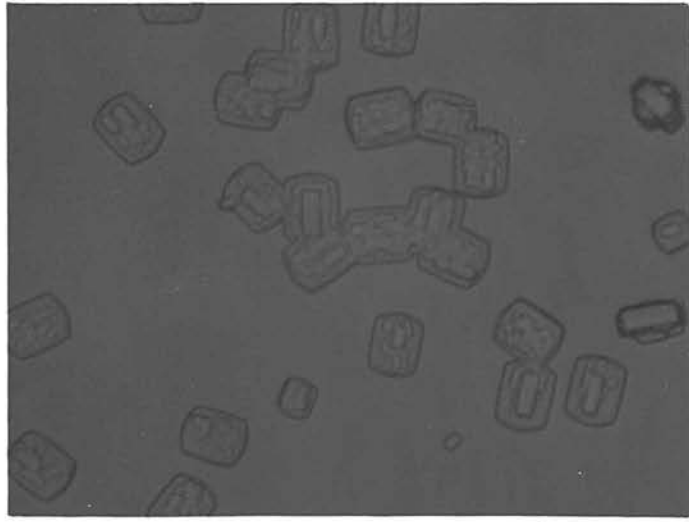
Optical photomicrographs of ZSM-5 crystals from a reaction mixture of composition $3\text{Na}_2\text{O}$, 60SiO_2 , $x\text{Al}_2\text{O}_3$, 240 EtOH, $4500\text{H}_2\text{O}$, 1.5TPABr at 433K.

(a) $x = 1.00$

(b) $x = 0.50$

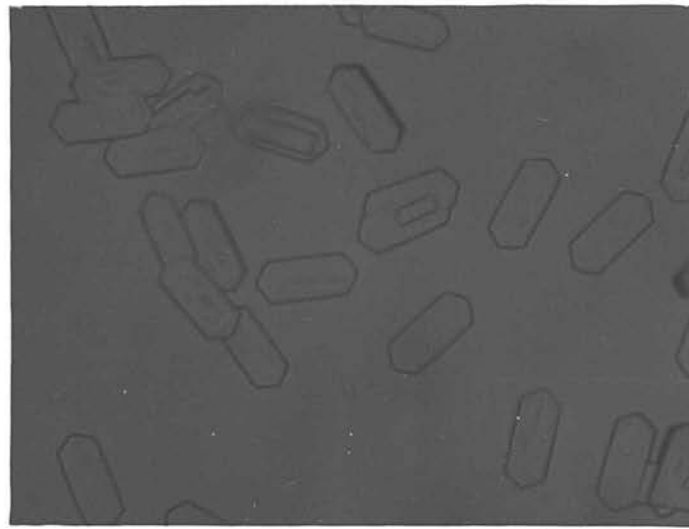
(c) $x = 0.00$





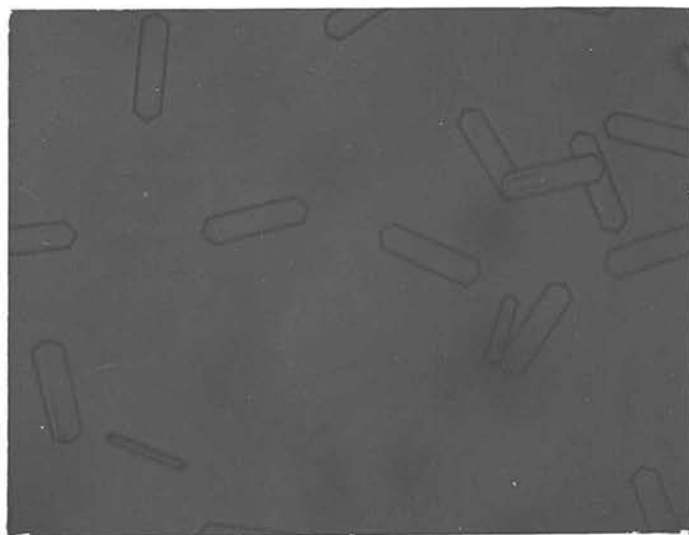
a

50 μ m



b

50 μ m



c

50 μ m

Table 4.13. Apparent activation energies (E_a) and pre-exponential factors (A) for width growth for different amounts of aluminium.

Run No.	Moles Al_2O_3 (x)	$E_a / \text{kJ mol}^{-1}$	$A / 10^7 \mu\text{m h}^{-1}$
1A	1.00	81	32
1B	1.00	78	16
2A	0.75	70	1.4
2B	0.75	74	4.2
3A	0.50	70	1.3
3B	0.50	73	3.8
4A	0.25	70	1.2
4B	0.25	68	0.72
5	0.00	68	0.69

transition state.

One of the practical implications of the addition of aluminium is that the shape of the crystal can be changed from long and narrow to short and fat. Table 4.14 lists the different length/width (l/w) ratios for the crystals shown in figure 4.12. A plot of the $\text{SiO}_2/\text{Al}_2\text{O}_3$ ratio of the reaction mixture against $\ln(l/w)$ shows that square crystals would be obtained for a $\text{SiO}_2/\text{Al}_2\text{O}_3$ ratio of about 50 (see figure 4.13). The minimum possible $\text{SiO}_2/\text{Al}_2\text{O}_3$ for ZSM-5 grown from TPA solutions is 48 since a maximum of 4 TPA can fit into the unit cell of 96 T atoms to balance the charge on the aluminium. Of course if alkali metal cations are also incorporated, as is possible with the compositions used in this work, lower $\text{SiO}_2/\text{Al}_2\text{O}_3$ ratios may be achieved. The shape of the crystals can also be altered by a change in the reaction temperature. Higher temperatures give crystals which are long and narrow while lower temperatures give less elongated crystals (see table 4.9). This means that a certain shape of ZSM-5 crystal can be obtained either by an alteration in the aluminium content in the synthesis mixture or by changing the reaction temperature.

Apart from its effect on crystal growth the addition of aluminium also had an effect on nucleation. When the reaction was completed the size and number of crystals were counted in a particular "volume" of the microslide. This data is shown for 413K reactions in

Table 4.14. Change in length / width ratio (l / w)
for different $\text{SiO}_2 / \text{Al}_2\text{O}_3$ ratios at 433K

Run No.	$\text{SiO}_2 / \text{Al}_2\text{O}_3$	l / w	$\ln l / w$
1B	60	1.28	0.25
2B	80	1.75	0.56
3B	120	2.30	0.83
4B	240	3.0	1.10
5	∞	4.0	1.39

Table 4.15. Number of crystals present in a "volume" of
microslide for different amounts of aluminium.

Temperature : 413K

Volume scanned : $0.9 \times 0.9 \times 0.1$ mm. (0.081 mm^3)

Run No.	Moles Al_2O_3 (x)	No. of crystals	Mean length $/ \mu\text{m}$	Std. dev. $/ \mu\text{m}$
1A	1.00	945	14.5	2.7
2A	0.75	628	23.1	3.2
3A	0.50	394	26.3	3.2
4A	0.25	449	26.6	3.4
5	0.00	481	31.7	3.2

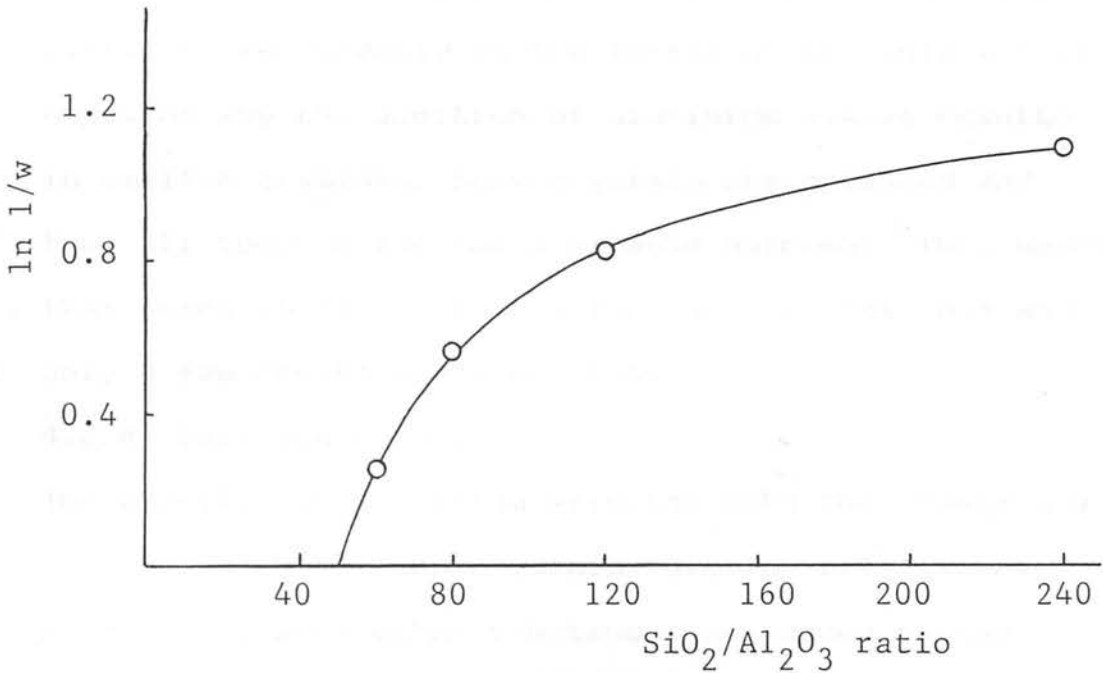


Figure 4.13. The effect of the SiO₂/Al₂O₃ ratio on the length/width (l/w) ratio (plotted as ln l/w) at 413K

table 4.15 where the length and standard deviation of the crystals is also given. It is clear that there is a large number of smaller crystals present per unit volume when the aluminium content is high. It seems that the aluminium makes nucleation easier and probably participates directly in the formation of nuclei. This explains why the addition of aluminium always results in smaller crystals. More crystals are produced and they all compete for the available nutrient. This means that there is less nutrient for each crystal than when only a few crystals are present.

4.3.4. Salt additions.

The addition of aluminium affected both the growth and the nucleation of the crystals. Similar effects are to be expected when other substances are added to the reaction mixture, even if unlike aluminium they are not incorporated into the zeolite framework. The addition of the foreign ions (in the form of salt additions) may affect the growth rates of the crystal faces and thereby modify the crystal shape. They may also affect nucleation. Any of these effects may be due to the cation or the anion. Work by Flanigen et. al.¹³ has shown that the addition of sodium fluoride resulted in larger silicalite-1 crystals. This was thought to be due to the fluoride ion rather than the sodium ion.

The effect of the addition of different amounts of sodium halide and tetramethylammonium (TMA) halide salts on silicalite crystallization was examined. The

composition chosen for this investigation had a higher water content than even the reaction mixtures to which aluminium was added (see section 4.3.3). This was necessitated by the high salt content of some of the reactions. A composition with a low water content would quickly form a "clear", solid gel which could not be placed inside a microslide. Thus a high water content was chosen. The compositions are shown in table 4.16 together with the pH of each initial solution at room temperature.

The addition of the salt always lowers the initial pH. It can be seen from table 4.16 that the initial pH for each different halide is approximately the same for a given number of moles of salt. The 16 moles of TMA salt did not have as large an effect on the pH as did the 16 moles of Na salt.

All the reactions were placed at 413K and the growth rate of the crystals followed by optical microscopy. The length and width growths for the sodium system are shown in figures 4.14 and 4.15. The results for each halide were exactly the same so that there is apparently only one length and one width growth curve shown in figure 4.14 (length) and 4.15 (width) for each composition. The final crystal sizes did vary slightly but not consistently i.e. a particular halide did not always give the largest or the smallest crystal. It would seem that these sodium salts do not influence the reaction. There was no indication that these "foreign"

Table 4.16. Initial pH for different amounts of added salt.

Composition : $3\text{Na}_2\text{O}$ 60SiO_2 240EtOH $6000\text{H}_2\text{O}$ 1TPABr
 \times salt

Cation	\times	Anion	pH	Anion	pH	Anion	pH
Na	1	Cl	11.08	Br	11.08	I	11.09
	4		10.92		10.92		10.90
	16		10.57		10.56		10.47
TMA	1		11.02		11.06		11.06
	4		10.92		10.92		10.92
	16		10.75		10.77		10.77

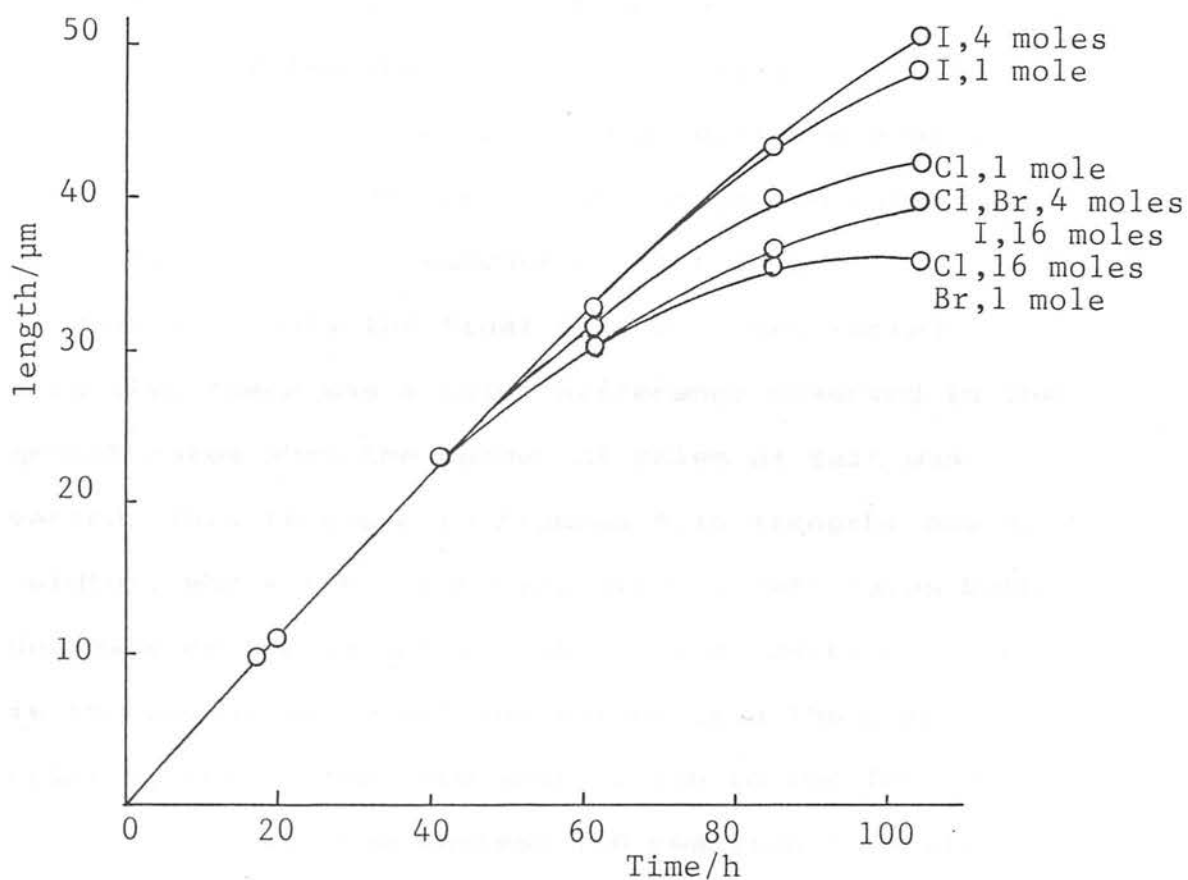


Figure 4.14. Crystal length growth for silicalite crystals.

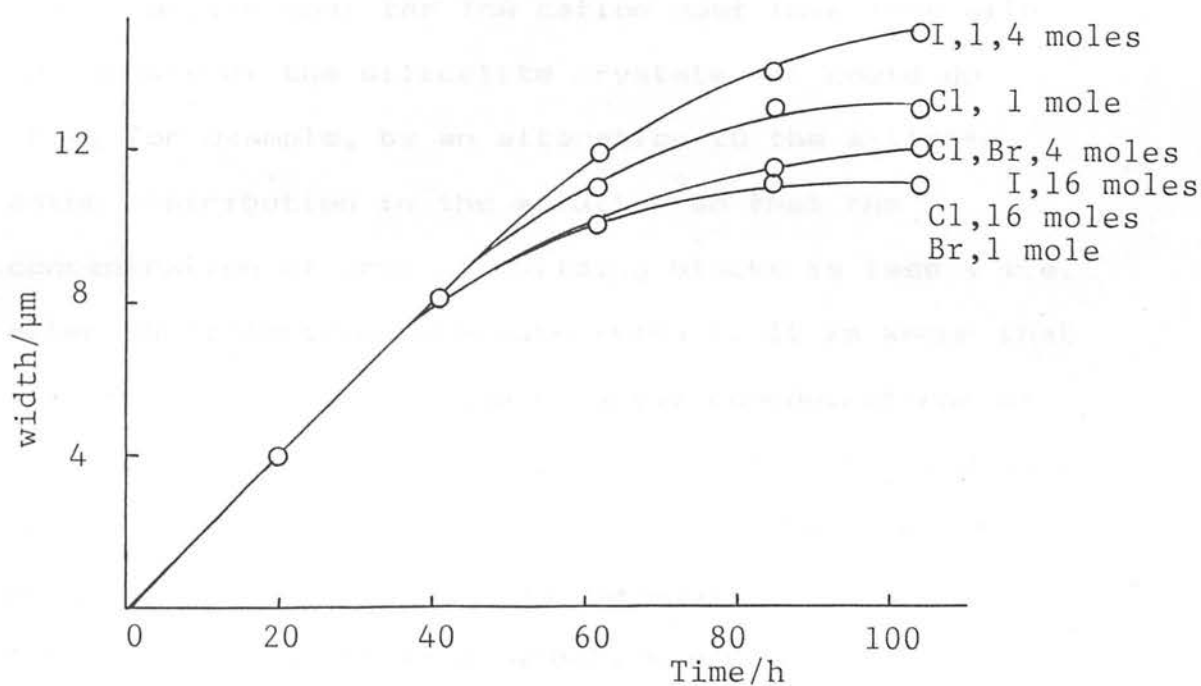


Figure 4.15. Crystal width growth for silicalite crystals.

Composition for figures 4.14 and 4.15: $3\text{Na}_2\text{O} \cdot 60\text{SiO}_2 \cdot 240\text{EtOH} \cdot 6000\text{H}_2\text{O} \cdot 1\text{TPABr} \cdot x\text{NaX}$, $X = \text{Cl}, \text{Br}, \text{or I}$, $x = 1, 4$ or 16.

ions affected the growth rates of any of the crystal faces or affected the final crystal size.

The TMA system also revealed no difference between the different anions. Again similar growth rates were obtained for similar amounts of salt in the composition. Only the final crystal sizes varied slightly. There was a major difference observed in the growth rates when the number of moles of salt was varied. This is shown in figures 4.16 (length) and 4.17 (width), where the length and width growth rates both decrease as the amount of salt in the reaction mixture is increased. Since all the anions give the same results, this difference must be due to the TMA ion. The rate of even the fastest TMA reaction is still slower than that for the sodium system. It follows from these results that the TMA cation must interfere with the growth of the silicalite crystals. It could do this, for example, by an alteration to the silicate anion distribution in the solution so that the concentration of crystal building blocks is less (i.e. alter the effective supersaturation). It is known that the TMA ion can change the relative concentrations of the small silicate ions in solution,¹⁸ and it could well be that the anions formed by TMA, e.g. the $\text{Si}_8\text{O}_{20}^{8-}$ cube, are unsuitable for silicalite formation. The shape of the TMA ion could offer an alternative explanation for the change in the growth rate. The TMA cation has a shape similar to that of the TPA cation except that it has

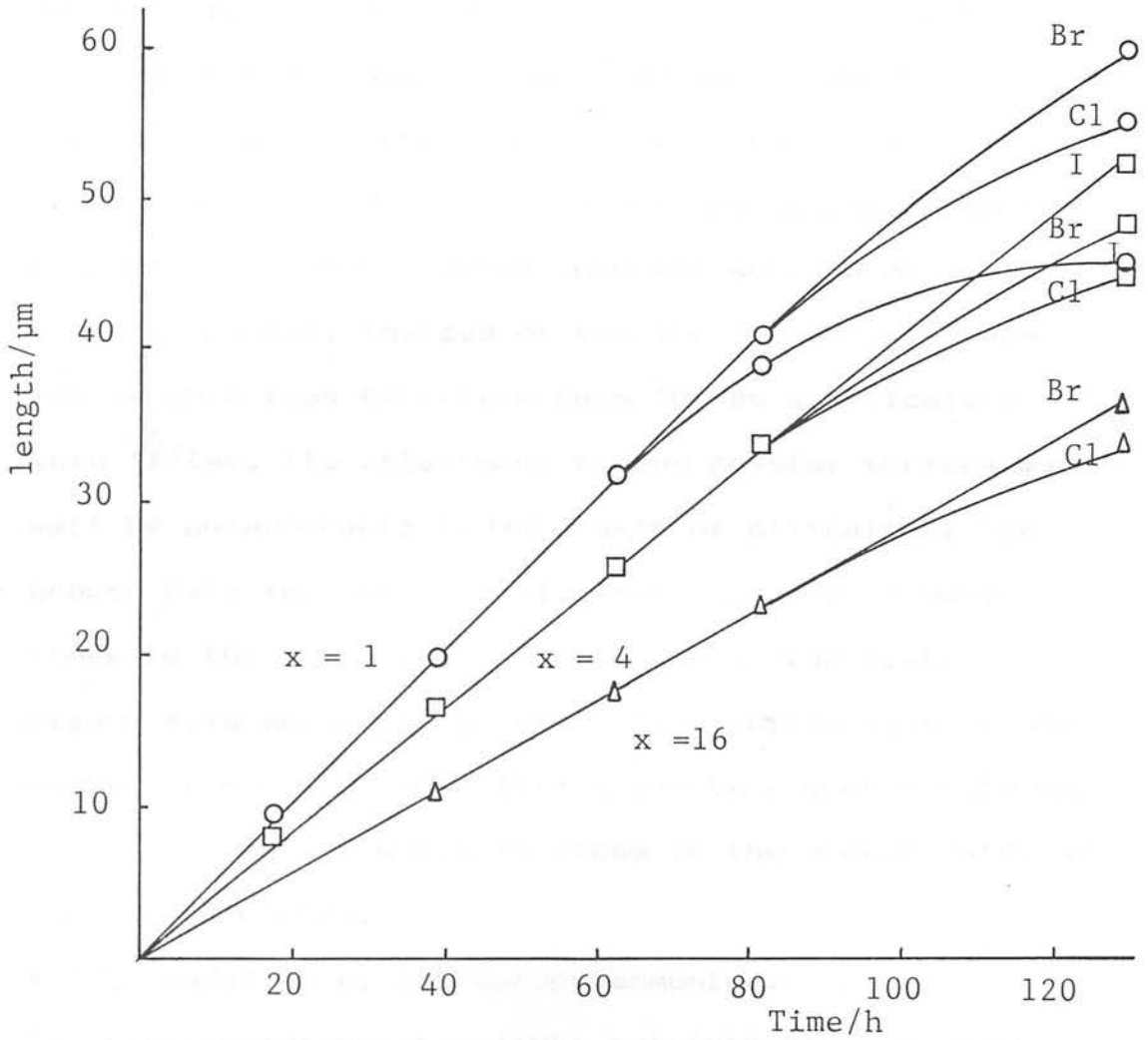


Figure 4.16. Crystal length growth for silicalite

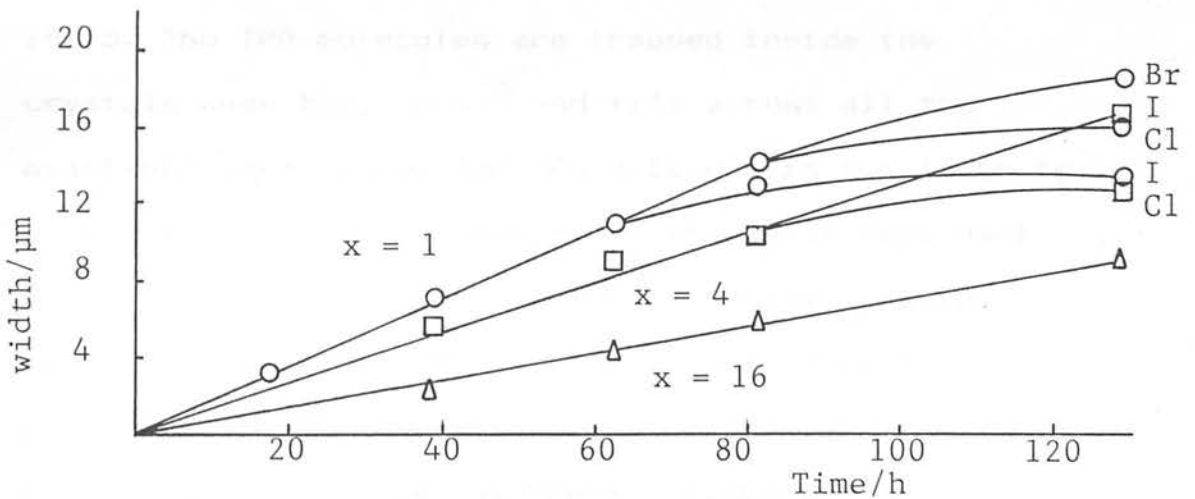


Figure 4.17. Crystal width growth for silicalite crystals.

Composition for figures 4.16 and 4.17: $3\text{Na}_2\text{O} \cdot 60\text{SiO}_2 \cdot 240\text{EtOH} \cdot 6000\text{H}_2\text{O} \cdot 1\text{TPABr} \cdot x\text{TMAX}$, $X = \text{Cl, Br or I}$, $x = 1, 4$ or 16 .

shorter "arms". The TPA molecule is built into the crystal as the crystal grows, and must play an important part in the growth of the crystal (see Section 4.3.5.). The TMA molecule may compete with the TPA molecule and be sorbed onto the surface of the growing crystal, instead of the TPA molecules. Since TMA is much less effective than TPA as a silicalite void filler, its attachment to the crystal surface may well be unfavourable to the growth of silicalite. The growth rate for only a small amount of TMA is very close to the value obtained for the sodium system. Figure 4.18 shows the growth rates plotted against the number of moles of TMA. This predicts a growth rate for no added TMA salt which is close to the growth rates of the sodium system.

4.3.5. Addition of tetrapropylammonium.

The tetrapropylammonium (TPA) molecule plays a very important role in the synthesis of silicalite-1 and ZSM-5. The TPA molecules are trapped inside the crystals when they grow²⁹ and fill almost all the available void space. The TPA molecule is too large to move along the channel system so it cannot move back out of the crystal (or be sorbed into the structure after crystallization). X-ray diffraction work has shown that the TPA molecules sit at channel intersections.²⁹ Thus the TPA ion plays a significant part in the formation of silicalite and ZSM-5 crystals. If TPA is very important, then the amount of TPA

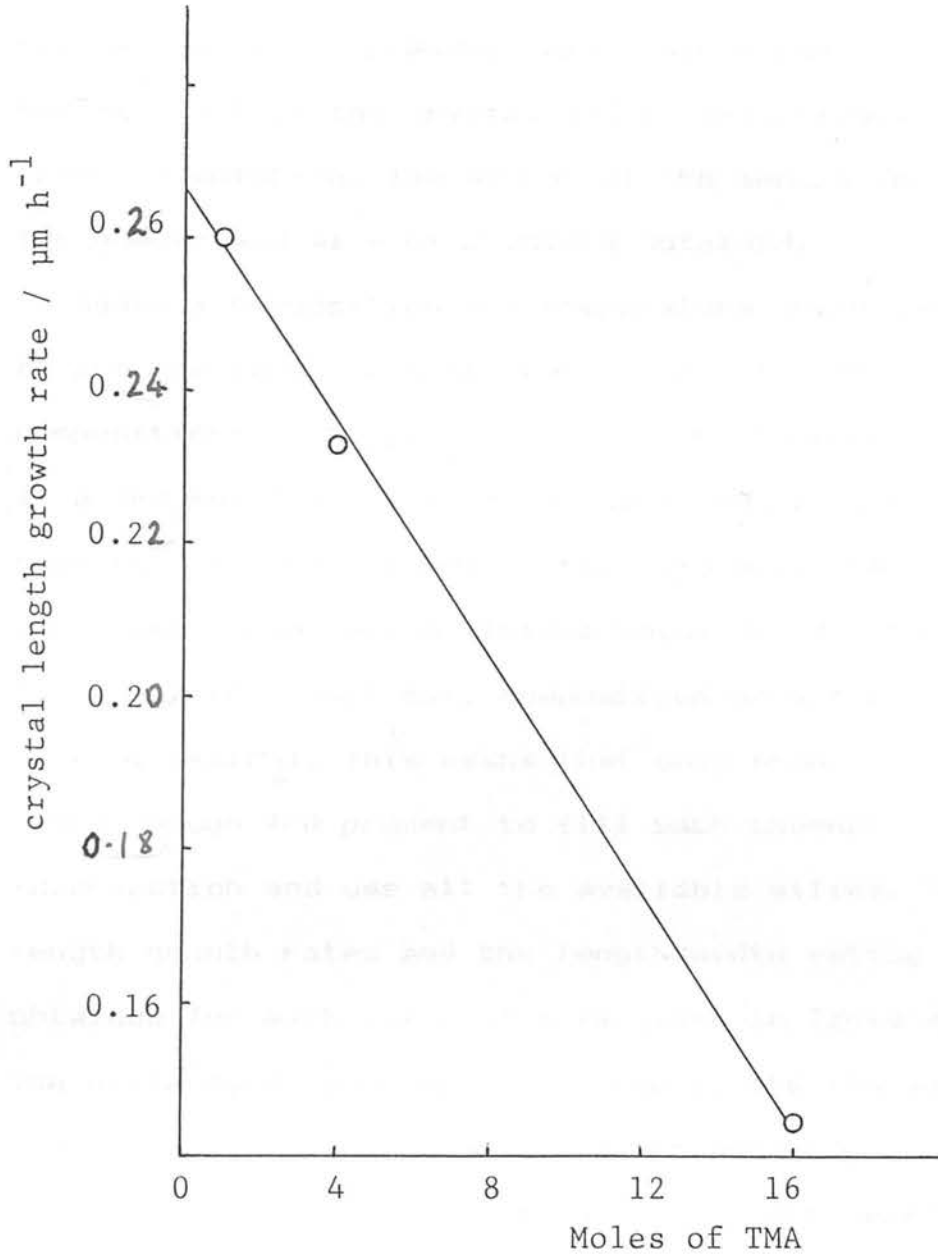


Figure 4.18. The effect of TMA ion concentration on silicalite crystal growth rate for a reaction mixture of composition $3\text{Na}_2\text{O} \cdot 6\text{SiO}_2 \cdot 24\text{EtOH} \cdot 600\text{H}_2\text{O} \cdot 1\text{TPABr} \cdot x\text{TMAX}$

present in the initial reaction mixture should influence the growth of the crystal. As TPA is a participant in the crystallization the supersaturation of the mother liquor will be affected by the change in the amount of TPA present. Also, since the TPA actually becomes part of the crystal and is effectively removed from the solution. The amount of TPA should influence the number and size of crystals obtained.

Again a composition and temperature which was known to produce large crystals was chosen ($T = 413\text{K}$, composition: $0.5\text{Na}_2\text{O}; 20\text{SiO}_2; 80\text{EtOH}; 750\text{H}_2\text{O}; x\text{TPABr}$). If a TPA molecule is sited at each channel intersection then the structure predicts that the SiO_2/TPA ratio of the crystal can have a minimum value of 24. (The stoichiometric unit cell composition of silicalite-1 is $4\text{TPADH}; 96\text{SiO}_2$). This means that only when $x > 0.83$ is there enough TPA present to fill each channel intersection and use all the available silica. The length growth rates and the length/width ratios obtained for each value of x is given in Table 4.17. The differences must be attributed to the TPA molecules and not the bromide anion since the addition of different amounts of sodium halide did not reveal any major differences to the growth rates (see Section 4.3.4).

Figure 4.19 shows the growth rates plotted against the amount of TPA. This graph shows clearly that as the amount of TPA is increased the growth rate also

Table 4.17. Length growth rates (R_1) and length / width ratios (l/w) for silicalite-1 for different amounts of tetrapropylammonium bromide (TPABr).

Temperature : 413 K

Composition : $0.5\text{Na}_2\text{O}$ 20SiO_2 80EtOH $750\text{H}_2\text{O}$ xTPABr

Run No.	Moles TPABr (x)	R_1 ($0.5 \Delta l / \Delta t$) / $\mu\text{m h}^{-1}$	l / w
1	0.01	0.06	~ 7
2	0.05	0.12	
3	0.1	0.22	5.6
4	0.5	0.28	2.7
5	1.0	0.28	2.7
6	5.0	0.27	2.5

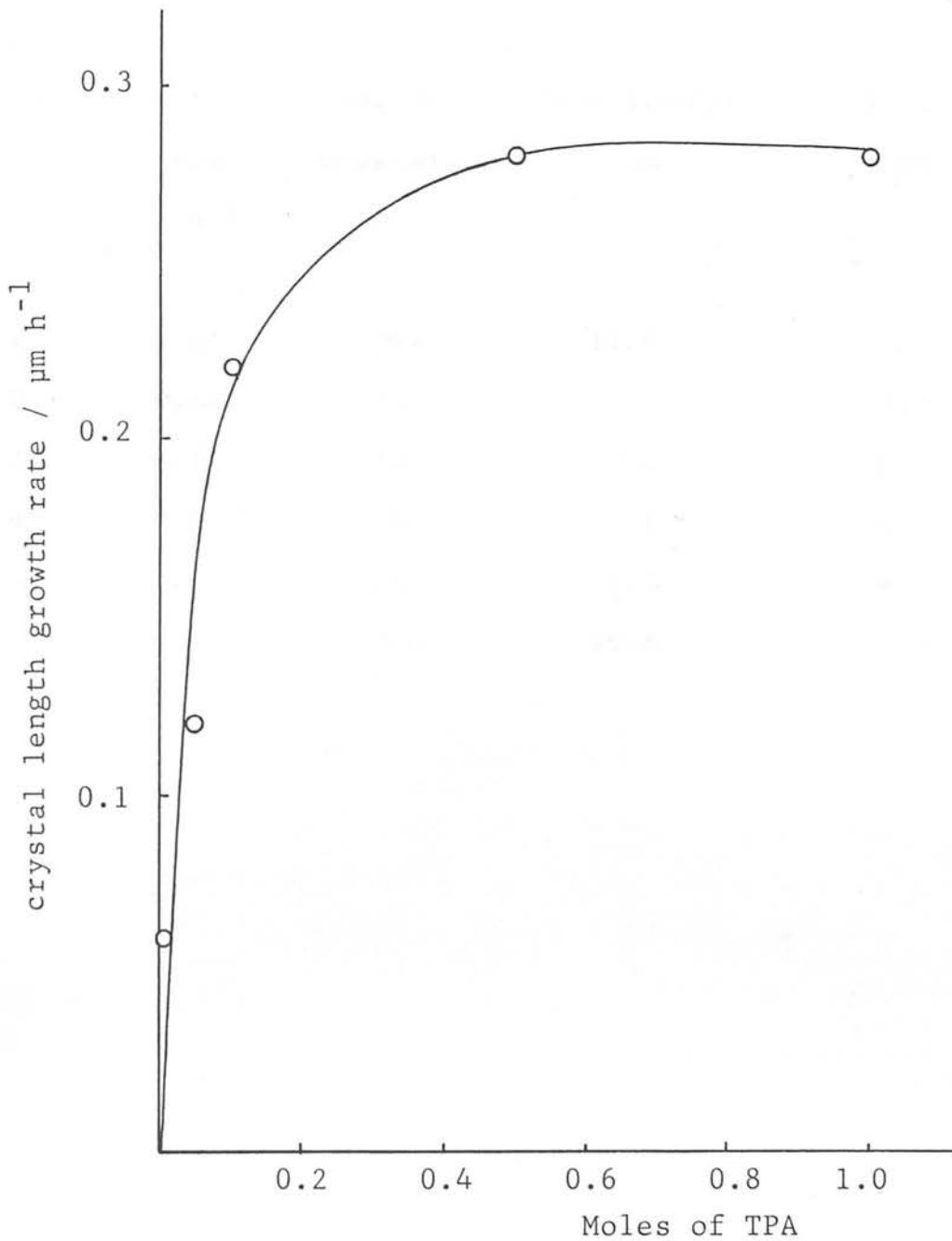


Figure 4.19. The effect of TPA ion concentration on silicalite crystal growth rate for a reaction mixture of composition $0.5\text{Na}_2\text{O} \cdot 20\text{SiO}_2 \cdot 80\text{EtOH} \cdot 750\text{H}_2\text{O} \cdot x\text{TPABr}$.

Table 4.18. Number of crystals present in a "volume" of microslide for different amounts of TPABr.

Temperature : 413K

Run No.	Moles TPABr (x)	No. of crystals	Mean length / μm	Std. dev. / μm
1	0.01	297	11.9	2.9
2	0.05	130	26.7	5.9
3	0.1	383	27.8	5.9
4	0.5	365	29.6	5.4
5	1.0	589	36.3	4.5
6	5.0	565	25.6	3.5

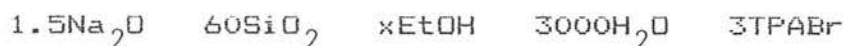
increases as is to be expected. However the leveling off in the growth rate which occurs at higher concentrations of TPA ($x > 0.5$) is much more difficult to understand. It could be that at low concentrations the growth rate is limited by the availability of TPA ions whereas at higher concentrations the crystal growth is limited by the availability of the silicate building units.

The TPA concentration also appears to affect nucleation. Table 4.18 lists the number and size of crystals found in a fixed "volume" of the microslide for each TPA concentration. In general, more and larger crystals were obtained when the amount of TPA was increased. Indeed in those runs with only small amounts of TPA ($x=0.1$ and 0.05) another (unidentified) phase appeared after the silicalite-1 crystals had stopped growing.

4.3.6. Ethanol additions.

All the reaction mixtures which were prepared from tetraethyl silicate have ethanol present as a result of the hydrolysis of the tetraethyl silicate. The presence of the ethanol may influence the reaction. The ethanol could perhaps compete with the TPABr and be absorbed by the growing crystal. The ethanol may even affect the supersaturation by influencing the silicate anion distribution. In order to investigate the effect of ethanol several reactions were carried out with different amounts of ethanol added. The composition

chosen for examination was the standard composition:



which gives crystals of a reasonable size. The number of moles of ethanol x was varied from 240 to 1680, where $x = 240$ is the number of moles of ethanol which result from the hydrolysis of 60 moles of tetraethyl silicate. Reactions were carried out at 393, 413 and 433K.

The results are shown in table 4.19 and figure 4.20. Table 4.19 shows clearly that a small additional amount of ethanol does not affect the growth rate but a large addition produces a substantial decrease in the growth rate. It was impossible to measure the width growth rates for the reactions with the high ethanol content because the crystals were very narrow (see figure 4.21) and similar in shape to the crystals obtained for low TPA concentrations. Crystals obtained at both 393K and 433K clearly show that the addition of ethanol has produced a more elongated crystal (see figure 4.21).

The high concentration of ethanol may compete with the TPA ions for access to the zeolite channels and slow down the growth of the crystal. ZSM-5 has been produced with ethanol as the organic void filler, and there is no reason why it could not be incorporated into the silicalite-1 crystals. However ethanol is not as good a "fit" as TPA and the overall effect is similar to the addition of TMA salt (see Section 4.3.4). The additional ethanol may also affect the

Table 4.19. Growth rates (R_1) for different amounts of ethanol.

Composition : 1.5Na₂O 60SiO₂ xEtOH 300OH₂O 3TFABr

Run No.	Moles EtOH (x)	R_1 (0.5 $\Delta l / \Delta t$) / $\mu\text{m h}^{-1}$		
		393K	413K	433K
1	240	0.067	0.23	0.62
2	480	0.065	0.22	--
3	720	0.063	--	0.56
4	1200	--	0.21	0.53
5	1680	0.047	0.14	0.36

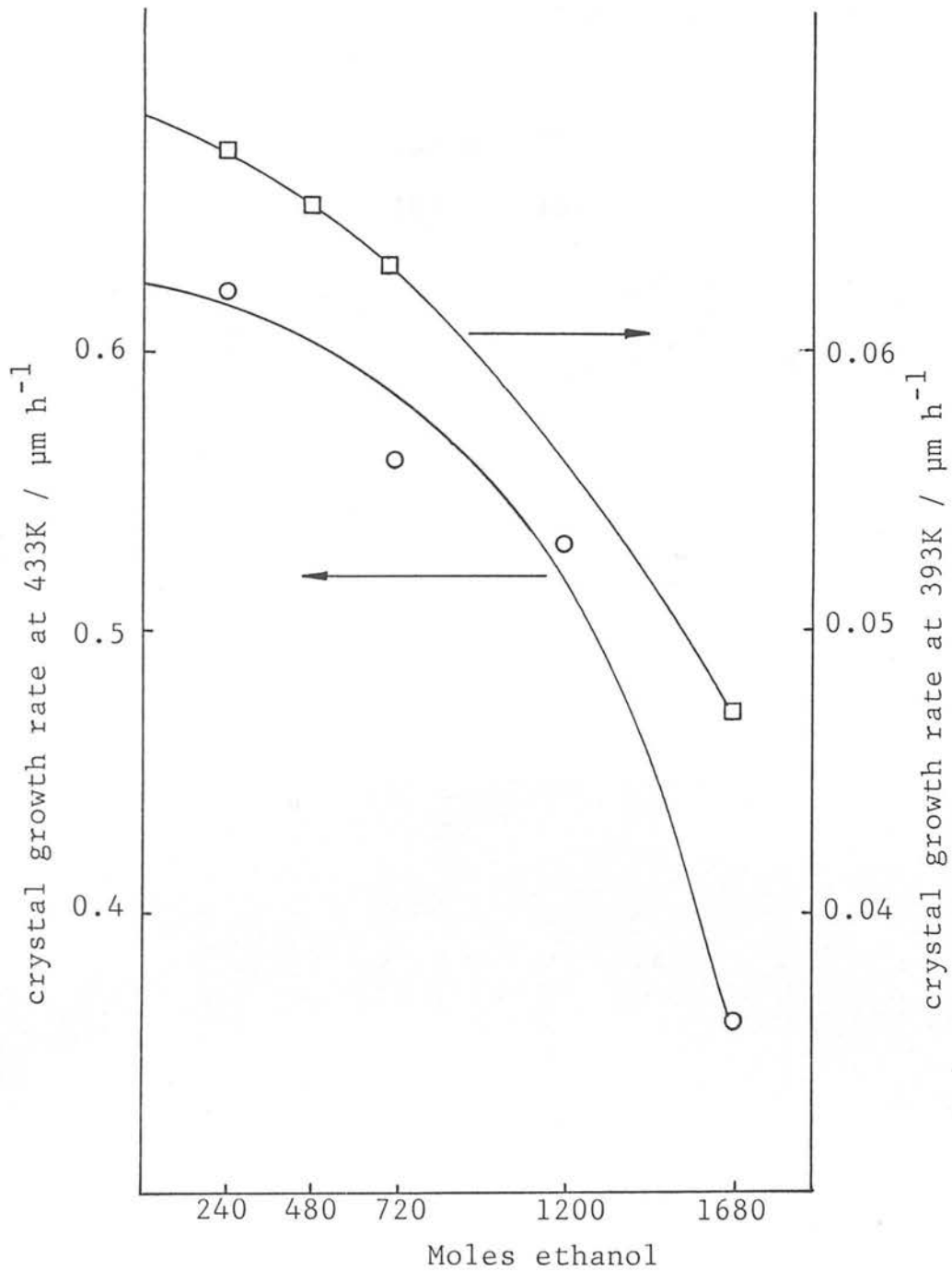


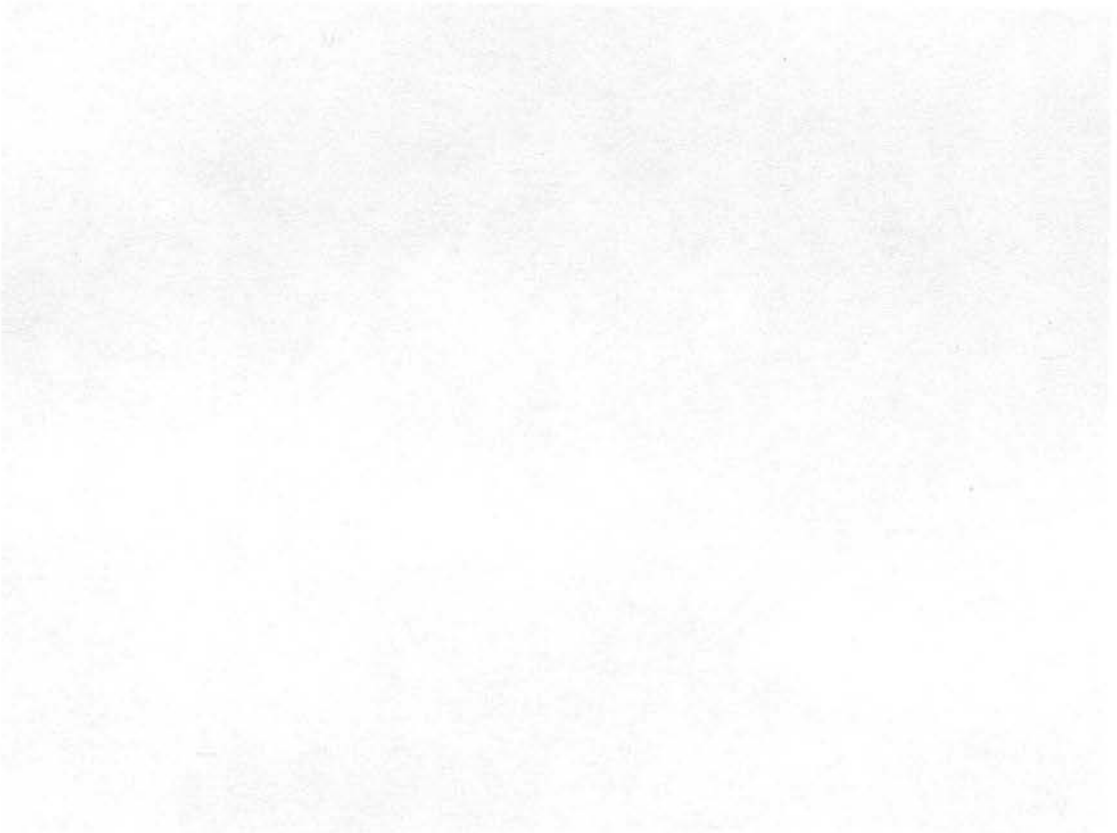
Figure 4.20. The effect of ethanol on the crystal growth rate for a reaction mixture of composition $1\text{Na}_2\text{O} \cdot 60\text{SiO}_2 \cdot x\text{EtOH} \cdot 3000\text{H}_2\text{O} \cdot 3\text{TPABr}$ at 393K and 433K.

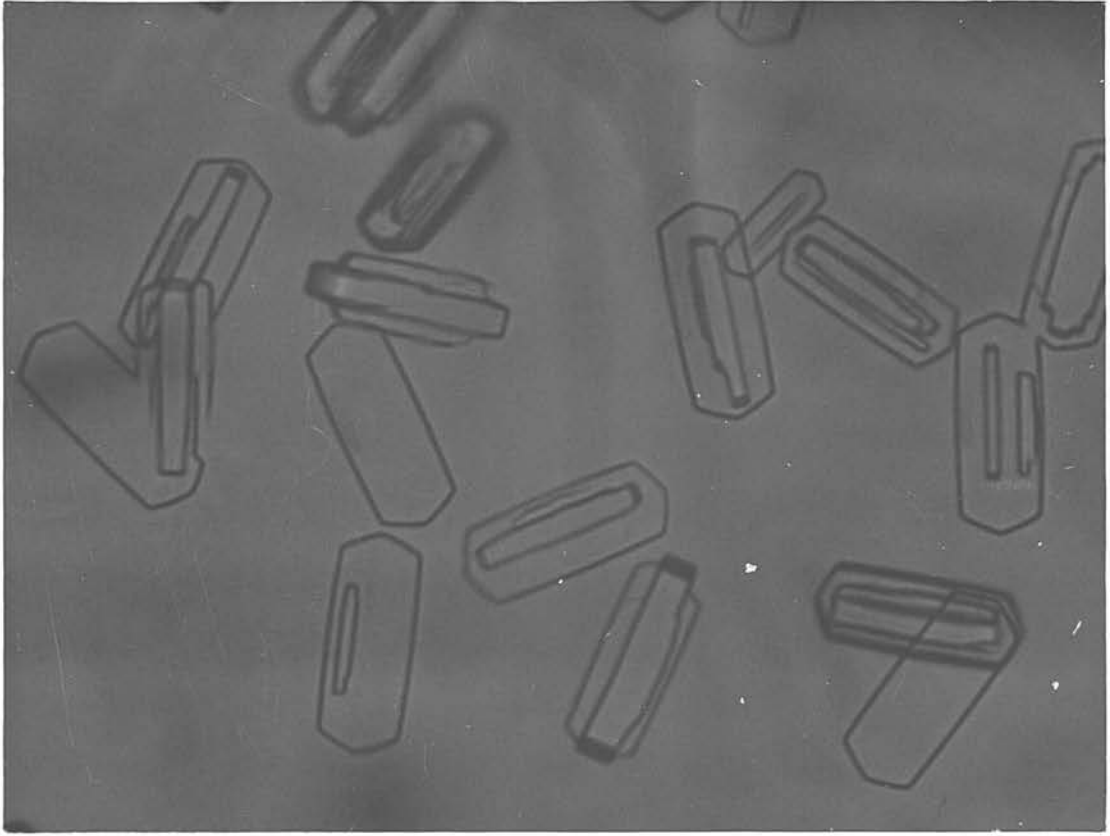
Figure 4.21. (overleaf).

Optical photomicrograph of silicalite crystals from a reaction mixture of composition $1.5\text{Na}_2\text{O} \cdot 60\text{SiO}_2 \cdot x\text{EtOH} \cdot 3000\text{H}_2\text{O} \cdot 3\text{TPABr}$ at 413K.

(a) $x = 240$

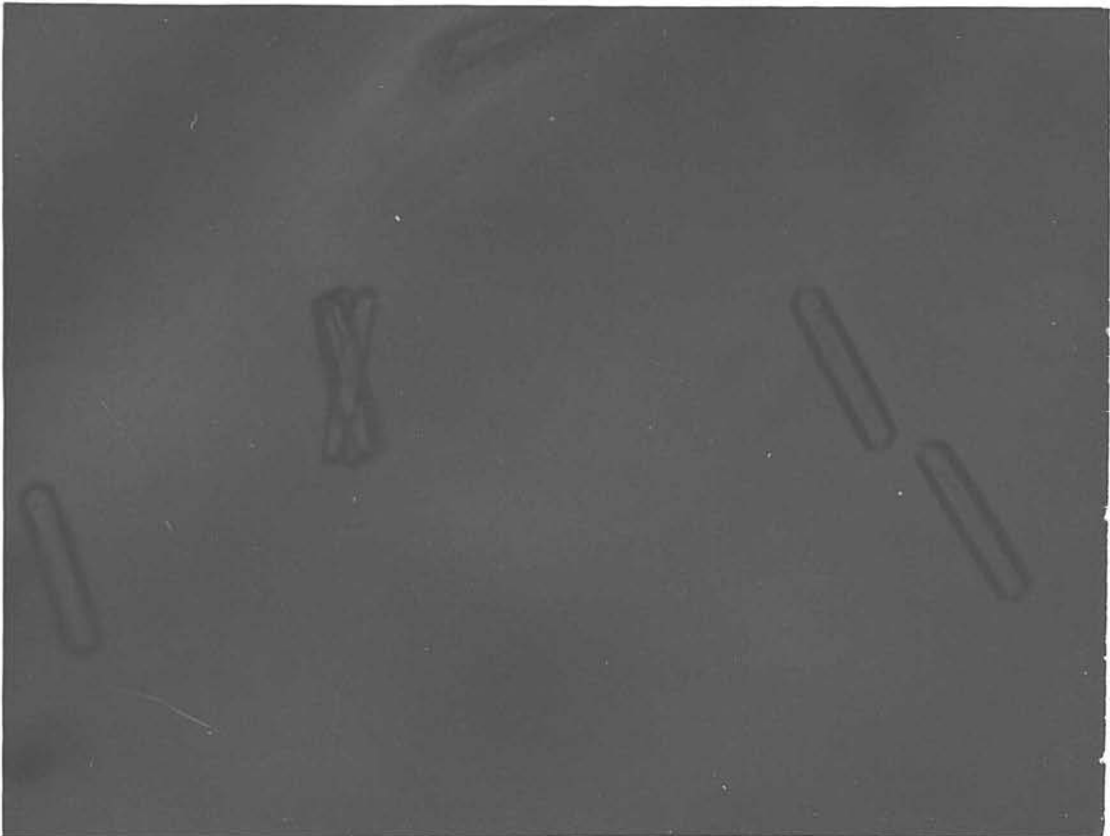
(b) $x = 1680$





a

50 μ m



b

50 μ m

supersaturation of the solution. If there are fewer building blocks in the solution then the growth rate will not be as fast.

4.3.7 Other systems.

The experiments so far described in this chapter established the conditions for the growth of larger than normal crystals of silicalite-1 and ZSM-5. The reactions have to have a low base content, high silica concentration, and a low inorganic cation content. These conditions allow the growth of crystals of a reasonable size at temperatures above 373K. The problem with low temperatures is that the crystal growth rate is so very small that it takes a very long time to obtain a large crystal. For example, reaction 5 (table 4.10) with a growth rate of $0.015 \mu\text{m h}^{-1}$ would take approximately 20 weeks to produce a $100 \mu\text{m}$ silicalite crystal, while reaction 1A (table 4.10) with a growth rate of $0.011 \mu\text{m h}^{-1}$ would take over 27 weeks to produce a $100 \mu\text{m}$ ZSM-5 crystal at 363K. This of course, assumes that there is enough nutrient available to allow a crystal to grow to such a size. The only way to produce large crystals within a reasonable time is to use higher temperatures. At 413K, reaction 5 (table 4.10) would only take approximately 6 days rather than 20 weeks to produce a $100 \mu\text{m}$ crystal (if enough nutrient were available). It was of considerable interest to establish whether the conditions used to grow larger silicalite crystals could be applied to

other zeolite systems. The zeolites chosen were all high silica zeolites; EU-1,¹⁸ ZSM-48¹⁹ and ZSM-39.²⁰

4.3.7.1. Zeolite EU-1

Zeolite EU-1 cannot as yet be synthesized in an all silica form, so it was necessary to include aluminium in the reaction mixture. This produced some practical problems. As with the ZSM-5 reaction in section 4.3.3 the addition of aluminium requires a higher base and water content to maintain a clear reaction mixture. Some of the mixtures used did, in fact, "gel" soon after being placed in the microslide and the gel is often obvious in the photographs. Zeolite EU-1 does not crystallize as easily as silicalite-1. Initial reactions at even 423K were very slow and other phases would often crystallize along with the EU-1. Some of the successful compositions are shown in table 4.20 along with the crystal sizes attained. X-ray powder diffraction confirmed that the product was EU-1.

The difficulty associated with the maintenance of a liquid reaction mixture which could be sucked into a microslide, yet achieving high silica, low base solutions meant that most success was achieved by using a fumed silica (cab-o-sil) as the silica source. It was found that the mixtures made using cab-o-sil remained fluid for longer and could still be sucked into a microslide. Table 4.20 shows that the reactions which are lower in base and more concentrated produce the largest crystals. Fumed silica proved to be easier to

Table 4.20. Production of large crystals: EU-1

Run No.	Composition						Temp. /K	Largest crystal present / μm
	Na_2O	SiO_2	EtOH	HexBr*	H_2O	Al_2O_3		
1	3	20	80	1	1500	0.3	448	10
2	2	20	80	1	1500	0.3	423	26 ^b
3	2	20	80	1	1500	0.2	423	34 ^b
4	2	20	80	1	1500	0.2	448	22
5 ^a	1	20	80	1	750	0.3	423	25
6	1	20	80	1	750	0.3	448	40 ^b
7	1	20 ^c	--	1	750	0.3	473	80
8 ^a	1	20 ^c	--	1	750	0.3	453	60 ^d
9 ^a	1	20 ^c	--	1	750	0.3	413	50 ^e
10	1	20 ^c	--	1	750	0.3	473	55
11	1	20 ^c	--	1	750	0.3	473	50

a steel bomb reaction

b other phases present

c fumed silica (cab-o-sil) used as silica source

d size after 10 days

e size after 5 months

* hexamethonium bromide $(\text{CH}_3)_3\text{N}^+(\text{CH}_2)_6\text{N}^+(\text{CH}_3)_3\text{2Br}^-$

use under these conditions and also gave reasonably large crystals. High temperatures were certainly needed for reasonable growth rates. Run 8 contained 60 μm crystals after 10 days at 453K. Run 9, which had the same composition, contained 50 μm crystals only after 5 months at 413K.

The measurement of growth rates was not as simple with these crystals. The crystals appeared to be "peanut" shaped; a somewhat unusual shape for a crystal! However they did give quite good extinctions between crossed polarizers when viewed with an optical microscope. This was quite promising as it suggested that they were single crystals. Nevertheless it was difficult to measure growth rates for these crystals. Figure 4.22 shows the growth curves for runs 10 and 11. These had identical reaction mixtures and were crystallized at the same temperature. Nevertheless they appear to have quite different growth curves. A closer examination of some of the optical micrographs suggested that the EU-1 crystals (see figure 4.23) had some additional structure. The initial electron micrographs did not show anything unusual, perhaps partly due to a coating of gel on the crystals (e.g. see figure 4.24). However later micrographs (figure 4.25) showed that the EU-1 "crystals" are in fact made from stacked plates all growing out from a common centre. So although the "crystals" are large they are not in fact single crystals and consequently not

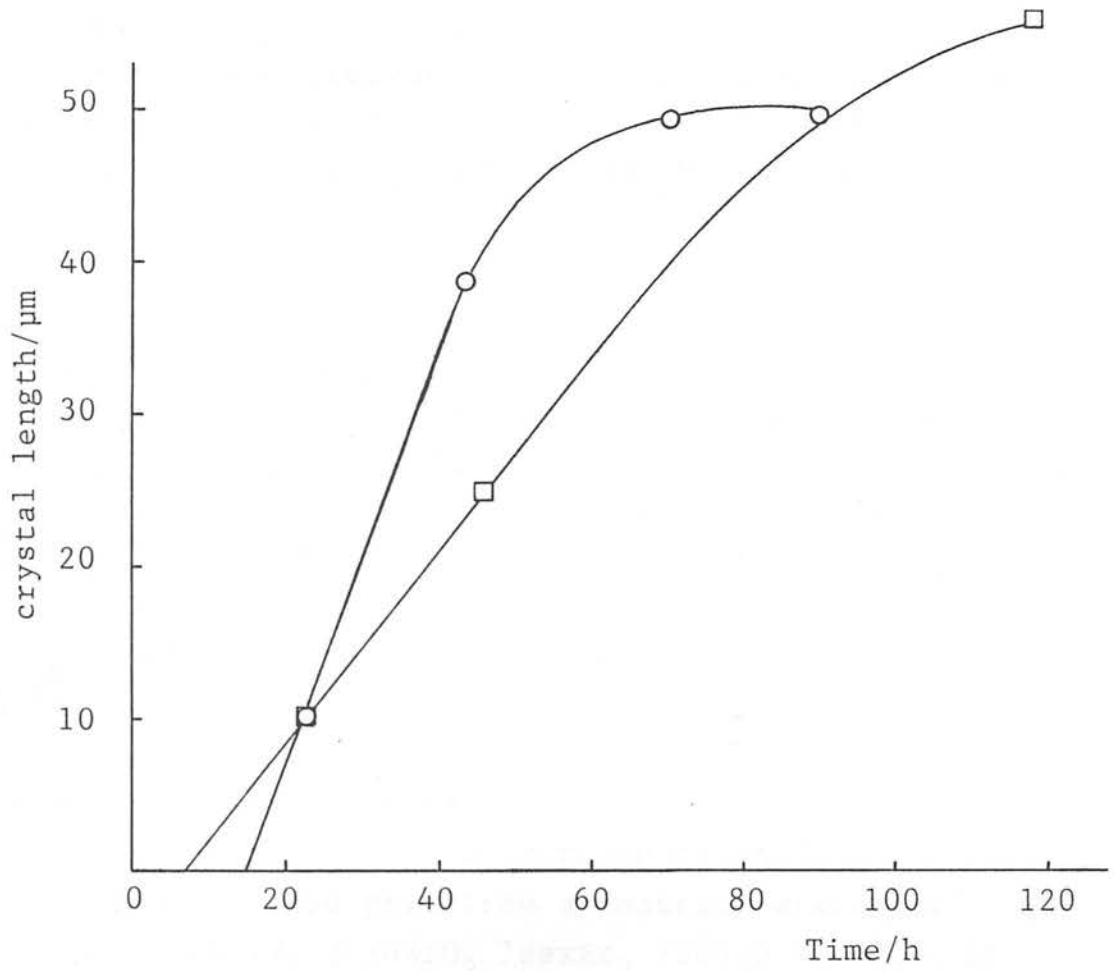


Figure 4.22. Crystal growth at 473K for runs 10 (\square) and 11 (\circ).

Figure 4.23. (overleaf).

Optical photomicrograph which suggests structure on an EU-1 "crystal" from a reaction mixture of composition $1\text{Na}_2\text{O}$ 20SiO_2 1HexBr_2 $750\text{H}_2\text{O}$ $0.3\text{Al}_2\text{O}_3$ at 473K.

Figure 4.24. (overleaf).

Scanning electron photomicrograph of an EU-1 "crystal" coated with dried gel, from a reaction mixture of composition $1\text{Na}_2\text{O}$ 20SiO_2 1HexBr_2 $750\text{H}_2\text{O}$ $0.3\text{Al}_2\text{O}_3$ at 453K.



Fig. 23.

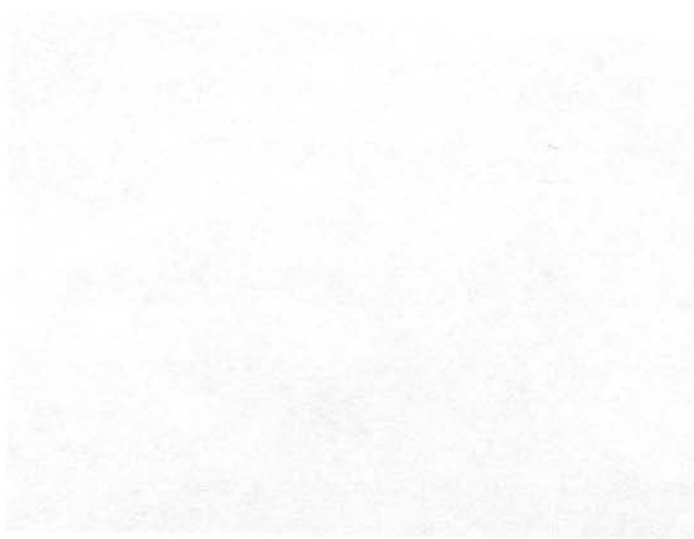
50 μ m

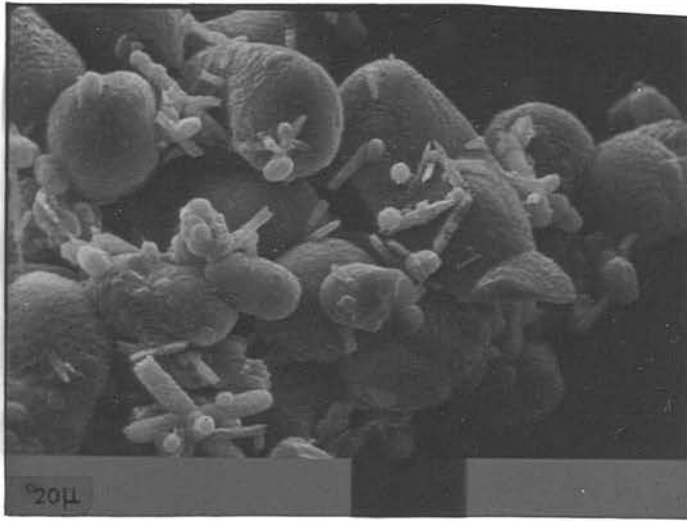


Fig. 24.

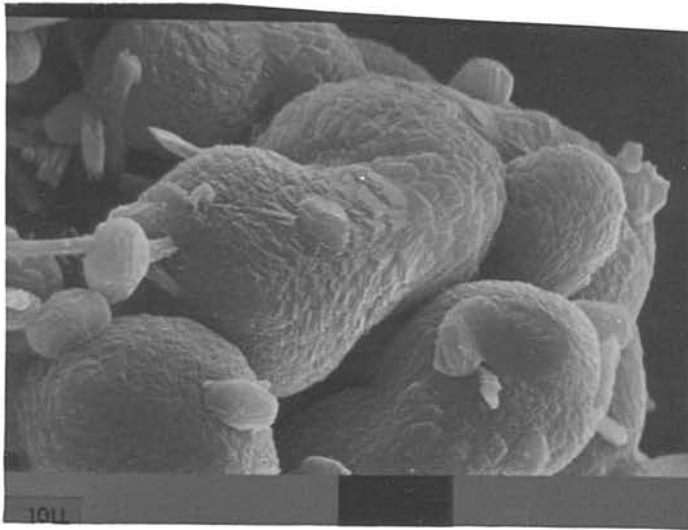
Figure 4.25. (overleaf).

Scanning electron photomicrographs of EU-1 "crystals" which show that these are not single crystals. Crystals obtained from a reaction mixture of composition $1\text{Na}_2\text{O}$ 20SiO_2 1HexBr_2 $750\text{H}_2\text{O}$ $0.3\text{Al}_2\text{O}_3$ at 413K.

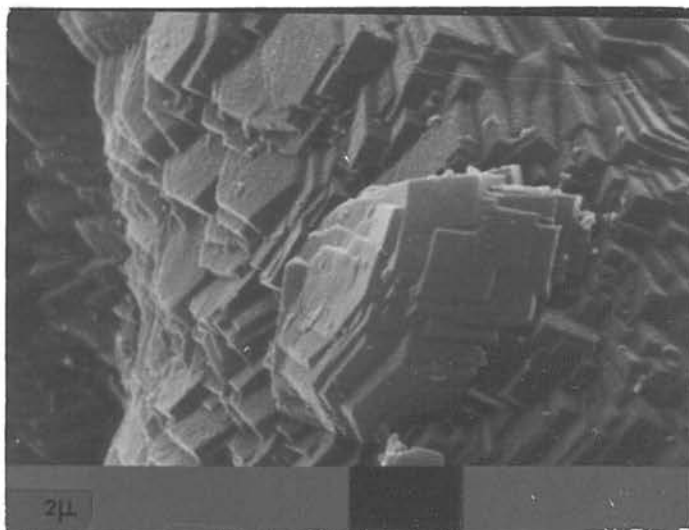




a



b



c

suitable for structure determination. It would seem that to grow a single EU-1 crystal it will be necessary to alter the composition so that several crystals do not grow together from the same nucleation centre (or at least if several do grow from the same centre then they grow as separate plates). Although this was not achieved with EU-1, work on the growth of ZSM-48 did suggest that this was possible (see section 4.3.7.2).

4.3.7.2. Zeolites ZSM-39 and ZSM-48

The work carried out on ZSM-5 and silicalite-1 crystallization had suggested that low alkali, alkali metal ion and high silica concentration should produce large crystals. This approach was therefore applied to the crystallization of ZSM-39 and ZSM-48. Table 4.21 shows the results for ZSM-48 crystallization. The initial reactions with sodium present (Runs 1 and 2) gave small "dog-bone" type crystals which, on examination by scanning electron microscopy, were found to be bundles of tightly packed fibres (see figure 4.26 a-c). When sodium was omitted from the composition a remarkable change occurred; the fibres opened out. Figures 4.27a to 4.27d show the effect of the removal of sodium ions and then those of altering the TMA, hydroxide and water content. ZSM-48 can be obtained as large "fluffy" bundles of fine fibres or thicker fibres can be obtained. Figure 4.26c is an electron micrograph of the ends of some of these fibres. The hexagonal ends are clearly seen.

Table 4.21. Production of large crystals: ZSM-48

Run No.	Composition					Temp. /K	Fig. No.	Shape
	M ₂ O	TMA ₂ O	SiO ₂	H ₂ O	MBr			
1	0.5 [*]	0.5	20	500	-	453	4.26a	tight
2	0.25 [*]	0.5	20	500	-	453	4.26b, c	bundles of fibres
3	-	0.5	20	500	-	473	4.27a	branched
4	-	0.5	20	750	-	473	4.27b	fibres
5	-	1	20	500	-	453	4.27c	loose
6 ^a	-	1	20	250	-	453	4.27d	bunches of fibres
7 ^a	0.25 [#]	0.5	20	500	-	453	4.28a	tight
8	-	1	20	250	0.25 [#]	453	4.28b	bundles of fibres
9	-	1	20	250	0.25 [*]	453	-	"

Silica source: fumed silica (cab-o-sil)

* M = Na

M = Cs

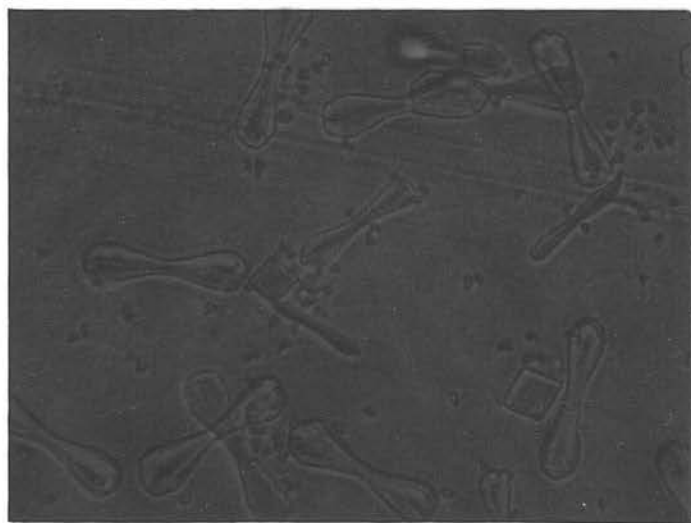
a steel bomb reaction

Figure 4.26. (overleaf).

(a) Optical photomicrograph of ZSM-48 "dog-bones".
(see run 1, table 4.21).

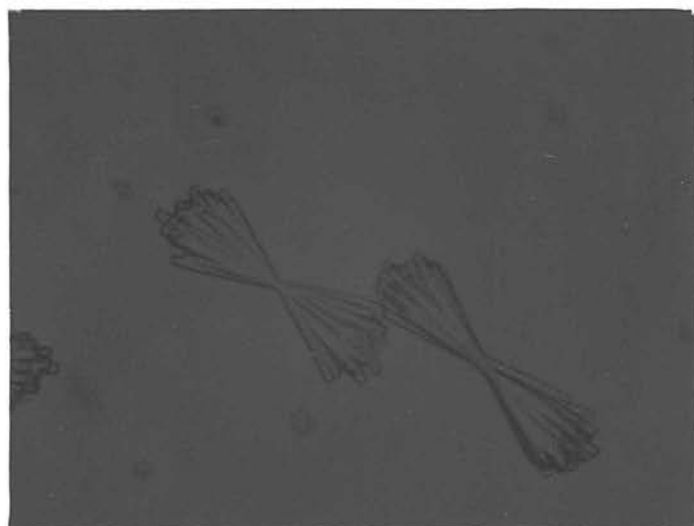
(b) Optical photomicrograph of ZSM-48 crystals.
(see run 2, table 4.21). The "dog-bones" are made of
fibres.

(c) Scanning electron photomicrograph of ZSM-48
fibre ends (see run 2, table 4.21).



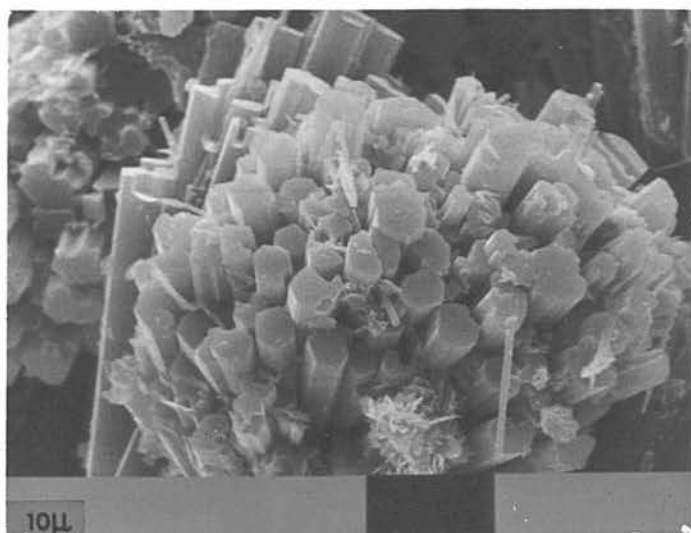
a

50 μ m



b

50 μ m



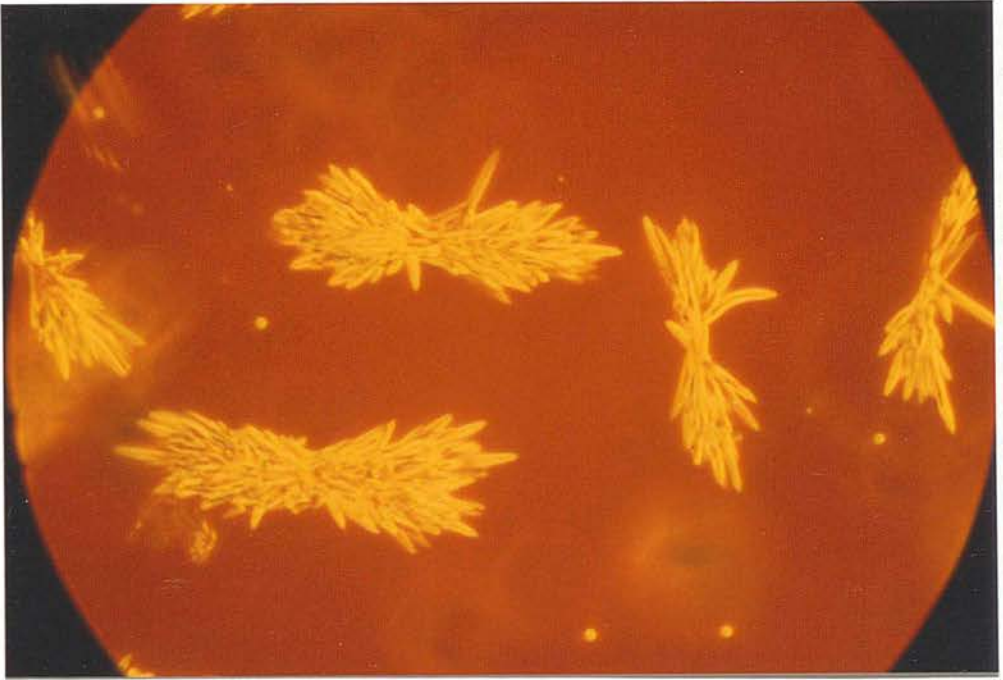
c

Figure 4.27. (overleaf).

Optical photomicrographs of bundles of ZSM-48 fibres.

		Composition	Temp/K
(a)	Run 3	$0.5\text{TMA}_2\text{O}$ 20SiO_2 $500\text{H}_2\text{O}$	473
(b)	Run 4	$0.5\text{TMA}_2\text{O}$ 20SiO_2 $750\text{H}_2\text{O}$	473
(c)	Run 5	$1\text{TMA}_2\text{O}$ 20SiO_2 $500\text{H}_2\text{O}$	453
(d)	Run 6	$1\text{TMA}_2\text{O}$ 20SiO_2 $250\text{H}_2\text{O}$	453

The more dilute system (b) has fewer fibres than the more concentrated system (d) which contains many fine fibres.



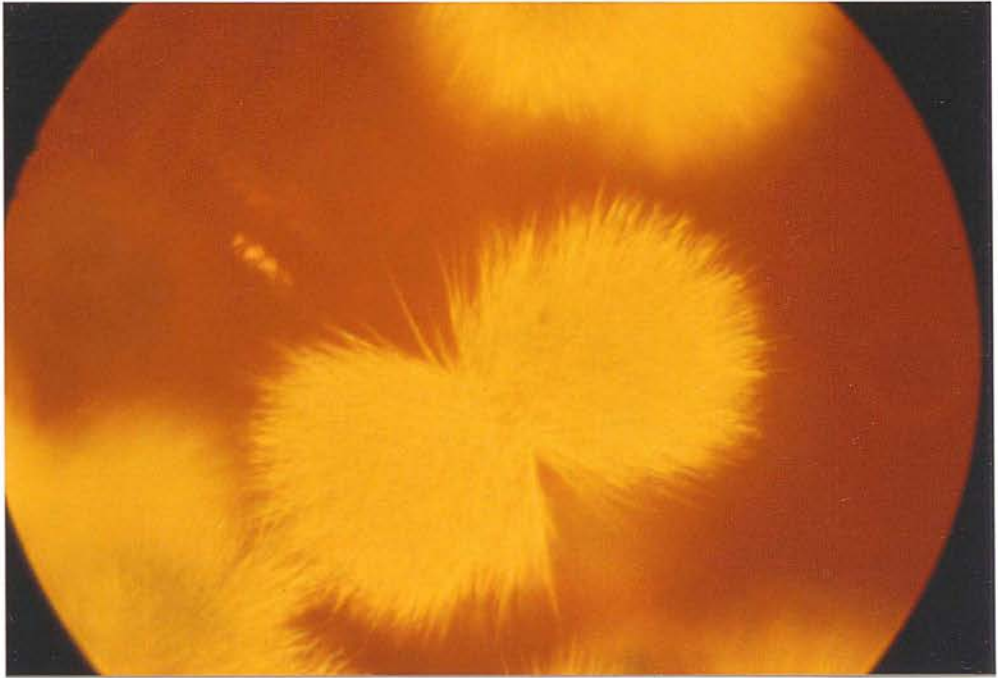
a

50µm



b

50µm



c

50µm



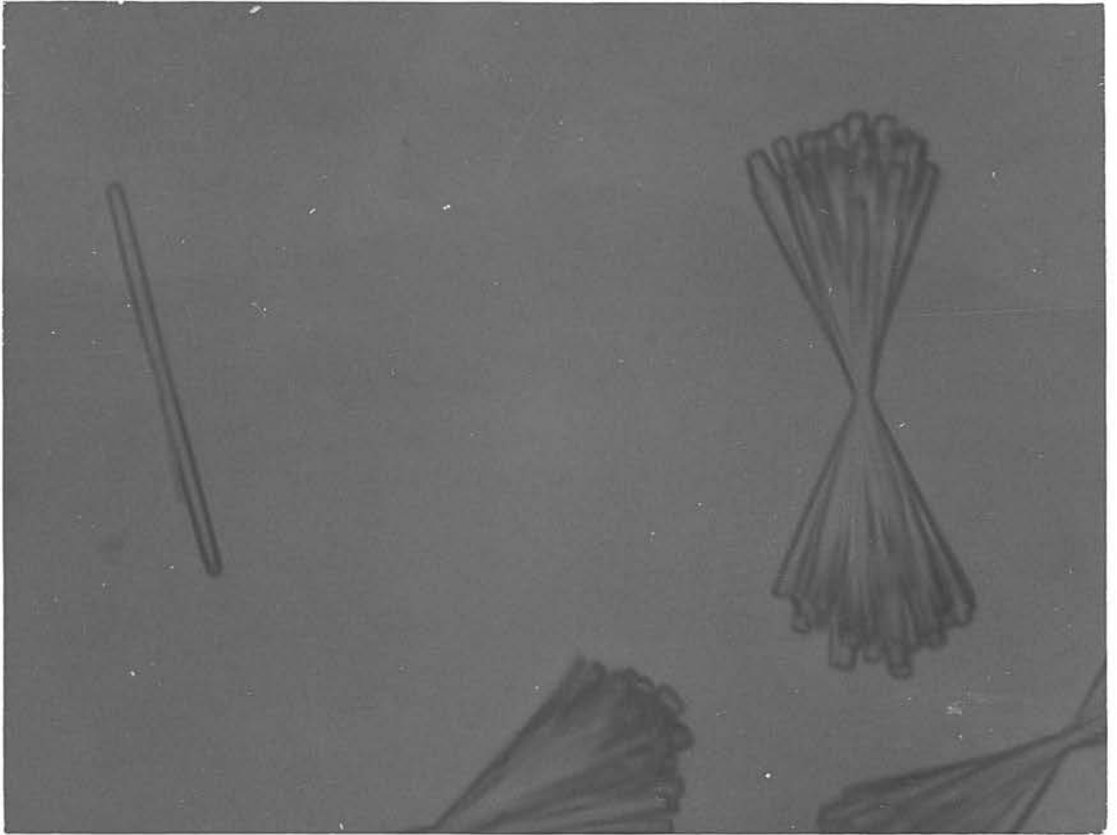
d

50µm

Figure 4.28. (overleaf).

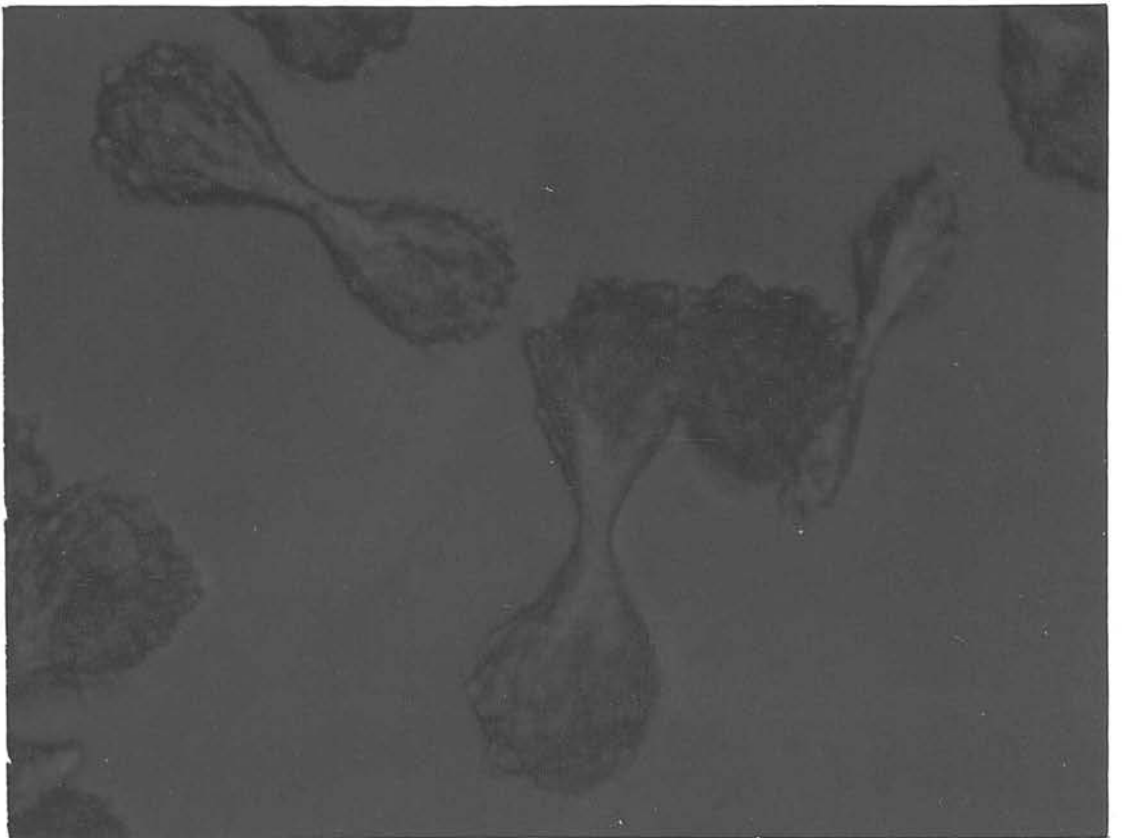
Optical photomicrograph of bundles of ZSM-48 fibres which show the effect of the addition of alkali metal ions (c.f. figure 4.27).

	Composition	Temp/K
(a)	Run 7 0.25Na ₂ O 0.5TMA ₂ O 20SiO ₂ 500H ₂ O	453
(b)	Run 8 1TMA ₂ O 20SiO ₂ 250H ₂ O	453



a

50 μ m



b

50 μ m

It would certainly seem that it is the metal cation which is responsible for the tight packing of the fibres. In Runs 8 and 9 sodium bromide and cesium bromide respectively were added. In both cases tightly packed bundles of fibres were obtained, similar to Runs 1 and 2. Perhaps if sodium were absent in the synthesis of EU-1, the plates produced in that system would also separate.

In most of the reactions shown in table 4.21 ZSM-39 crystallized along with ZSM-48. Only in Runs 3 and 4 was there no evidence of ZSM-39. In general, the system with a higher concentration of silica is more likely to produce ZSM-39. This is shown in table 4.22, where the composition with the highest concentration of silica (Run 11) did not appear to contain any ZSM-48. Very large crystals of ZSM-39 could be easily obtained (e.g. see figure 4.30a). An interesting example of the co-crystallization of ZSM-39 and ZSM-48 is shown in figure 4.30d where a ZSM-39 crystal surrounds a bundle of ZSM-48 fibres.

Table 4.22. Production of large crystals: ZSM-39.

Run No.	Composition				Temp. /K	Figure No.
	Na ₂ O	TMA ₂ O	SiO ₂	H ₂ O		
10	-	0.5	20	250	453	4.29a
5	-	1	20	500	453	4.29b
6 ^a	-	1	20	250	453	4.30a
11 ^a	-	1	20	150	453	4.30b
2	0.25	0.5	20	500	453	4.30c
1	0.5	0.5	20	500	453	4.30d

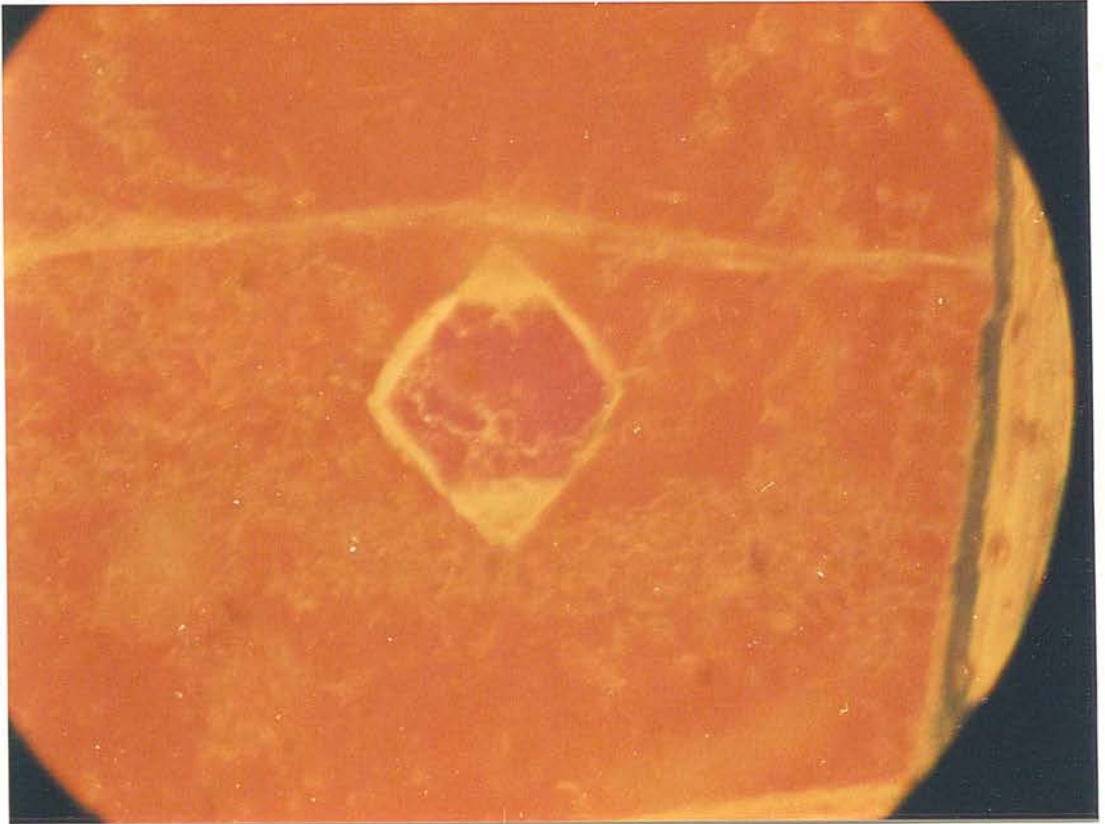
Silica source: fumed silica (cab-o-sil)

a steel bomb reaction

Figure 4.29. (overleaf).

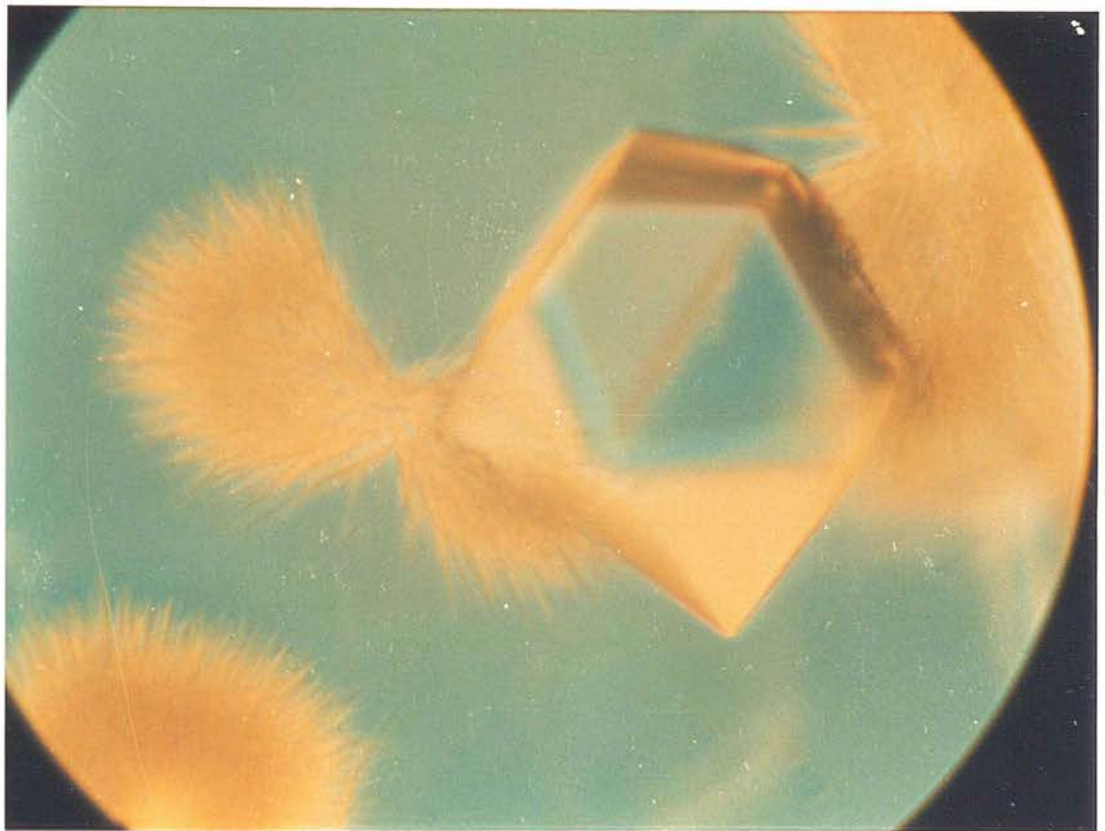
Optical photomicrographs of ZSM-39 crystals.

		Composition	Temp/K
(a)	Run 10	$0.5\text{TMA}_2\text{O}$ 20SiO_2 $250\text{H}_2\text{O}$	453
(b)	Run 5	$1\text{TMA}_2\text{O}$ 20SiO_2 $500\text{H}_2\text{O}$	453



a

100μm



b

50μm

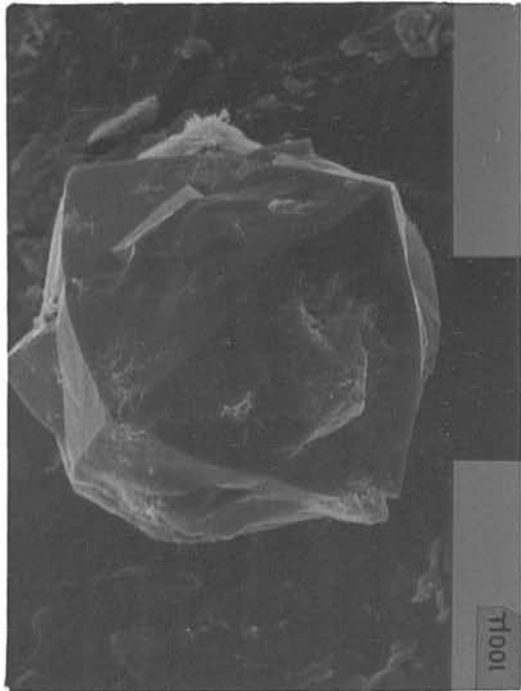
Figure 4.30. (overleaf).

(a) Scanning electron photomicrograph of a large ZSM-39 crystal from a reaction mixture of composition $1\text{TMA}_2\text{O}$ 20SiO_2 $250\text{H}_2\text{O}$ at 453K (Run 6, table 4.22)

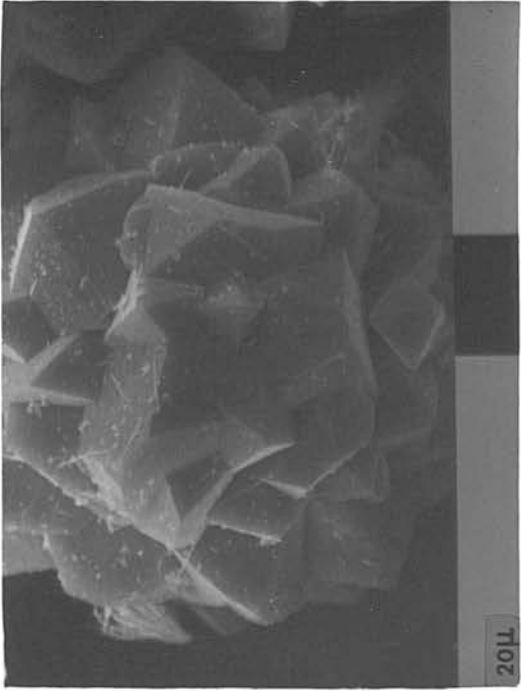
(b) Scanning electron photomicrograph of a ZSM-39 crystal from a reaction mixture of composition $1\text{TMA}_2\text{O}$ 20SiO_2 $150\text{H}_2\text{O}$ at 453K (Run 11, table 4.22).

(c) Scanning electron photomicrograph of a ZSM-39 crystal from a reaction mixture of composition $0.25\text{Na}_2\text{O}$ $0.5\text{TMA}_2\text{O}$ 20SiO_2 $500\text{H}_2\text{O}$ at 453K (Run 2, table 4.22).

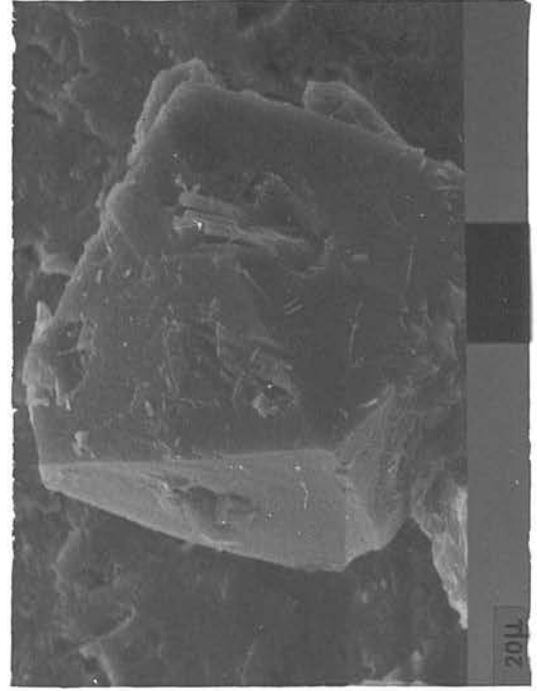
(d) Optical photomicrograph of a ZSM-39 crystal which surrounds a bundle of ZSM-48 fibres. From a reaction mixture of composition $0.5\text{Na}_2\text{O}$ $0.5\text{TMA}_2\text{O}$ 20SiO_2 $500\text{H}_2\text{O}$ at 453K (Run 1, table 4.22).



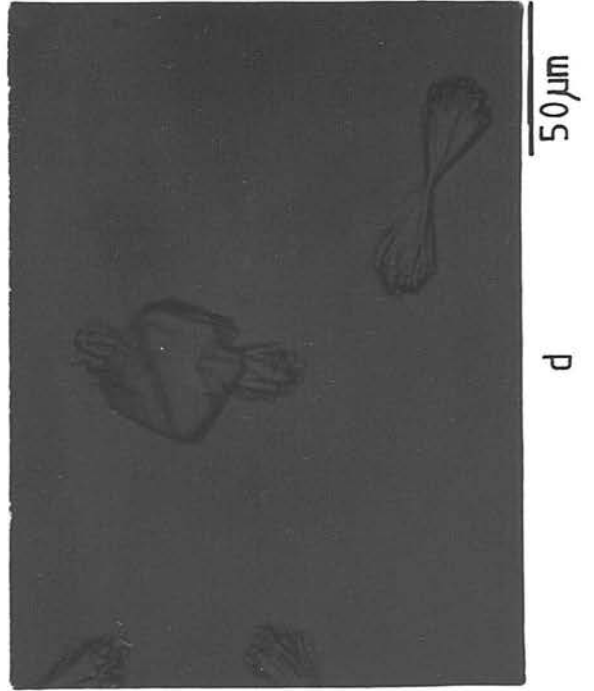
a



b



c



d

4.4 Conclusions.

The production of large crystals of some high silica zeolites can be achieved by careful control of the reaction mixture composition and the crystallization conditions. Low supersaturations achieved by a reduction in the hydroxide content is desirable, as is a high concentration of silica (as large polymers or colloidal species) required to feed the growing crystals. The absence of alkali metal ions is also an advantage. The growth of these crystals can now be followed directly by optical microscopy, and the growth of single crystals can, by the methods developed in this work, be followed with comparative ease.

4.5. References.

1. L.B. Sand, "Proceedings of the 5th. International Conference on Zeolites", Ed. L.V.C. Rees, Heyden, London, 1980, 1
2. G.W. Dodwell and L.B. Sand, Recent Progress Report, 4th. Int. Zeolite conference, U. Chicago, 1977.
3. R.M. Barrer, "Hydrothermal Chemistry of Zeolites", Academic Press, London, 1982, 178.
4. R.M. Barrer, Brit. Ceram. Soc., 1957, 56, 155.
5. Bye and E.A.D. White, J. Cryst. Growth, 1970, 6, 355.
6. J.Ciric, Science, 1967, 155, 689.
7. J.F. Charnell, J. Cryst. Growth, 1971, 8, 291.
8. H. Khatami, E.M. Flanigen and N.R. Mumbach, "Molecular Sieves", Ed. W.M. Meier and J.B. Uytterhoeven, American Chemical Society Advances in Chemistry series No.121, 1973, 183.
9. L. Falth, "Proceedings of the 5th. International Conference on Zeolites", Ed. L.V.C. Rees, Heyden, London, 1980, 45.
10. R. von Ballmoos and W.M Meier, Nature, 1981, 289, 782.
11. D.H. Olson and E.W. Valyocsik, EPA O 026 963, 1981.
12. A.Nastro and L.B.Sand, Zeolites, 1983, 3, 57.
13. E.M.Flanigen and R.L.Parton, USP 4 073 865, 1978.
14. E.V. Khamskii, "Crystallization from Solutions", Consultants Bureau, New York, 1969, 19.
15. D. Domine and J. Quobex, "Molecular Sieves",

- Society for Chemical Industry, 1968, 78.
16. P.H. Egli and S. Zerfoss, Faraday Soc. Discussion No.5, 1949, 61.
17. "Microslides" produced by CAMLAB Ltd.
18. J.L. Casci, Ph.D. Thesis, University of Edinburgh, 1982.
19. P. Chu, EPA O 023 089, 1981.
20. F.G. Dwyer and E.E. Jenkins, USP 4 287 166, 1981.
21. J.L. Schlenker, F.G. Dwyer, E.E. Jenkins, W.J. Rohrbaugh, G.T. Kokotailo and W.M. Meier, Nature, 1981, 294, 340.
22. H. Gies, F. Liebau and H. Gerke, Angew. Chem., 1982, 21, 206.
23. A. Erdem and L.B. Sand, J. Catal., 1979, 60, 241.
24. K-J. Chao, T.C. Tasi, M-S. Chen and I. Wang, J. Chem. Soc. Faraday Trans. 1, 1981, 77, 547.
25. V. Lecluze and L.B. Sand, "Proceeding of the 5th. International Conference on Zeolites", Ed. L.V.C. Rees, Heyden, London, 1980, 41.
26. R. Mostowicz and L.B. Sand, Zeolites, 1982, 2, 143.
27. S.B. Kulkarni, V.P. Shiralkar, A.N. Kotasthane, R.B. Borade, and P.Ratnasamy, Zeolites, 1982, 2, 313.
28. M.Ghamami and L.B. Sand, Zeolites, 1983, 3, 155.
29. G.D. Price, J.J. Pluth, J.V. Smith, J.M. Bennett and R.L. Patton, J. Am. Chem. Soc., 1982, 104, 5971.

Chapter 5. *Nucleation and Crystal Growth of Silicalite.*

5.1. Introduction.

The studies described in the previous chapter gave information on the growth of zeolite crystals but not on their nucleation, especially in bulk crystallization. The work described in this chapter tells how several different techniques were combined to give a better understanding of not only the growth but also the nucleation stage of the crystallization process.

In Chapter 1 it was noted that the determination of particle size distribution can play an important part in the study of crystallization kinetics. The final particle size distribution is the result of the crystal growth rate and the nucleation rate. Zhdanov¹ reported in 1971 that it was possible to obtain information about nucleation from the final particle size distribution and the crystal growth rate. The largest crystals present at different times during a zeolite A synthesis were measured and a length growth curve plotted. The curves obtained appeared to indicate that the rate of crystal growth gradually decreased as crystallization progressed (see figure 5.1). Zhdanov also examined the crystal size distribution of the final product. He suggested that if the linear rate of crystal growth is assumed to be independent of its size then it should be possible to use the linear growth rate curve for the largest crystals to calculate the time at which crystals of a particular final size

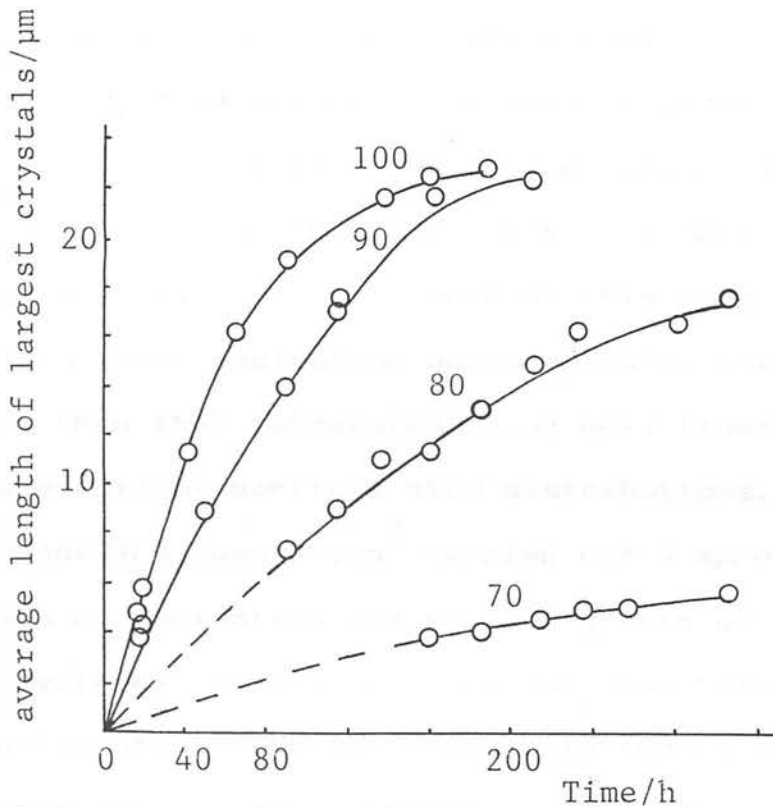


Figure 5.1. Rates of growth at a series of temperatures (in °C) of the largest crystals of zeolite A from aluminosilicate gels of the same composition. $(2.8\text{Na}_2\text{O}, \text{Al}_2\text{O}_3, 1.9\text{SiO}_2, 427\text{H}_2\text{O})^1$

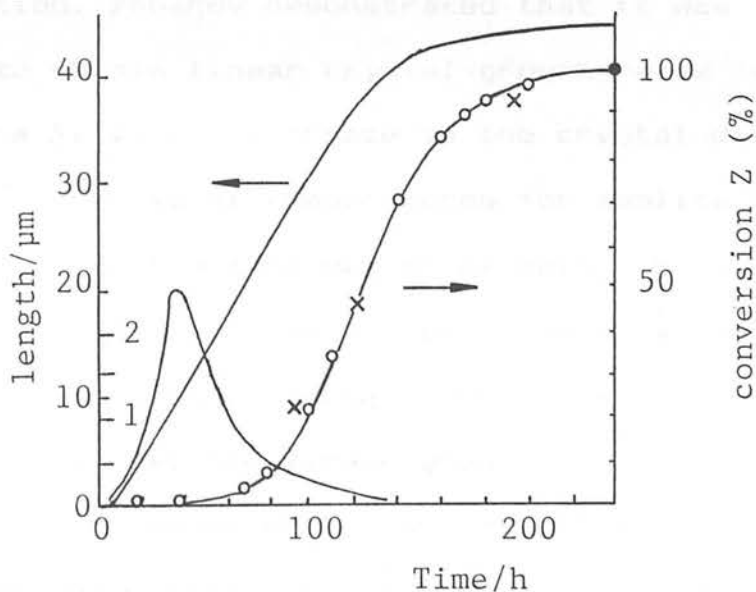


Figure 5.2. Rate of growth of the largest crystals (curve 1); nucleation kinetics (curve 2) (ordinate = $(\Delta F/\Delta t) \times 10^2$); and the crystal mass growth (curve 3) for zeolite Na-X (x = experimental points, o = calculated points) as a function of time.²

actually nucleated. The assumption that the growth rate is independent of size will be most in error for the early stages of crystal growth, i.e. when the actual nuclei are growing. The tiny nuclei are more soluble so that growth will be much slower at this stage. This would mean that nucleation would actually take place earlier than that calculated using only linear growth curves and final particle size distributions.

Zhdanov and Samulevich² carried out a more complete analysis of nucleation and crystal growth of low Si/Al ratio zeolites. Zhdanov pointed out that the majority of experimental S-shaped crystallization curves are well described by the equation :

$$Z_t / Z_f = 1 - \exp(-kt^n) \quad (\text{equation 1.16})$$

However this equation contains no quantitative information about the crystal growth rate or the rate of nucleation. Zhdanov demonstrated that it was possible to obtain linear crystal growth rates (as $0.5 \Delta l / \Delta t$ where Δl is the increase in the crystal diameter in time Δt) at several temperatures for zeolite Na-X. This was done in the same manner as before by simply measuring the largest crystals observed in a sample at various time intervals during crystallization. His results showed that the linear growth rate of the largest crystals appeared to remain constant for a wide interval of the crystallization time. From the final

yield of crystals a histogram of crystal size distribution was constructed from a sample of 300 crystals. The crystal size growth of the largest crystals (for zeolite Na-X crystallized at 363 K from a gel of composition $3.72\text{Na}_2\text{O}$, Al_2O_3 , $x\text{SiO}_2^*$, $542\text{H}_2\text{O}$) is shown in figure 5.2 (curve 1). If it was assumed that the linear rate of growth was the same for all the crystals even during the decay period of growth (after 115 h) the time of nucleation of a particular crystal can now be determined. For example, figure 5.2, curve 1 could be used to find the approximate time of nucleation of a crystal of final mean length of $16.5\ \mu\text{m}$ by merely subtracting $16.5\ \mu\text{m}$ from the maximum crystal size (l_{max}) and then noting the time equivalent to this crystal size ($l_{\text{max}} - 16.5$) i.e. about 90 hours. This process could be repeated for all the crystal bands in the final crystal size distribution graph. If n_i crystals of length l_i are present at time t_i , then;

$$f_i = n_i / N$$

where N is the total number of crystals. If the fraction of crystals which nucleate at time t_i is f_i and the fraction which nucleate at time t_{i+1} is f_{i+1} then;

$$\Delta f / \Delta t = (f_{i+1} - f_i) / (t_{i+1} - t_i)$$

The value of $\Delta f / \Delta t$ indicates whether the nucleation rate is increasing ($\Delta f / \Delta t$ is positive) or decreasing

* the value of x is not given

($\Delta f / \Delta t$ is negative). The nucleation curve shows the sum of these changes given by;

$$\Delta F / \Delta t = \sum_i \Delta f_i / \Delta t_i$$

The nucleation curve obtained by Zhdanov is shown in figure 5.2, curve 2.

In order to check the validity of this curve, Zhdanov calculated a crystal mass growth curve from the nucleation and crystal growth data. The ratio of the mass of crystals at time t (Z_t) to the mass of crystals in the final product (Z_f) is equivalent to the ratio of the volume of the crystals at time t (V_t) to the final volume (V_f). The volume of (cubic) crystals in the final product, or at time t , can be obtained from :

$$V_f = \sum_i f_i l_i^3 \quad (5.1)$$

$$V_t = \sum_i f_i l_i^3(t) \quad (5.2)$$

Therefore the ratio V_t/V_f is equivalent to Z_t/Z_f . The calculated curve V_t/V_f (X100%) is shown in figure 5.2 along with the actual experimental results obtained for Z_t/Z_f (X100%) (crosses).

Zhdanov discovered that his calculated curve for the crystal mass growth of zeolite Na-X was very close to the experimental crystallization curve. This close agreement led him to believe that the assumption about the independence of the linear growth rate on crystal size was valid.

This chapter describes the application of the Zhdanov and Samulevich approach to the crystallization of a high silica zeolite. The crystallization of (TFA,Na)-silicalite-1 was studied. Silicalite-1 is the pure silica form of the zeolite ZSM-5. High silica zeolites like ZSM-5 have very important catalytic and sorption properties, as is evident from the large number of patents on the uses of such zeolites. It is important to obtain as much information about the crystallization of such systems in order to prepare crystals which are a more suitable size and shape for catalysis or other practical uses. Chapters 3 and 4 described how silicalite-1 was found to be relatively easy to crystallize from silicate solutions prepared from tetraethyl silicate. The omission of aluminium from the reaction mixture meant that the composition was relatively simple. Furthermore, reaction mixtures prepared from tetraethyl silicate did not produce a thick gel phase, instead they were water clear, the crystals could be readily seen and could be separated by filtration from samples taken throughout the crystallization. The mass of crystals produced at each stage of the crystallization could then be recorded. This method of following the crystallization had to be used instead of the normal method of X-ray powder diffraction. X-ray powder diffraction can only reveal the percentage of crystals in amorphous material. It is unable to detect when the first small crystals have

been formed. When tetraethyl silicate is used as the silica source the first small crystals are revealed much earlier and can then be examined by optical or electron microscopy.

In the investigation described in this chapter two different stirring speeds were chosen in order to find the extent to which agitation affects the crystal growth rate. When the solution is stirred any control of growth due to diffusion should be reduced. This is because agitation increases the relative velocity between the crystals and the solution, it thereby reduces the diffusion layer thickness, so that the growth rate depends mainly on the rate of the chemical reactions taking place at the crystal surface.

If there are any differences between the relative velocities of crystals of different sizes then correspondingly different linear growth rates would be obtained, especially at low stirring speeds. In stirred systems, small crystals tend to have smaller relative velocities than larger particles. However, as the effect is most marked at low velocities, high stirring speeds should reduce the problem so that only the very smallest crystals would be affected. The growth rate of sodium thiosulphate³ is unaffected by speeds greater than 20 r.p.m., while Casci⁴ observed that crystal mass growth curves for zeolite EU-1 were independent of stirrer speed at speeds greater than 300 r.p.m. As agitation will also increase the nucleation rate 300

r.p.m. is likely to be well beyond the stirrer speed needed to allow the same growth rate for all crystals. The two different speeds used in this study were 150 and 300 r.p.m. The former was chosen as it was also the standard speed used for all stirred reactions carried out at 368K in the water bath, while 300 r.p.m. was the standard speed used for autoclave reactions. A larger difference would have been better for the detection of a stirring effect, but it was also desirable to know if there was any major difference between a water bath reaction at 150 r.p.m. and an autoclave reaction at 300 r.p.m..

In this work some of the techniques described in earlier chapters were used to follow the course of the crystallization. It was decided that for each reaction the amount of crystalline material at each stage of the reaction would be obtained by the separation of the solid from the mother liquor followed by weighing (as described in Chapter 3). The product formed was also confirmed by X-ray powder diffraction whenever enough solid sample was available.

The size and shape of the crystals was observed at each stage of the crystallizations by both optical and electron microscopy. The crystals were measured and their length growth rate determined. In Chapter 4 it was shown that in a static system the growth rate of the same crystal would remain constant for most of the crystallization and was the same for all the crystals

in that reaction. The pH of the solutions was also determined to gain an insight into the course of the reaction.

The composition chosen for this study was :

1Na₂O 20 SiO₂ 80EtOH 1960H₂O 2TPABr

This composition had proved to reliably produce silicalite-1 from "clear" solutions.

The investigations described in this chapter show how a greater understanding of zeolite crystallization can be achieved by the combination of several experimental techniques. The use of "clear" solutions meant that a direct measurement of the precipitated crystal mass could be obtained just as for conventional crystallizations from solution. The crystal mass growth was measured directly and not as percentage mass conversion from amorphous solid as calculated by X-ray diffraction. The appearance of even a small amount of solid could be detected quite early in the reaction and even if it could not be weighed it could be examined by scanning electron microscopy. The results showed that there were crystals present at a very early stage in the reaction and certainly well before one might have predicted from the crystal mass growth curve. However, calculations show that it is these crystals which ultimately contribute the largest amount to the crystal mass growth curve.

5.2 Experimental

5.2.1 Materials

The following materials were used:

Tetraethyl silicate (B.D.H. , GPR grade)

Sodium hydroxide (Fisons, analar grade)

Tetrapropylammonium bromide (Fluka, purum)

Distilled water was always used.

5.2.2 Preparation of silicate solutions.

The mixture was prepared in one litre polypropylene bottles. The quantity prepared was approximately 1000g per batch. The sodium hydroxide was dissolved in the required amount of water. For batch (1) the TPABr was then added to this solution and allowed to dissolve. No TPABr was added to batch (2). The tetraethyl silicate was then added to both batches. Teflon-coated magnetic followers were then added and lids fitted. The solutions were stirred quite rapidly for at least 16 hours until all of the tetraethyl silicate had disappeared and a single phase produced. The solutions were allowed to remain static at room temperature for seven days after the addition of the tetraethyl silicate (as recommended in Chapter 3).

5.2.3 Crystallization

The required amount of TPABr was added to batch (2) in order to give the desired composition. The TPABr was added with vigorous stirring until it had all dissolved. This addition was made just before the solutions were to be placed at reaction temperature.

The reactions were carried out in two stainless steel 500 ml autoclaves and two 1 litre polypropylene bottles. (The autoclaves and stirred bottles were described in chapter 2). The autoclaves were agitated by magnetic stirrers at a stirring speed of 300 r.p.m. The reactions could be sampled by means of dip-pipes fitted on the autoclaves. Each autoclave was filled with 400g of solution, with batch (1) in one autoclave and batch (2) in the other (reactions A1A and A2A respectively). The stirrers were started immediately and the temperatures raised to 368K. The reactions were timed from the moment that heat was applied.

The polypropylene reactors were agitated by means of stainless steel stirrer bars connected to electric motors (stirring speed 150 r.p.m.). The reactions could be sampled by means of a hole drilled into the bottle lid. This was firmly stoppered after sampling. Each bottle was filled with 500g of solution, with batch (1) in one reactor and batch (2) in the other (reactions P1S and P2S respectively). The larger quantity was used here since the plastic bottles were liable to leak slightly. The larger quantity helped to minimise the effect of any loss. The reactors were placed in a 368K water bath and allowed to remain static for 24 hours before stirring commenced. (This was the procedure recommended for these reactions in chapter 3)

5.2.4. Analysis

Samples (8ml) were collected in glass sample bottles.

$$\begin{aligned} \text{Weight of liquid} &= 5.9626 \text{ g} \\ \text{Density of liquid} &= 1.0102 \text{ g ml}^{-1} \\ \text{Volume} = \text{mass/density} &= 5.9626/1.0102 \\ &= 5.9024 \text{ ml} \end{aligned}$$

Thus the weight of solid silica (in the form of calcined silicalite) per ml could be obtained. For example for the example given above:

$$\begin{aligned} \text{Weight of dried solid} &= 0.0510\text{g} \\ &(\text{equilibrated over} \\ &\text{saturated sodium} \\ &\text{chloride solution}) \\ \text{Weight loss by t.g.a.} &= 13.5\% \\ \text{Weight of calcined silicalite} &= (86.5/100) \times 0.0510 \\ &= 0.0441 \text{ g} \\ \text{Weight of solid per ml} &= (0.0441/5.9024) \\ &= 0.0075 \text{ g ml}^{-1} \end{aligned}$$

Scanning electron micrographs of each sample were obtained using a Cambridge Stereoscan 604 instrument. Final particle size analysis was carried out in a semi automatic manner, by viewing the sample with an optical microscope (Nikon Optiphot Pol.) connected to a Vickers Magiscan instrument. A light pen was used to mark crystal lengths. The final crystal size distribution was obtained using a program called DIATEST. The size distribution was checked by manual measurements of crystal size on scanning electron micrographs. There was reasonable agreement between the two methods but results obtained from the "Magiscan" were used in all

calculations as many more crystals were measured by this method.

When enough sample was available it was examined by X-ray powder diffraction using a Philips powder diffractometer (Cu K α radiation). These confirmed that the material obtained was silicalite-1.

5.3. Results and Discussion.

5.3.1 Crystal growth

The linear growth rate was obtained by measuring the length of between 10 and 20 of the largest crystals present in each sample taken at separate time intervals. An idealized drawing of a silicalite crystal is portrayed in figure 4.3 (chapter 4), and the dimension measured is shown. Normally the rate of displacement of a crystal face parallel to itself is measured but, under the growing conditions used, the 101 faces of the crystal were not very well developed. However the length of the crystal is geometrically related to the displacement of the 101 faces and is much easier to measure, so this was the dimension measured.

The major assumption made in the analysis of the results is that the linear rate of growth is the same for all sizes of crystal within the same reaction mixture. This is a standard assumption and is true for static systems, but the system used here was agitated which is a common procedure in crystallization. Agitation increases the relative velocity between the crystals and the solution which reduces any control due to diffusion until the growth rate depends mainly on the rate of the chemical reaction at the surface.

The linear growth rate obtained for all the reactions agreed, within experimental error. The length growth rate ($0.5 \Delta l / \Delta t$) was found to be $(2.0 \pm 0.1) \times$

$15^2 \mu\text{m h}^{-1}$ at 368K . The measurement of the length / width (l/w) ratio for crystals of various sizes, from the same batch of crystals, indicated that this ratio was constant and equal to 1.3. This gives a width growth rate ($0.5 \Delta w / \Delta t$) of $(1.5 \pm 0.1) \times 10^{-2} \mu\text{m h}^{-1}$. The final particle size distribution for reaction A1A is shown as a histogram in figure 5.3. This was constructed from the results of size measurements of over 500 crystals in the final product. The number of crystals n_i in each band is expressed as the percentage of the total number of crystals N. The curve in figure 5.3 attempts to smooth irregularities in the histogram. In further calculations results from the curve are used. The linear growth rate curve for reaction A1A is shown in figure 5.4. If it is assumed that the growth rates of all the crystals in this reaction are the same, even at the time of reduced growth after 190 hours, then the approximate time of nucleation of any crystal can be calculated. For example, crystals of 4 μm and 6 μm in the final product would have nucleated at approximately 108 hours and 58 hours respectively as shown by the arrows in figure 5.4. It is possible to continue this process for other crystal sizes so that the product size distribution curve can be converted into a nucleation curve (figure 5.5, curve 1) as described in section 5.1.

A check on the validity of these curves can be made by the construction of the curve for crystal mass

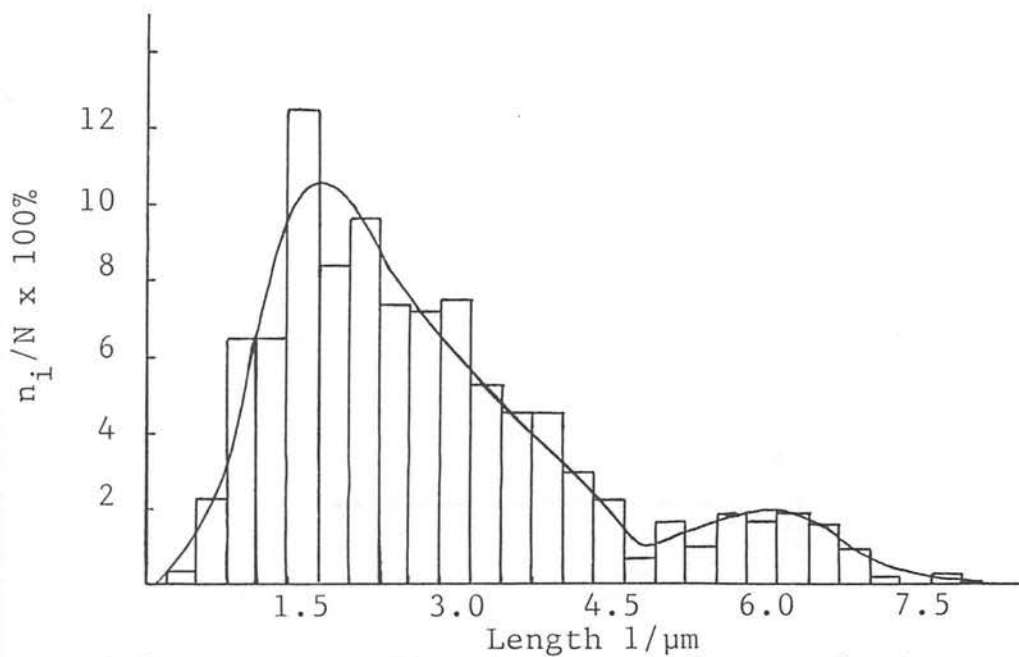


Figure 5.3. Reaction A1A: Histogram of crystal size distribution in the final product.

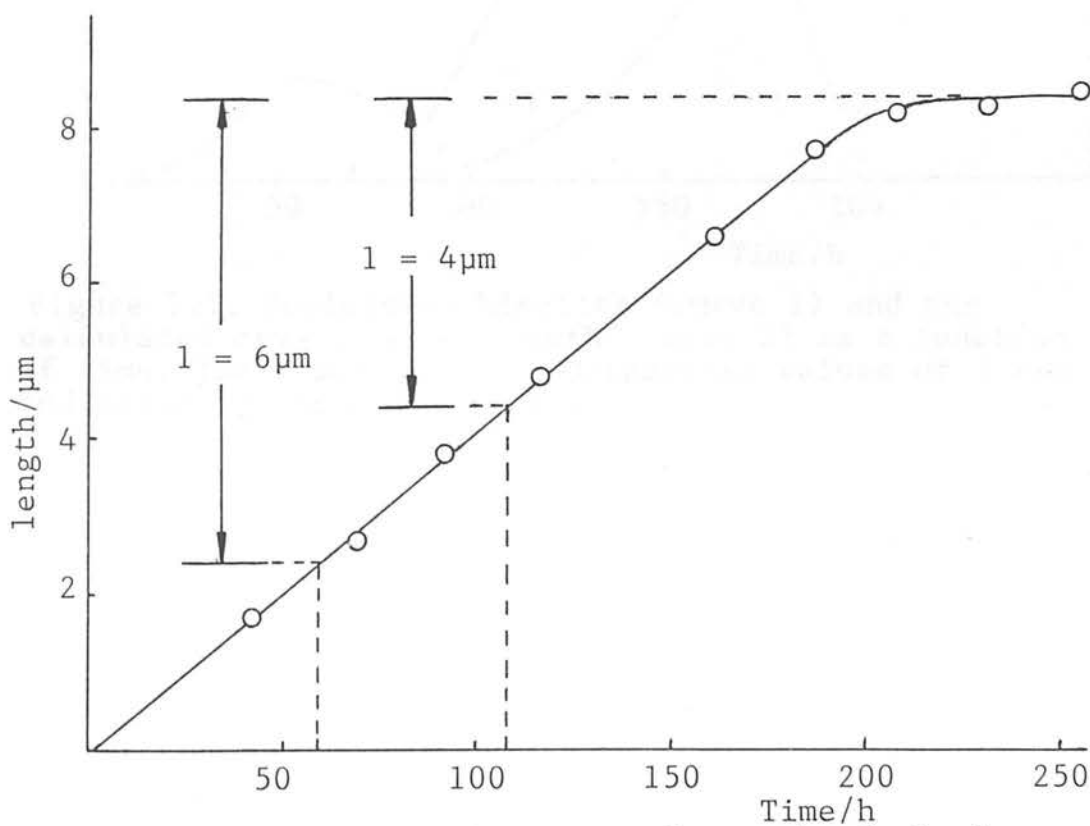


Figure 5.4. Reaction A1A: Rate of growth of the largest crystals of silicalite.

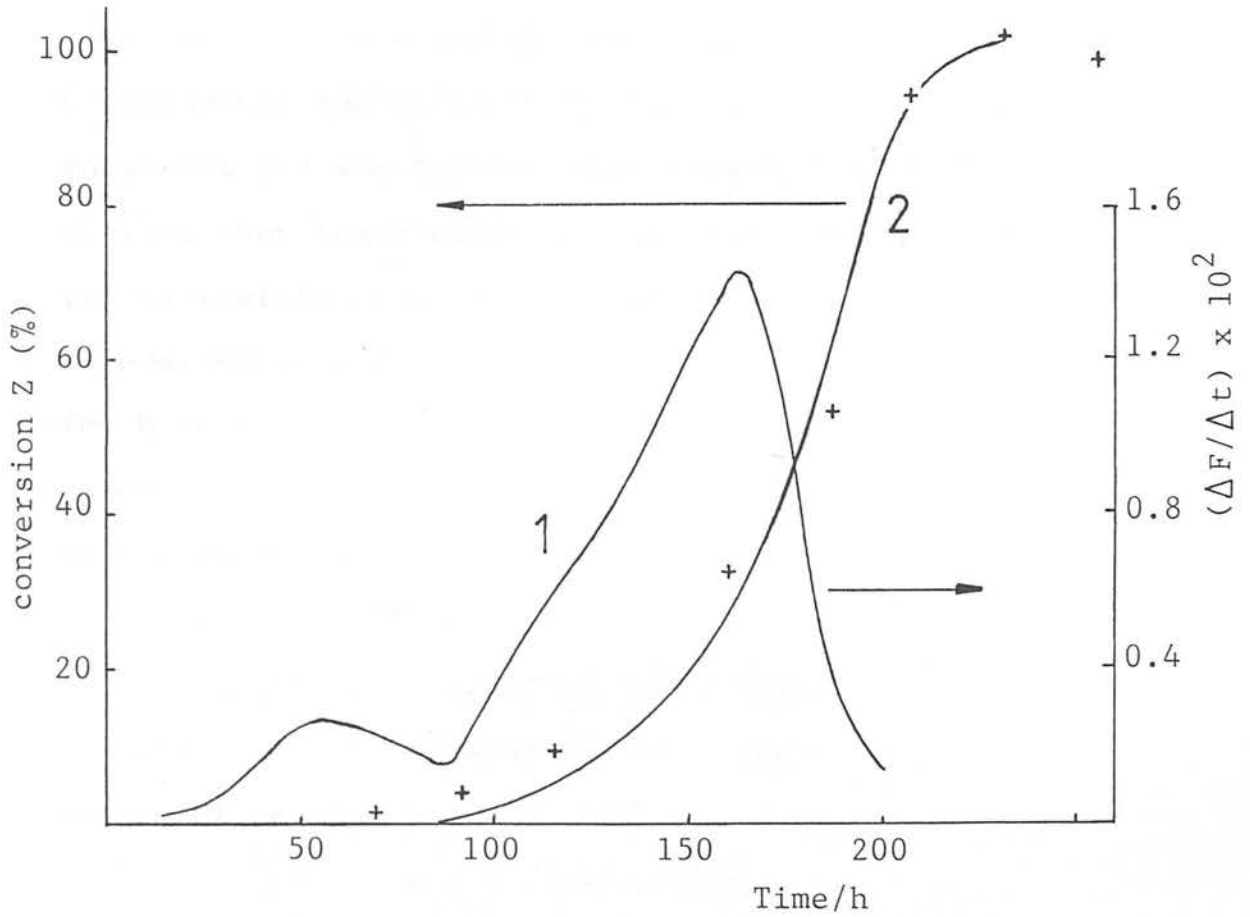


Figure 5.5. Nucleation kinetics (curve 1) and the calculated crystal mass growth (curve 2) as a function of time. The experimentally determined values of Z are indicated by the crosses (+).

growth from the product size curve and the linear growth rate curve. As discussed in section 5.1., the ratio of the mass of crystals at time t (Z_t) to the mass of crystals in the final product (Z_f), Z_t/Z_f is equivalent to the ratio V_t/V_f where V_t is the volume of crystals at time t and V_f the final volume.

Consequently the ratio V_t/V_f can be calculated using equations 5.1 and 5.2 for each crystal fraction. It is obvious that these equations are for cubic crystals, yet silicalite crystals are not cubic but lozenge shaped. Fortunately the length/width ratio is the same for both large and small crystals in any particular batch. This also appears to be true for the length/depth ratio.

Thus:

$$\text{length } (l) = \text{constant } (a) \times \text{width } (w)$$

$$\text{and } l = \text{constant } (b) \times \text{depth } (d)$$

$$\text{Volume of crystal} = l \times w \times d$$

$$= l \times (l/a) \times (l/b)$$

$$= l^3 / ab$$

Consequently equations 5.1 and 5.2 should be altered

$$\text{to: } V_f = \sum_i f_i \frac{l_i^3}{ab}$$

$$\text{and } V_t = \sum_i f_i \frac{l_i^3(t)}{ab}$$

However, since it is the ratio, V_t/V_f which is required then the constant ab cancels. This means that it is not necessary to calculate the constant ab . For the purposes of this calculation points were taken from the curve on figure 5.3 at $0.3 \mu\text{m}$ intervals i.e. the same

interval as used in the histogram. A computer program was used to help carry out this calculation. The program is shown in appendix 2. The curve for mass growth calculated in this way is shown in figure 5.5 (curve 2). The crosses in figure 5.5 indicate the experimentally determined values of $(Z_t/Z_f) \times 100\%$. These were determined from the values of the calcined silicalite shown in table 5.1. For reaction A1A, 0.03 g ml^{-1} (the average of the last two values) was taken as Z_f . Thus at $t = 187\text{h}$, when $Z_t = 0.0157 \text{ g ml}^{-1}$

$$Z = Z_t/Z_f \times 100\% = 157/300 \times 100\% = 52\%.$$

This was repeated for all the other values of A1A. It should be noted that if all the silica in the reaction mixture had converted to silicalite then a value of 0.0334 g ml^{-1} would be expected. The final values for reactions A1A, A2A and P1S indicate that about 90% of the silica was converted to silicalite. Reaction P2S gave a slightly higher value (95%).

These values of Z were obtained from the weight of the crystals per ml at each stage divided by the final weight of crystals per ml. The reaction mixtures used in these experiments did not separate to form a gel plus a solution but remain "clear" solutions throughout the reaction. This meant that it was a relatively simple operation to remove the solid from the solution by filtration. The solid material was normally completely crystalline according to X-ray diffraction methods, but the initial samples taken at the beginning

Table 5.1. Weight per ml of calcined silicalite for each reaction.

Time/h	Weight per ml / $\text{g ml}^{-1} \times 10^4$			
	A1A	A2A	P1S	P2S
70	5	-	3	-
92	12	9	7	-
116	28	19	19	3
161	96	56	75	21
187	157	90	118	38
208	280	153	166	60
232	308	232	264	109
256	293	300	303	160
334				319

of the crystallization contained some amorphous material. This was revealed by scanning electron microscopy as shown in the photos in figure 5.6 for some of the different stages of the crystal growth of reaction P1S. The sample obtained after 42 hours shows small crystals sitting on amorphous material (figure 5.6a). This may explain why the experimental points are slightly higher than the calculated curve at the early stages of crystallization.

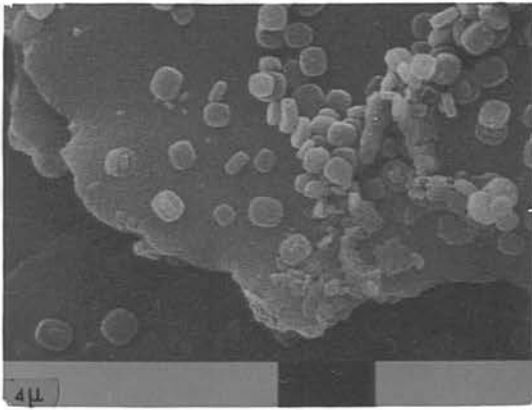
The experimental and calculated curves are very close so that it appears that the assumptions made in the calculations are, in the main, valid. One problem which was not allowed for in the volume calculation was that of twinning. It was assumed that twins would be equally spread throughout the whole product range but this may not always be the case and could result in a discrepancy between calculated and experimental curves. The product of reaction A1A appeared to contain fewer twinned crystals than did the other products. This can be seen in figure 5.7 which shows the final products for all four reactions.

The product distribution histograms and curves, crystal growth, nucleation and mass growth curves for the other three reactions (A2A, P1S and P2S) are shown in figures 5.8 - 5.13. The experimental points and calculated crystal mass growth curve agree quite well for each reaction although the experimental points for reaction P2S appears to come slightly later than the

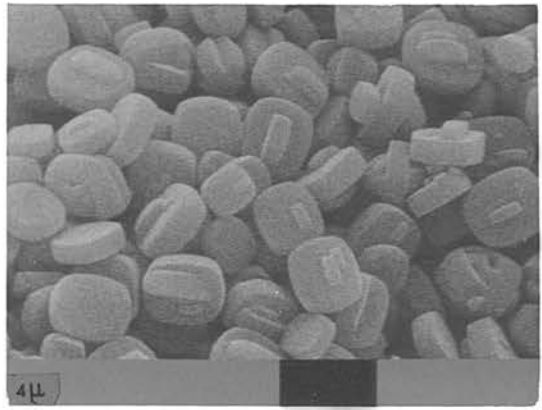
Figure 5.6. (overleaf) Scanning electron photomicrographs of different stages of crystal growth.

Reaction P1S: (a) after 42 h
(b) after 92 h
(c) after 161 h
(d) after 208 h
(e) after 232 h
(f) after 334 h

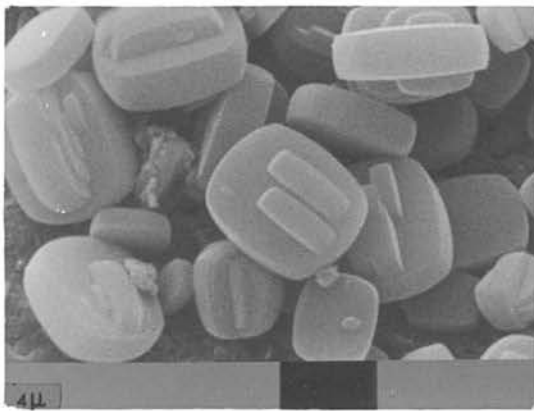




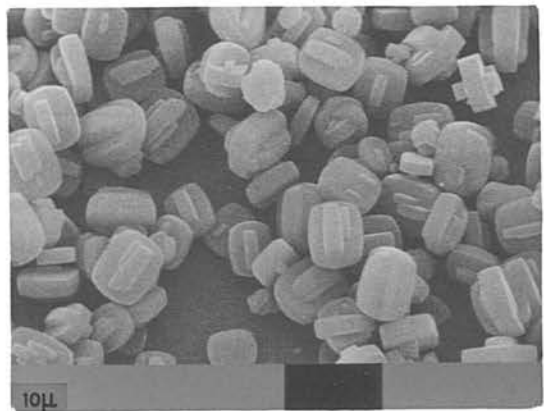
a



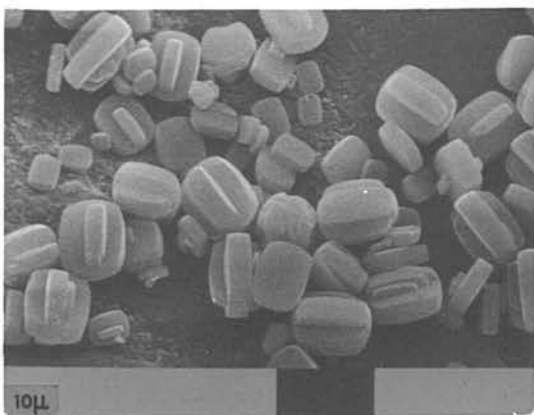
b



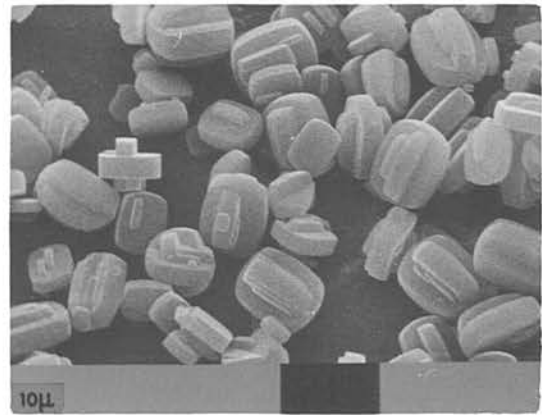
c



d



e



f

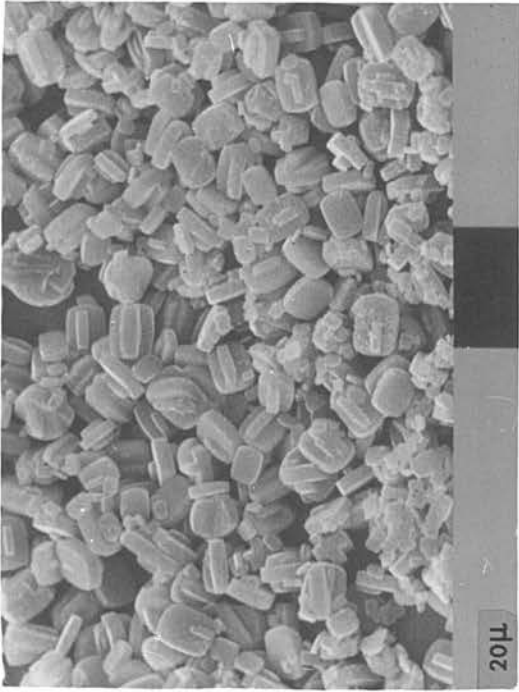
Figure 5.7. (overleaf) Scanning electron photomicrographs of the final products;

(a) A1A

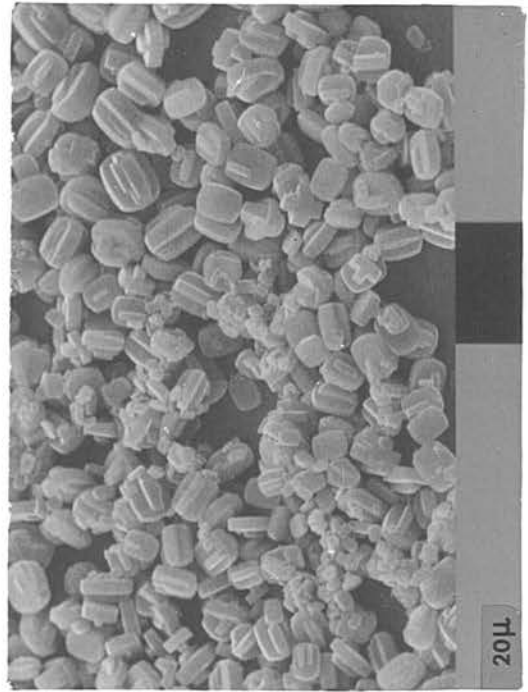
(b) A2A

(c) P1S

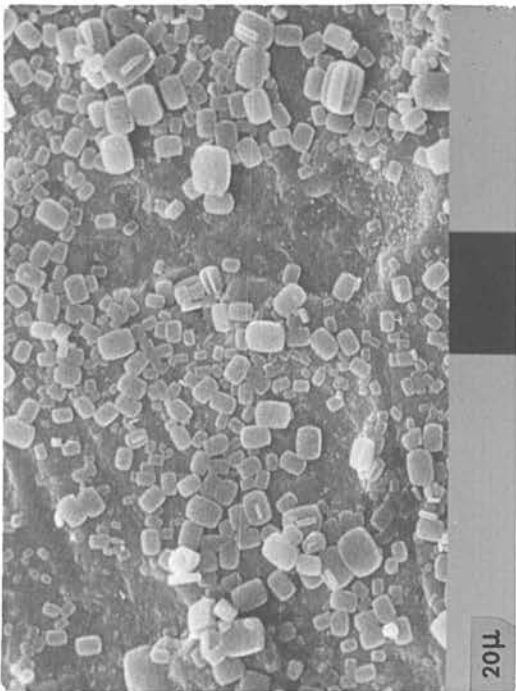
(d) P2S



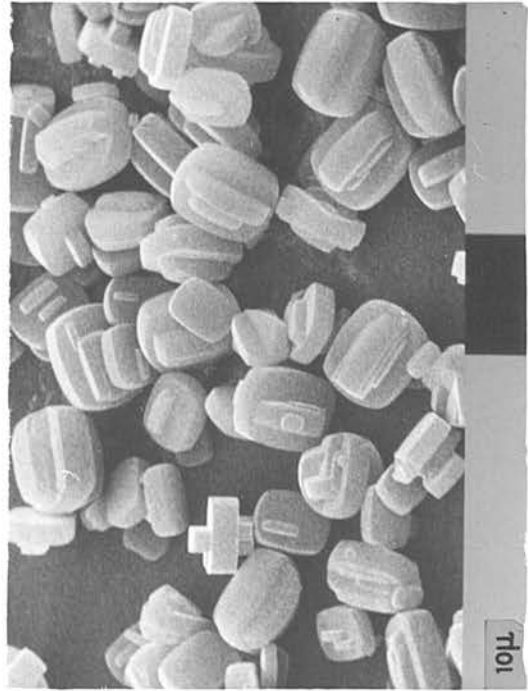
b



d



a



c

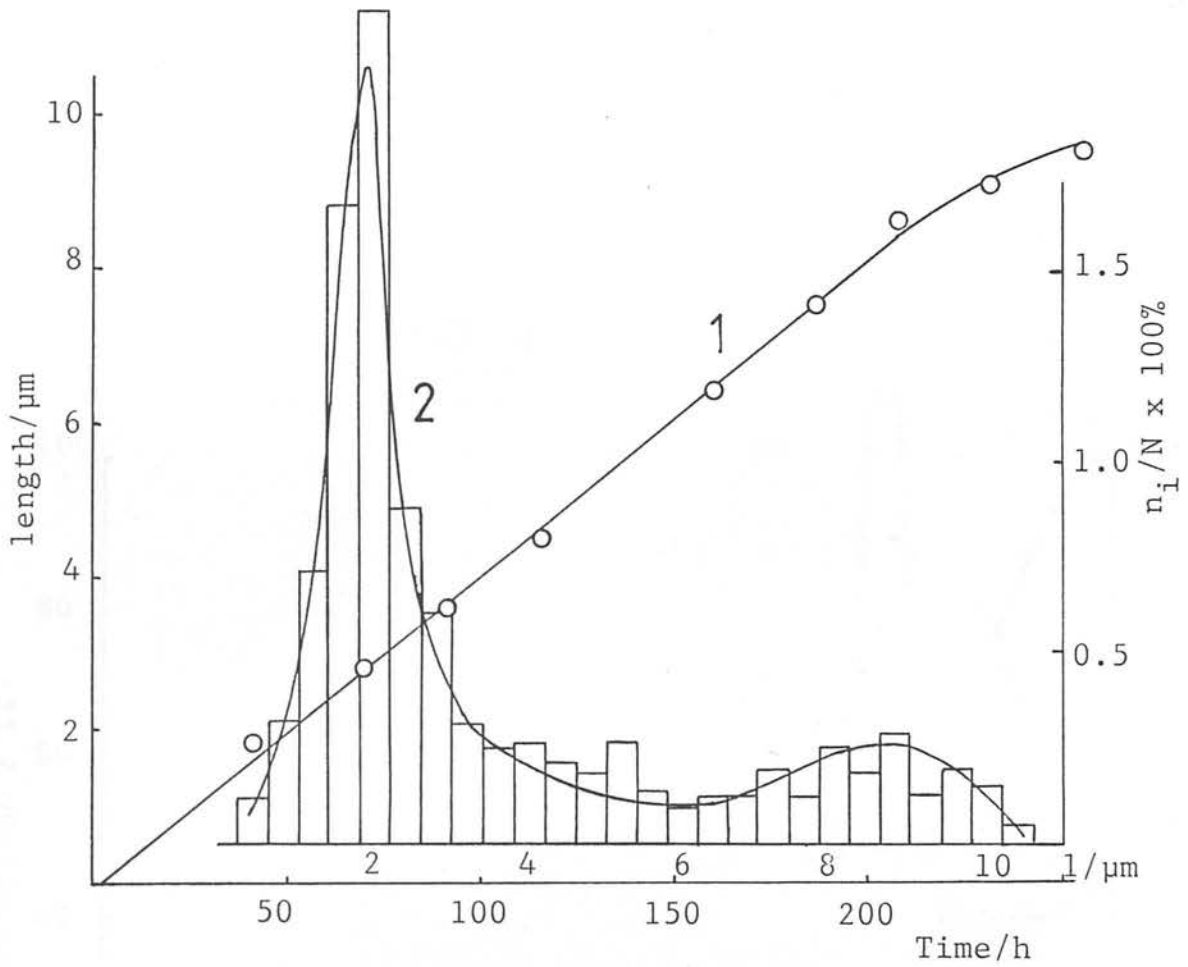


Figure 5.8. Reaction A2A: Rate of growth of the largest crystals (curve 1) and histogram of the crystal size distribution in the final product (curve 2).

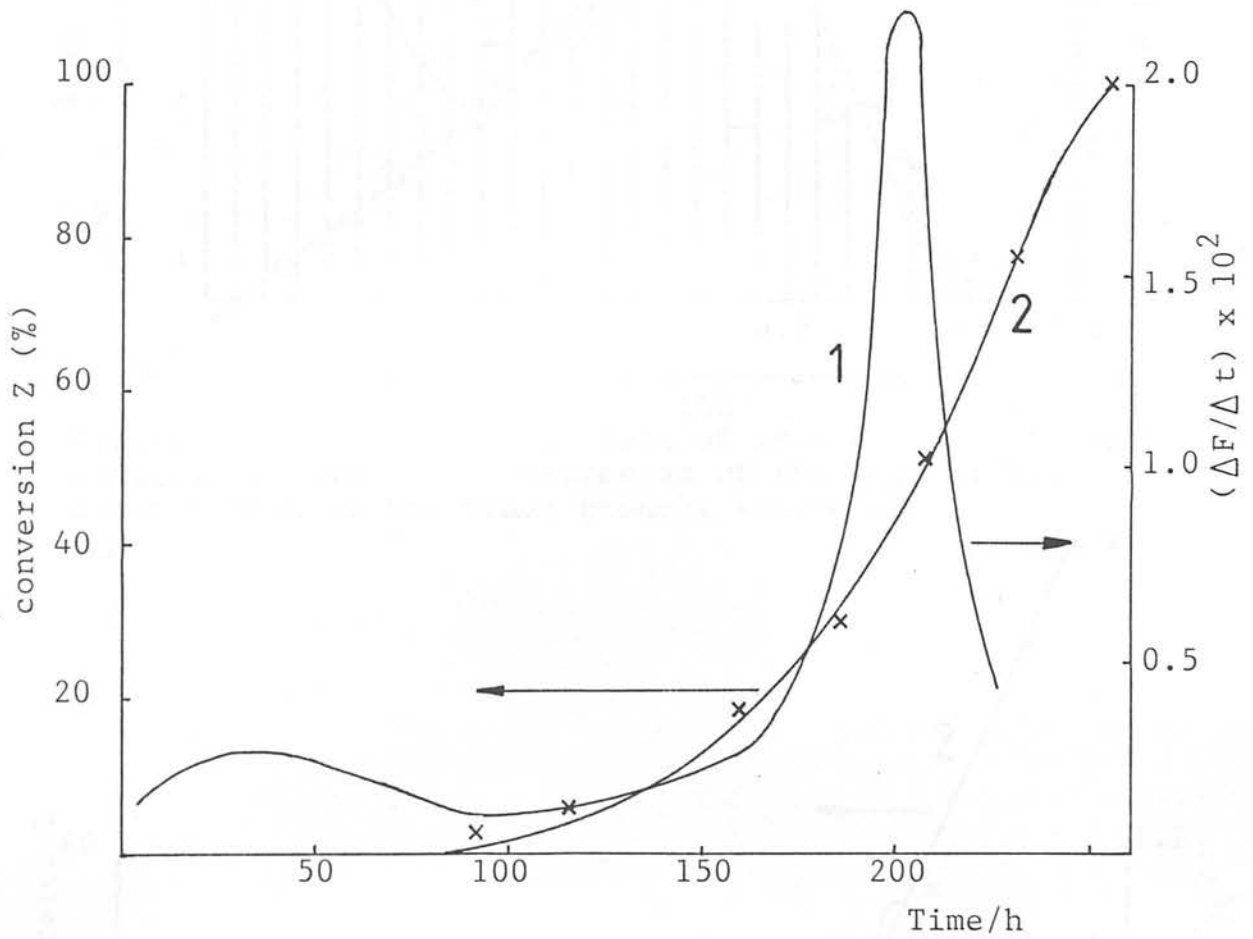


Figure 5.9. Reaction A2A: Nucleation kinetics (curve 1) and the crystal mass growth (curve 2) as a function of time.

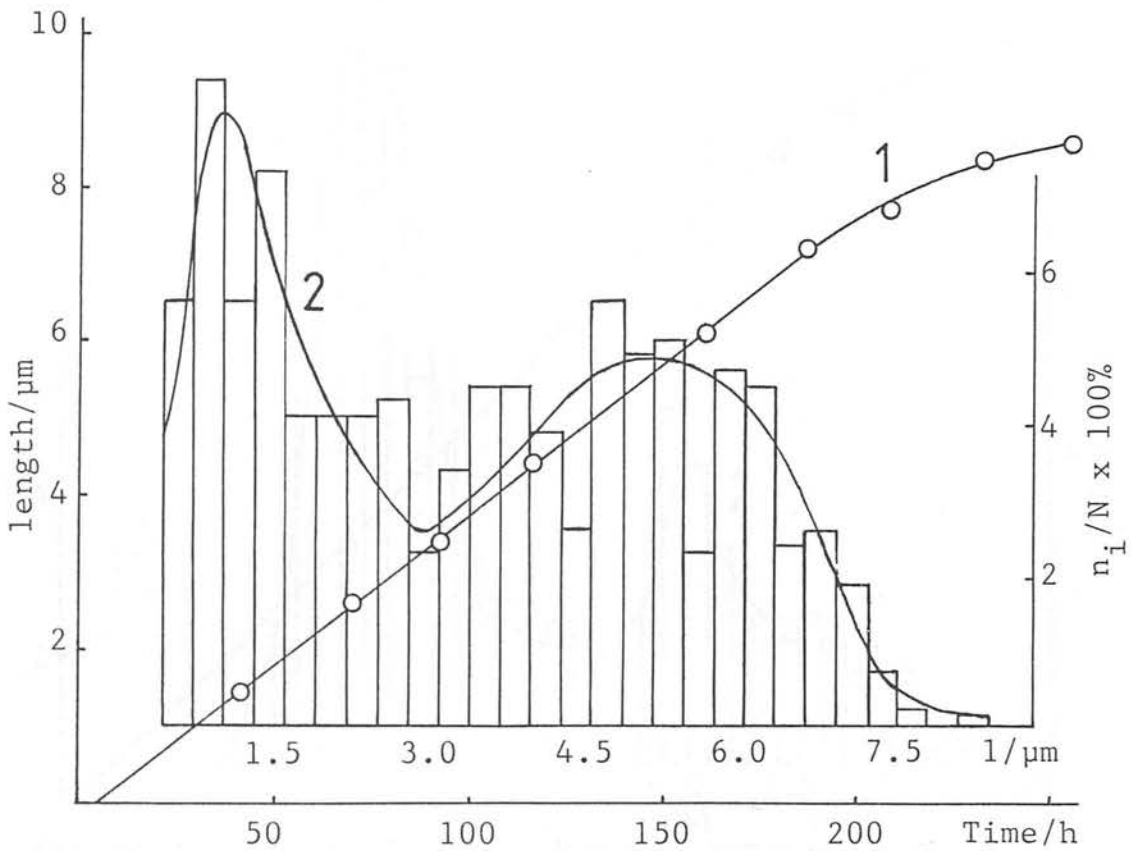


Figure 5.10. Reaction P1S: Rate of growth of the largest crystals (curve 1) and histogram of the crystal size distribution in the final product (curve 2).

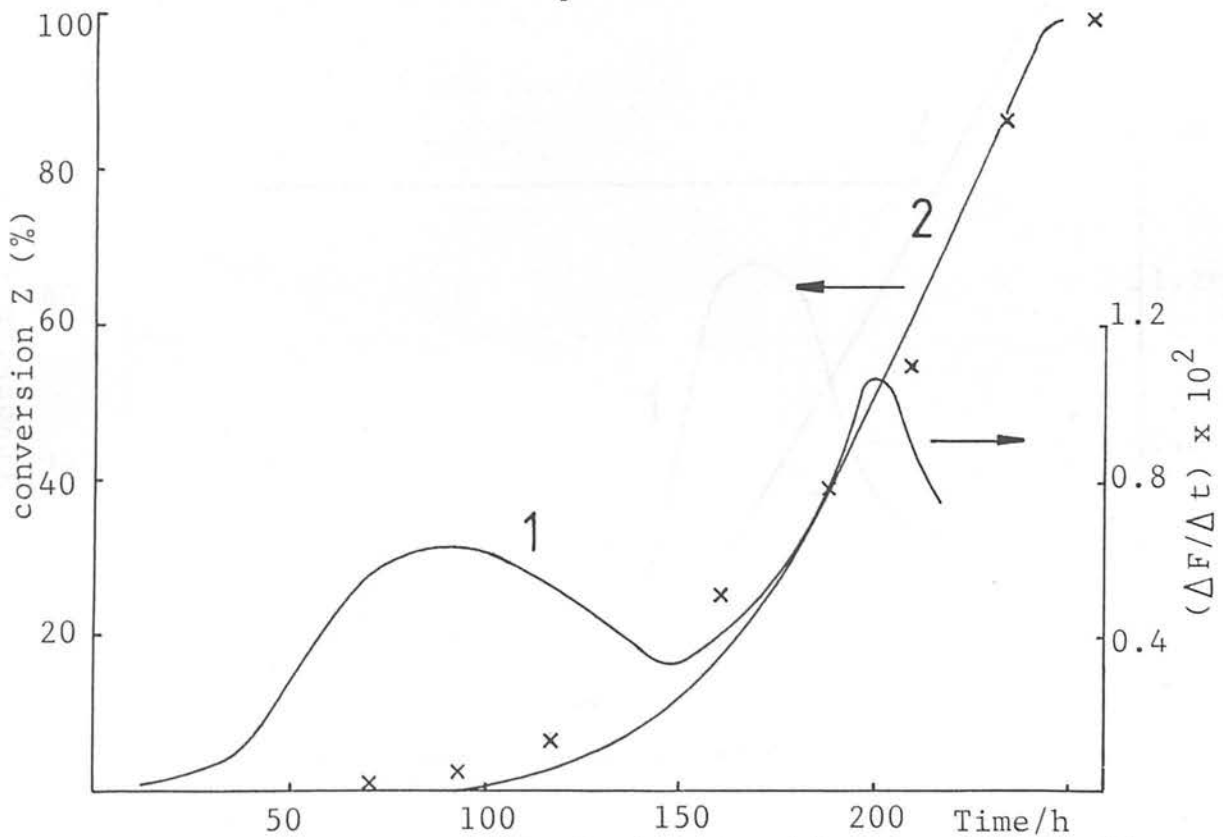


Figure 5.11. Reaction P1S: Nucleation kinetics (curve 1) and the crystal mass growth (curve 2) as a function of time.

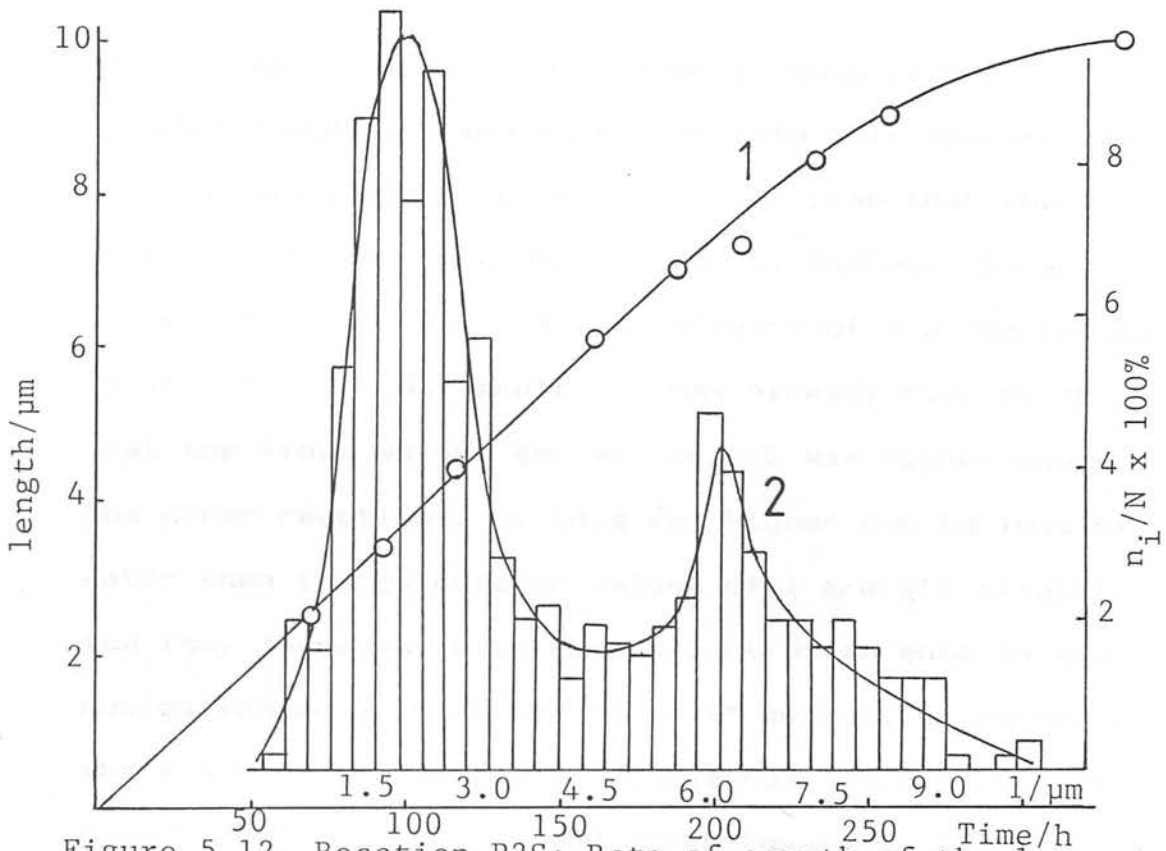


Figure 5.12. Reaction P2S: Rate of growth of the largest crystals (curve 1) and histogram of the crystal size distribution in the final product (curve 2).

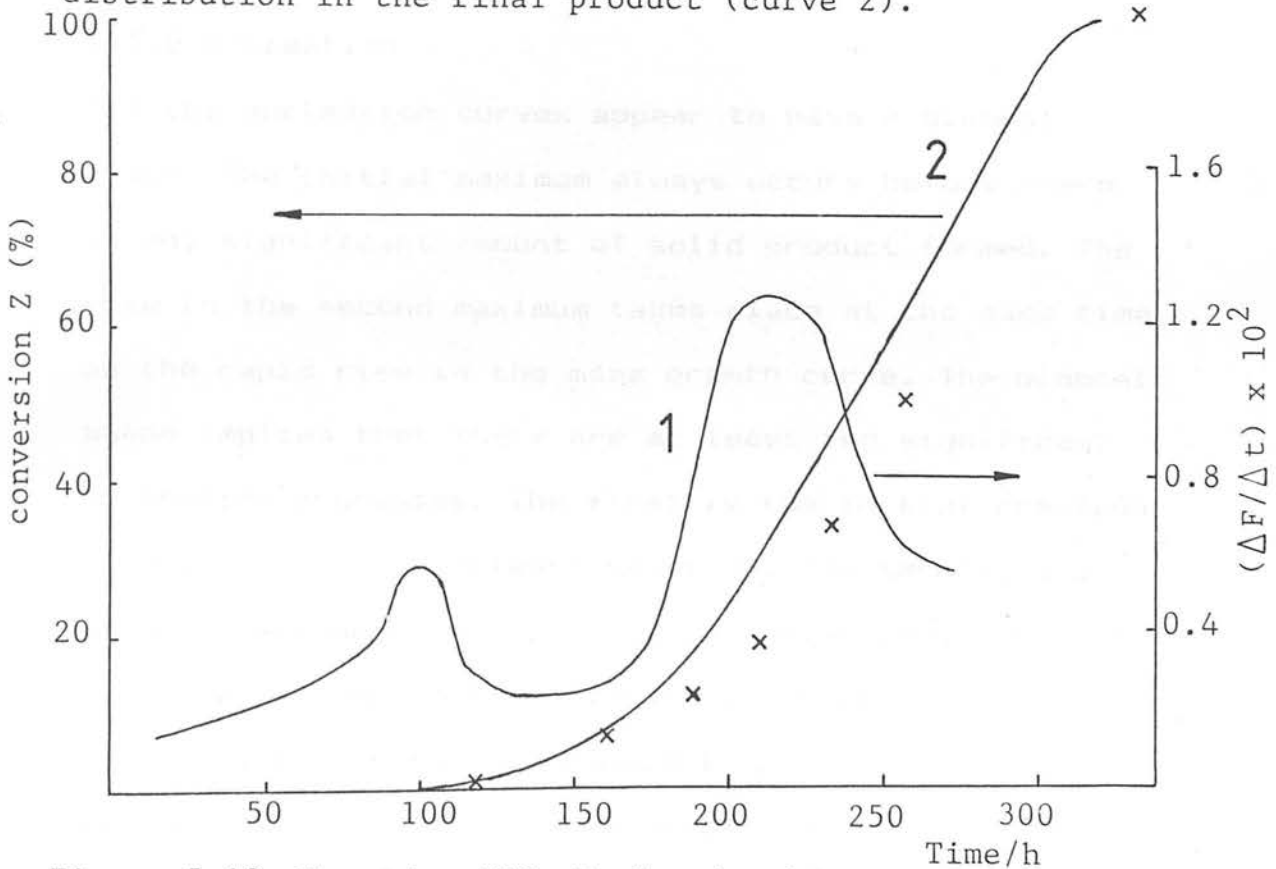


Figure 5.13. Reaction P2S: Nucleation kinetics (curve 1) and the crystal mass growth (curve 2) as a function of time.

calculated curve. This discrepancy could be due to several reasons. A major problem with this reaction is that it had a longer crystallization time than the others. This led to a gap in results between 250 and 330 hours which has made the estimate of the completion of the reaction difficult. It has already been noted that the final weight per ml for P2S was higher than the other reactions. If this was higher due to loss of water then the calculated values of Z are all slightly too low. There may also be a slight difference in the nucleation curve from the "actual" nucleation curve. If the start of the nucleation curve rose more slowly this could "push" the calculated curve towards the experimental curve.

5.3.2 Nucleation

All the nucleation curves appear to have a bimodal shape. The initial maximum always occurs before there is any significant amount of solid product formed. The rise to the second maximum takes place at the same time as the rapid rise in the mass growth curve. The bimodal shape implies that there are at least two significant nucleation processes. The first is the initial creation of nuclei from the "clear" solution. The second, and larger, maximum in the nucleation curves coincides with the obvious rise in the crystal mass growth curve. It is possible that this is caused in part by ;

(a). fracturing and abrasion of crystals due to collisions between crystals in the stirred reactor. The

pieces of crystal can then act as nuclei (i.e. secondary nucleation)

and /or

(b). the depolymerisation of the large polymeric species (colloidal particles) in the solution occurring at a much faster rate because of demand for nutrient from the growing crystals. This may introduce additional "active" sites where nuclei can form or alternatively the depolymerisation may expose structures which can themselves form nuclei.

If process (a) is mainly responsible then a difference should be observed between the reactions stirred at 300 r.p.m. and the reactions stirred at 150 r.p.m. The nucleation curves for each reaction are compared in figure 5.14. This shows that all the nucleation curves have a large second maximum with very little difference between the reactions stirred at 300 r.p.m. (A1A and A2A) when compared with those stirred at 150 r.p.m. (P1S and P2S). It may, be that a mechanism like (b) is involved since the "potential nuclei would be present from the start of the reaction and would depend on how the solution was prepared. The reactions A2A and P2S show a more rapid rise to the second maximum which may suggest that more "potential" nuclei have been locked away at the preparation stage. The early addition of TPABr in A1A and P1S may affect this.

The fact that the initial solutions are different is

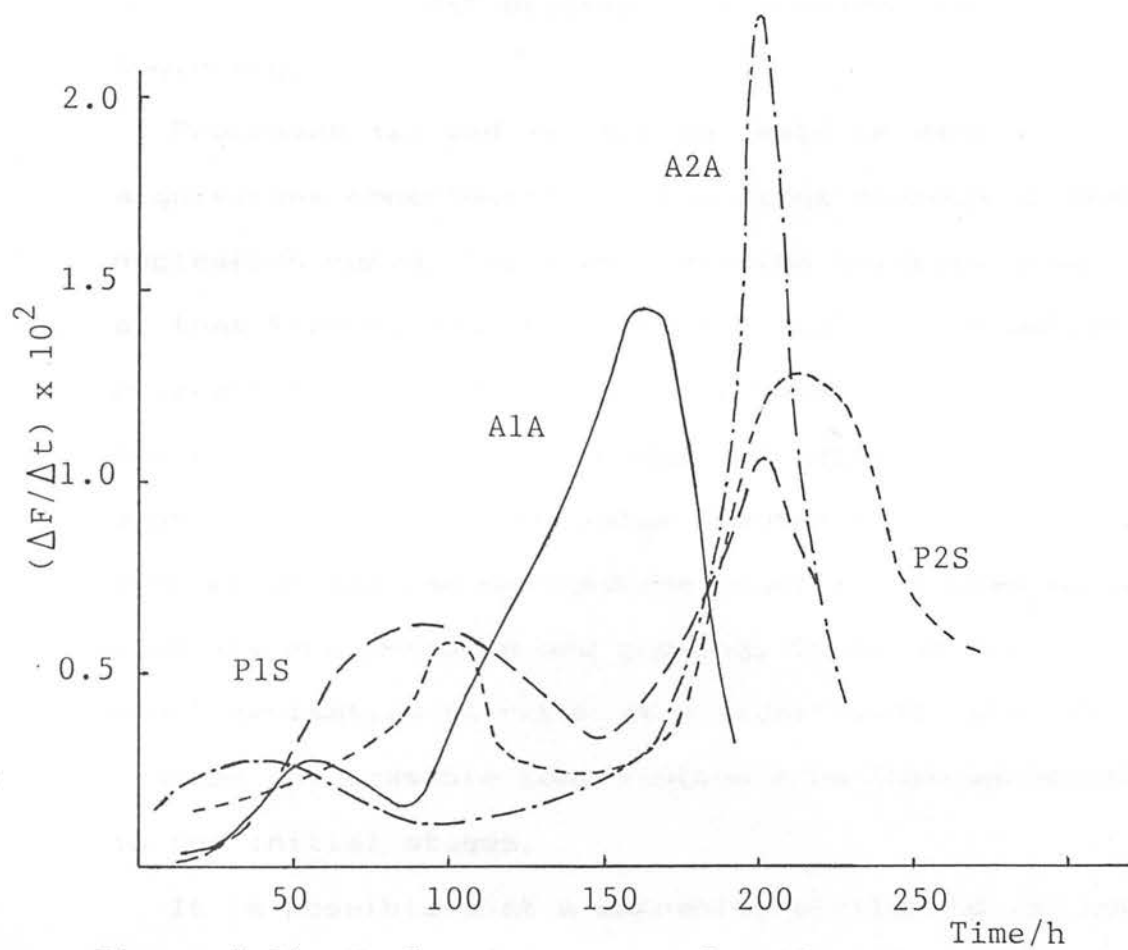


Figure 5.14. Nucleation curves for AlA, A2A, P1S and P2S.

shown by the pH results for the initial solutions (see Table 5.2). The reactions A2A and P2S have much higher initial pH values than the corresponding reactions A1A and P1S. Since hydroxide is released when silicate species polymerise, it implies that these reactions had a different polymer distribution from the very beginning.

Processes (a) and (b) are unlikely to make a significant contribution to the first maximum in the nucleation curve. There are very few crystals present at that time so that the chance of collisions between crystals is quite small, which reduces any possible contribution from (a). Process (b) relies upon the depolymerisation of the large species in the colloidal dispersion and can only become significant when enough crystals are produced and growing, to cause the depolymerisation to occur at a significant rate. This reduces any possible contribution from this mechanism in the initial stages.

It is possible that a mechanism similar to (b) could operate in the early stages if nuclei can be formed from the small polymers. These are the species which would dissolve from the colloidal silica particles first as they have a higher solubility than the large polymers. However it is hard to believe that the change from this mechanism to mechanism (b) could result in a decrease in the nucleation rate.

The first maximum always occurs before it is

Table 5.2. Initial pH for the reaction after a short period (t) of heating.

Run No.	t/h	pH
A1A	0.5	10.55
A2A	0.5	10.88
P1S	1	10.75
P2S	1	11.00

apparent that any crystalline material has been produced. Crystal growth measurement on the largest crystals indicate that these crystals start to grow at virtually zero time, i.e. as soon as the solutions are heated, crystals begin to grow. This suggests that nuclei are either already present or can be formed very quickly. Any proposed mechanism must take this into account.

One mechanism involves the participation of impurities and amorphous particles present in the solution. It has already been noted that the earlier samples, taken at times close to that of the first maximum in the nucleation curve contain a proportion of amorphous material (see figure 5.6). Most of these pieces of gel had crystals on their surface. The amorphous particles probably induce nucleation by adsorbing molecules onto their surface and lowering the free energy needed to form nuclei. This type of process should give an initial fast rate of nucleation due to the large number of "active" sites. Although some of the sites will be vacated as crystals fall off (probably a rare occurrence), the majority will probably be removed, especially when the crystals grow and cover several possible sites. This would cause the rate of nucleation to decrease. This type of mechanism is likely for all four reactions.

Further support for this mechanism comes from the work of Aiello et.al.⁵ These workers found that

dilute, "clear" aluminosilicate solutions, prepared from amorphous silica powder, (about 0.03 to 0.05 mol SiO_2 per dm^3) would produce amorphous laminae when held under static conditions at 353K. Zeolites would then appear as crystallites in association with the lamellae. These lamellae then developed holes as if being consumed. This nucleation of the zeolites was heterogeneous under the conditions used. The "clear solutions used in the work described in this chapter are much more concentrated (about 0.5 mol SiO_2 per dm^3) but a similar process appears to operate. Amorphous gel "rafts" nucleate first and then the zeolite nucleates on the "raft".

Another possibility is homogeneous nucleation. The rate of homogeneous nucleation is proportional to the supersaturation so it will remain constant as long as the supersaturation is constant. This means that this type of mechanism is unlikely to produce an increase in rate, but it will act as a "base-line" throughout the reaction. Thus nucleation is unlikely to reach zero unless the supersaturation is at zero, which is a condition which is also required for the end of a reaction.

Bimodal distributions have also been observed by Zhdanov¹ for zeolite A (figure 5.15) and Mostowicz and Sand⁶ for zeolite ZSM-5 (figure 5.16). Mostowicz and Sand used static autoclaves at 443K and obtained a distribution which appears to be composed of two

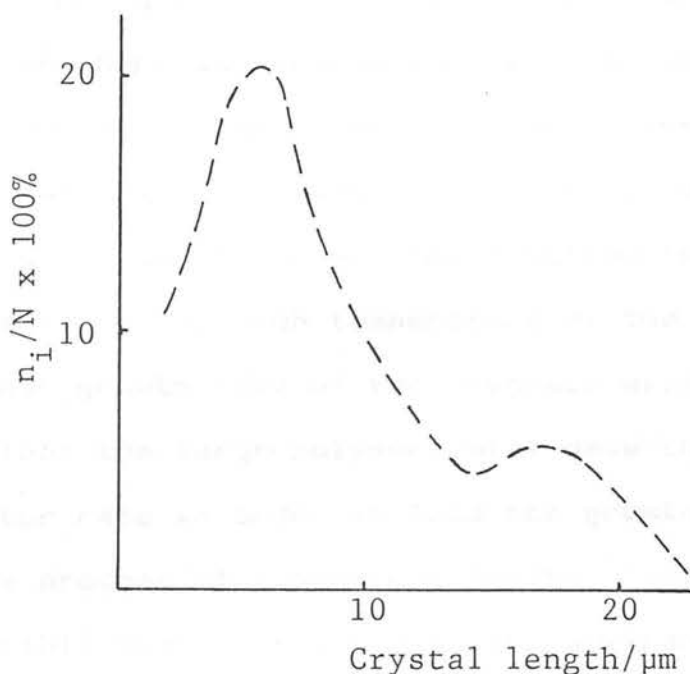


Figure 5.15. Crystal size distribution of zeolite A obtained at 363K (see figure 5.1).¹ No information was given about whether the reaction is stirred or static.

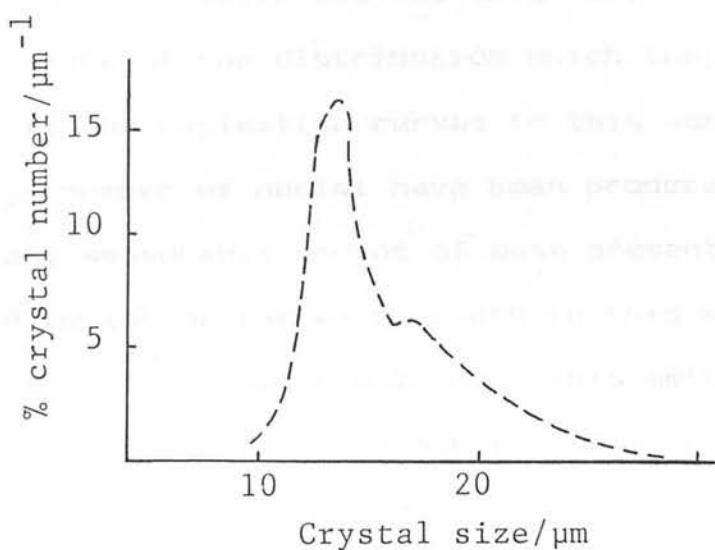


Figure 5.16. Crystal size distribution for zeolite ZSM-5, crystallized at 443K from the composition: $4.5(\text{TPA})_2\text{O}$, Al_2O_3 , 90SiO_2 , $2000\text{H}_2\text{O}$, $12(\text{NaHCO}_3)_2$ prepared from Ludox silica sol, TPAOH and sodium bicarbonate⁵. The reaction was not agitated.

overlapping peaks. A mechanism like (a) cannot really operate here as secondary nucleation usually involves forced motion. An alternative mechanism such as type (b) must be quite important. It is interesting to speculate about whether the distribution is this shape because of the high temperature of the reaction. The linear growth rate of the crystals will be much higher so that the large polymers will have to dissolve at a faster rate in order to feed the growing crystals. If this process also produces further nuclei it is possible that this would be the dominant mechanism. This would start much earlier than at the lower temperatures so that it is possible to contemplate a temperature where this mechanism is so dominant that it hides any other and produces only a single peak. Sand and Mostowicz did not offer any explanation for the shape of the distribution which they had obtained.

All the nucleation curves in this work show that a large number of nuclei have been produced before there is any measurable amount of mass present. The technique used to follow the mass growth in this work involved weighing the product obtained. This method is probably more sensitive than the normal X-ray method used for conventional crystallization from amorphous solid gel. Despite this, it was still not possible to detect the very small quantities of material which are present in the early stages of the reaction. The only method that could be used to detect the small amounts of crystals

present in these circumstances was scanning electron microscopy. This emphasizes the importance of electron microscopy in the study of zeolite crystallization. The induction period observed for the crystal mass growth curves simply corresponds to the period during which the crystals grow to sufficient dimensions and in sufficient quantities that the formation of the new phase becomes apparent. This definition of the induction period has been made for other crystallizations besides those of zeolites.⁷

Some investigators^{6,8} have tried to obtain activation energies for nucleation from induction periods obtained at different temperatures. These results may not be very satisfactory as it can be easily seen that the nucleation process is very complicated and the rate of nucleation does not remain constant. The induction period does not just depend on the rate of nucleation. It also depends on the rate of linear growth because the crystals must grow to a size which can be detected whether it be by X-ray diffraction, weighing or microscopy.

All of the reactions show that nucleation carries on throughout almost all of the crystallization period and only decreases when over 40% of the available material has been used. Nucleation appears to effectively stop at about the same time as the linear growth rate begins to decrease. This is to be expected because both are a function of the decreasing supersaturation. These

changes cause the mass growth rate to slow down.

5.3.3 pH.

The pH of the solution also starts to rise at about this time. The hydroxide which is released on the formation of the zeolite is normally used to depolymerise the polymers which provide material for the growth of the zeolite. This hydroxide will build up rapidly when there is no more material and result in a rise in pH. A typical pH profile is shown in figure 5.17 for reaction A1A, along with the mass growth curve for comparison. The pH profiles and mass growth curves for the other reactions are shown in figures 5.18 - 5.20. Each pH profile shows a sharp rise in pH at the start of the reaction when the solutions are heated from room temperature to 368K. This implies that further polymerization takes place at this time to produce colloidal silicate species and release hydroxide.

5.3.4 Comparison of reactions.

Although all the reactions give the same linear growth rate $(2.0 \pm 0.1) \times 10^{-2} \mu\text{m h}^{-1}$, it is obvious that the mass growth curves are not the same. Figure 5.21 shows all four mass growth curves together. The differences between these curves must be caused by the differences in the nucleation curves. The nucleation curves for all four reactions were compared in figure 5.14. Figures 5.21 and 5.14 show clearly that the fastest reaction is A1A while the slowest reaction is P2S, i.e. reaction

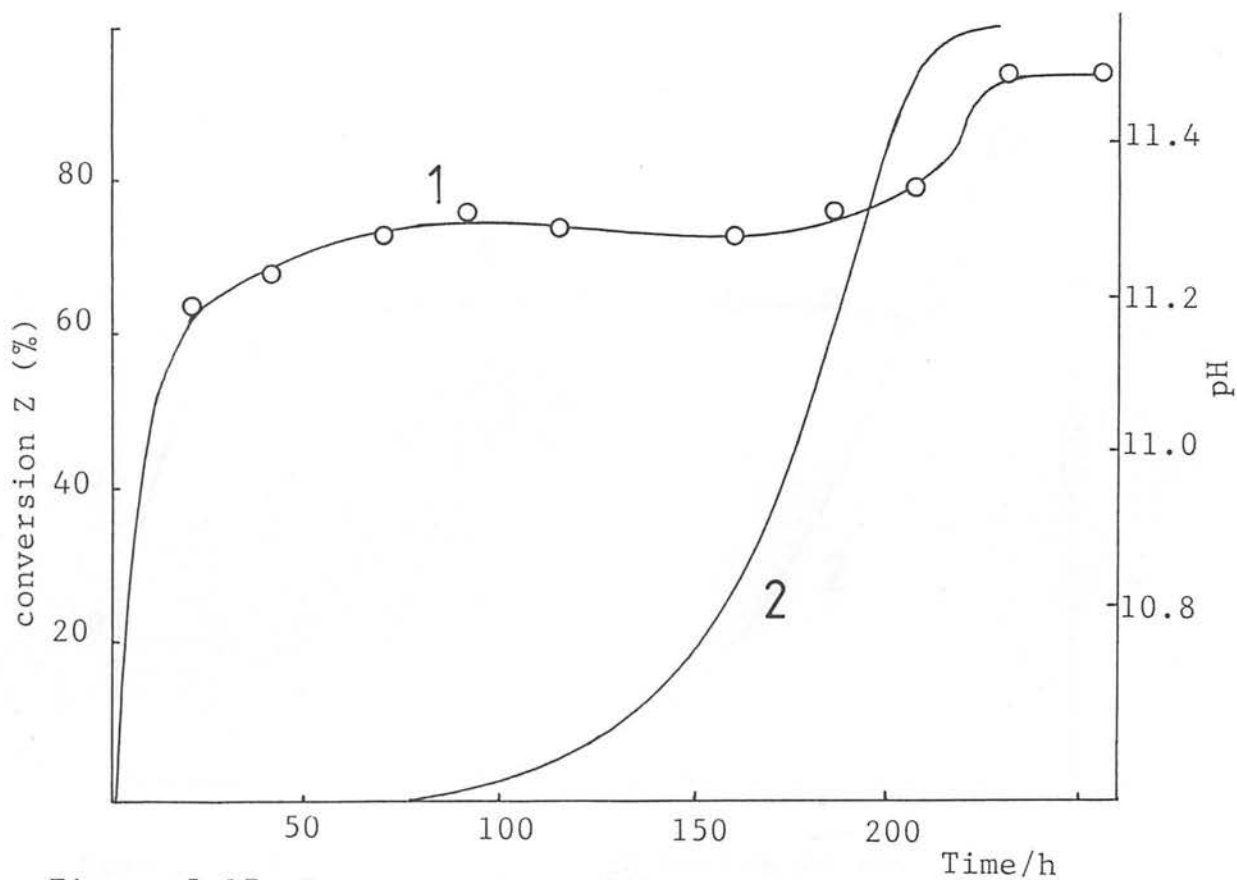


Figure 5.17. Reaction A1A: pH (curve 1) and crystal mass growth (curve 2).

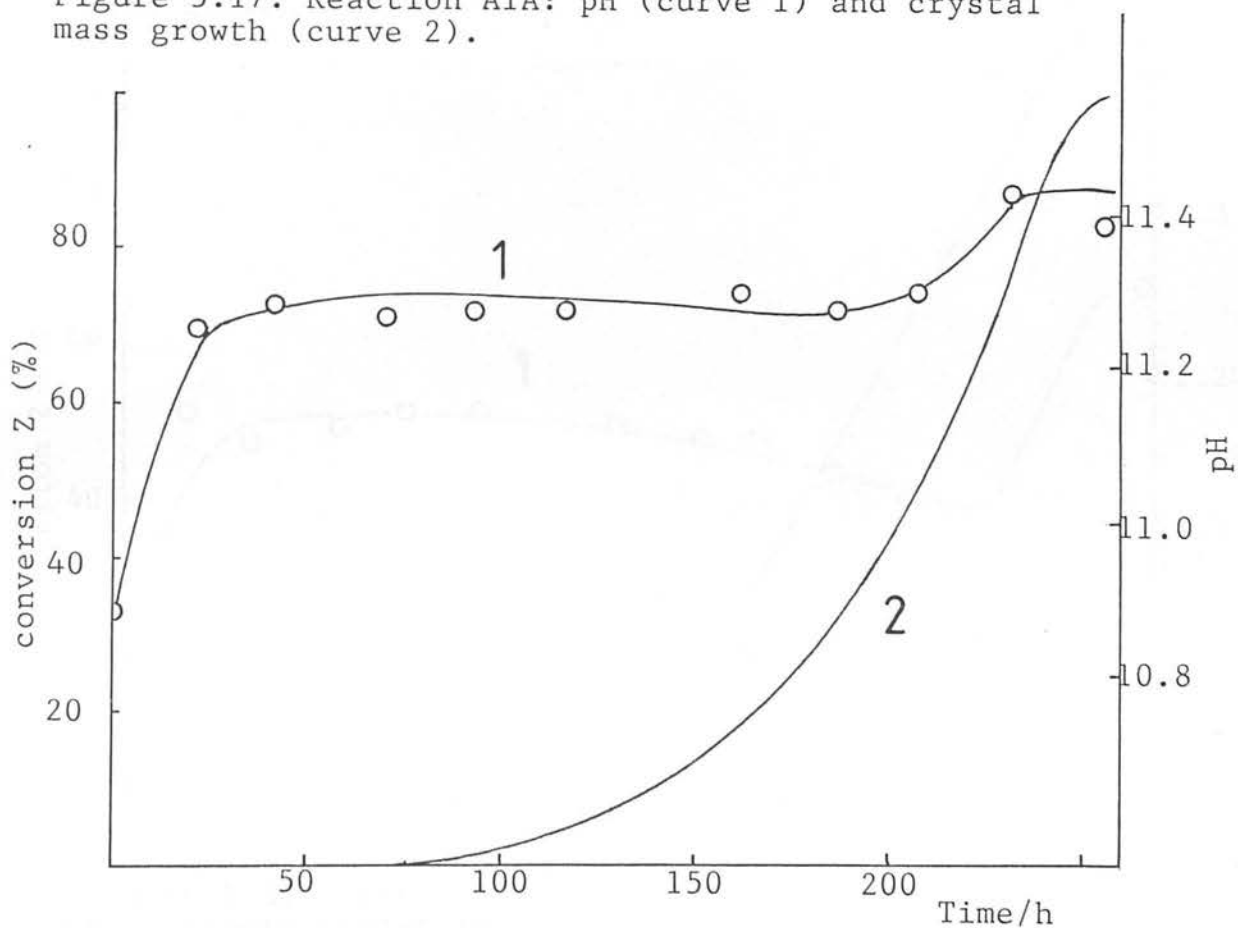


Figure 5.18. Reaction A2A: pH (curve 1) and crystal mass growth (curve 2).

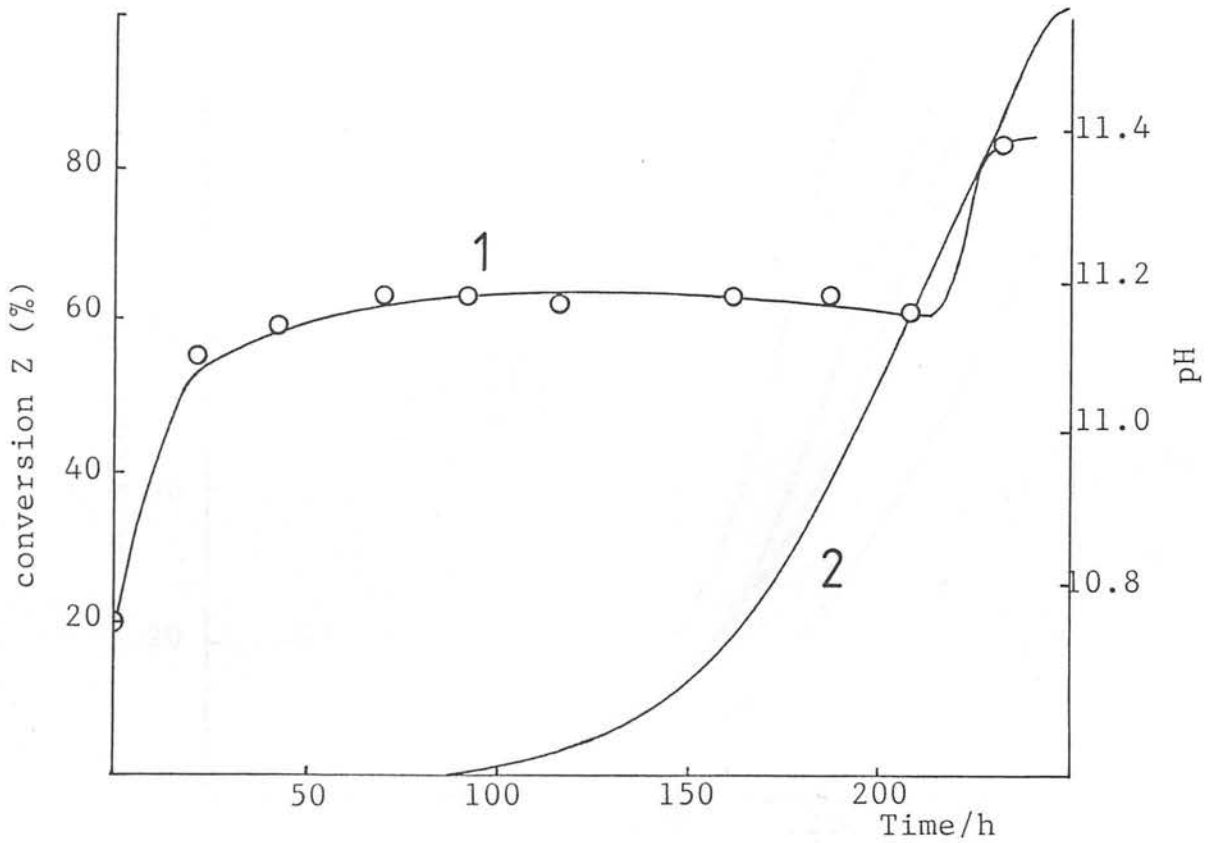


Figure 5.19. Reaction P1S: pH (curve 1) and crystal mass growth (curve 2).

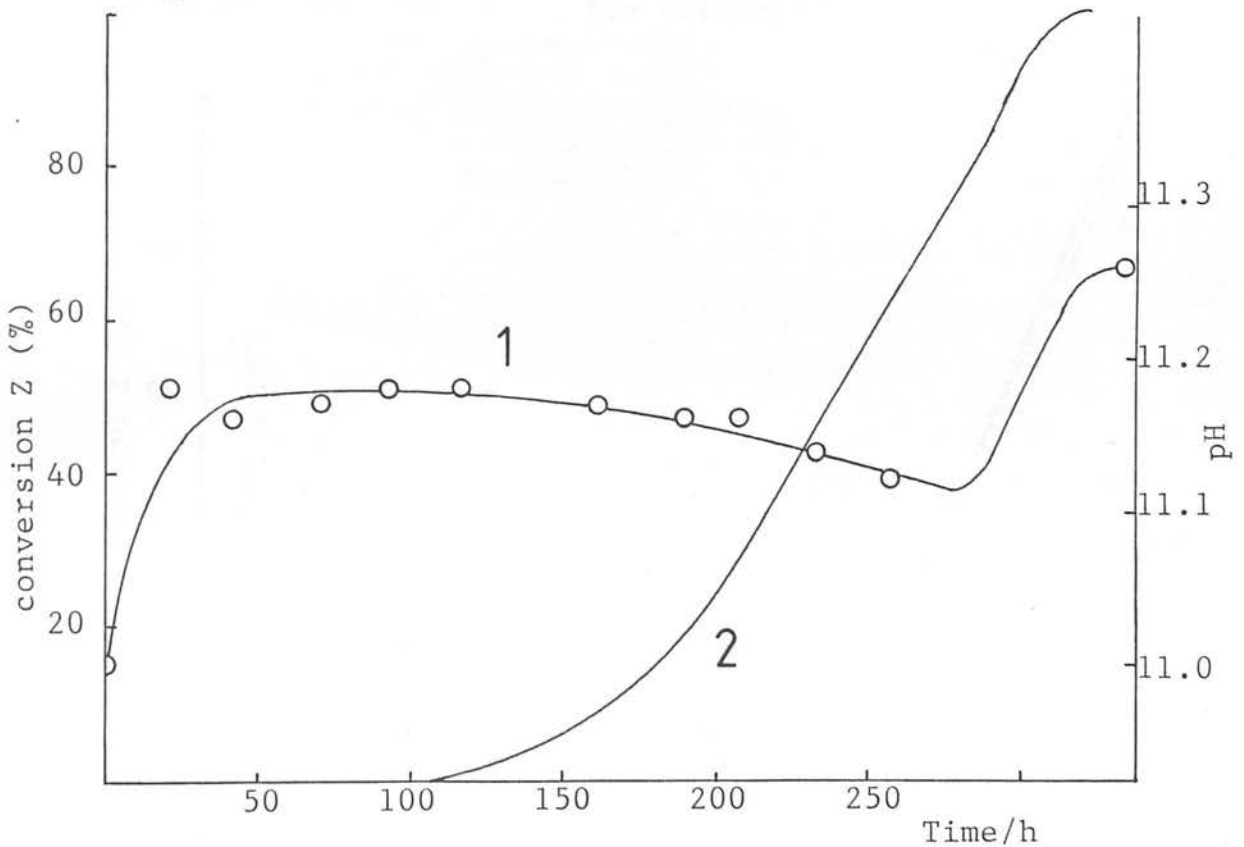


Figure 5.20. reaction P2S: pH (curve 1) and crystal mass growth (curve 2).

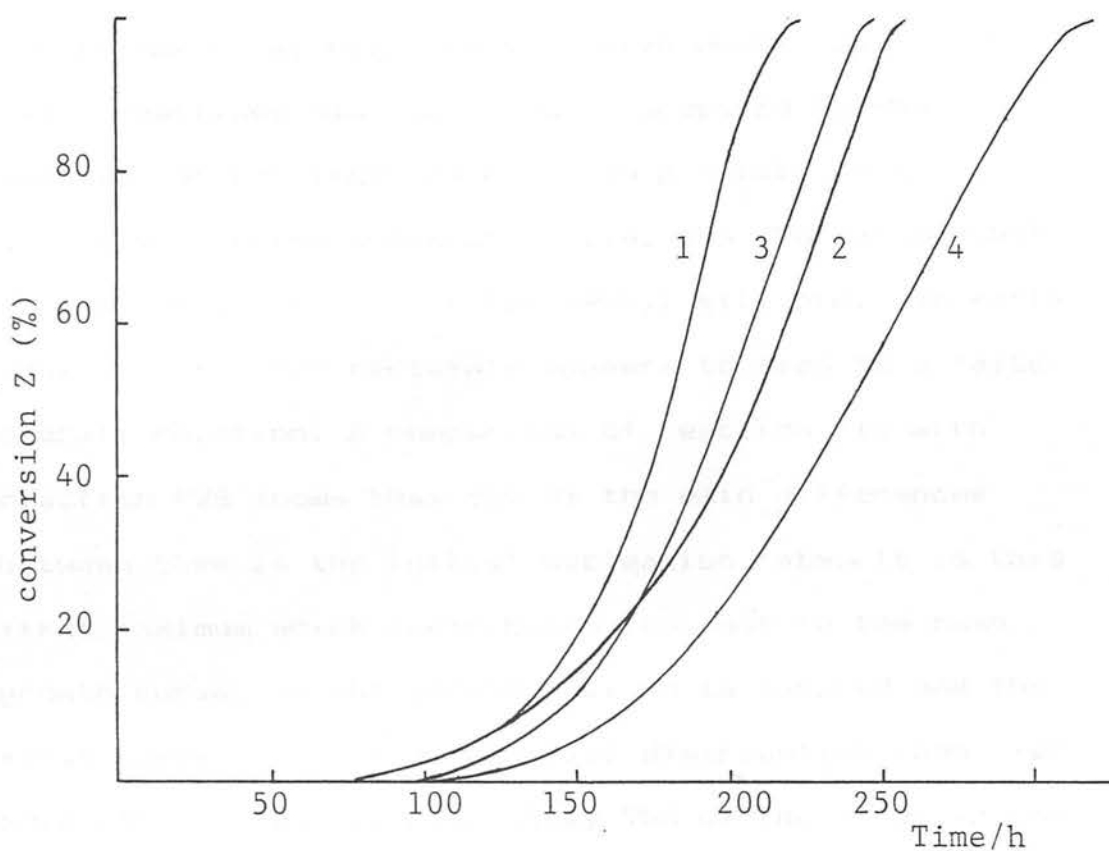


Figure 5.21. Crystal mass growth for AlA (curve 1), A2A (curve 2), PlS (curve 3), P2S (curve 4).

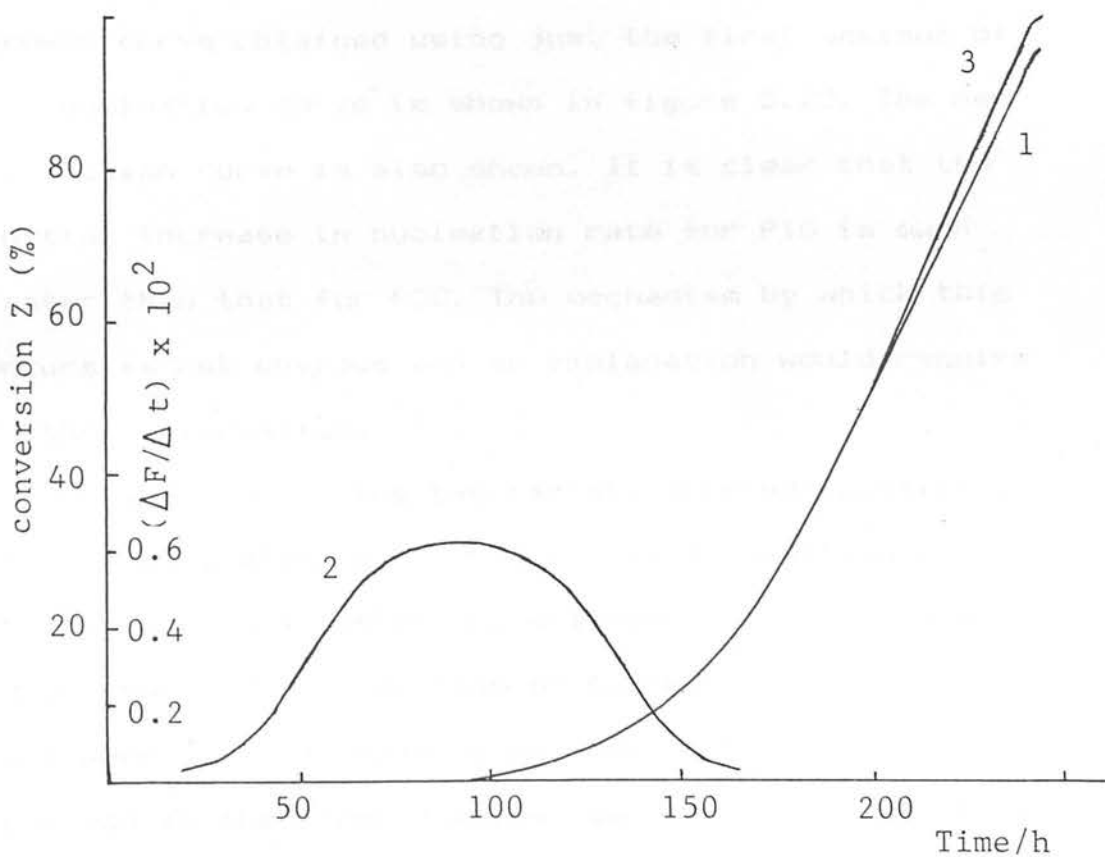
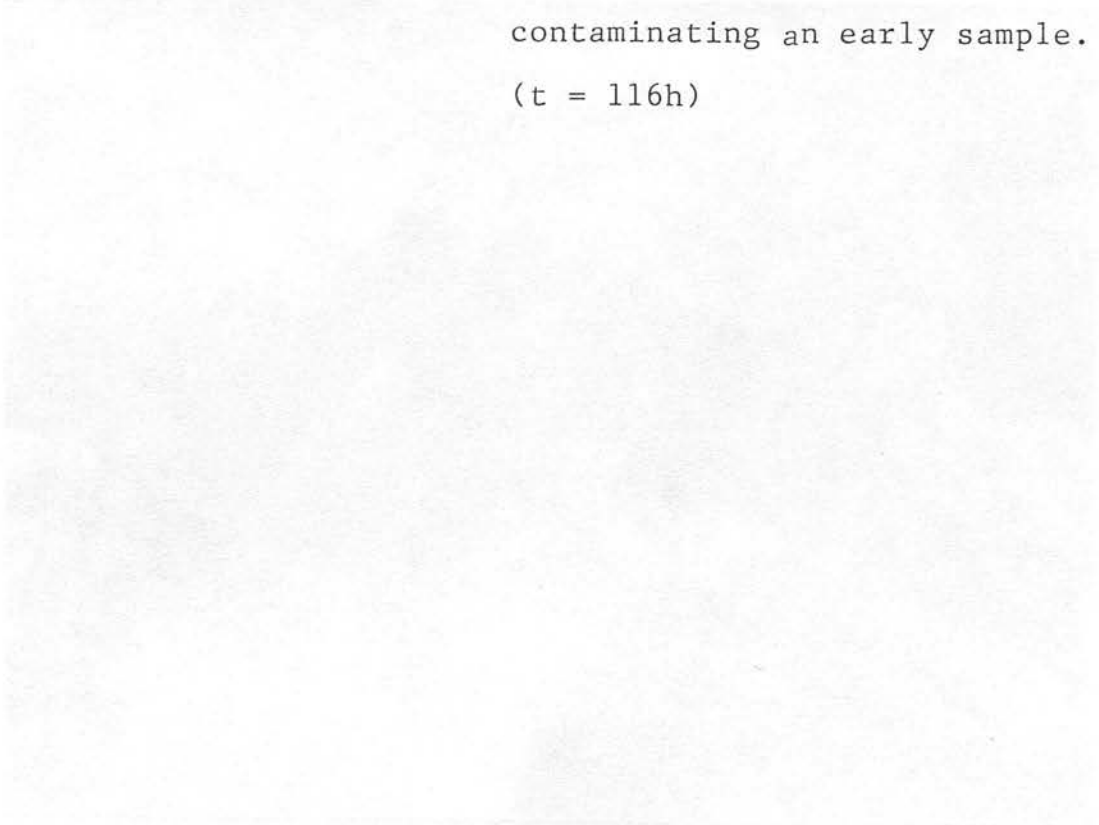


Figure 5.22. Reaction PlS: New crystal mass growth (curve 1) generated by assuming the nucleation kinetics (curve 2). The actual crystal mass growth (curve 3) is also shown.

A1A is the first reaction to finish while P2S is the last. Reactions A1A and P1S were prepared by the addition of the TPABr as early as possible in the silicate solution preparation i.e. the TPA was present during the hydrolysis of tetraethyl silicate. The early addition of TPABr certainly appears to lead to a faster overall reaction. A comparison of reaction P1S with reaction P2S shows that one of the main differences between them is the initial nucleation rate. It is this first maximum which contributes the most to the mass growth curve. If the second maximum is ignored and the first curve taken to be a normal distribution then, for both P1S and P2S, approximately 95% of the final volume of crystals is contributed by the first maximum. A comparison of the mass growth curve for P1S with the growth curve obtained using just the first maximum of the nucleation curve is shown in figure 5.22. The new nucleation curve is also shown. It is clear that the initial increase in nucleation rate for P1S is much faster than that for P2S. The mechanism by which this occurs is not obvious and an explanation would require further information.

A comparison of the two rapidly stirred reactions, A1A and A2A, also shows that the early addition of TPABr leads to a faster overall reaction. It should be noted that the initial rate of nucleation for A2A may have been aided by seeding as some seed crystals were observed in the first samples (see figure 5.23). These

Figure 5.23. (overleaf) Reaction A2A: Seed crystal
contaminating an early sample.
($t = 116\text{h}$)



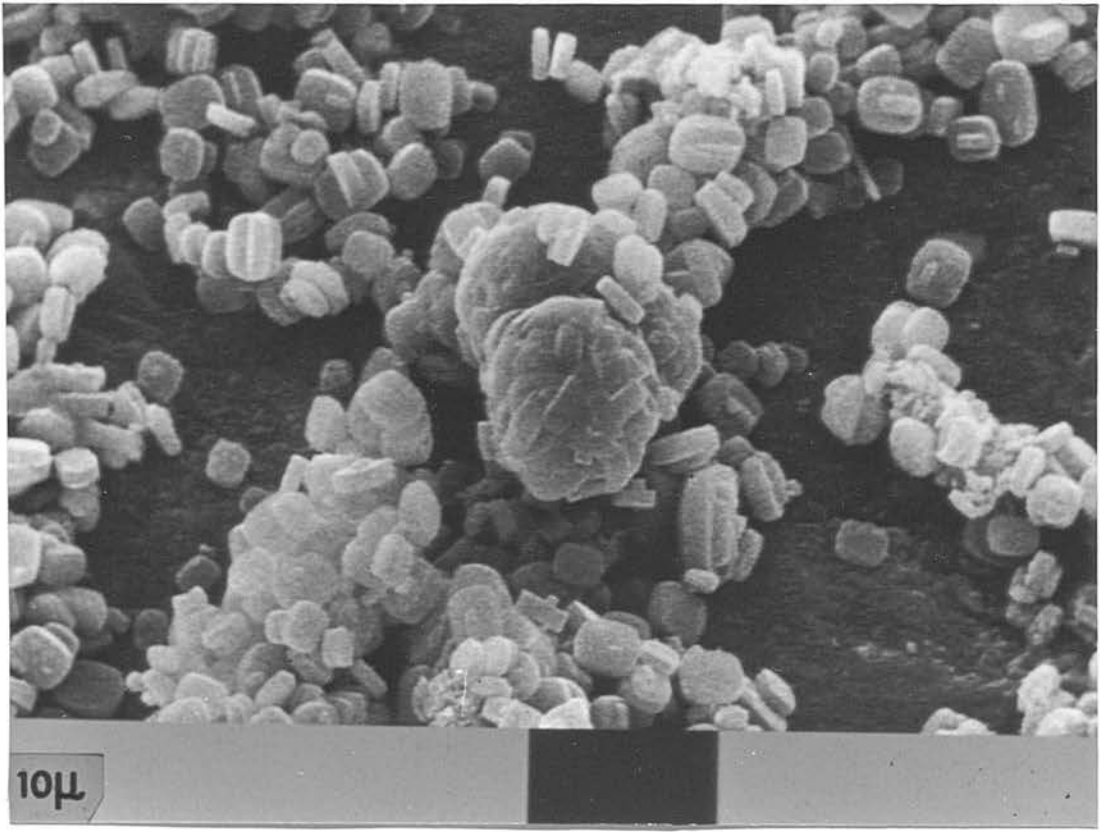


Fig. 5.23.

seeds must have been trapped in the sampling tube and some may have been washed into the main solution.

The broad initial maximum for P1S and P2S may be associated with the 24 hour static period that they underwent. This quiescent period at high temperature is likely to have produced different changes in the solution compared to the continuously stirred reactions. It may also have produced more amorphous particles as it is known (Chapter 2) that amorphous material can form at the solution / vapour / container boundary. An increase in the number of amorphous particles would probably lead to an increase in nucleation. This could partly explain the difference between P1S and A1A but it is not possible to make a similar comparison between P2S and A2A because the latter reaction may have been seeded.

An equation which is often found to fit crystallization curves is equation (1.16) which was mentioned in the introduction.

$$Z_t/Z_f = 1 - \exp(-kt^n)$$

The values of n and k can vary quite widely and yet still give a reasonable fit to the curves obtained here; e.g. for reaction A1A, $n = 6.75$ and $k = 5.11 \times 10^{-16}$ fits the curve only slightly better than $n = 7.58$ and $k = 5.95 \times 10^{-18}$. The values for n are greater than 4 so this indicates an increasing nucleation rate. It is obvious that the equation is unable to predict a nucleation rate which increases, decreases then

increases again, as was actually observed. The crystallization process is probably too complicated for one single general equation to be applicable in all situations.

5.4 Conclusions.

The mass growth curves normally obtained for zeolite crystallizations are of limited use as an aid to the understanding of zeolite crystallization. The shapes of these growth curves are a result of both nucleation and crystal growth processes. As a result, it is not possible to take a mass growth curve in isolation and use it to obtain information about either the nucleation or the growth rate. Mathematical models of the crystallization curve which provide a good fit to experimental results may well be based upon mechanisms which do not occur, so that they are of little practical use. The crystallization process is very complex and should really be broken down into different components for separate examination. An example of this is the study of linear growth rates and particle-size analysis, given in this chapter.

The final particle-size distribution can give an insight into the mechanism of nucleation, especially when it is linked with the linear crystal growth rate to produce a nucleation curve. This approach allows us to understand why apparently minor changes in reaction conditions can alter the reaction time. It may also reveal ways in which different crystal distributions may be obtained, a factor which may be of use in the production of zeolites as catalysts and sorbents. Further work on the crystallization kinetics of zeolites should use techniques which give as detailed a

picture of the process as possible, rather than just relying upon the mass growth curve. An attempt should be made to determine zeolite solubilities at the reaction temperature and hence to acquire some knowledge of the supersaturation of the solutions used to crystallize zeolites. The degree of supersaturation is of primary importance in crystallization as both nucleation and growth rates depend upon it.

An objection which may be made about any attempt to obtain a value for the supersaturation is that the building blocks of the zeolites are unknown, so how can the concentration of these blocks be measured? A very simple approach would be to obtain the concentration (C_0) of monomer when zeolite crystals are allowed to equilibrate in buffered solutions at various pH values and temperatures. The concentration (C) of monomer in several reactions could then be determined. If a parameter, e.g. linear growth rate, was found to depend strongly on the value $C - C_0$ (absolute supersaturation) then it may indicate that the monomer concentration could be used to compare various reactions. It would not matter for kinetic purposes if the monomer was not the actual crystal "bricks" so long as the conversion of monomer to the "bricks" is extremely fast.

5.5 References

1. S.P. Zhdanov, *Advan. Chem. Ser.*, 1971, 101, 20
2. S.P. Zhdanov and N.N. Samulevich, "Proceedings of the 5th. International Conference on Zeolites", Ed. L.V.C. Rees, Heyden, London, 1980, 75
3. J.M. Coulson and J.F. Richardson, "Chemical Engineering", Vol.2 p817, Pergamon Press, London 1955
4. J.L. Casci, Ph.D. Thesis, University of Edinburgh, 1982
5. R. Aiello, R.M. Barrer and I.S. Kerr, *Advan. Chem. Ser.*, 1971, 101, 41
6. R. Mostowicz and L.B. Sand, *Zeolites*, 1983, 3, 219
7. E.V. Khamskii, "Crystallization from Solutions", p45, Consultants Bureau, New York, 1969
8. For example,
 - (a) M. Dirringer and F. Fajulo, *Zeolites*, 1983, 3, 163
 - (b) S.B. Kulkarni, V.P. Shiralkar, A.N. Kotasthane, R.B. Borads and P. Ratnasamy, *Zeolites*, 1982, 2, 313
 - (c) K.J. Chao, T.C. Tasi, M.S. Chem and I. Wangy, *J. Chem. Soc. Faraday Trans. 1*, 1981, 77, 547

Appendix 1. Computer program to calculate the weights required for a reaction mixture, from a composition given in mole ratios.

```

100  REM  PROG. TO CALC. WEIGHTS
      REQ.   FOR REACTION MIXTURES

120  INPUT "RUN NO. ";NO
140  INPUT "DATE:";D$
200  MN = 61.98
210  MH = 40.00
220  MS = 60.08
230  MT = 208.33
240  MA = 101.96
250  ML = 78.00
260  MW = 18.015
265  INPUT "FORMULA OF HYDROXIDE(
      EXC.NAOH),ROH";R$
268  INPUT "MOL. WT. OF ROH ";MR
270  INPUT "NO. OF SALTS TO BE AD
      DED(<4)";M
275  DIM SALT$(4): DIM P(4): DIM
      H(4): DIM Q(4): DIM AW(4): DIM
      V(4)
277  SUM = 0:MUS = 0:CR = 0
280  IF M = 0 THEN GOTO 400
285  FOR N = 1 TO M
290  INPUT "FORMULA OF SALT ";SAL
      T$(N)
292  INPUT "MOL WT OF SALT ";P(N)

294  INPUT "NO. OF WATERS OF HYDR
      ATION ";H(N)
300  INPUT "NO. OF MOLES REQD. ";
      Q(N)
305  NEXT N
315  FOR N = 1 TO M
320  V(N) = P(N) * Q(N)
325  PROD = H(N) * Q(N)
330  SUM = PROD + SUM
335  MUS = MUS + V(N)
340  NEXT N
400  INPUT "NO. MOLES NA2O REQ.?"
      ";E
405  INPUT "NO. MOLES R2O REQ.?"
      R
410  INPUT "NO. MOLES SiO2(CABOSI
      L) REQ.?" ";S
420  INPUT "NO. MOLES Si(OET)4 RE
      Q.?" ";T
450  INPUT "NO. MOLES AL2O3 REQ.?"
      ";A
460  INPUT "NO. MOLES H2O REQ.?" "
      ;W
464  IF T = 0 THEN GOTO 470
466  W = W + 2 * T
470  WR = 2 * R * MR

```

```

500 WH = 2 * B * MH
510 WS = S * MS
520 WT = T * MT
540 WL = 2 * A * ML
550 WW = MW * (W - B - R - (3 * A
    ) - SUM)
560 TT = WR + WH + WS + WT + MUS +
    WL + WW
570 INPUT "TOTAL WT REQ. ";ZZ
580 F = ZZ / TT
600 HR = F * WH
605 RR = F * WR
610 SR = F * WS
620 TR = F * WT
622 IF M = 0 THEN GOTO 640
623 FOR N = 1 TO M
625 AW(N) = F * V(N)
630 NEXT N
640 LR = F * WL
650 WV = F * WW
690 PR# 1
692 PRINT "RUN NO. ";NO
694 PRINT "DATE: ";D#
695 IF M = 0 THEN GOTO 700
696 FOR N = 1 TO M
697 PRINT "MOL. WT. ";SALT$(N);"
    =";P(N)
698 NEXT N
700 PRINT "WTS REQ. ARE "
702 PRINT
705 IF R = 0 THEN GOTO 710
708 PRINT R#;"=";RR;" GRAMS"
710 PRINT "NAOH=";HR;" GRAMS"
715 IF S = 0 THEN GOTO 725
720 PRINT "CABOSIL=";SR;" GRAMS"

725 IF T = 0 THEN GOTO 733
730 PRINT "SI(OET)4=";TR;" GRAMS
    "
733 IF M = 0 THEN GOTO 750
735 FOR N = 1 TO M
740 PRINT SALT$(N);"=";AW(N);" G
    RAMS"
742 CR = CR + AW(N)
745 NEXT N
750 PRINT "AL(OH)3=";LR;" GRAMS"

760 PRINT "H2O=";WV;" GRAMS"
762 PR# 0
765 ZZ = HR + SR + TR + CR + LR +
    WV + RR
768 PR# 1
770 PRINT "TOTAL WT. IS ";ZZ
790 PRINT
792 PRINT

```

```

800 PRINT "MOLE COMPOSITION IS "
802 PRINT
806 IF R = 0 THEN GOTO 810
808 PRINT R;" R2O, FROM ";R$
810 PRINT B;" NA2O"
812 PR# 0
815 IF S = 0 THEN GOTO 825
818 PR# 1
820 PRINT S;" SIO2 CABOSIL "
822 PR# 0
825 IF T = 0 THEN GOTO 840
828 PR# 1
830 PRINT T;" SIO2, FROM SI(OET)4
"
832 E = 4 * T
834 PRINT E;" ETOH"
835 PR# 0
840 PR# 1
845 PRINT A;" AL2O3"
848 W = W - 2 * T
850 PRINT W;" H2O"
851 IF M = 0 THEN GOTO 870
852 FOR N = 1 TO M
855 PRINT Q(N);" ";SALT$(N)
860 NEXT N
870 PR# 0
900 END

```

Appendix 2. Computer program to calculate a mass growth curve from a size distribution curve.

```

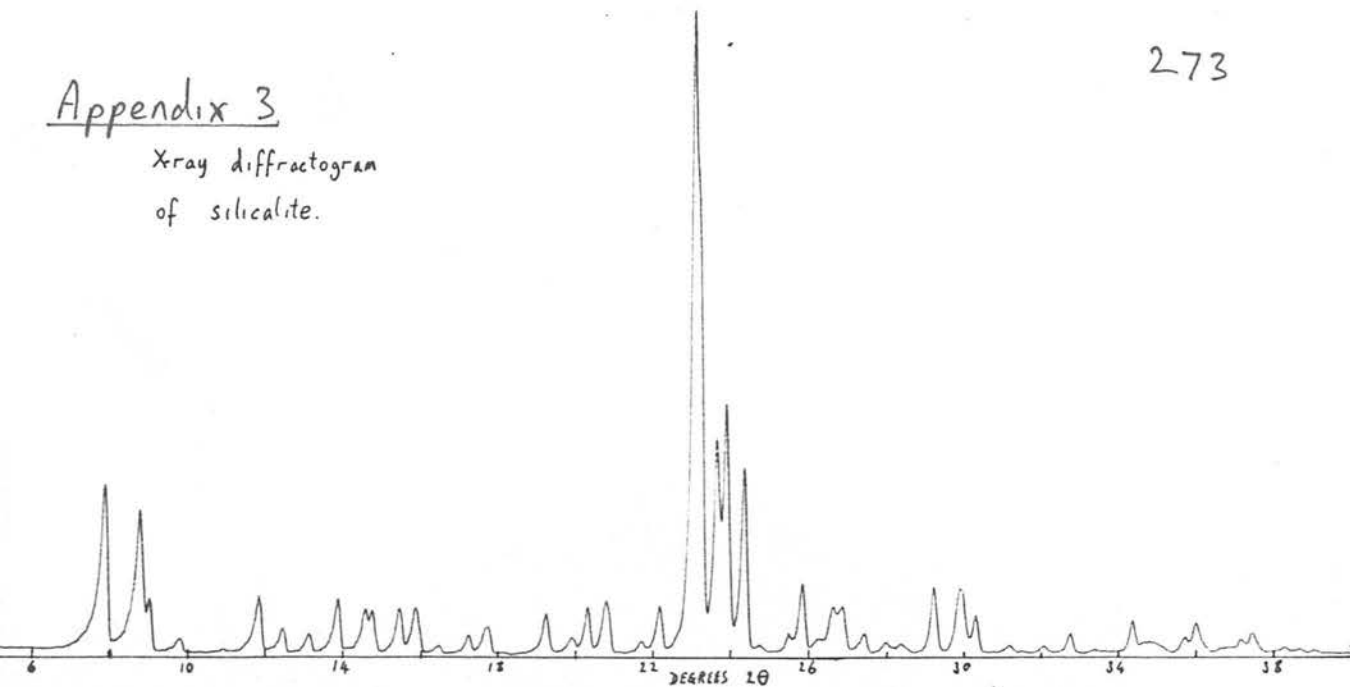
10  REM  PROG TO CONVERT SIZE DIS
    TR. TO GROWTH CURVE
12  INPUT "SAMPLE CODE:";SC$
20  PRINT "NO. OF DIVISIONS:";
30  INPUT M
40  DIM Z(M)
50  DIM DIST(M)
60  DIM TIME(M)
70  PRINT "INPUT NO. OF CRYSTALS
    AND TIME:CRYSTALS SHOULD NOT
    BE ZERO SIZE"
75  PRINT "START AT BEGINNING OF
    NUCLEATION CURVE"
80  FOR I = 0 TO M - 1
90  INPUT "NO. OF CRYSTALS:";DIST
    (I)
100  PRINT "TIME:";
110  INPUT TIME(I + 1)
120  NEXT I
122  FOR N = 0 TO M - 1
125  PRINT DIST(N);" ";TIME(N +
    1)
128  NEXT N
130  INPUT "DO YOU WANT TO CHANGE
    ANY OF THESE (YES OR NO)?";
    D$
135  IF D$ = "NO" THEN GOTO 150
137  INPUT "INPUT N FOR (N)TH BAT
    CH OF RESULTS TO BE CHANGED:
    ";N
140  INPUT "NO. OF CRYSTALS:";DIS
    T(N - 1)
143  INPUT "TIME:";TIME(N)
145  GOTO 122
150  PRINT "GIVE SIZE BETWEEN DIV
    ISIONS.THIS IS ALSO ASSUMED
    TO BE THE SMALLEST CRYSTAL S
    IZE IN ANY DIVISION"
155  INPUT "SIZE:";INCR
160  FOR J = 1 TO M
165  X = INCR
170  Z(J) = 0
200  FOR K = 1 TO J
220  Z(J) = X * X * X * DIST(J - K
    ) + Z(J)
225  X = X + INCR
230  NEXT K

```

```
240 NEXT J
245 PRF 1
250 PRINT "SAMPLE:";SC$
252 PRINT
253 PRINT "SIZE BETWEEN DIVISION
S:";INCR
255 PRINT CHR$(27);"Q"; CHR$(
80)
258 PRINT "DIST "; "TIME "; "Z(
T) "; "%FINAL MASS"
260 FOR L = 1 TO M
270 PRINT DIST(L - 1); " "; TIM
E(L); " "; Z(L); "
"; Z(L) / Z(M) * 100
280 NEXT L
290 PRF 0
300 END
```


Appendix 3

X-ray diffractogram
of silicalite.



UNKNOWN MATERIAL IS: DEGR
LE OF KNOWN ZEOLITES IS: HST HIGH SILICA AND NEW ZEOLITES.
COMPARISON WITH UPTO FOUR ZEOLITES IN FILE OF UNKNOWN

ZSM5-SILICATE
ZSM5 A
ZSM5 B
ZSM5 C

ZSM5-SILICATE		ZSM5 A		ZSM5 B		ZSM5 C	
11.173	27.	11.120	75.	11.177	75.	11.357	29.
17.753	22.	10.707	75.	10.707	75.	17.132	22.
9.874	3.	0.000	?	0.000	?	0.000	?
8.717	2.	0.000	?	0.000	?	0.000	?
8.229	0.	0.000	?	0.000	?	0.000	?
7.455	4.	7.400	25.	7.477	25.	7.547	13.
7.252	4.	7.177	25.	7.177	25.	7.167	7.
6.712	5.	6.277	?	0.000	?	6.707	9.
6.355	6.	0.000	?	6.307	25.	6.457	11.
6.075	7.	6.700	25.	0.000	?	0.000	?
5.553	7.	6.040	25.	6.047	25.	6.097	13.
5.717	7.	5.977	25.	0.000	?	0.000	?
5.594	7.	0.000	?	0.000	?	5.777	10.
7.000	?	5.567	25.	5.567	25.	5.677	11.
5.322	1.	0.000	?	0.000	?	5.427	5.
5.175	3.	0.000	?	0.000	?	5.227	6.
4.931	4.	5.217	25.	5.017	25.	5.257	9.
4.626	6.	4.607	25.	4.607	25.	4.657	9.
4.457	2.	0.000	?	0.000	?	4.477	12.
4.377	7.	4.250	25.	4.250	25.	4.307	13.
4.277	8.	0.000	?	0.000	?	0.000	?
4.347	2.	0.000	?	0.000	?	4.127	7.
4.017	7.	0.000	?	0.000	?	4.047	11.
0.000	0.	0.000	?	0.000	?	0.000	?
0.000	0.	0.000	?	0.000	?	0.000	?
0.000	0.	0.000	?	0.000	?	0.000	?
0.000	0.	0.000	?	0.000	?	0.000	?
0.000	0.	0.000	?	0.000	?	0.000	?
3.852	100.	3.850	100.	3.850	100.	7.007	120.
3.835	76.	0.000	?	0.000	?	3.757	52.
3.759	50.	3.717	75.	3.717	75.	3.757	48.
3.723	38.	0.000	?	0.000	?	0.000	?
3.652	28.	0.000	?	0.000	?	0.000	?
3.584	1.	0.000	?	0.000	?	0.000	?
3.484	3.	0.000	?	0.000	?	3.527	10.
3.444	11.	0.000	?	0.000	?	3.477	17.
3.392	2.	0.000	?	0.000	?	3.347	20.
3.342	7.	0.000	?	0.000	?	3.297	11.
3.317	7.	0.000	?	0.000	?	0.000	?
3.247	3.	0.000	?	0.000	?	0.000	?
3.184	2.	0.000	?	0.000	?	0.000	?
3.140	1.	0.000	?	0.000	?	0.000	?
3.051	10.	3.040	25.	3.047	25.	3.077	14.
2.981	10.	2.990	25.	2.990	25.	3.007	21.
2.948	6.	2.940	25.	2.947	25.	0.000	?
2.955	1.	0.000	?	0.000	?	0.000	?
2.787	1.	0.000	?	0.000	?	0.000	?
2.733	3.	0.000	?	0.000	?	0.000	?
2.681	1.	0.000	?	0.000	?	0.000	?
2.658	0.	0.000	?	0.000	?	0.000	?
2.609	5.	0.000	?	0.000	?	0.000	?
2.566	2.	0.000	?	0.000	?	0.000	?
2.510	2.	0.000	?	0.000	?	0.000	?
2.492	4.	0.000	?	0.000	?	0.000	?
2.451	1.	0.000	?	0.000	?	0.000	?
2.438	1.	0.000	?	0.000	?	0.000	?
2.419	2.	0.000	?	0.000	?	0.000	?
2.400	3.	0.000	?	0.000	?	0.000	?
2.352	0.	0.000	?	0.000	?	0.000	?